4.0 ANALYSIS OF PERFORMANCE

The purpose of this section is to provide the technical basis for the analyses of performance for the closed HTF facilities over time based on the total remaining inventory.

Section 4.1 provides an overview of the ICM comprised of three components: 1) closure cap, 2) vadose zone, and 3) saturated zone.

Section 4.2 describes the ICM approach for contaminant release.

- 4.2.1 presents details of the source term release, the analyses performed to estimate the leaching of contaminants from the CZ by the pore fluid, based on solubility controls used for modeling the transport of contaminants from their initial closure locations within the waste tanks and ancillary equipment to the underground aquifers.
- 4.2.2 describes the assumed radionuclide transport mechanisms and parameters used for groundwater pathways modeling to estimate exposures to MOP and the inadvertent intruder for various scenarios.
- 4.2.3 defines the MOP and intruder exposure pathways used for dose calculation.

Section 4.3 describes various computer codes, their purpose, and integration utilized in this PA. The computer codes discussed in the section are HELP, PORFLOW, GoldSim, The Clean Air Act Assessment Package - 1988 (CAP-88), and The Geochemist's Workbench (GWB).

Section 4.4 describes the integrated closure system, including the assumed waste tank modeling dimensions, scenarios of potential conditions of the waste tanks, and scenarios of potential conditions of ancillary equipment. The modeling processes used in PORFLOW and GoldSim are detailed in this section.

Section 4.5 describes the ICM and modeling assumptions to estimate the potential flux of gaseous radionuclides at the ground surface for the air pathway analyses. Results are provided based on the assumed inventory of radionuclides susceptible to volatilization. A radon analysis is also completed by presenting the ICM, modeling assumptions, and the results of the radon (Rn-222) surface flux analysis based on source inventories of the parent radionuclides that generate Rn-222.

Section 4.6 presents the factors for each element necessary in the biotic dose pathway model.

- 4.6.1 presents the bioaccumulation factors used in the analysis.
- 4.6.2 presents consumption rates for human health exposure.

Section 4.7 presents the internal and external Dose Conversion Factors (DCFs) utilized in the various dose pathway models.

Section 4.8 describes the risk evaluation, including the ICM and protocols for the assessment of human health and ecological risk from radioactive and chemical contaminants contained within the closed HTF.

4.1 Overview of Analyses

The purpose of this section is to describe the ICM to be used for evaluating the performance of the HTF closure system during the 10,000-year compliance period following closure.

This ICM is used to evaluate the migration of contaminants from the HTF and is illustrated in Figure 4.1-1. It comprises three related conceptual models that represent the HTF closure system and the environmental media through which contaminants may migrate, 1) the conceptual closure cap model, 2) the vadose zone model, and 3) the saturated zone model. This section compiles and organizes relevant data associated with these three component conceptual models to facilitate use of mathematical models to implement the ICM in the evaluation of potential HTF impacts.

The ICM described in this section is for use in simulating the release of radiological and chemical contaminants and their migration through soil and groundwater from the 29 underground waste tanks of the HTF and the associated ancillary equipment. The ancillary equipment of interest includes three evaporators, nine pump tanks, and the network of underground waste transfer lines in the area. The ICM focuses on contaminant migration via groundwater. The model output is used to predict effects of contaminants on human receptors through various pathways and exposure routes. Although the ICM focuses primarily on the groundwater exposure pathway, the air pathway is also taken into account (e.g., inhalation of volatile radioactive contaminants in water taken from a contaminated well or stream is accounted for in the inputs related to human receptor impacts). This section does not address inadvertent intrusion into the CZ, nor does it describe the mathematical models of the various computer codes used to implement the ICM to predict future behavior of the contaminants. Figure 4.1-1 graphically depicts the relationship between the HTF modeling inputs.

Figure 4.1-1: H-Area Tank Farm Modeling Input Relationships

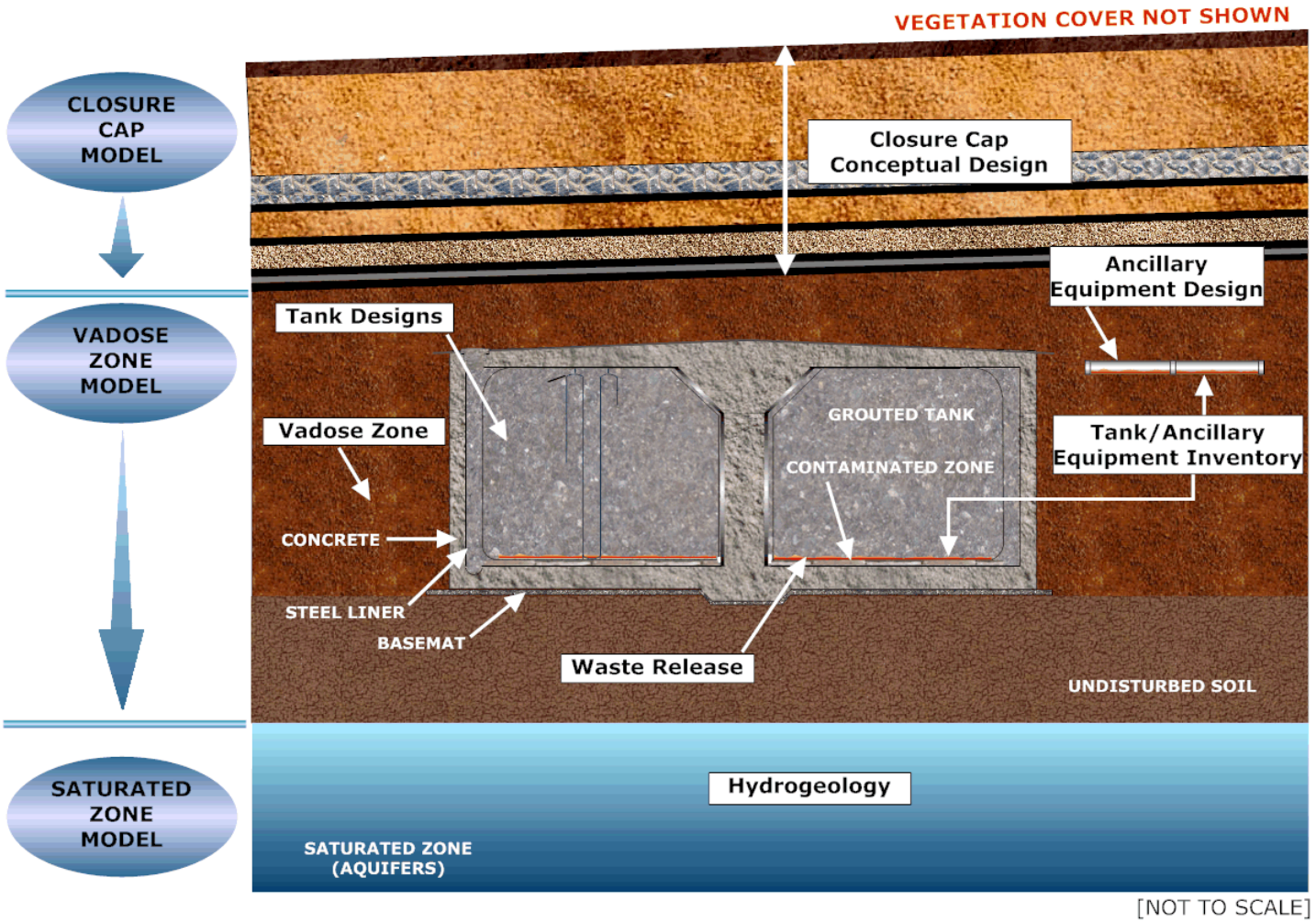

4.2 Integrated Conceptual Model of Facility Performance

The ICM simulates radiological and chemical contaminant release from the 29 waste tanks and associated ancillary equipment in the HTF. An independent conceptual waste release model was used to simulate stabilized contaminant release from the grouted waste tanks based on various chemical phases in the waste tank controlling solubility and thereby affecting the timing and rate of release from the CZ.

This ICM approach considers the integrity of the waste tank steel liners and cementitious barriers in waste tank modeling. In the ICM, steel liner failure triggers waste release from the waste tanks. After failure, the carbon steel liner is assumed to be absent, or otherwise not a hindrance to advection and diffusion.

With this approach, the time of initial waste release is tied to the integrity of the waste tank primary liners (waste tank secondary liners were assumed to fail at the same time as the primary liner). This time calculation is based on steel corrosion rates under different conditions (e.g., differing diffusion coefficients for CaO_2). The failure times varied with waste tank design, owing to differences in liner properties. [WSRC-STI-2007-00061, SRNL-STI-2010-00047] The failure analyses considered general and localized corrosion mechanisms of the waste tank steel. Consumption of the waste tank steel encased in grouted conditions was estimated due to carbonation of the concrete leading to low pH conditions, or the chloride-induced depassivation of the steel leading to accelerated corrosion. The modeling approach used for predicting steel liner failure is discussed in Section 4.2.2.2.6. Steel liner failure for four waste tanks (Type 1, Tank 12 and Type II, Tanks 14, 15, and 16) does not utilize data from the liner degradation reports. Instead, these waste tanks are assumed to have liner degradation at the time of HTF closure, based on present leak site numbers and physical locations. [C-ESR-G-00003]

The time of initial waste release from the closed waste tanks was caused by through-wall thinning due to general corrosion. Since corrosion was assumed to occur uniformly, liner failure occurs when the thinnest segment has been completely corroded. Under conservative diffusion coefficient conditions (i.e., when holes from pitting begin to occur), the earliest liner failures are predicted to occur 75 years after HTF closure for the Type IV tanks. The latest liner failures were predicted to occur 12,751 years after HTF closure in the Type III/IIIA tanks, through general corrosion under grouted conditions. Prior to failure, the primary liner is considered impermeable with respect to both advection and diffusion. After failure, the liner is not a hindrance to advection and diffusion (i.e., there would be no retardation).

Flow in-to and out-of the CZ is controlled by the material properties of the waste tank cementitious materials. The expected degradation rate and timing for the waste tank cementitious materials is based on SRNL-STI-2010-00035 and SRR-CWDA-2010-00019, and can vary dependent on waste tank type. The waste tank grout can begin degrading as early as year 800 (Type IV tanks) with full degradation being reached as early as year 13,200 (Type I tanks). The waste tank concrete can begin degrading as early as year 400 (Type IV tanks) with full degradation occurring as early as year 800 (Type IV tanks).

Soil-solute distribution coefficients for the cementitious materials depend on pore water flow through the material. These values will increase over time in stages as the concrete ages with increasing pore water flow. The infiltrating liquid will initially be characterized as Region I, it

will transition to Region II, then Region III as the liquid's pH changes over time. Because each individual waste tank grout and concrete will be aged at the time of overall HTF closure, none of the waste tank cementitious materials were characterized as young (Region I). The differences between the chemical phases are summarized in Table 4.2-1. The waste tank concrete properties are originally characterized as Oxidizing Region II transitioning to Oxidizing Region III. The waste-tank grout properties are initially characterized as Reduced Region II, then transition to Oxidized Region II after 371 pore volumes and to Oxidizing Region III after 2,131 pore volumes. [ISSN 1019-0643, WSRC-STI-2007-00544] This aging process is directly related to flow through the grout, and is therefore accelerated when liner failure allows additional liquid to encounter the cementitious materials inside the waste tank liner.

Table 4.2-1: Summary of Chemical Phases

Chemical Phase	Description
Region I	The pH lies between approximately 13.3 and 12.5. The pore water composition is dominated by potassium, sodium, and hydroxide. The solution is saturated with respect to portlandite ($Ca(OH)_2$ approximately 2.0E-03 moles). The major solid phases present in cement have already formed, though hydration may be continuing.
Region II	Contact with "flowing" groundwater has removed virtually all of the highly soluble (potassium, sodium) hydroxide. The pore water composition is now dominated by portlandite ($Ca(OH)_2$ approximately 2.0E-03 moles) which fixes the pH at approximately 12.5. The portlandite is also being slowly removed by groundwater flow but the quantities contained in the cement are so large that this phase buffers the system over very long periods. There are no significant changes in the major solid phases present in Region I and II.
Region III	The removal of $Ca(OH)_2$ has become significant and the pH falls continuously. The CSH gel is no longer stable and begins to dissolve incongruently. The Ca^2 concentration decreases continuously to approximately 1.0 to 5.0E-03 mol at pH of approximately 11.

[ISSN 1019-0643]

The pump tanks (HPT-2 through HPT-10) and evaporators (242-H, 242-16H, and 242-25H) are modeled as point sources located in the HTF at a central point of the individual components. Transfer line inventory is modeled by distributing the assumed inventory equally over the entire HTF. Other ancillary equipment is not modeled explicitly.

Based on stainless steel corrosion rate calculations, the earliest failure of a stainless steel transfer line is predicted to occur 510 years after HTF closure. [WSRC-STI-2007-00460] Failure is assumed after 25% pitting penetration of the transfer line wall. Predicted failure times are dependent on the thickness of the transfer lines. A more detailed discussion of ancillary equipment corrosion failure is provided in Section 4.2.2.2.6.

4.2.1 Source Term Release

A fundamental part of estimating and understanding the release of stabilized contaminants from closed HTF waste tanks is a conceptual model of contaminant leaching from residual waste. This section presents a conceptual model followed by an achievable method of implementing the ICM in the framework of a flow and transport model. [WSRC-STI-2007-00544] In the most general sense, the model assumes that the residual waste remains as a discrete layer at the bottom of the waste tanks after they are filled with grout. This discrete layer is referred to as the CZ. Infiltration from the surface that passes through the waste tanks provides the pore fluids necessary to leach contaminants from the CZ.

Previous models of waste tank closure performance have used a constant leach rate for stabilized contaminant release from the CZ. [DOE-EIS-0303] This is unrealistic because conditions within the waste tanks will evolve over the period of time and leaching of radionuclides from the CZ depends on the chemical composition of pore fluid passing through the CZ. Adsorption and solubility of all of the radionuclides of concern vary with the pH, and most vary with redox potential as well. Other parameters, such as carbonate concentration, can also affect the leaching of some of the radionuclides. As the grout filled waste tanks age, chemical composition of the pore fluid passing through the waste tanks will change resulting in changes to the solubility and adsorption controls on stabilized contaminant release.

Most HTF waste tanks do not encounter the water table (non-submerged waste tanks). For these waste tanks, this is captured in the conceptual model of radionuclide leaching from the CZ by dividing waste tank evolution into four potential conditions shown schematically in Figure 4.2-1.

Figure 4.2-1: Potential Physical Conditions of Closed Waste Tanks in Conceptual Model

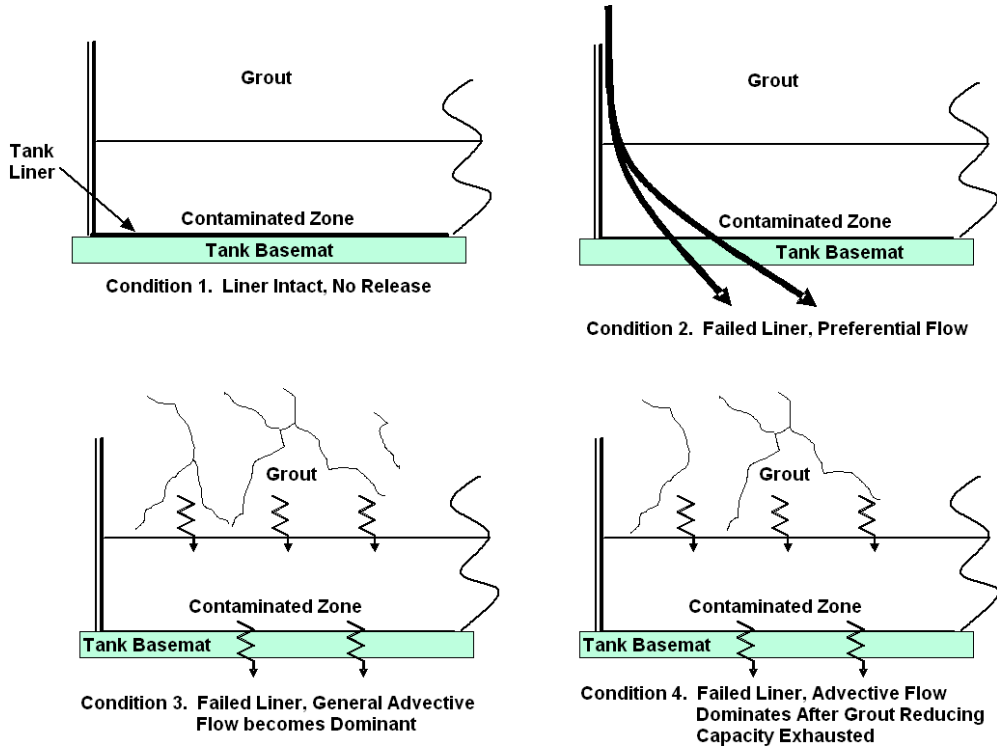

[WSRC-STI-2007-00544]

Condition 1: Commences immediately following pouring of grout. The steel primary liner is assumed intact. It is assumed that pore fluids in the CZ that remain after washing are forced upward into the grout. No stabilized contaminants are released from the waste tank.

Condition 2: Commences when steel primary liner is breached, and infiltration flow is predominantly along preferential flow paths. The assumption is that initially the waste tank grout will be too impermeable to allow significant advective flow, so flow along preferential paths will dominate. These paths could be at the interface of the grout and the steel primary liner or the grout and waste tank infrastructure such as piping. It is assumed that the reducing capacity of the grout along these preferential flow paths is rapidly depleted, thus, conditions of fluid reaching the CZ are relatively oxidizing.

Condition 3: Commences when general advective flow becomes dominant over flow along preferential pathways. For this conceptual model, general advective flow is defined as flow through a porous medium or along a fracture network extensive enough to be considered homogeneous on the scale of the waste tanks. If this is the case when the steel primary liner is breached, then Condition 2 does not occur, and the waste tank evolution proceeds to Condition 3. It is assumed that general advective flow through the grout will produce reducing conditions in the pore water passing through the CZ.

Condition 4: Commences when reducing capacity of the waste tank grout is exhausted. In this condition, general advective flow dominates and pore water passing through the CZ is relatively oxidizing.

These four conditions only reflect changes in redox potential of the pore fluids. The pH of the pore fluids will also evolve as the waste tanks age. *Sorption Databases for the Cementitious Near-Field of a L/ILW Repository for Performance Assessment* described evolution of pore fluid pH in cementitious waste forms in three regions, of which the latter two are pertinent to this conceptual model. [ISSN 1019-0643] It is assumed in ISSN 1019-0643 that cement in Region II had pore fluids in equilibrium with portlandite ($Ca(OH)_2$) and a pH above 12. However, the grout to be used in waste tank closure will not have free portlandite at full hydration. Rather, the CSH gel will control the pH at approximately 11.1. Eventually, the cement will become fully carbonated and evolve to Region III in which pore fluids are in equilibrium with calcite ($CaCO_3$) and have a pH near 8.

The conceptual model that emerges from this multi-condition approach results in a non-uniform leaching rate that is dependent on the chemical state of pore fluid contacting the stabilized contaminant at any given time. To allow maximum flexibility, the waste release model addresses four chemical states, shown in Table 4.2-2, and the corresponding waste tank conditions that are represented by these four states. The chemical states do not apply to Condition 1 (Figure 4.2-1) because the waste tank primary liner is intact and there is no fluid flow through the CZ.

Table 4.2-2: Chemical States and Condition of the Waste Tanks

Chemical State	Tank Condition
Oxidizing Region II	2 and 4 (CSH dominant)
Oxidizing Region III	2 and 4 ($CaCO_3$ dominant)
Reducing Region II	3 (CSH dominant)
Reducing Region III	3 ($CaCO_3$ dominant)

[WSRC-STI-2007-00544]

In the waste release model, there are three phase types considered, 1) an aqueous pore fluid phase, 2) a matrix phase composed primarily of non-radionuclide elements, and 3) discrete radionuclide phases embedded in the matrix. Each radionuclide is partitioned between the aqueous pore fluid, the surfaces of matrix phases in an adsorbed state, and discrete radionuclide phases. As long as the concentration of a radionuclide dissolved in the aqueous phase equals the solubility limit, release of that radionuclide is solubility controlled. Thus, as long as there are discrete particles of a radionuclide present, the rate of that radionuclide release is controlled by the flux of water through the CZ and the solubility of the discrete phase. If enough water passes through the CZ, the discrete phases of a particular radionuclide will be completely removed by dissolution and control of stabilized contaminant release will be by desorption from the surface of the matrix phases. Hence, adsorption controls only dominate the stabilized contaminant release when the mass of contaminant is insufficient to exceed the adsorption capacity of the non-radionuclide matrix phases. This can occur at any point during stabilized contaminant release, depending upon the inventory of a radionuclide and the adsorption capacity of the matrix. From there forward adsorption dominates stabilized contaminant release. Figure 4.2-2 shows this aspect of the waste release conceptual model.

Figure 4.2-2: States of Stabilized Contaminant Release

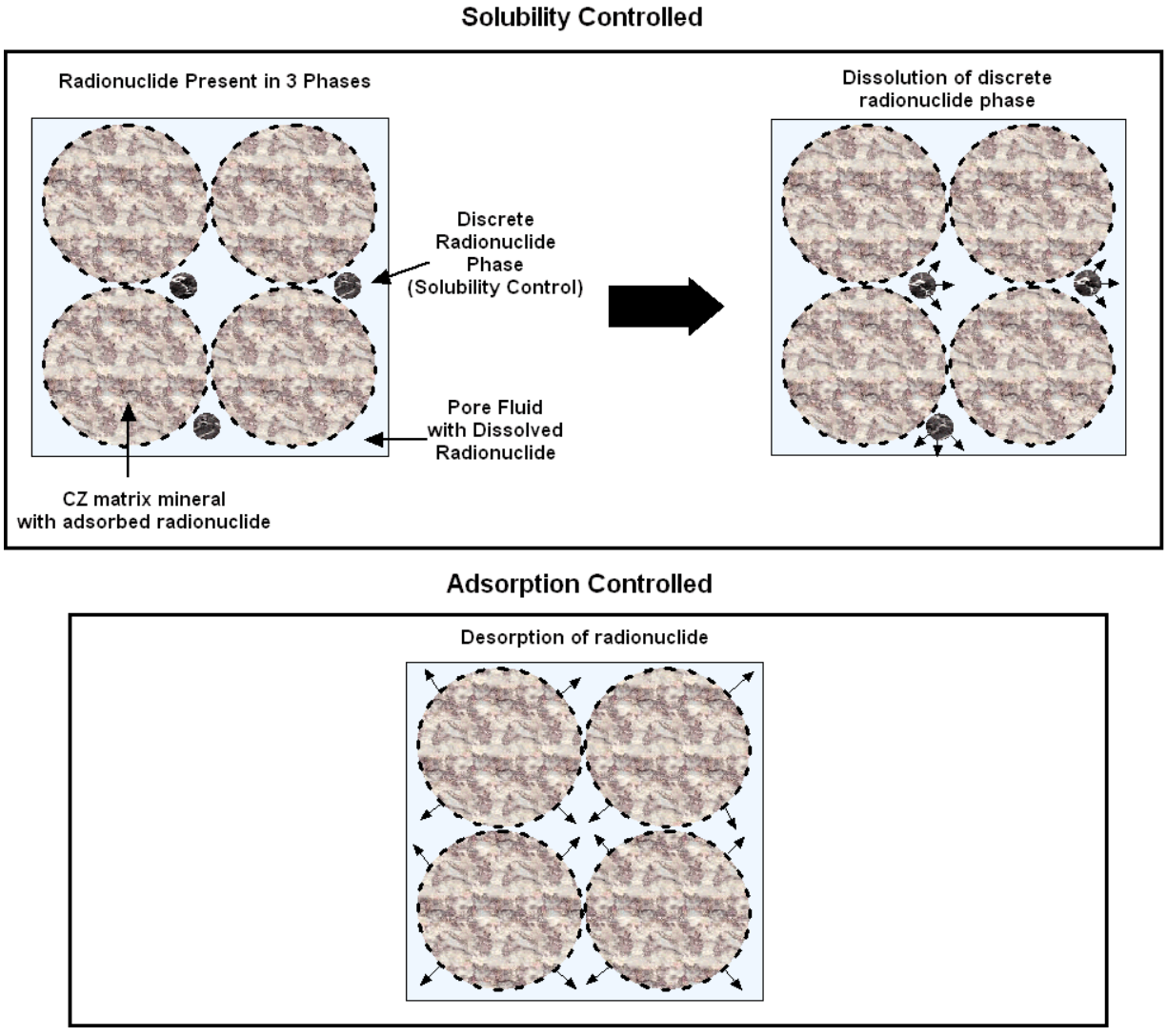

Note Solubility controlled until inventory is less than adsorption capacity of matrix. [WSRC-STI-2007-00544]

4.2.1.1 Submerged Waste Tanks

There are eight waste tanks in H Area in which the CZ is currently below or nearly below the water table. Groundwater could influence the solubility of radionuclides in these waste tanks when the primary liner fails. For this to occur, lateral flow of groundwater through the waste tank would have to predominate over vertical flow of infiltrate. In this case, the changes in grout pore fluid chemistry do not greatly influence the solubility of radionuclides in the CZ, because there is little vertical flow from the grout into the CZ. To evaluate the potential influence of groundwater on radionuclide solubility, four different chemical conditions were established showing varying degrees of groundwater influence. The basis for these is shown in Figure 4.2-3. The groundwater composition used is from a background water table well, designated P27D, located approximately 450 meters east of Tank 43.

Condition A: Groundwater flows laterally into the CZ with no effect on the outer concrete

Condition B: Groundwater attains equilibrium with outer concrete before passing through the CZ

Condition C: Groundwater flows laterally into the CZ and mixes with a minimal portion (fluid fraction = 0.1) of Reducing Region II grout pore fluid with no effect on the outer concrete

Condition D: Groundwater flows laterally into the CZ with no effect on the outer concrete and mixes with a minimal portion (fluid fraction = 0.1) of Oxidizing Region II grout pore fluid

[WSRC-STI-2007-00544]

Figure 4.2-3: Basis for Conditions Controlling Pore Fluid Chemistry in CZ of Submerged Waste Tanks

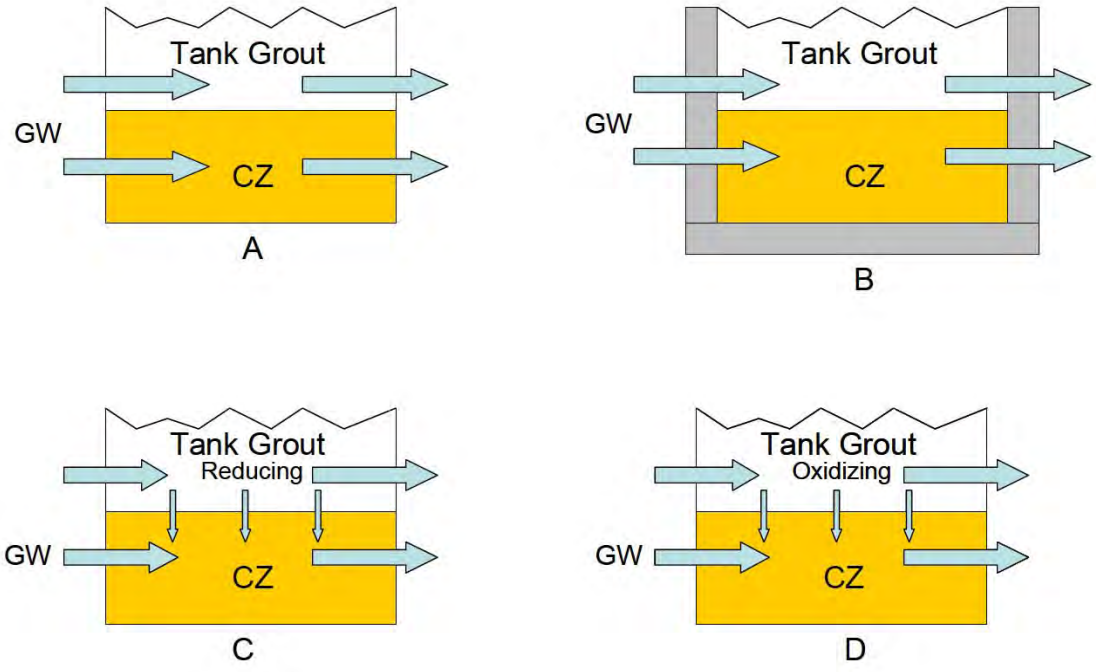

[WSRC-STI-2007-00544]

For Conditions C and D, a grout pore fluid fraction of 0.1 was chosen because it is the approximate fraction at which the final CZ pore fluid is most different from either end-member in the mixture of groundwater and grout pore fluid. This is illustrated by mixing curves of the two end-members calculated using GWB (Figure 4.2-4). The extreme composition of the waste tank grout, pore fluids dominates the mixtures until the groundwater fluid fraction is approximately 0.9, at which point, groundwater begins to dominate. [WSRC-STI-2007-00544]

Figure 4.2-4: Mixing Curves of Groundwater and Waste Tank Grout Pore Fluid

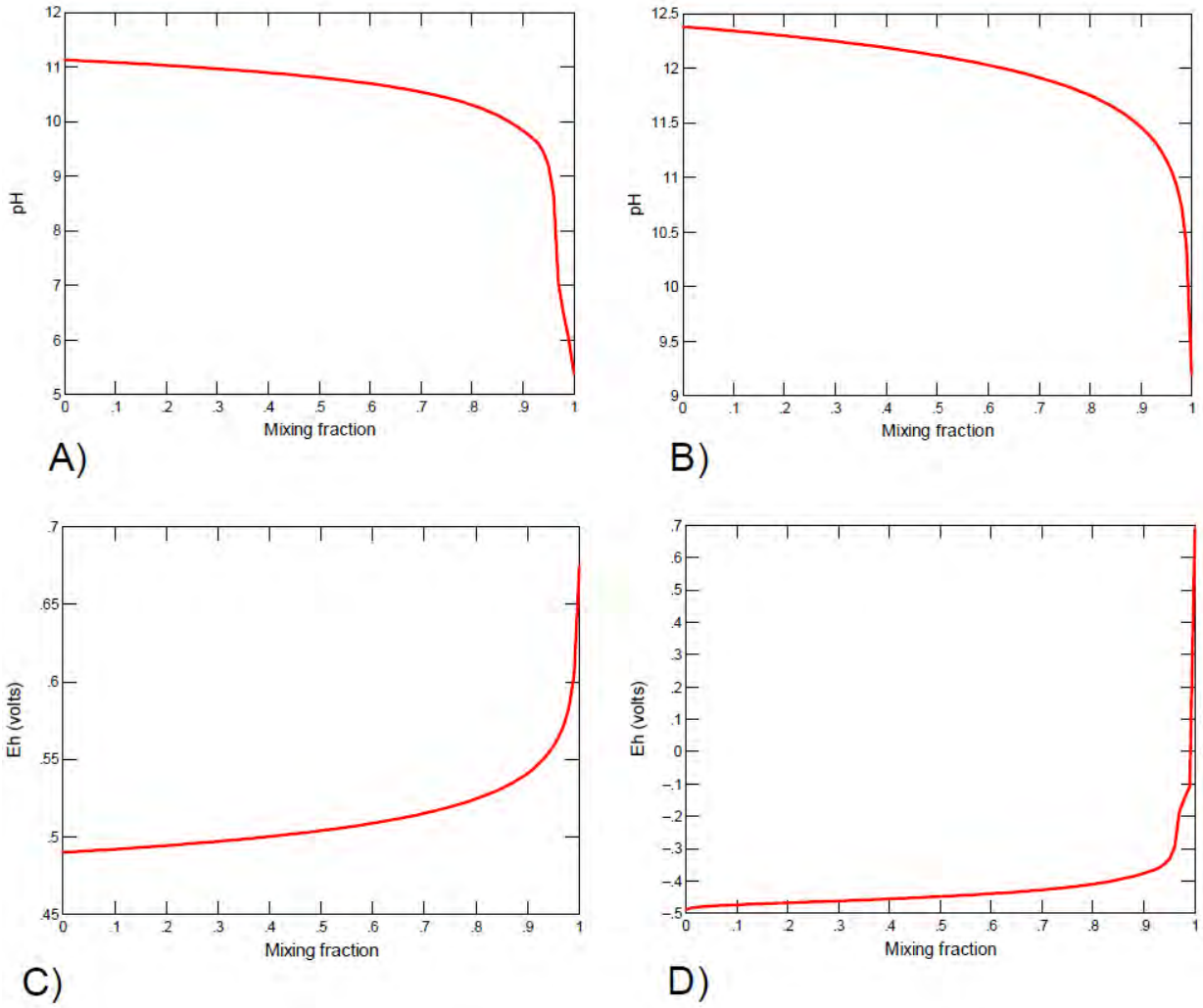

A) pH of groundwater + Reduced Region II
B) pH of groundwater + Oxidized Region II
C) E_h of groundwater + Reducing Region II
D) E_h of groundwater + Oxidizing Region II
[WSRC-STI-2007-00544]

The chemical compositions of the four conditions with groundwater influence are shown in Table 4.2-3. These are treated here as independent cases rather than as conditions linked by the progression of grout degradation. Conditions C and D could be linked, as Reduced Region II pore water would evolve into Oxidized Region II pore water.

Table 4.2-3: Calculated Pore Water Compositions for Conditions in the CZ of Submerged Waste Tanks

	Pore Water Conditions			
Parameter	**A**	**B**	**C**	**D**
pH	5.4	9.30	9.83	9.84
E_h (V)	0.369	0.266	-0.380	0.620
Ca (mol/L)	6.2E-05	2.0E-04	2.1E-04	2.1E-04
Na	4.4E-05	4.3E-05	4.0E-05	4.1E-05
Cl	8.5E-05	1.5E-04	2.7E-04	2.6E-04
HCO_3^-	9.8E-05	2.4E-04	4.2E-05	4.2E-05
SO_4^{-2}	6.3E-06	6.2E-06	5.4E-06	6.5E-06

Condition A: Pore Water = Groundwater
Condition B: Pore Water = Groundwater equilibrated with calcite
Condition C: Pore Water = Mixture 0.9 Groundwater + 0.1 Reduced Region II Pore Water
Condition D: Pore Water = Mixture 0.9 Groundwater + 0.1 Oxidized Region II Pore Water
[WSRC-STI-2007-00544]

4.2.1.2 Implementation of Waste Release Model

The first step in the calculation of radionuclide solubility is to estimate the chemical conditions associated with each chemical state listed in Table 4.2-2. This is done under the assumption of thermodynamic equilibrium using the geochemical modeling program, GWB. The thermodynamic database used for solubility calculations in Table 4.2-4 was "thermo.com.V8.R6+" provided by GWB as an alternative an earlier thermodynamic database utilized by Lawrence Livermore National Laboratory. As noted in Table 7 of WSRC-STI-2007-00544, additional thermodynamic data for becquerelite was obtained and added to the database. [WSRC-STI-2007-00544]

Table 4.2-4 shows composition of pore water estimated for each of the chemical states listed in Table 4.2-2. Establishing the pore water composition of the four states allows solubility for each radionuclide to be calculated by attaining equilibrium of a selected radionuclide phase with the pore water for each state. A total sulfur concentration of 1.0E-05 moles (equivalent to 1.0 mg/L SO_4^{-2}) is added to the pore fluids to be equilibrated with various solubility controlling radionuclide phases. This is a reasonable concentration based on the fact that at pH equals 12 equilibrium of common cement phases ettringite ($Ca_6Al_2O_6(SO_4)_3 \cdot 32H_2O$) with C4AH13 ($Ca_4Al_2O_7 \cdot 13H_2O$) produces a sulfate concentration of 3 mg/L.

Table 4.2-4: Chemical Grout State Estimates for Pore Water Composition

Chemical State	**pH**	**E_h(v)**	**Ca^{+2}(mol/dm^3)**	**CO_3^{-2}(mol/dm^3)**
Oxidizing Region II	11.13	0.58	3.20E-03	3.50E-08
Oxidizing Region III	8.23	0.73	4.60E-04	1.70E-06
Reducing Region II	11.12	-0.48	3.33E-03	3.45E-08
Reducing Region III	8.23	-0.34	4.60E-04	2.40E-03

[WSRC-STI-2007-00544]

4.2.1.2.1 Selecting Solubility Controlling Phases

A fundamental part of establishing solubility-controlled stabilized contaminant release rates is selection of a solubility-controlling phase for each radionuclide. For some of the radionuclides of interest there are studies that can guide selection, for others there are no studies. For this reason, selection of solubility controlling phases is generally very conservative, meaning that where multiple phases of a radionuclide are possible, that with the highest solubility is selected.

Two factors determine the solubility of a phase, the composition, and the structure. For phases with the same composition, amorphous forms usually have higher solubility than crystalline forms. Thus, where thermodynamic data existed, the amorphous forms are selected for solubility controls. For most, hydroxides were chosen over oxides because the hydroxide of an element usually has a higher solubility than the oxide. For many radionuclides, carbonate phases are selected. This was particularly true for the Region III chemical states because of the higher partial pressures of carbon dioxide. [ISSN 1019-0643] Carbonate phases normally precipitate easily from solution and their occurrence in the grouted waste tanks is considered plausible.

Two special cases of mineral selection are becquerelite for uranium and Tc_2S_7 for technetium. These phases are selected because they have been identified elsewhere in samples subject in conditions similar to those expected for the closed waste tanks. Becquerelite is stable in cementitious conditions and has been identified in experiments in these conditions. Likewise, Tc_2S_7 was identified in experiments at conditions near those expected for closed H-Area waste tanks. [WSRC-STI-2007-00544]

The professional judgment used in selecting solubility controlling phases followed the general flow of Figure 4.2-5. For each radionuclide, the process began with an examination of the literature for occurrence of a stable phase with reliable thermodynamic data at conditions prevalent in the waste tanks or cementitious systems. If a stable phase was found, it was selected. Examples of stable phases are becquerelite for uranium and Tc_2S_7 for technetium in reduced grout. If none were found, a list of other phases that contain components found in the waste tanks and having reliable thermodynamic data was assembled. If there were appropriate geologic or industrial process analogues cited in the literature, they were selected. Examples of analogues are radium sulfate and strontium carbonate. If there were no analogues cited in the literature, but the hydroxide was stable, it was retained. If reliable thermodynamic data was available for the amorphous hydroxide then it was selected. If not, the crystalline hydroxide was selected. If hydroxide was not stable, an appropriate non-hydroxide with the highest solubility was selected (i.e., $mOHCO_3$). The process attempted to balance scientific knowledge with the need to be cautious and biased toward higher solubility.

Figure 4.2-5: General Flow in the Use of Professional Judgment to Select Solubility Controlling Phases

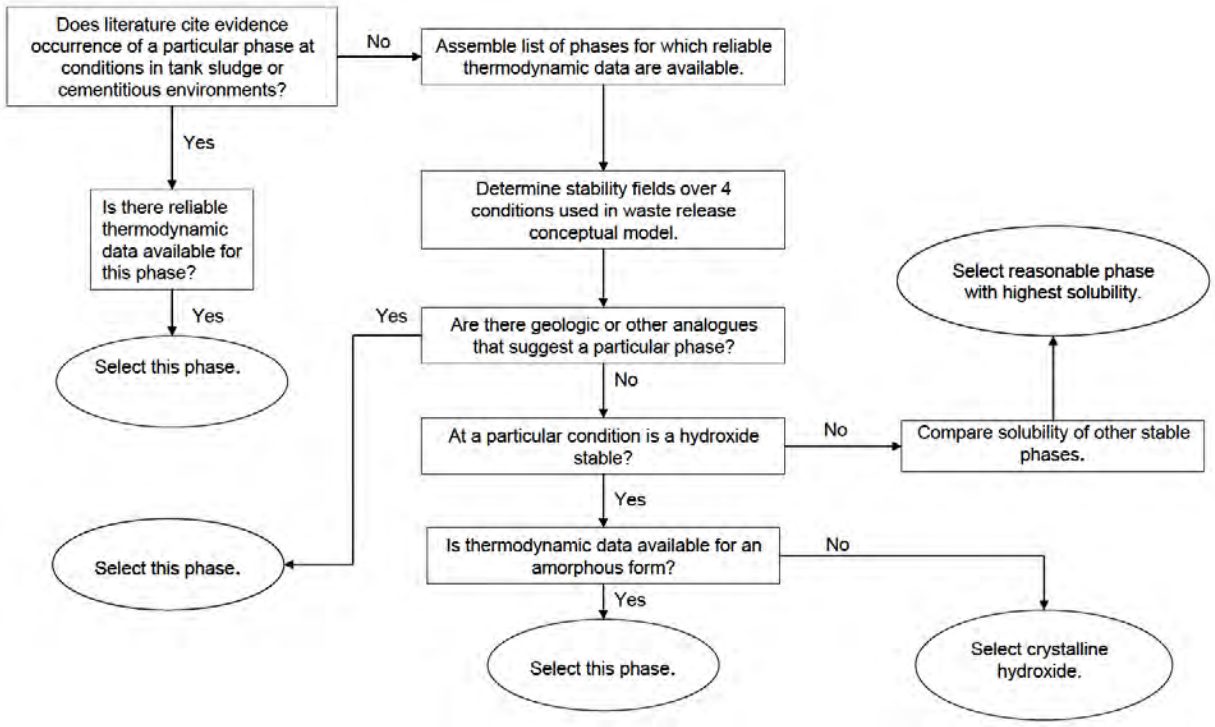

[WSRC-STI-2007-00544]

4.2.1.2.2 Solubility Values

Table 4.2-5 shows solubility values and controlling phases for all of the elements of interest at each of the chemical states of interest. For neptunium, plutonium, technetium, and uranium, the Region II solubility values listed correspond to iron co-precipitation (discussed in detail later in this section) as the controlling mechanism. The solubility of four elements was not calculated (Bk-249, Cf-249, Rh-106, and Te-125m) because of insufficient thermodynamic data. However, each of these has either a very small inventory or a short half-life and is unlikely to be an issue at exposure points. Several of the elements have no identified solubility controls and their release is modeled as instantaneous (within the first pore volume). Technetium and selenium concentrations in a Tank 18 dip sample were much lower than expected for identifiable solubility controls. This suggests that there may be phases present that are not well known or that may co-precipitate with another phase.

4.2.1.3 Solubility for Partially Submerged HTF Waste Tanks

The solubility of discrete phases of radionuclides, partially in submerged waste tanks in H Area, were calculated using pore fluid composition for the four conditions shown in Table 4.2-5. These are shown with the assumed solubility controlling phases in Table 4.2-6.

Table 4.2-5: Calculated Solubility and Controlling Phases of Radionuclides of Interest

	Oxidized Region II		Oxidized Region III		Reduced Region II		Reduced Region III	
	Controlling Phase	**Solubility (mol/L)**	**Controlling Phase**	**Solubility (mol/L)**	**Controlling Phase**	**Solubility (mol/L)**	**Controlling Phase**	**Solubility (mol/L)**
Ac	La(OH)3	4.00E-05	La2(CO3)3: 8H2O	1.60E-08	La(OH)3	4.00E-05	La2(CO3)3:8 H2O	1.40E-08
Am	Am(OH)3 (am)	8.60E-09	AmOHCO3	4.90E-08	Am(OH)3	8.80E-09	AmOHCO3	7.70E-08
Ba	Witherite(BaCO3)	6.40E-07	Witherite(Ba CO3)	8.70E-09	Witherite(BaCO3)	6.50E-07	Witherite (BaCO3)	5.60E-09
Bk	Short half-life	Modeled as instantaneous release	Short half-life	Modeled as instantaneous release	Short half-life	Modeled as instantaneous release	Short half-life	Modeled as instantaneous release
C	Calcite	9.60E-06	Calcite	5.80E-04	Calcite	9.60E-06	No solubility control	Modeled as instantaneous release
Ce	Ce(OH)3	1.20E-05	Ce(OH)3	3.40E-04	Ce(OH)3	1.10E-05	Ce(OH)3	4.50E-05
Cf	Tiny inventory	Modeled as instantaneous release	Small inventory	Modeled as instantaneous release	Small inventory	Modeled as instantaneous release	Small inventory	Modeled as instantaneous release
Cm	Cm(OH)3	5.10E-10	CmOHCO3	4.20E-07	Cm(OH)3	5.20E-10	CmOHCO3	5.10E-08
Co	CoFe2O4	5.00E-10	CoFe2O4	5.90E-13	CoFe2O4	4.80E-10	CoFe2O4	5.40E-13
Cs	No solubility control	Modeled as instantaneous release	No solubility control	Modeled as instantaneous release	No solubility control	Modeled as instantaneous release	No solubility control	Modeled as instantaneous release
Eu	Eu(OH)3	1.20E-08	EuOHCO3	1.20E-06	Eu(OH)3	1.20E-08	EuOHCO3	1.20E-06
I	No solubility control	Modeled as instantaneous release	No solubility control	Modeled as instantaneous release	No solubility control	Modeled as instantaneous release	No solubility control	Modeled as instantaneous release

Table 4.2-5: Calculated Solubility and Controlling Phases of Radionuclides of Interest (Continued)

	Oxidized Region II		Oxidized Region III		Reduced Region II		Reduced Region III	
	Controlling Phase	**Solubility (mol/L)**	**Controlling Phase**	**Solubility (mol/L)**	**Controlling Phase**	**Solubility (mol/L)**	**Controlling Phase**	**Solubility (mol/L)**
Nb	No solubility control	Modeled as instantaneous release	No solubility control	Modeled as instantaneous release	No solubility control	Modeled as instantaneous release	No solubility control	Modeled as instantaneous release
Ni	NiFe2O4	1.20E-10	NiFe2O4	1.20E-07	Heazlewoodite (Ni3S2)	4.30E-11	Polydimite (Ni3S4)	1.20E-10
Np	Fe co-precipitation	2.00E-15	Fe co-precipitation	5.00E-17	Fe co-precipitation	2.00E-14	Np(OH)4	1.60E-09
Pa	No solubility control	Modeled as instantaneous release	No solubility control	Modeled as instantaneous release	No solubility control	Modeled as instantaneous release	No solubility control	Modeled as instantaneous release
Pm	Pm(OH)3(am)	1.30E-08	Pm2(CO3)3	1.80E-07	Pm(OH)3(am)	1.30E-08	Pm2(CO3)3	1.80E-07
Pr	Pr(OH)3	7.90E-06	Pr(OH)3	9.70E-08	Pr(OH)3	7.80E-06	Pr2(CO3)3	9.50E-08
Pu	Fe co-precipitation	9.00E-15	Fe co-precipitation	2.00E-16	Fe co-precipitation	7.00E-14	Pu(OH)4	2.90E-09
Ra	RaSO4	9.10E-06	RaSO4	3.80E-06	RaSO4	6.00E-06	RaSO4	4.60E-04
Rh	Short half-life	Modeled as instantaneous release	Short half-life	Modeled as instantaneous release	Short half-life	Modeled as instantaneous release	Short half-life	Modeled as instantaneous release
Ru	RuO2.2H2O(am)	1.50E-03	RuO2.2H2O (am)	7.60E-07	RuS2	3.30E-50	RuS2	9.00E-11
Sb	Sb(OH)3	9.50E-08	Sb(OH)3	8.00E-08	Sb(OH)3	9.40E-08	Sb(OH)3	8.00E-08
Se	No solubility control	Modeled as instantaneous release	No solubility control	Modeled as instantaneous release	Ferroselite (FeSe2)	8.70E-06	Ferroselite (FeSe2)	2.40E-02

Table 4.2-5: Calculated Solubility and Controlling Phases of Radionuclides of Interest (Continued)

	Oxidized Region II		Oxidized Region III		Reduced Region II		Reduced Region III	
	Controlling Phase	**Solubility (mol/L)**	**Controlling Phase**	**Solubility (mol/L)**	**Controlling Phase**	**Solubility (mol/L)**	**Controlling Phase**	**Solubility (mol/L)**
Sm	Sm(OH)3(am)	5.60E-06	Sm(OH)3(am)	4.40E-06	Sm(OH)3(am)	5.50E-06	Sm(OH)3 (am)	2.60E-04
Sn	Cassiterite (SnO2)	2.70E-08	Cassiterite (SnO2)	2.70E-08	Cassiterite (SnO2)	2.70E-08	Cassiterite (SnO2)	2.70E-08
Sr	Strontianite (SrCO3)	2.20E-05	Strontianite (SrCO3)	4.10E-06	Strontianite (SrCO3)	2.30E-05	Strontianite (SrCO3)	2.70E-06
Tc	Fe co-precipitation	7.00E-14	Fe co-precipitation	2.00E-15	Fe co-precipitation	6.00E-13	Tc2S7	2.80E-38
Te	Short half-life	Modeled as instantaneous release	Short half-life	Modeled as instantaneous release	Short half-life	Modeled as instantaneous release	Short half-life	Modeled as instantaneous release
Th	Th(OH)4	4.20E-07	Th(OH)4	4.20E-07	Th(OH)4	4.20E-07	Th(OH)4	4.20E-07
U	Fe co-precipitation	9.00E-13	Fe co-precipitation	2.00E-14	Fe co-precipitation	7.00E-12	UO2(am)	3.50E-05
Y	Y(OH)3	1.90E-08	Y(OH)3	5.10E-05	Y(OH)3	1.80E-08	Y(OH)3	1.80E-04

[WSRC-STI-2007-00544]

Note The elements aluminum, hydrogen, and sodium are not controlled by solubility, and thus are not included in the table, rather they are assumed to release instantaneously.

Table 4.2-6: Calculated Solubility and Controlling Phases in Submerged Waste Tanks

	Submerged Condition A		Submerged Condition B		Submerged Condition C		Submerged Condition D	
	Controlling Phase	**Solubility (mol/L)**	**Controlling Phase**	**Solubility (mol/L)**	**Controlling Phase**	**Solubility (mol/L)**	**Controlling Phase**	**Solubility (mol/L)**
Ac	La2(CO3)3·8H2O	3.10E-05	La2(CO3)3· 8H2O	1.40E-08	La2(CO3)3· 8H2O	2.20E-08	La2(CO3)3·8 H2O	2.30E-08
Am	AmOHCO3	1.10E-04	Am(OH)3(am)	6.00E-08	Am(OH)3(am)	1.30E-07	Am(OH)3(a m)	1.20E-07
Ba	Witherite(BaCO3)	2.00E-05	Witherite (BaCO3)	3.90E-04	Witherite(BaCO3)	6.20E-09	Witherite (BaCO3)	6.10E-09
Bk	Short half-life	Modeled as instantaneous release	Short half-life	Modeled as instantaneous release	Short half-life	Modeled as instantaneous release	Short half-life	Modeled as instantaneous release
C	No solubility control	Modeled as instantaneous release	No solubility control	Modeled as instantaneous release	Calcite (CaCO3)	5.20E-04	Calcite (CaCO3)	2.10E-04
Ce	Ce2(CO3)3 8H2O	3.80E-05	Ce2(CO3)3 8H2O	6.40E-08	Ce2(CO3)3 8H2O	5.10E-07	Ce2(CO3)3 8H2O	5.90E-07
Cf	Tiny inventory	Modeled as instantaneous release	Small inventory	Modeled as instantaneous release	Small inventory	Modeled as instantaneous release	Small inventory	Modeled as instantaneous release
Cm	Cm(OH)3	7.40E-04	CmOHCO3	6.30E-09	Cm(OH)3	1.10E-08	Cm(OH)3	1.00E-08
Co	CoFe2O4	9.90E-11	CoFe2O4	6.80E-12	CoFe2O4	2.30E-11	CoFe2O4	2.40E-11
Cs	No solubility control	Modeled as instantaneous release	No solubility control	Modeled as instantaneous release	No solubility control	Modeled as instantaneous release	No solubility control	Modeled as instantaneous release
Eu	Eu2(CO3)3 8H2O	1.30E-05	Eu(OH)3	1.50E-06	Eu(OH)3	1.20E-07	Eu(OH)3	1.20E-07
I	No solubility control	Modeled as instantaneous release	No solubility control	Modeled as instantaneous release	No solubility control	Modeled as instantaneous release	No solubility control	Modeled as instantaneous release

Table 4.2-6: Calculated Solubility and Controlling Phases in Submerged Waste Tanks (Continued)

	Submerged Condition A		Submerged Condition B		Submerged Condition C		Submerged Condition D	
	Controlling Phase	**Solubility (mol/L)**	**Controlling Phase**	**Solubility (mol/L)**	**Controlling Phase**	**Solubility (mol/L)**	**Controlling Phase**	**Solubility (mol/L)**
Nb	No solubility control	Modeled as instantaneous release	No solubility control	Modeled as instantaneous release	No solubility control	Modeled as instantaneous release	No solubility control	Modeled as instantaneous release
Ni	No solubility control	Modeled as instantaneous release	NiFe2O4	1.40E-09	NiFe2O4	1.70E-10	NiFe2O4	1.60E-10
Np	Fe co-precipitation	2.20E-14	Fe co-precipitation	7.90E-17	Fe co-precipitation	1.80E-14	Fe co-precipitation	1.50E-16
Pa	No solubility control	Modeled as instantaneous release	No solubility control	Modeled as instantaneous release	No solubility control	Modeled as instantaneous release	No solubility control	Modeled as instantaneous release
Pm	Pm2(CO3)3	5.60E-05	Pm2(CO3)3	1.90E-07	Pm(OH)3(am)	2.30E-08	Pm(OH)3(am)	1.30E-08
Pr	Pr2(CO3)3	4.70E-05	Pr2(CO3)3	1.00E-07	Pr2(CO3)3	2.70E-07	Pr2(CO3)3	2.80E-07
Pu	Fe co-precipitation	9.60E-14	Fe co-precipitation	3.50E-16	Fe co-precipitation	8.20E-14	Fe co-precipitation	6.50E-16
Ra	RaSO4	6.70E-06	RaSO4	7.40E-06	RaSO4	7.50E-06	RaSO4	7.20E-06
Rh	Short half-life	Modeled as instantaneous release	Short half-life	Modeled as instantaneous release	Short half-life	Modeled as instantaneous release	Short half-life	Modeled as instantaneous release
Ru	Ru(OH)3 H2O (am)	7.60E-08	RuO2.2H2O (am)	7.10E-07	RuS2	4.60E-48	RuO2.2H2O (am)	1.20E-06
Sb	Sb(OH)3	8.00E-08	Sb(OH)3	8.10E-08	Sb(OH)3	8.10E-08	Sb2O5	7.50E-22
Se	No solubility control	Modeled as instantaneous release	No solubility control	Modeled as instantaneous release	No solubility control	Modeled as instantaneous release	No solubility control	Modeled as instantaneous release
Sm	Sm2(CO3)3	6.00E-05	Sm(OH)3(am)	2.00E-06	Sm(OH)3(am)	3.40E-07	Sm(OH)3(am)	3.40E-07

Table 4.2-6: Calculated Solubility and Controlling Phases in Submerged Waste Tanks (Continued)

	Submerged Condition A		Submerged Condition B		Submerged Condition C		Submerged Condition D	
	Controlling Phase	**Solubility (mol/L)**	**Controlling Phase**	**Solubility (mol/L)**	**Controlling Phase**	**Solubility (mol/L)**	**Controlling Phase**	**Solubility (mol/L)**
Sn	Cassiterite (SnO2)	2.70E-08	Cassiterite (SnO2)	2.70E-08	Cassiterite (SnO2)	2.70E-08	Cassiterite (SnO2)	2.70E-08
Sr	Strontianite (SrCO3)	1.00E-03	Strontianite (SrCO3)	1.40E-06	Strontianite (SrCO3)	3.00E-06	Strontianite (SrCO3)	2.90E-06
Tc	Fe co-precipitation	7.90E-13	Fe co-precipitation	2.90E-15	Fe co-precipitation	6.70E-13	Fe co-precipitation	5.30E-15
Te	Short half-life	Modeled as instantaneous release	Short half-life	Modeled as instantaneous release	Short half-life	Modeled as instantaneous release	Short half-life	Modeled as instantaneous release
Th	Th(OH)4	4.50E-07	Th(OH)4	4.20E-07	Th(OH)4	4.20E-07	Th(OH)4	4.20E-07
U	Fe co-precipitation	9.00E-12	Fe co-precipitation	3.30E-14	Fe co-precipitation	7.60E-12	Fe co-precipitation	6.10E-14
Y	No solubility control	Modeled as instantaneous release	Y(OH)3	3.80E-07	Y(OH)3	8.50E-09	Y(OH)3	8.40E-09

Condition A Pore Water = Groundwater
Condition B Pore Water = Groundwater equilibrated with calcite
Condition C Pore Water = Mixture 0.9 Groundwater + 0.1 Reduced Region II Pore Water
Condition D Pore Water = Mixture 0.9 Groundwater + 0.1 Oxidized Region II Pore Water
[WSRC-STI-2007-00544]

In the implementation of the conceptual model for waste release, it was evident that adsorption controls would play only a minor role as discussed later in this section. It is thought that the importance of adsorption controls is minimal because for most of the radionuclides the mass of matrix minerals in the stabilized contaminant will be too low to adsorb a substantial fraction of the radionuclide inventory (e.g., the inventories of most radionuclides exceed the adsorption capacity of the stabilized contaminant). The fact that the radionuclides currently present in the residual material remain after extensive washing supports the assumption that they occur in a form less labile than adsorbed.

Due to this, in addition to the inability to calculate reliable adsorption parameters for most of the radionuclides of interest, it was decided to model only solubility controls to account for stabilized contaminant release in fate and transport models. Doing so removed the need to make assumptions about the mineralogy of the stabilized contaminant layer, the abundance of minerals, and their surface areas based on limited information.

In an equilibrium model, the assumption that solubility rather than adsorption controls stabilized the contaminant release is conservative, resulting in faster overall release of radionuclides. This assumption is based on the fact that the maximum contaminant that can desorb is controlled by solubility. In effect, if the distribution coefficient is low enough that a concentration is released that exceeds solubility, some of the radionuclide will precipitate bringing the concentration down to solubility. The stabilized contaminant release rate will drop below that dictated by solubility when the radionuclide inventory is depleted to where the concentration released is below solubility. At higher distribution coefficient values, the concentration released at any given time will always be below the concentration dictated by solubility. Thus, the time until complete release of a radionuclide using adsorption controls will always be longer than when only solubility controls are used. This is demonstrated in Figure 4.2-6, where an example of uranium release from the CZ under reducing conditions was examined using a total inventory of 10 moles and a solubility of 3.5E-05 mol/L. Adsorption controls result in an overall slower release of uranium.

Figure 4.2-6: Comparison of Solubility and Adsorption Controls Only on Uranium Release

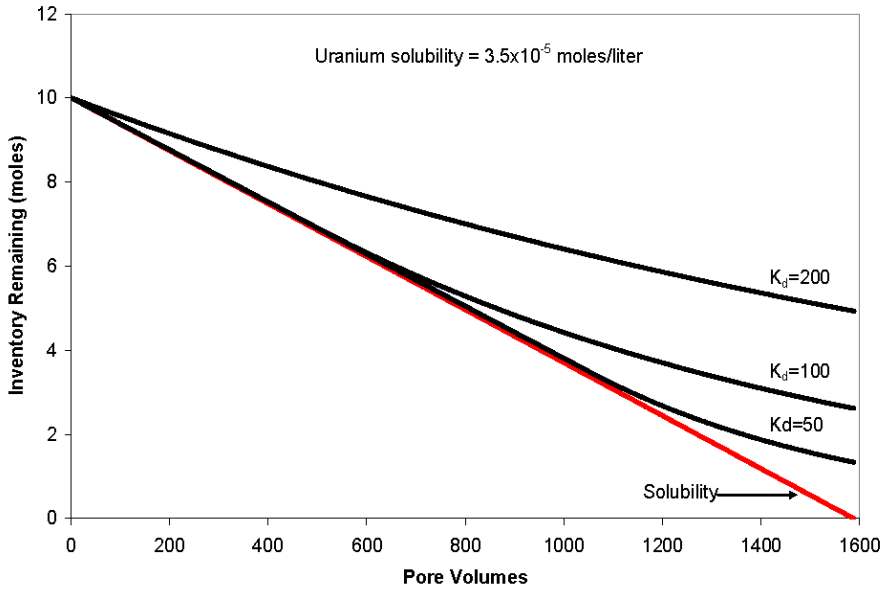

Note Assumes a total inventory of 10 moles and a solubility of 3.5E-05 mol/L.
K_d = mL/g
[WSRC-STI-2007-00544]

4.2.1.4 Solubility Control vs. Adsorption Controls

The conceptual model for stabilized contaminant release from the CZ assumes the stabilized contaminant release is solubility controlled. This is based on inventories of radionuclides and the volume of stabilized contaminants that remain in the waste tanks after cleaning. For isotopes uranium and plutonium, Tc-99, Np-237, and Am-241, the post-wash inventories per single pore volume are much higher than would be soluble in a single pore volume. More importantly, apparent distribution coefficients calculated from the post-wash inventories and amount of matrix are generally too high to conclude that adsorption controls dominate stabilized contaminant release.

The distribution coefficient values were calculated by assuming a waste tank bottom area of 527.2 m^2 and a theoretical CZ thickness of 1.6E-03 meters, to give a total post-wash waste volume of 0.84 m^3. The effective porosity of the CZ was assumed the same as the grout, 21.1%, giving a pore volume of 0.18m^3 and a matrix mineral volume of 0.66 m^3. The density of the matrix minerals was assumed that of hematite, 5.3 g/cm^3. Thus, the estimated mass of the CZ was assumed 3.5E+06 grams. [WSRC-STI-2007-00544]

The distribution coefficient is defined as:

$$K_d = \frac{C_{solid}}{C_{aqueous}}$$

where:

C_{solid} is the concentration of the radionuclide in the solid phase, $C_{aqueous}$ is the concentration in the aqueous phase, and Mcz is the mass of the CZ. The inventory in the solid phase is the total inventory (I_T) minus the inventory in the aqueous phase. For these calculations, the inventory in the aqueous phase is defined as the calculated solubility (S) in mol/L of the radionuclide multiplied by the total fluid pore volumes (V_p) in the CZ of a waste tank. Thus, the distribution coefficient in milliliters per gram (mL/g) is defined by:

$$C_{solid}\left(\frac{moles}{g}\right) = \frac{I_T - 1000V_P S}{M_{CZ}}$$

$$C_{aqueous}\left(\frac{moles}{ml}\right) = 0.001S$$

$$K_d\left(\frac{ml}{g}\right) = \frac{I_T - 180S}{3500S}$$

where:

Total radionuclide inventory in moles is the total inventory in the CZ and solubility is the calculated solubility in moles per liter. Table 4.2-7 shows the minimum, maximum, and median values of distribution coefficient calculated for all HTF waste tanks for total uranium, plutonium, Tc-99, Np-237, and Am-241. The solubility under Reducing Region II conditions is used because it is assumed that these would be the equilibrium conditions when the waste tank primary liner is breached and allowing initial leaching of stabilized contaminants to the environment. Low distribution coefficient values occur in a few waste tanks, particularly for Np-237, because the inventory in these waste tanks is low. It is important to note that if adsorption controls are used to estimate stabilized contaminant release rates and the median distribution coefficient values are used, the release rates would be slower than those estimated from solubility controls. This is true even if super saturation of the pore fluids is allowed. These same values have been applied to the HTF conceptual model.

Table 4.2-7: Calculated K_d Values if Adsorption Controlled Stabilized Release

Radionuclide/Element	Min K_d (mL/g)	Max K_d (mL/g)	Median K_d (mL/g)
Am-241	4.5E+14	7.0E+18	1.3E+16
Np-237	3.2E+00	1.2E+05	2.8E+03
Plutonium	6.1E+03	1.8E+06	2.6E+04
Tc-99	1.9E+42	2.4E+45	1.2E+44
Uranium	8.6E+01	2.4E+04	2.8E+02

[WSRC-STI-2007-00544]

4.2.1.5 Uncertainty in Solubility Calculations

There are uncertainties in the calculation of the solubility. Much of the uncertainty is because of unknowns related to the evolution of the CZ over time due to conditions experience. Some is the result of the limited amount of thermodynamic data available for many of the radionuclides of interest. The uncertainty can be reduced by laboratory studies,

but significant uncertainty will always remain. For example, with very careful and detailed analyses, the actual form the dominant radionuclides take in the CZ might be determined. Nevertheless, considerable uncertainty would remain because conditions evolve from the initial waste tank grouting to that of several thousand years in the future, thus the radionuclide forms are likely to change as well. The best way to manage this uncertainty during implementation of the ICM is to make conservative assumptions as is reasonable. The uncertainty on solubility control has been incorporated into Section 5.6. The potential variability in solubility limits and chemical transition times discussed in Section 5.6 are two of the parameters specifically evaluated in the probabilistic HTF GoldSim Model (Section 5.6.3.3 and 5.6.3.8).

4.2.1.5.1 Choice of Controlling Phase

The choice of the solubility-controlling phase has the largest uncertainty when calculating solubility for many radionuclides. The choice of controlling phase in this analysis is biased toward higher solubility phases by not considering many phases with low solubility. For example, where there is thermodynamic data available for both amorphous and crystalline phases of the same stoichiometry, the amorphous phase is chosen because amorphous phases generally have higher solubility than that of their crystalline counterparts. Thus, this solubility reported may be biased high by many orders of magnitude for many elements (e.g., uranium). Table 4.2-8 compares uranium solubility calculated for Oxidized Region II and Reduced Region II with solubility calculated for other potential solubility controlling phases. The choice of becquerelite for Oxidized Region II yields a calculated controlling solubility seven orders of magnitude higher than if $CaUO_4$ was chosen. A choice of the amorphous form of UO_2 in Reduced Region II rather than the crystalline form (uraninite) yields a solubility five orders of magnitude higher. The issue is further complicated by ample evidence that suggests uranium concentrations may also be limited by silicate and phosphate phases that were not considered in this analysis. [ISSN 1019-0643]

Table 4.2-8: Comparison of Calculated Solubility of Various Uranium Phases

Phase Chosen for Oxidizing Region II	**Solubility (mol/L)**
Becquerelite	3.4E-07
Other Potential Solubility Controlling Phases for Oxidizing Region II	
$CaUO_4$	1.8E-14
Schoepite	1.8E-05
Phase Chosen for Reducing Region II	
UO_2 (amorphous)	3.5E-05
Other Potential Solubility Controlling Phases for Reducing Region II	
Uraninite (crystalline UO_2)	3.9E-10
$CaUO_4$	6.9E-06

[WSRC-STI-2007-00544]

The main reason for choosing high solubility phases over low solubility phases is the precipitation of high solubility phases are often kinetically favored over a low solubility phases. If the low solubility phases were chosen, it would always be the controlling

phases. Selecting the higher solubility phases eliminates consideration of kinetic arguments for why a lower solubility phase would be expected.

Phases other than the amorphous hydroxides are chosen for some elements. Phases with the stoichiometry of XFe_2O_4 are chosen for nickel and cobalt because there is a strong possibility that precipitation of these phases would be catalyzed at the surface of hematite or other ferric iron phases present. Sulfate or carbonate phases are chosen because these are known to precipitate readily as pipe or waste tanks scale, and thus it is assumed that kinetics would not inhibit their precipitation in the waste tanks. The database with the appropriate solid phases for tin is so small that cassiterite (SnO_2) is considered the most likely phase to precipitate of those in which data exists.

One way to manage uncertainty related to choice of solubility controlling phase is to consider the probability of different phases occurring. For example, $Pu(OH)_4$ is selected here as the solubility controlling phase. Yet, the more thermodynamically stable PuO_2 is practical, particularly at the elevated temperatures (approximately 80°C) that will occur from initial grout hydration. [WSRC-TR-97-0102] However, if PuO_2 was the controlling phase, it would have a large effect on stabilized contaminant release because its calculated solubility under Reducing Region II conditions is 1.3E-17 mol/L compared to the $Pu(OH)_4$ solubility of 1.7E-09 mol/L. Tables 4.2-9 and 4.2-10 show a possible distribution of phases for plutonium, uranium, neptunium, and technetium, where the probabilities are weighted to account for the possibility of different phases. The probabilities chosen here are not rigorous or mathematical. They are based on professional judgment that accounts for observations in the literature (e.g., thermodynamic stability, etc).

Table 4.2-9: Probability Distributions for Various Phases Controlling Reduced Region II Solubility

	Controlling Phase [a]	Solubility (mol/L)	Probability
Plutonium	$Pu(OH)_4$	1.7E-09	0.4
	PuO_2	1.3E-17	0.1
	Fe co-precipitation	7.0E-14	0.5
Neptunium	$Np(OH)_4$	4.8E-09	0.4
	NpO_2	2.6E-20	0.1
	Fe co-precipitation	2.0E-14	0.5
Technetium	Tc_2S_7	1.2E-32	0.4
	$TcO_2.2H_2O$	3.3E-08	0.1
	Fe co-precipitation	6.0E-13	0.5
Uranium	UO_2(am)	3.5E-05	0.25
	Uraninite	3.9E-10	0.15
	$CaUO_4$	6.9E-06	0.1
	Fe co-precipitation	7.0E-12	0.5

a Iron co-precipitation assumed to be controlling 50% of the time.
[WSRC-STI-2007-00544]

Table 4.2-10: Probability Distributions for Various Phases Controlling Oxidized Region II Solubility

	Controlling Phase [a]	Solubility (mol/L)	Probability
Plutonium	$Pu(OH)_4$	3.0E-07	0.35
	PuO_2	2.3E-15	0.1
	$PuO_2(OH)_2$	1.9E-11	0.05
	Fe co-precipitation	9.0E-15	0.5
Neptunium	$NpO_2(OH)(am)$	6.8E-07	0.35
	Np_2O_5	9.6E-10	0.1
	NpO_2	1.2E-10	0.05
	Fe co-precipitation	2.0E-15	0.5
Technetium	No solubility control	instantaneous release	0.5
	Fe co-precipitation	7.0E-14	0.5
Uranium	Becquerelite	3.4E-07	0.25
	$CaUO_4$	1.8E-14	0.15
	Schoepite	1.8E-05	0.1
	Fe co-precipitation	9.0E-13	0.5

a Iron co-precipitation assumed to be controlling 50% of the time.
[WSRC-STI-2007-00544]

4.2.1.5.2 Uncertainty in Thermodynamic Data

Uncertainty in thermodynamic data can result in large discrepancies in mineral solubility. For any given solubility calculation, there are numerous thermodynamic quantities involved, each of which has an uncertainty. The uncertainties in each of these compound and can lead to solubility calculations that have a range of uncertainty that spans several orders of magnitude. Typically, the least studied constituents have the highest uncertainty in their thermodynamics, but even well studied constituents can have high thermodynamic uncertainties if their chemistries are complicated. For example, uranium is well studied but has multiple oxidation states, can form aqueous complexes with a variety of anions and cations, and can form dozens of solid phases. Accounting for all of these complexities in experiments, measuring thermodynamic quantities is extremely difficult, often resulting in vastly different values reported for the same quantity. The solubility of the uranium mineral becquerelite is an example. Table 4.2-11 shows values for the log of the equilibrium constants (Log K) measured in four studies for the dissolution reaction:

$$Ca(UO_2)_6O_4(OH)_6{\cdot}8H_2O_{(s)} + 14H^+ = 6UO_2^{+2} + Ca^{+2} + 18H_2O$$

Table 4.2-11: Values of Log K for Reaction from Various Studies

LOG K
41.89
43.6
29
41.4

[WSRC-STI-2007-00544]

The solubility calculated for becquerelite using these values varies by two orders of magnitude for the chemical composition associated with Condition 1 (Figure 4.2-1). The reason the calculated solubility only varies by two orders of magnitude despite the 14.6 orders of magnitude variation in the equilibrium constant is that, at these conditions, other thermodynamic quantities exert greater control on the solubility of becquerelite. With a pH equal to 12.3 and the oxidizing conditions, the primary control on the solubility is the association constant of the dominant aqueous uranium complex, $UO_2(OH)_4^{-2}$.

Figure 4.2-7 shows the results of a simple analysis of the sensitivity of calculated becquerelite solubility to the equilibrium constant of the dissolution reaction and the association constant of the dominant aqueous species of uranium. In Scenario A, the equilibrium constant of the dissolution reaction is varied ± 1 order of magnitude from that used in the original calculation and all other constants are the same as used in the original calculation. In Scenario B, the association constant for the dominant aqueous uranium species, $UO_2(OH)_4^{-2}$, is varied by ±1 order of magnitude while all other constants remain the same as in the original calculation. In Scenario C, the association constant of the dominant species and the equilibrium constant for the dissolution reaction are varied in the same direction ±1 order of magnitude. In Scenario D, the two constants are varied in opposite directions ±1 order of magnitude.

Figure 4.2-7: Effect of Varying Different Thermodynamic Parameters on Solubility of Becquerelite

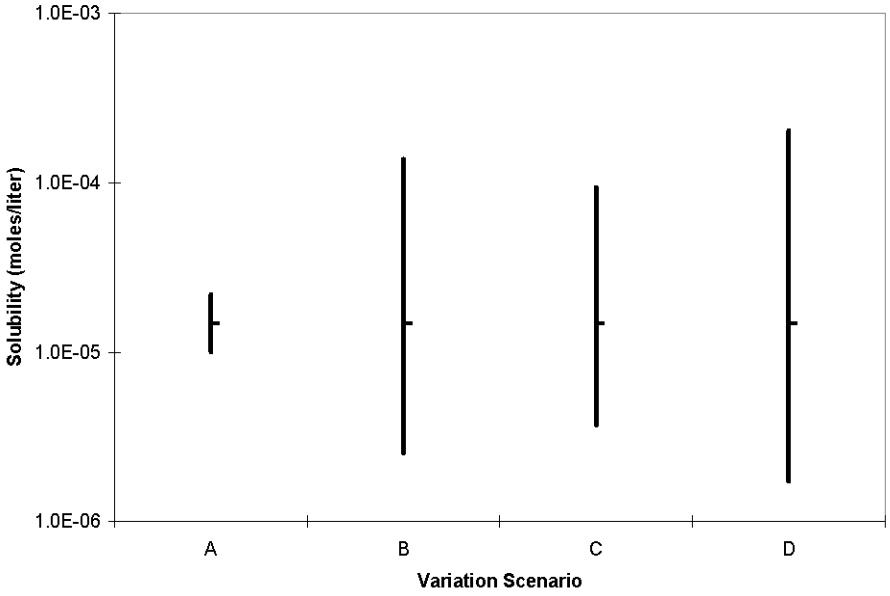

Note Vertical lines show variation in solubility in each scenario, horizontal tick marks show the solubility reported in this study.

[WSRC-STI-2007-00544]

The results show that when the two constants are varied in the opposite directions by one order of magnitude, Scenario D, the calculated solubility varies by about ± one order of magnitude. The results also show the relative insensitivity of the calculated solubility to the equilibrium constant of the dissolution reaction compared to the association constant of the dominant species, at a pH of 12.3 and these oxidizing conditions. As chemical conditions approach the stability of the uranium species in the dissolution reaction, $UO2^{+2}$. the calculated solubility becomes more sensitive to the equilibrium constant of this reaction.

The Nuclear Energy Agency's Organization for Economic Co-Operation and Development is developing a thermodynamic database for species and reactions pertinent to the nuclear industry and has published volumes specific to several radioactive elements. Table 4.2-12 shows the range in uncertainty reported in this database for association constants of aqueous species of several radioactive elements.

Table 4.2-12: Variation in Association Constants of Aqueous Species of Various Elements of Interest

Element	Range Of Uncertainty In Log K
Uranium	±0.02 to ±2.00
Plutonium	±0.09 to ±3.00
Neptunium	±0.06 to ±2.69
Technetium	±0.15 to ±1.7

[WSRC-STI-2007-00544]

From the sensitivity analysis shown in Figure 4.2-7 and Table 4.2-12, a maximum uncertainty of two orders of magnitude for all elements was assumed due to changing thermodynamic conditions.

4.2.1.6 Stabilized Contaminants Release Control by Co-Precipitation

Co-precipitation as defined here as the incorporation of an element into the crystal structure of a solid phase that is predominantly made of other elements or the trapping of an element within the bulk mass of a phase made up of other elements, but not necessarily within the crystal lattice. The incorporated element is often referred to as a trace or minor element in the solid phase. This differs from adsorption where an element is bound to the surface layers of a solid phase and is available for equilibration with pore fluids. The bulk of a co-precipitated trace element is not available for interaction with pore fluids until the parent phase is dissolved.

An example of co-precipitation that can be treated thermodynamically is Cr^{+3} incorporated into the structure of $Fe(OH)_3$. This can be considered thermodynamically in a simple way by the reaction:

$$Cr^{+3} + Fe(OH)_3 = Cr(OH)_3 + Fe^{+3}$$

With an equilibrium constant of:

$$K = \frac{aFe^{+3} \times ACr(OH)_3}{aCr^{+3} \times AFe(OH)_3}$$

where:

aFe^{+3} and aCr^{+3} are the activities of the aqueous species and $ACr(OH)_3$ and $AFe(OH)_3$ are the activities of these components in the precipitated solid.

The equilibrium relationship can be rearranged to:

$$K \times \frac{AFe(OH)_3}{ACr(OH)_3} = \frac{aFe^{+3}}{aCr^{+3}}$$

Thus, the amount of chromium that precipitates with $Fe(OH)_3$ is related to the ratio of Fe^{+3} to Cr^{+3} in the aqueous solution by the equilibrium constant, sometimes referred to as the distribution coefficient.

Co-precipitation in which the element of interest is not part of the crystal structure of the main phase cannot be treated thermodynamically. Yet, when the molality ratio in a solution of an element of interest to a "carrier" element is very small, co-precipitation with the carrier phase can remove much of the element of interest from the solution providing that the element of interest has not already precipitated and settled out of solution. Table 4.2-13 presents the molality ratios of Pu-239, Np-237, Tc-99, and U-238 to the iron in Tanks 19 and 20 residual wastes. Work has been reported that plutonium was co-precipitated with iron or aluminum in Hanford Site waste tanks. [WSRC-STI-2007-00544]

Table 4.2-13: Ratios of Pu-239, U-238, Tc-99, and Np-237 to Iron in FTF Tanks 19 and 20

Tank	Pu-239/Fe (mol)	U-238/Fe (mol)	Tc-99/Fe (mol)	Np-237/Fe (mol)
19	5.0E-05	2.0E-02	2.0E-04	2.0E-06
20	4.0E-05	5.0E-03	4.0E-04	3.0E-06

[WSRC-STI-2007-00544]

Many of the radionuclides of interest may be co-precipitated with solid iron or other metal hydroxides or oxides in the residual waste. This is supported by concentrations of rare earth elements, often considered surrogates for actinides, in natural iron oxides and oxyhydroxides formed at low temperature environments. WSRC-STI-2007-00544 provides multiple examples of reports that discuss co-precipitation. For example, rare earth element concentrations have been reported in low temperature hematite, and goethite that range from about 0.1 parts per million to nine parts per million (one sample of goethite contained 132 parts per million of cerium). If all iron and Pu-239 in Tank 19 residual waste resided in hematite, the Pu-239 would have a concentration of 1.4 parts per million in the hematite. Thus, it is plausible that a large fraction of plutonium and other radionuclides might be in a co-precipitated form. Supporting this idea are reports that document both plutonium and uranium co-precipitated with iron and found that uranium and plutonium were both effectively removed from solution by co-precipitation with iron oxide/hydroxides in a water treatment process. [WSRC-STI-2007-00544] Similarly, removing plutonium from residual waste solutions by co-precipitating it with magnetite and co-precipitation with iron oxide/hydroxides quantitatively remove plutonium from liquid samples prior to analysis have been discussed in applicable reports. In the magnetite co-precipitation experiments, decontamination factors in the range of 1.0E+04, to 1.0E+05 were achieved, and the

experimental data suggests a plutonium distribution coefficient of about 1,000 in the magnetite produced. [WSRC-STI-2007-00544] Co-precipitation with iron oxide/hydroxides has also been used quantitatively to remove plutonium from liquid samples prior to analysis. Thus, it is likely that most of the plutonium and perhaps the uranium in SRS waste tanks are co-precipitated in iron phases known to be prevalent.

Technetium may also be co-precipitated with iron phases in the waste tanks. A significant fraction of Tc-99 in Hanford Site waste tank sludge was relatively insoluble (a sample at 20% and 80% in another) and the insoluble Tc-99 was correlated with iron oxide/hydroxides in selective extraction experiments. Experiments were conducted with perrhenate (an analogue for pertechnitate, ReO4) under the sludge conditions of the Hanford Site waste tanks. These experiments concluded that up to 14% of the Tc-99 in waste tank sludge may be irreversibly sorbed, possibly co-precipitated, in iron and aluminum solids. It was also believed that Tc-99 was removed from solution during titration experiments of acidic groundwater by co-precipitation with iron and aluminum phases. [WSRC-STI-2007-00544]

There is also evidence in the literature that neptunium may readily co-precipitate with ferric iron oxides (Fe_2O_3) and found that Np(V) and Np(VI) sorbs strongly to ferric oxyhydroxides ($Fe(OH)^3$) at a high pH, while Np(IV) forms true mixed oxide co-precipitates. If neptunium sorbed strongly to ferric iron phases as they formed, and these particles settled to the bottom of the waste tanks to form a lithified heel, the neptunium would be effectively co-precipitated. Its release to pore fluids would require dissolution of the ferric iron phases. Likewise, it was observed that Np(IV) sorbed strongly on magnetite in anaerobic conditions, while Np(V) sorbed strongly to hematite under aerobic conditions. [WSRC-STI-2007-00544]

It is likely that co-precipitation of technetium, uranium, neptunium, and plutonium in iron oxide/hydroxides is initiated by adsorption of these radionuclides on particles of ferric iron phases as they precipitate. As the particles grow or become agglomerated into larger masses, the radionuclides are effectively co-precipitated (isolated from pore fluid by their entrapment) in ferric iron phases. The co-precipitation of technetium is postulated to be by adsorption within the microporosity of precipitating ferrihydrite. As the ferrihydrite recrystallizes to hematite or goethite, the microporosity is closed off and the technetium is isolated from interparticle pore fluids. This is likely also the case for uranium and plutonium because none of these radionuclides fit well into the crystal lattice of ferric iron oxides or hydroxides. Thus, a thermodynamic treatment is not applicable.

Nevertheless, an apparent solubility can be estimated for radionuclides co-precipitated by this mechanism by assuming that the radionuclides are homogenously distributed within the mass of ferric iron phase. This is reasonable if soluble iron was added to the waste stream during or after the radionuclides of interest. Ferrous sulfamate was added during the Plutonium Recovery and Extraction (PUREX) process used at SRS to reduce plutonium. It is possible that this iron precipitated upon neutralization of the pH prior to disposition in the waste tanks. Ferric iron precipitated by an increase in the pH generally occurs initially as colloidal-sized particles of an amorphous hydroxide. The particles subsequently agglomerate and settle out. With time, the amorphous hydroxide becomes increasingly crystalline and usually converts to hematite or goethite. A relatively homogenous distribution of radionuclide

within an aged ferric iron phase would be expected if the radionuclide were initially adsorbed to the early colloidal particles. The ratio of the radionuclide to iron in solution as the iron phase dissolves is equal to the ratio in the solid phase is the inherent assumption in WSRC-STI-2007-00544 to calculate the apparent solubility of technetium co-precipitated with iron.

Recent work reported in WSRC-STI-2007-00544 suggests that uranium co-precipitated with hydrous ferrous oxides becomes less extractable with age as the originally amorphous hydrous ferrous oxide becomes increasingly crystalline and hematite and goethite begin to crystallize. This is consistent with the recent observations of technetium leachability when co-precipitated with iron. However, other recent studies reviewed and documented in WSRC-STI-2007-00544 showed that uranium is preferentially leached compared to iron when the solid is exposed to extractants. It should be noted that the aged iron phase still contained appreciable ferrihydrite, which suggests that the preferential leaching of uranium by a carbonate extractant may be the result of dissolution of the ferrihydrite with subsequent re-precipitation of the iron. The other possibility is that the uranium is not homogenously distributed in the aged particles, but is concentrated near the surface. This is a reasonable explanation considering the aged particles are very small (approximately 0.2 micrometers). Radionuclide-bearing iron mineral particles present after waste tank washing are likely to be fused together in much larger agglomerates/crystals or the washing process would remove all of the radionuclide. Thus, on the sub-micrometer scale radionuclides may not be homogenously distributed in iron minerals, but on larger scales can be considered homogenously distributed for modeling purposes. [WSRC-STI-2007-00544]

Analyses of representative samples from HTF waste tanks are not available to determine the radionuclide to iron ratios. Therefore, calculations of apparent solubility of co-precipitated uranium, plutonium, technetium, and neptunium were based on analysis of WCS. A radionuclide to iron ratio was calculated for each waste tank based on the WCS. The solubility of each radionuclide of interest for each HTF waste tank was calculated from these ratios and the solubility of iron at the different pore fluid compositions of interest. The median, maximum, and minimum apparent solubility in non-submerged waste tanks for H Area are reported in Table 4.2-14. Similar information for the partially submerged waste tanks in H Area is shown in Table 4.2-15.

Table 4.2-14: Solubility of Co-Precipitated Radionuclides in Non-Submerged Waste Tanks

		Pore Water Conditions (mol/L)		
Element	**Molality**	**Reducing Region II**	**Oxidizing Region II**	**Oxidizing Region III**
Uranium	Median	7.0E-12	9.0E-13	2.0E-14
	Maximum	2.0E-10	2.0E-11	5.0E-13
	Minimum	4.0E-15	6.0E-16	1.0E-17
Plutonium	Median	7.0E-14	9.0E-15	2.0E-16
	Maximum	9.0E-13	1.0E-13	3.0E-15
	Minimum	4.0E-15	5.0E-16	1.0E-17
Technetium	Median	6.0E-13	7.0E-14	2.0E-15
	Maximum	2.0E-12	2.0E-13	6.0E-15
	Minimum	1.0E-14	2.0E-15	4.0E-17
Neptunium	Median	2.0E-14	2.0E-15	5.0E-17
	Maximum	4.0E-14	5.0E-15	1.0E-16
	Minimum	3.0E-17	3.0E-18	8.0E-20

[WSRC-STI-2007-00544]

Table 4.2-15: Solubility of Co-Precipitated Radionuclides in Partially Submerged Waste Tanks

		Submerged Pore Water Conditions (mol/L)			
Element	**Molality**	**A**	**B**	**C**	**D**
Uranium	Median	9.0E-12	3.0E-14	8.0E-12	6.0E-14
	Maximum	2.0E-11	8.0E-14	2.0E-11	1.0E-13
	Minimum	2.0E-13	5.0E-16	1.0E-13	1.0E-15
Plutonium	Median	1.0E-13	4.0E-16	8.0E-14	7.0E-16
	Maximum	3.0E-12	1.0E-14	3.0E-12	2.0E-14
	Minimum	1.0E-14	5.0E-17	1.0E-14	1.0E-16
Technetium	Median	8.0E-13	3.0E-15	7.0E-13	5.0E-15
	Maximum	1.0E-10	4.0E-13	1.0E-10	8.0E-13
	Minimum	2.0E-13	8.0E-16	2.0E-13	1.0E-15
Neptunium	Median	2.0E-14	8.0E-17	2.0E-14	2.0E-16
	Maximum	7.0E-14	3.0E-16	6.0E-14	5.0E-16
	Minimum	6.0E-15	2.0E-17	5.0E-15	4.0E-17

Condition A: Pore Water = Groundwater
Condition B: Pore Water = Groundwater equilibrated with calcite
Condition C: Pore Water = Mixture 0.9 Groundwater + 0.1 Reduced Region II Pore Water
Condition D: Pore Water = Mixture 0.9 Groundwater + 0.1 Oxidized Region II Pore Water
[WSRC-STI-2007-00544]

The assumption that radionuclide release is controlled by solubility of discrete radionuclide phases rather than co-precipitation is conservative if equilibrium prevails and the choice of solubility controlling minerals is biased towards those with high solubility. This is because apparent solubility from a co-precipitated form only controls the release of the radionuclide to solution if it does not exceed the solubility of the selected discrete phase. Otherwise, the solubility of the selected discrete phase controls radionuclide release. [WSRC-STI-2007-00544]

4.2.1.7 Affect of Partial Pressure of Carbon Dioxide on Solubility

Several elements are known to form aqueous carbonate complexes at elevated pH. Those that have radionuclides with high inventories in the HTF waste tanks and long half-lives that are known to form aqueous carbonate complexes are plutonium, neptunium, uranium, and americium. At a constant elevated pH, as PCO_2 increases the solubility of these elements will increase. The pressure of carbon dioxide (PCO_2) is considered differently in calculation of solubility in Regions II and III. In Region II it is assumed that the PCO_2 would be very low, controlled by the reaction of carbon dioxide with portlandite producing calcite. This was modeled with the infiltrating pore fluid in equilibrium with atmospheric carbon dioxide prior to contact with the waste tank grout. As it passes through the grout, increasing amounts of carbon dioxide is removed from solution, and thus the gas phase, by precipitation of calcite. For Region III, where the grout is completely carbonated, it is assumed that the radionuclide solubility reactions were at the PCO_2 of the atmosphere (atm), because there is no reaction to remove carbon dioxide as infiltrates passes through the grout. [ISSN 1019-0643]

It is possible, though, that the PCO_2 at the CZ is influenced by soil PCO_2, which is typically higher than atmosphere. A sample from a water table well near F Area was in equilibrium with a calculated PCO_2 of 2.51E-03 atmosphere rather than the atmospheric PCO_2 of 3.16E-04 atmosphere. [WSRC-RP-92-450] This PCO_2 is typical of groundwater in water table aquifers at SRS in which there is little organic matter to drive the PCO_2 values higher. To evaluate how the elevated PCO_2 affects the solubility of plutonium, neptunium, uranium, and americium curves of solubility versus PCO_2 are calculated. The calculations are done using geochemical modeling program GWB, and assuming that the CZ is a mixing zone of infiltrate from the grout and carbon dioxide gas diffusing from soil. The rate that carbon dioxide diffuses into the CZ relative to the rate of infiltrate advection and/or ion diffusion from the grout may result in different PCO_2 values at steady state. Thus, the composition of the pore fluid in the CZ is assumed to be the same as that in the original solubility calculations, but the PCO_2 is varied up to a PCO_2 equal to 1.0E-02 atmosphere. Reaction of carbon dioxide with the infiltrate produces calcite and lowers the pH by the overall reaction:

$$CO_2(aq) + Ca^{+2} = CaCO_3 + 2H^+$$

At a PCO_2 of 2.51E-03 atmosphere, the grouted waste tank system has equilibrium pH values that range from about 7.3 to 7.7, depending on the original chemical state of the infiltrate. The calculated curves for Region II infiltrate are shown in Figure 4.2-8. The curves for Region III are not shown because the variation in solubility of the four elements is less than one order of magnitude because the assumed PCO_2 in Region III was already at PCO_2, which is equal to 3.16E-04 atmosphere. [ISSN 1019-0643]

Figure 4.2-8: Calculated Solubility Curves for Uranium, Plutonium, Neptunium, and Americium vs. PCO_2

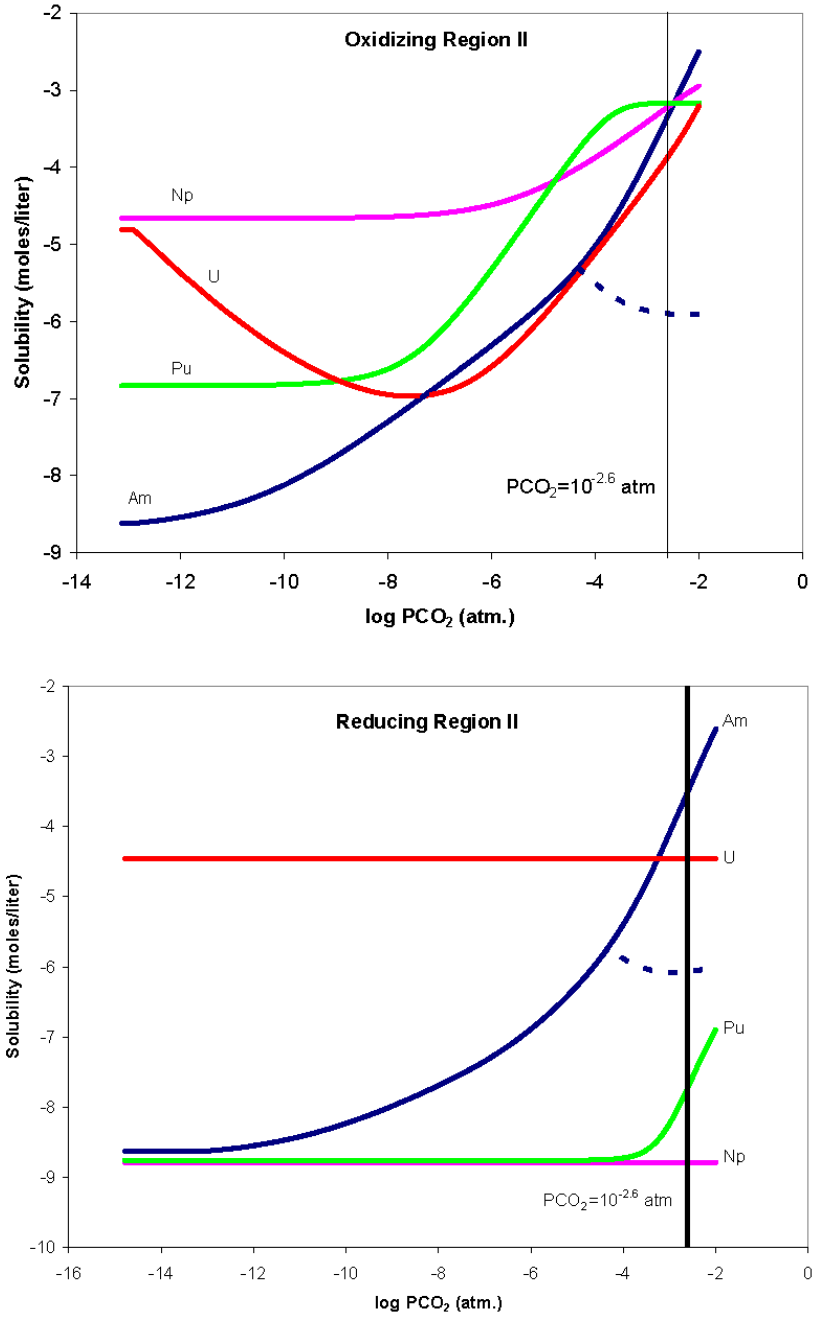

Note Dashed line is solubility of americium allowing carbonate phases to precipitate.
[WSRC-STI-2007-00544]

The solubility of uranium, plutonium, neptunium, and americium are most affected in the oxidizing chemical state, because known aqueous carbonate complexes are more influential at oxidizing conditions. Table 4.2-16 shows the solubility at a PCO_2 of 2.51E-03 atmosphere compared to the original calculated values. Under oxidizing conditions, the solubility of plutonium and uranium increase about three orders of magnitude and that of americium increases by about five orders of magnitude. The solubility of neptunium increases by less than about one and a half orders of magnitude.

Under reducing conditions, the solubility of uranium and neptunium do not increase as the PCO_2 increases and that of plutonium increases by one order of magnitude. The solubility of americium increases by five orders of magnitude under reducing conditions. However, if carbonate phases of americium are allowed to precipitate the increases in solubility under both oxidizing and reducing conditions are much less (the dashed lines in Figure 4.2-8).

Precipitation of calcite during equilibration with elevated soil PCO_2 values may eventually occlude porosity around the CZ and limit stabilized contaminant release. About 0.5 cm^3 of calcite is precipitated for each liter of pore fluid equilibrated with a PCO_2 of 2.51E-03 atmosphere. Therefore, after a few hundred-pore volumes of infiltrate equilibrate with the elevated PCO_2 the porosity may be completely occluded.

Table 4.2-16: Impact of Partial Pressure of CO_2 Variability on Solubility

Element	Calculated Solubility (mol/L)	Solubility at PCO_2 = 2.51E-03 atm (mol/L)
Oxidizing Region II		
Uranium	3.4E-07	1.5E-04
Plutonium	3.0E-07	6.8E-04
Neptunium	6.8E-07	6.4E-04
Americium	8.6E-09	5.4E-04 ($Am(OH)_3$)
		1.3E-06 ($Am_2(CO_3)_3$)
		3.2E-07 ($AmOHCO_3$)
Reducing Region II		
Uranium	3.5E-05	3.5E-05
Plutonium	1.7E-09	1.7E-08
Neptunium	4.8E-09	1.6E-09
Americium	8.8E-09	2.8E-04 ($Am(OH)_3$)
		8.5E-07 ($Am_2(CO_3)_3$)
		2.5E-07 ($AmOHCO_3$)

[WSRC-STI-2007-00544]

4.2.1.8 Chemical Degradation of Grout

Evolution of the chemical conditions in the grout was modeled using GWB. Details of these calculations are presented in Appendix B of WSRC-STI-2007-00544. The database used for grout degradation simulations was "thermo.data", as recommended by WSRC-STI-2007-00544. It was modified to include cementitious minerals as reported in WSRC-STI-2007-00544.

The first step in the grout degradation simulation is to estimate the hydrated mineralogy of the grout from the grout formula presented in procurement specification C-SPP-F-00047. This formula, together with chemical compositions of the grout components, allows calculation of the final chemical composition of the grout. From this composition, a normative mineralogy is estimated by assuming all calcium in the phase CSH, all magnesium in hydrotalcite, excess aluminum in gibbsite, and remaining silica is inert to pore fluids. The amount of pyrrhotite in the grout is estimated from the measured reducing capacity of the slag, the amount of slag, and the following reaction: [WSRC-RP-2005-01674]

$$FeS + 2O_{2(aq)} = Fe^{+2} + SO_4^{-2}$$

Table 4.2-17 presents the grout formula and the estimated hydrated mineralogy used in the model. For the non-submerged waste tanks, the grout mineralogy in Table 4.2-17 is reacted with an infiltrate calculated to simulate rainwater passing through a kaolinitic soil assuming no interaction with waste tank capping materials. For the submerged waste tanks, the grout mineralogy was reacted with a groundwater composition obtained from a well near the HTF. The reactions were done in the "flush" mode meaning as water enters the block of grout it pushes out an equivalent volume of water that has equilibrated with the grout. The simulations were done in two steps because the model becomes unstable and terminates at the abrupt change in oxidation potential when reducing capacity is exhausted. This results in minor inconsistencies between the end of the first step and the beginning of the second. The results for the non-submerged and submerged waste tanks are shown in Figure 4.2-9 and Figure 4.2-10.

Table 4.2-17: Grout Formula and Estimated Hydrated Mineralogy

Grout Formula	
Grout Component	**Amount (lbs/yd^3)**
Portland Cement	75
Class F Fly Ash	375
Slag	210
Quartz Sand	2,300
Water	501
Estimated Hydrated Mineralogy	
Mineral	**Amount (g/m^3)**
CSH	192,583
Hydrotalcite	47,475
Gibbsite	50,505
Pyrrhotite	967

[WSRC-STI-2007-00544]

Figure 4.2-9: Pore Fluid pH (A) and E_h (B) During Simulated Degradation of Reduced Grout of Non-Submerged Waste Tanks

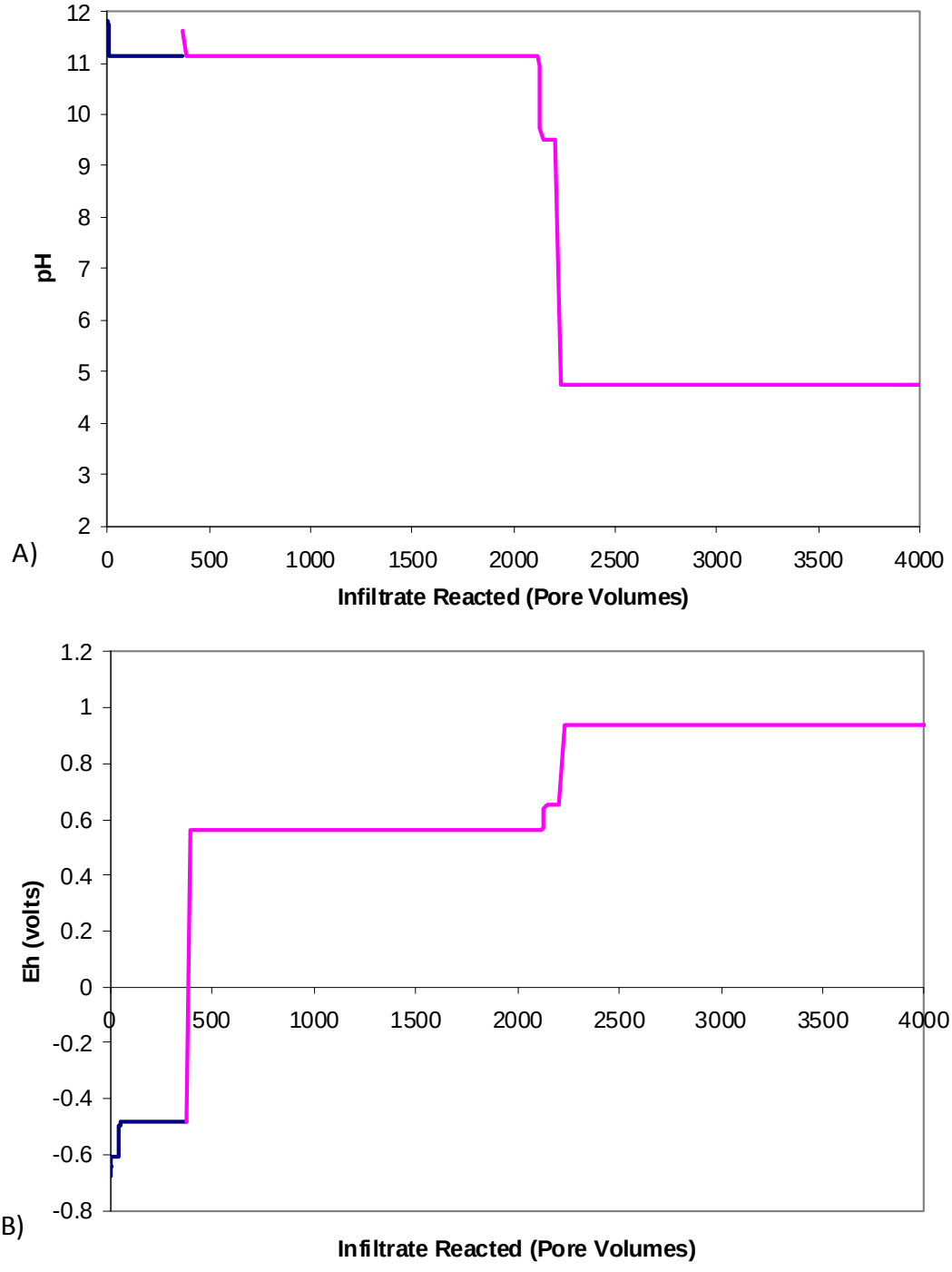

[WSRC-STI-2007-00544]

Figure 4.2-10: Pore Fluid pH (A) and E_h (B) During Simulated Degradation of Reduced Grout of Submerged Waste Tanks

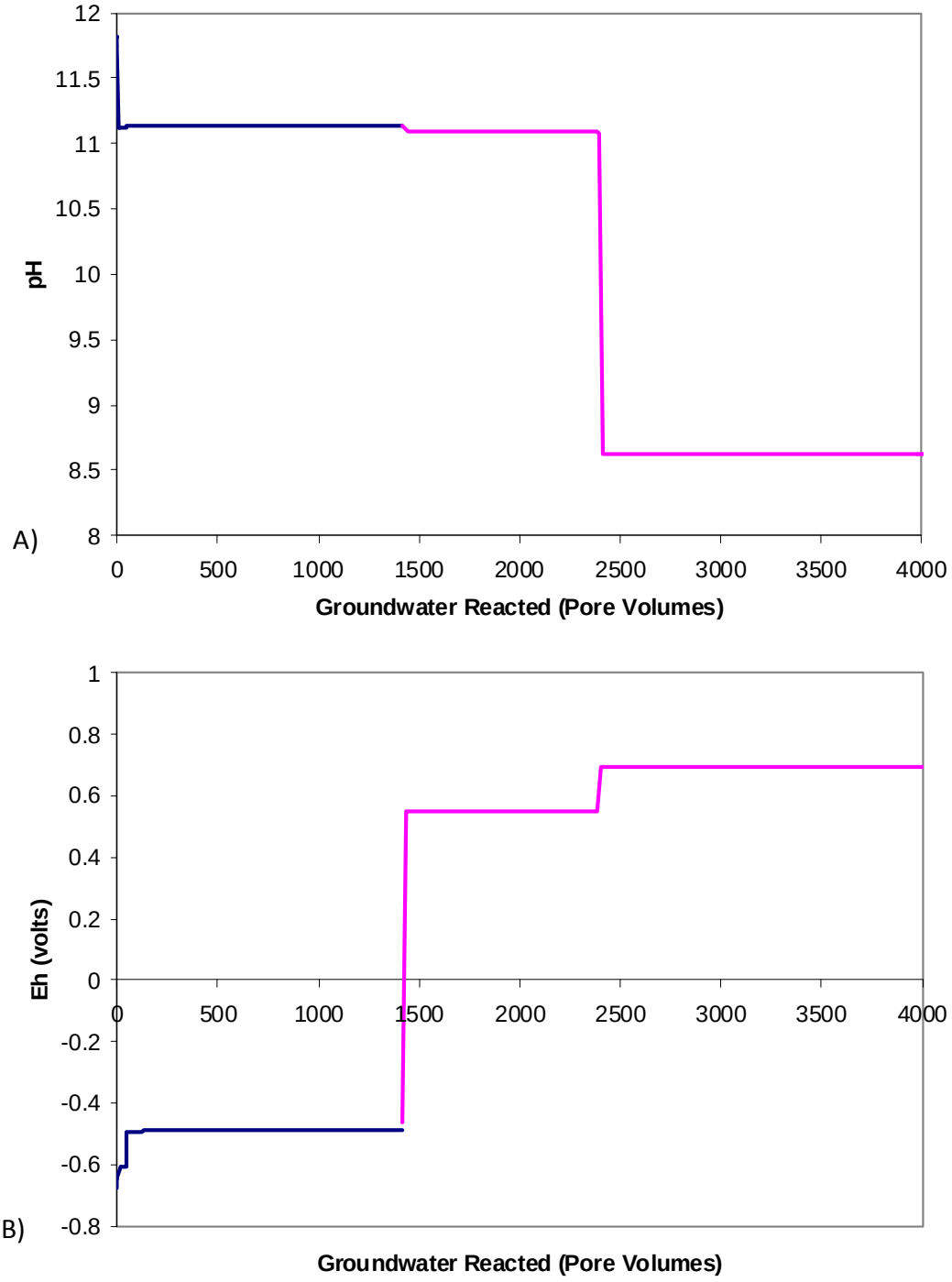

[WSRC-STI-2007-00544]

Table 4.2-18 provides a summary of the number of pore volumes of infiltrate required to bring about the various step changes in pore fluid conditions for the non-submerged and submerged waste tanks. [WSRC-STI-2007-00544]

Table 4.2-18: Grout Degradation Simulations Pore Volumes of Infiltrate Reacted Required to Cause Step Changes in Chemical Conditions

Tank Position	Transition	Pore Volumes
Non-Submerged	Reduced Region II to Oxidized Region II	371
	Oxidized Region II to Oxidized Region III	2,131
Submerged	Condition C to Condition D	1,414
	Condition D to Oxidized Region III	2,383

[WSRC-STI-2007-00544]

4.2.2 Radionuclide Transport

Over the course of time, the mobile contaminants in the closed waste tanks and ancillary equipment are likely to release and gradually migrate downward through unsaturated soil to the hydrogeologic units comprising the shallow aquifers underlying the HTF. Some contaminants will be transported via groundwater through near surface aquifers and discharge to either Fourmile Branch or UTR streams. Exposure to contaminants could occur through various pathways associated with groundwater, surface water uses, and air exposure. Figure 3.1-4 shows the location of the HTF within the GSA, which is bounded by UTR to the north and by Fourmile Branch to the south.

In model simulations, HTF contaminant transport processes in cementitious materials and soils included advection, dispersion, and sorption, but not colloidal transport. Contaminant transport through the cementitious materials and soils is impeded by sorption, as represented through the distribution coefficient of the soils (Section 4.2.2.2.2) and cementitious materials (Section 4.2.2.2.4). The distribution coefficient values used are based primarily on SRS site-specific experimental data, some central value of literature, or on expert judgment, with SRS site-specific experimental data being the preferred information source. [SRNL-STI-2009-00473]

Geochemical Data Package for Performance Assessment Calculations Related to the Savannah River Site (SRNL-STI-2009-00473) discusses field studies of colloid facilitated transport of plutonium that were conducted at SRS by two groups, the University of Georgia/SRNL and Woods Hole Oceanographic Institution. Together their results indicate little or perhaps no colloidal transport of plutonium occurring within the GSA of the SRS, which includes both the F-Area and H-Area tank farms.

In the University of Georgia/SRNL study conducted in 1994 as discussed in SRNL-STI-2009-00473, plutonium associated with a filterable fraction was measured in groundwater recovered in F Area, near the E-Area burial grounds and the Saltstone Disposal Facility (SDF). This filterable fraction was presumed to be a colloidal fraction based on specialized low-flow collection and filtering techniques. Minimal plutonium was found in association with colloids, 0.003 pCi/L Pu-239/240 (5,000 times less than the MCL).

The percent of plutonium retained by filters, increased as the pH of the plume increased, which was also coincidental with distance from the point source. Inversely, the percent of plutonium that passed through the smallest membrane, 500-molecular weight cut-off (MWCO) or approximately 0.5 nanometer decreases with an increase in distance from the point source. The ratio between the plutonium concentration of colloids in well water and liquid in the source zone did not change in a systematic manner with distance (or pH) in the field. [SRNL-STI-2009-00473]

A colloid study was conducted in F Area by the Woods Hole Oceanographic Institution in 1998 and concluded that colloids were not involved in plutonium transport. [SRNL-STI-2009-00473] The difference between these two (1994 study and 1998 study) is that one reported little colloidal plutonium and the other reported no colloidal plutonium. These results may be attributed to sampling 8 years later in a more basic pH plume and with significant differences in sampling and analytical techniques. The study reporting no colloidal plutonium used more sensitive analytical methods but larger MWCO membranes permitting larger particles to pass through (1,000 MWCO or approximately 1 nanometer) to separate colloidal from the dissolved fractions).

Woods Hole Oceanographic Institution and the SRNL returned to F Area in 2004 to characterize changes in plutonium oxidation states and plutonium association with colloids in groundwater samples collected six years earlier. They reported small concentrations of plutonium associated with colloids. The percentage of plutonium associated with colloids, 1.0 to 23%, fell between the results of the previous two studies. They concluded that plutonium moved primarily in the dissolved state (and in the higher plutonium oxidation states). They reported that colloidal plutonium increased systematically with decreases in redox conditions. They observed greater dynamic shifts in plutonium speciation, colloid association, and transport in groundwater on both seasonal and decadal time scales and over short field spatial scales than commonly believed. [SRNL-STI-2009-00473]

Based on the information available to date, colloid-facilitated radionuclide transport would not have a significant effect on contaminant movement in the HTF transport models. Potential effects on radionuclide transport as modeled due to colloid-facilitated transport is addressed indirectly through varying various inputs related to transport in the UA/SA (e.g., by varying radionuclide inventory and distribution coefficient values as described in PA Sections 5.6.3.1 and 5.6.3.4, respectively).

4.2.2.1 Model Approach

The ICM modeling domain is organized vertically from top to bottom as shown in Figure 4.2-11. For the purposes of this document, the ICM has been broken up into its three component conceptual models:

- Conceptual closure cap
- Vadose zone
- Saturated zone (i.e., the aquifers)

Simplifying model assumptions have been made for each of these distinct zones or layers and are summarized below and discussed in detail in Section 4.4.

Figure 4.2-11: Conceptual Closure Model for HTF

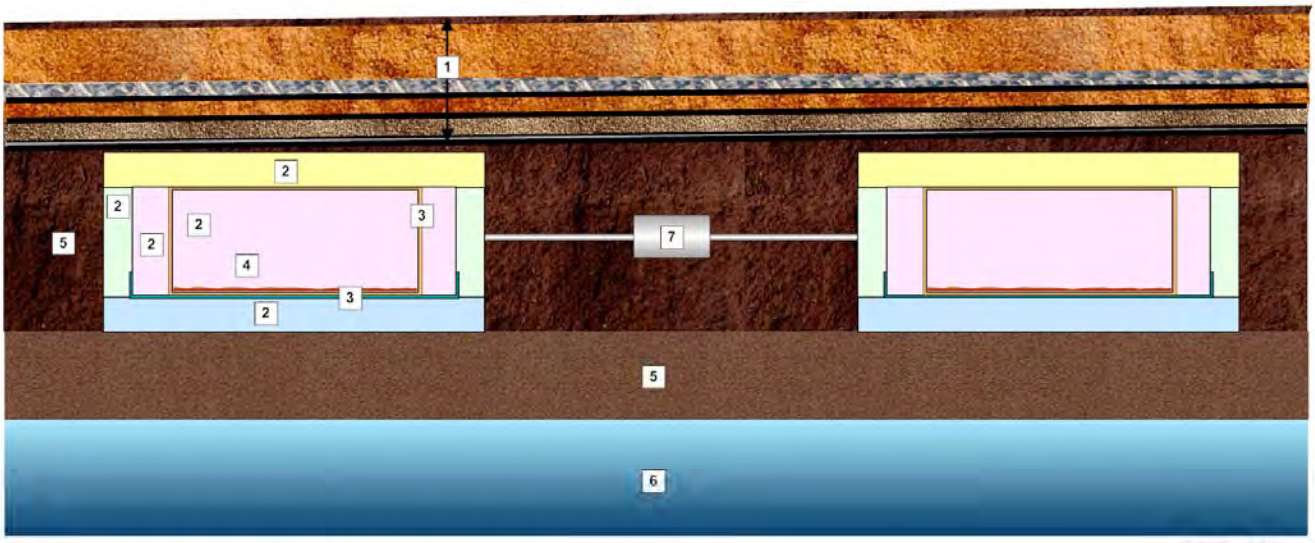

1 **Closure Cap** - Provides water flux to the top of tank from infiltrating rainwater.

2 **Vault Concrete and Tank Fill Grout** - Provides degradation description of the concrete and grout based materials in the tank system.

3 **Carbon Steel Tank Liner (Primary and Secondary)** - Provides degradation description of the carbon steel liners in the tank system.

4 **Waste Release** - Provides waste contamination release rates of residual inventory based on solubility and sorption rates per nuclide.

5 **Vadose Zone and Backfill** - Provides hydraulic related values for the unsaturated undisturbed soil beneath the tanks and the backfill soil surrounding the tanks.

6 **Hydrogeology** - Provides hydraulic related values for the saturated soil beneath the tanks.

7 **Ancillary Equipment** - Provides waste contamination release rates of residual waste associated with ancillary equipment.

4.2.2.1.1 Conceptual Closure Cap

The design concept for the HTF assumes it will be covered by two large closure caps, one over the "West Hill" area and one over the "East Hill" area, and a small closure cap over PPs 5 and 6. The conceptual design and expected performance of the closure caps are described in Section 3.2.4. Figure 4.2-12 illustrates the conceptual design of the HTF closure caps.

Figure 4.2-12: Closure Cap Concept for HTF

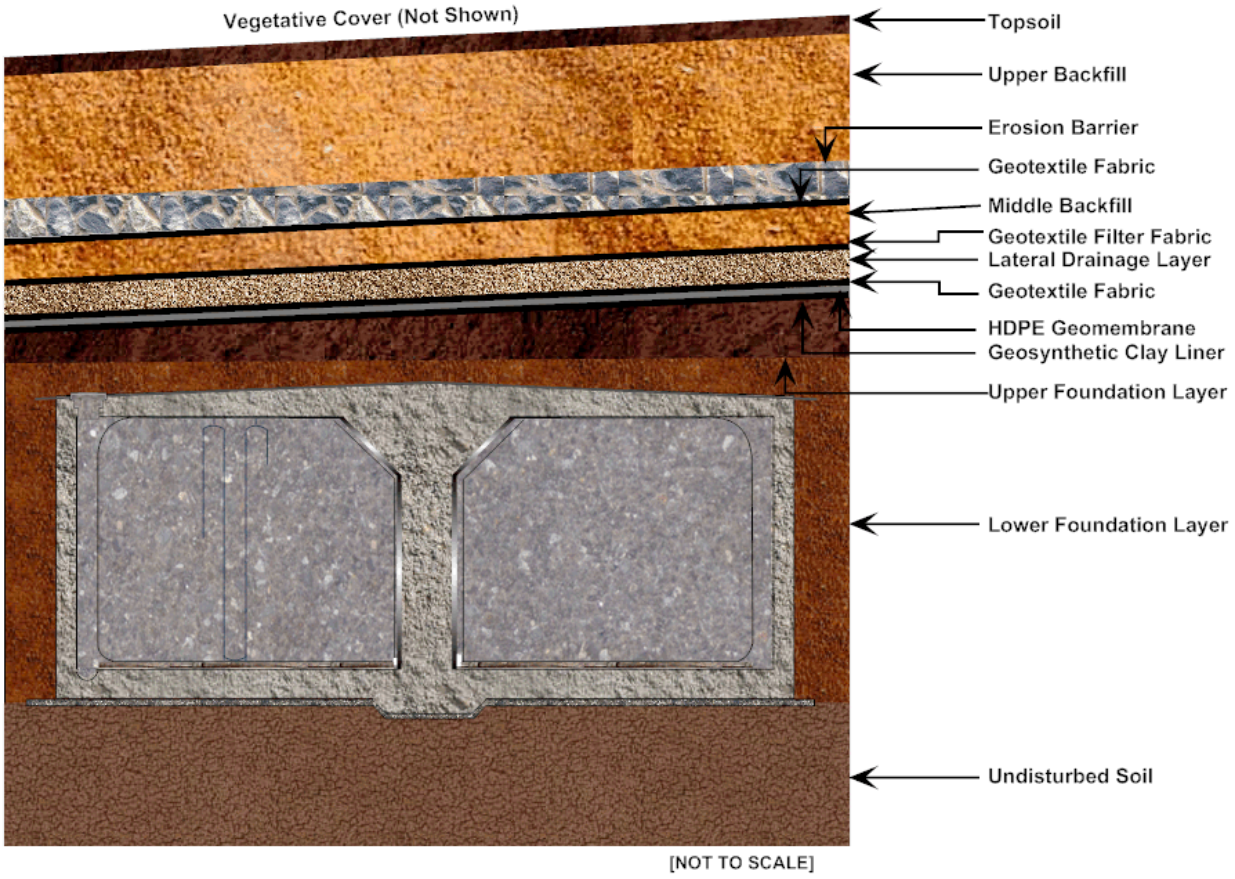

4.2.2.1.2 Vadose Zone

Although the conceptual closure cap has a certain physical thickness (a minimum of 10 feet), the cap is viewed as a surface feature in the ICM, as it is simulated separately. The area directly beneath the conceptual closure cap in the ICM is considered the vadose zone. The vadose zone and the surrounding soil, both undisturbed and backfill, contain the majority of the potential contamination sources in HTF (i.e., 21 waste tanks and ancillary equipment). In addition, eight waste tanks, along with some ancillary equipment, are either fully submerged or partially submerged in the saturated zone. The residual inventories are classified as waste tanks or ancillary equipment. Table 4.2-19 shows the thickness of the vadose zone under each of the 29 HTF waste tanks.

Table 4.2-19: Vadose Zone Thickness beneath HTF Waste Tanks

Tank Group Numbers	Tank Type	Average Concrete Working Slab Top Elevation (ft above MSL)	Group Median Water Table Elevation (ft above MSL)	Distance from Working Slab to Water Table (ft)
9 - 12	I	240.65	276.14	-35.5
13 - 16	II	270.33	276.93	-6.6
21 - 24	IV	281.75	274.65	7.1
29 - 32	III	281.88	273.80	8.1
35 - 37	IIIA	283.37	268.98	14.4
38 - 43	IIIA	292.09	273.93	18.2
48 - 51	IIIA	286.89	274.40	12.5

[SRNL-STI-2010-00148, Table 4]

The waste tanks will be modeled slightly differently, depending on the type. The segmentation approach and a discussion of different model elements for each waste tank type are described in Section 4.4.1. The material properties of waste tank and waste tank system behavior over time are discussed in later sections.

The transfer lines in the HTF are not concentrated in any geographical area, but transverse under all areas between waste tanks and transfer facilities. Therefore, the transfer line inventory was modeled by distributing the assumed inventory equally over all of the HTF area around the waste tanks and transfer facilities as indicated by the orange solid lines presented in Figure 4.2-13. Pump tanks (HPT 2 through 10), CTS pump tanks (242-3H and 242-18H), and evaporator pots (242-H, 242-16H, and 242-25H) were modeled as point sources located in the HTF at a central point of an individual component. The inventory associated with these waste sources was assumed to have had contact with the soil (so that any waste release is direct) after an assumed transfer line/waste tank degradation time.

Figure 4.2-13: HTF PORFLOW Model Streamtraces and 100m Boundary

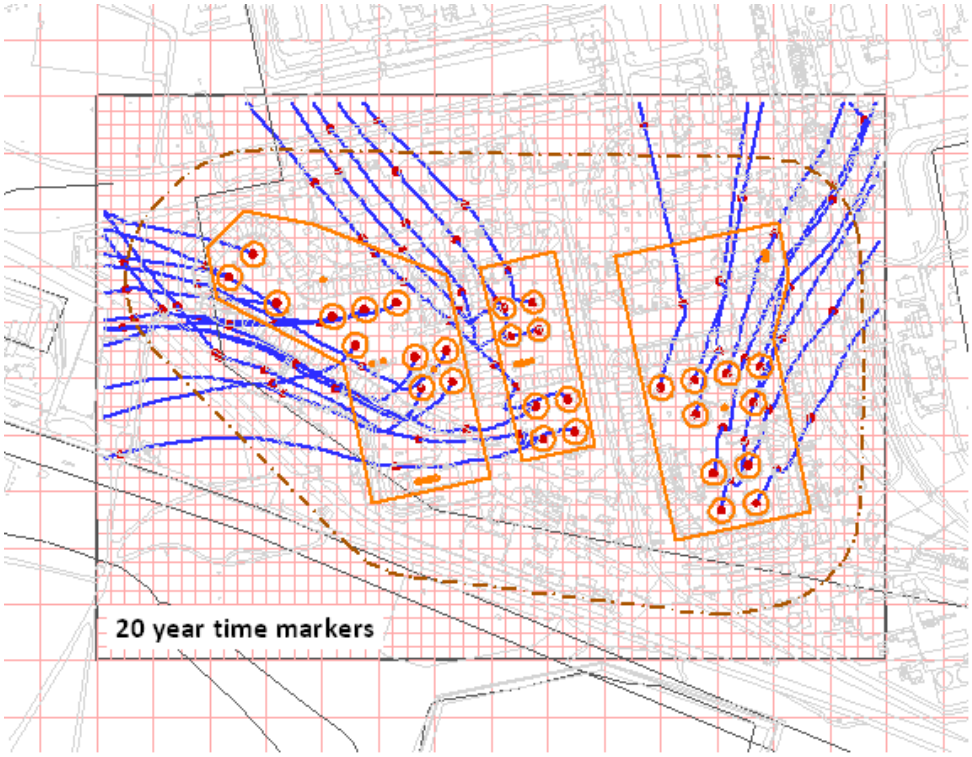

Other ancillary equipment was not modeled, based on the assumed inventories being insignificant or not inventory containment (e.g., catch tank).

4.2.2.1.3 Saturated Zone

After contaminants have left the vadose zone, they will be transported into the aquifers beneath the HTF. A description of the HTF hydrogeology is provided in SRNL-STI-2010-00148 and states that the GSAD and WSRC-STI-2006-00198 soil data should be applied for the HTF. The GSAD, comprising SRS characterization and monitoring data and interpretations, will be used as the basis of hydrogeologic input values into the computational model for groundwater flow and contaminant transport. The GSAD was developed using field data and interpretations for the GSA and vicinity and is documented in WSRC-TR-96-0399, Volumes 1 and 2.

The aquifers of primary interest for HTF modeling are the UTR and Gordon Aquifers. Potential contamination from the HTF is not expected to enter the deeper Crouch Branch Aquifer because an upward hydraulic gradient exists between the Crouch Branch and Gordon Aquifers near UTR. [SRNL-STI-2010-00148]

Groundwater flow in the UTR Aquifer is predominantly horizontal with a smaller, vertically downward component. Near groundwater divides located between surface water drainages, the vertical component of groundwater flow is stronger and downward due to the decreasing hydraulic head with increasing depth. In areas along Fourmile Branch, shallow groundwater moves generally in a horizontal direction and deeper

groundwater has vertically upward potential to the shallow aquifers. In these areas, hydraulic heads increase with depth. To the north of HTF, however, the rising elevation of the UTR Aquifer and the deep incision of UTR stream result in truncation of the entire aquifer. In these areas, shallow groundwater may seep out along the major tributaries to UTR above the valley floor or may seep downward to the next underlying aquifer zone and discharge along the stream valley.

The Gordon Aquifer is overlain by the UTR Aquifer UTR-LZ along the valley of Fourmile Branch. Along UTR, the Gordon Aquifer has been partially eroded by the deep streambed incision. The aquifer discharges to UTR and is locally recharged by leakage from overlying aquifers near the HTF. A southeast-to-northwest hydraulic gradient is observed for this aquifer layer in the GSA.

Because the HTF is located over a groundwater divide between UTR and Fourmile Branch, contaminants could eventually discharge to both streams, depending on the contaminant's origination point.

Within the GSA, for defining transport properties, soils with a saturated hydraulic conductivity greater than 1.0E-07 cm/s are defined as sandy and those with a saturated hydraulic conductivity less than 1.0E-07 cm/s are defined as clay. Within the GSA model the saturated zone soils that are defined as sandy will be assigned the effective diffusion coefficient of the upper vadose zone (i.e., 5.3E-06 cm^2/s) and those soils defined as clay will be assigned that of the vadose zone clay (i.e., 4.0E-06 cm^2/s). These property definitions are done to remain consistent with the soils of the vadose zone. [WSRC-STI-2006-00198]

Table 4.2-20 provides a summary of the saturated zone soils hydraulic properties (as represented by the vadose zone soil properties) and the model input used to represent these values.

Table 4.2-20: Upper Vadose Zone and Effective Saturated Zone Soil Properties

Actual/Model	**η (%)**	**ρ_h(g/cm^3)**	**ρ_n(g/cm^3)**	**Saturated D_e (cm^2/s)**
Upper Vadose Zone	39 (total)	1.65	2.70	5.3E-06
Saturated Zone Soil (Effective Properties for Modeling Purposes)	25 (effective)	1.04 (effective)	1.39 (effective)	Sandy: 5.3E-06 Clay: 4.0E-06

[WSRC-STI-2006-00198]
η = Porosity
ρ_h = Dry Bulk Density
ρ_n = Particle Density
D_e = Effective Diffusion Coefficient

4.2.2.1.4 Groundwater Flow Simulation

The simulation model for groundwater flow constructed from the GSAD using the PORFLOW code is referred to as the GSA/PORFLOW Model. In the model, groundwater from the UTR Aquifers (UTR-UZ and UTR-LZ) assumed to discharge equally from each side to UTR and Fourmile Branch Aquifers in the GSA. Therefore, these streams provide natural, no-flow boundary conditions for most of the UTR Aquifer Unit. The GSA boundary conditions are graphically displayed in Figure 4.2-14. On the west side of the unit, hydraulic head values from a contour map of measured water elevations are prescribed. The Gordon Aquifer is assumed to discharge equally from both sides of UTR and a no-flow boundary condition is specified over the north face of the model. Lacking natural boundary conditions, hydraulic heads are specified over the west, south, and east faces of the model within the Gordon Aquifer. Areas of groundwater recharge and discharge consistent with computed hydraulic head at ground surface are computed as part of the model solution using a combined recharge/drain boundary condition applied over the entire top surface of the model. Using this hybrid boundary condition, groundwater discharges to surface water in regions where the computed head is above ground elevation. Flows across the Crouch Branch Confining Unit are small compared to surface recharge and flow across the Gordon Confining Unit, and are neglected in the model.

Figure 4.2-14: GSA Boundary Conditions

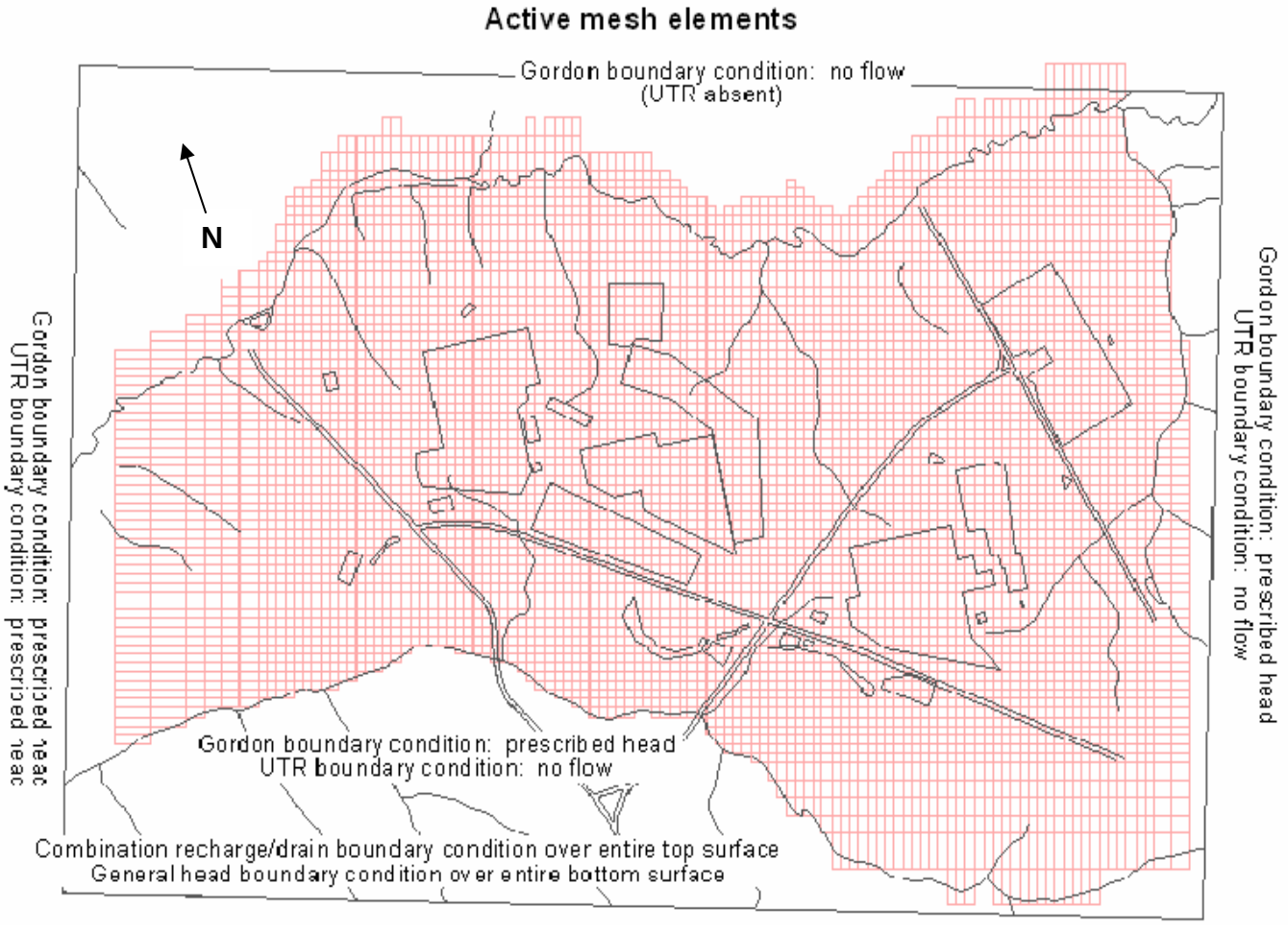

[WSRC-TR-2004-00106]

The area resolution of the GSA aquifer model is 200 square feet except in peripheral areas. There are 108 grid blocks along the east-west axis, and 77 blocks along the north-south axis. The vertical resolution varies depending on hydrogeologic unit and terrain/hydrostratigraphic surface variations as depicted in Figure 4.2-15. Each hydrostratigraphic surface is defined by numerous "picks" ranging in number from approximately 52 to 225 depending on the surface. The UTR-UZ represented with up to 10 finite elements in the vertical direction. The vadose zone is included in the model. The UTR-LZ contains five finite-elements while the TCCZ separating the aquifer zones is modeled with two vertical elements. The Gordon Confining Unit and Gordon Aquifer each contain two elements, totaling 21 vertical elements from ground surface to the bottom of the Gordon Aquifer. The 3-D grid comprises 102,295 active cells as depicted in Figure 4.2-16. [WSRC-TR-2004-00106]

Figure 4.2-15: North-South Cross-Section of GSA/PORFLOW Computational Mesh

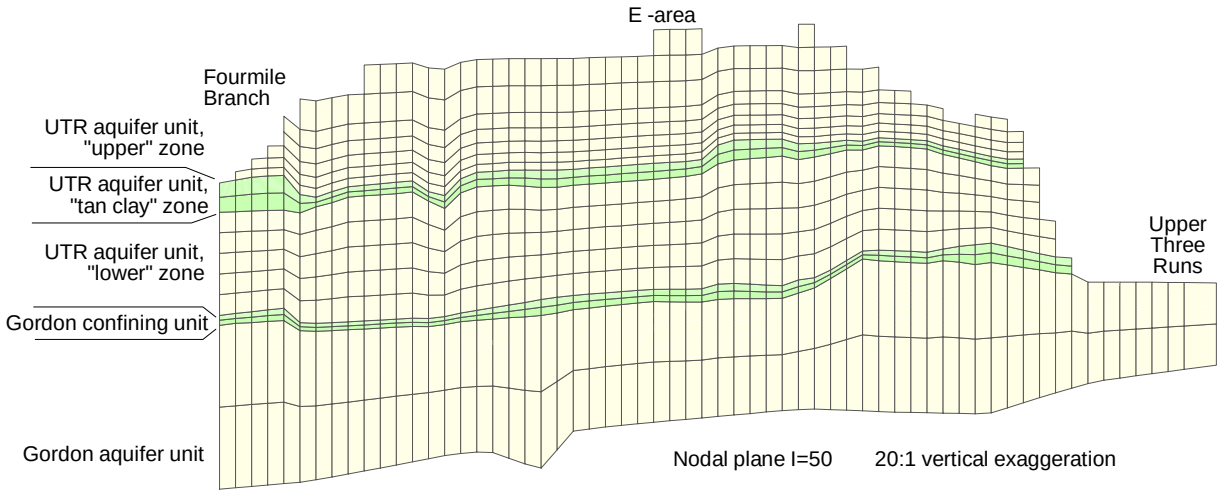

[WSRC-TR-2004-00106]

Figure 4.2-16: Perspective View of GSA/PORFLOW Computational Mesh

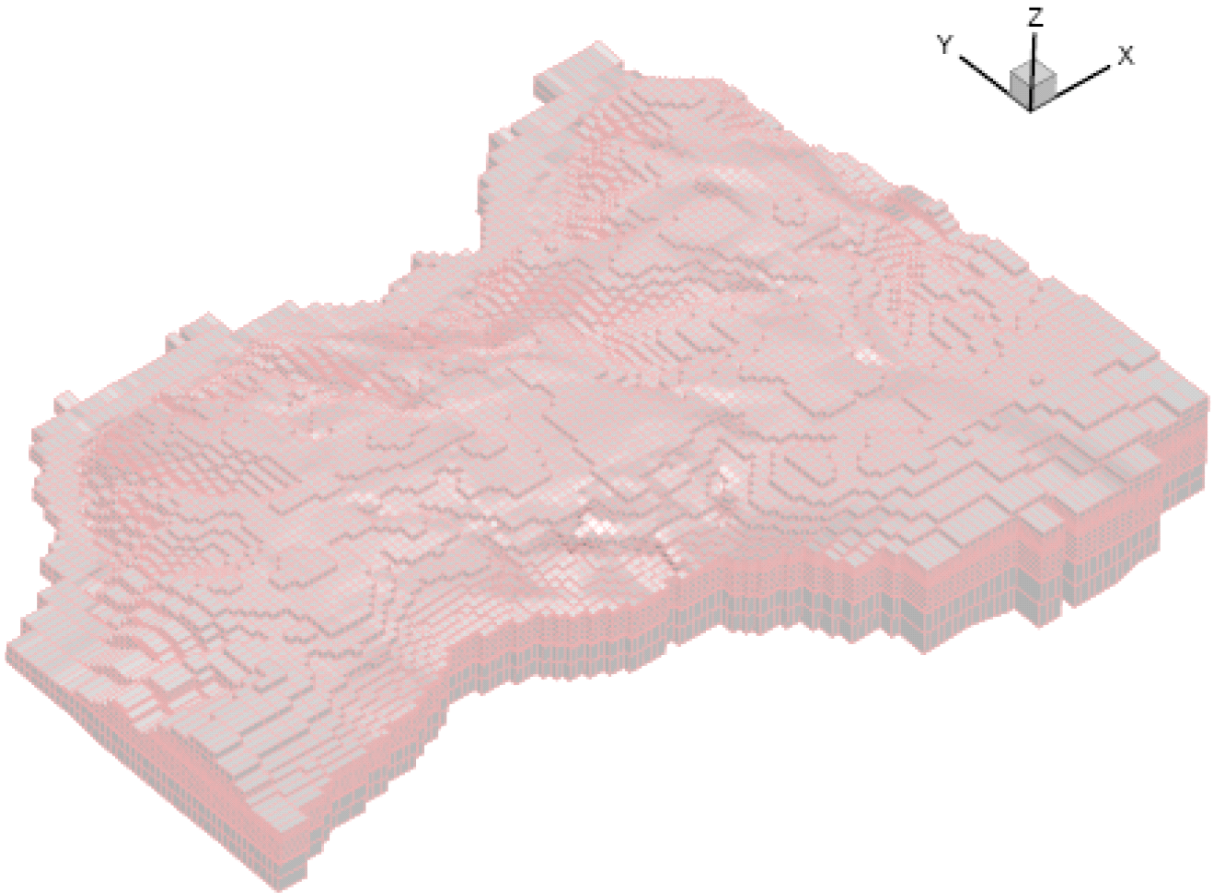

[WSRC-TR-2004-00106]

Hydraulic conductivity values in the model are based on a characterization GSAD discussed in Section 3.1.5. The conductivity field is heterogeneous within hydrogeologic units and reflects variations present in the characterization data. The average horizontal conductivities in the saturated UTR-UZ, UTR-LZ, and Gordon Aquifer are approximately 10, 13, and 38 ft/d, respectively. The average vertical conductivities for the TCCZ and the Gordon Confining Unit are 6.0E-03 and 1.0E-05 ft/d, respectively. [WSRC-TR-96-0399] Figure 4.2-17 illustrate typical horizontal and vertical model hydraulic conductivity fields, respectively, along a representative cross-section through the GSA. The GSA/PORFLOW Model calibration and validation used measured, well water levels.

Figure 4.2-17: North-South Cross Sections of GSA/PORFLOW Model - Horizontal and Vertical Hydraulic Conductivity Variations Views

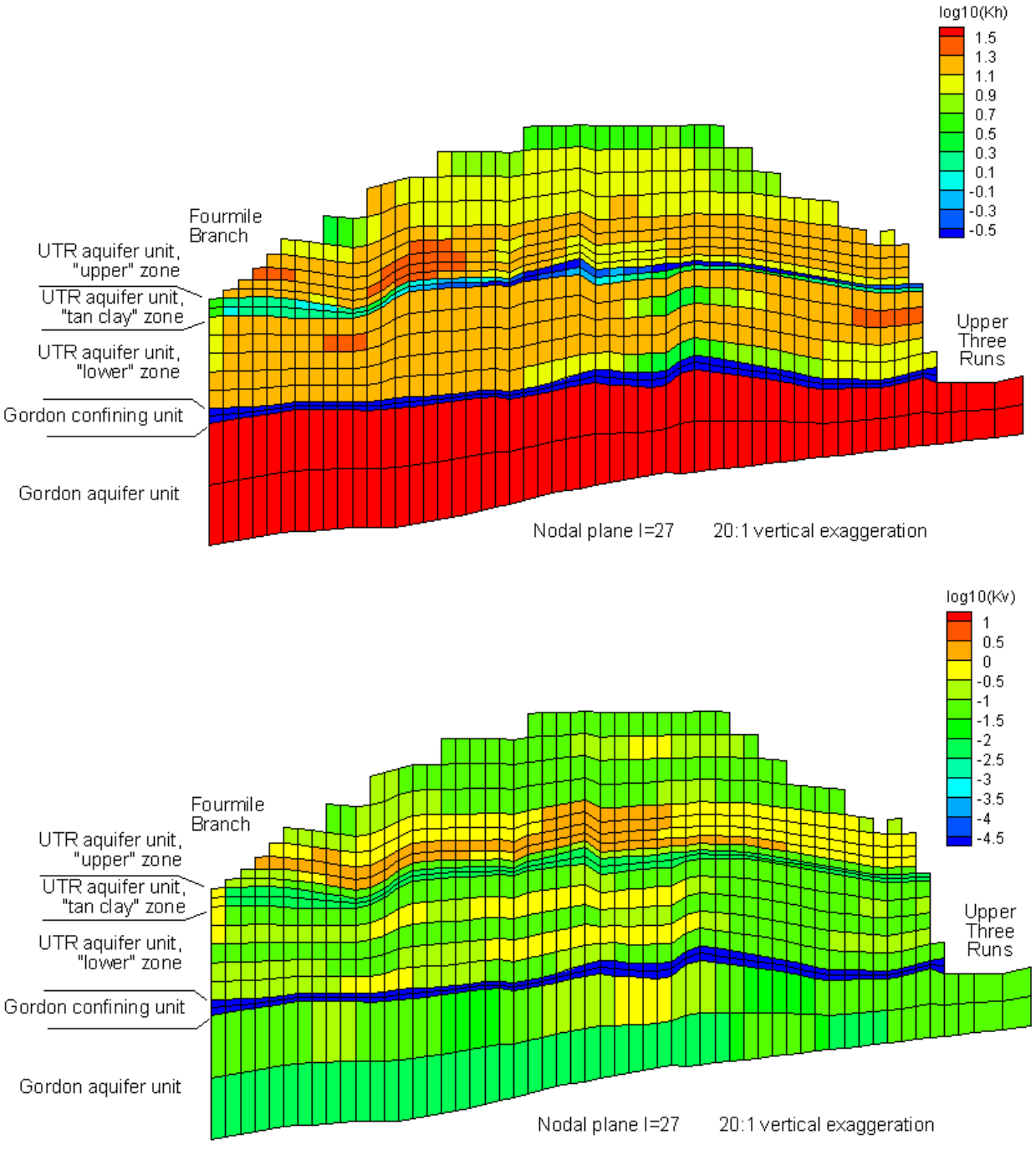

The average natural recharge over the entire model domain is 14.7 in/yr compared to approximately 15 in/yr from prior groundwater budget studies. [WSRC-TR-2004-00106] Various man-made features (e.g., basins) provide additional recharge in localized areas. The estimated discharge rates to UTR and Fourmile Branch, within the model domain, are 18.2 and 2.6 ft^3/sec, respectively. [WSRC-TR-2004-00106] The simulated discharge rates are 11.4 and 3.8 ft^3/sec, respectively. Predicted seepage faces are consistent with field observations. Simulated hydraulic heads, vertically averaged over the entire thickness of the UTR-LZ, UTR-UZ, and Gordon Aquifer, agree with potentiometric maps based on measured heads. The evaluation of simulated versus measured heads utilized GSA/PORFLOW results for the vertically averaged head and the residuals between computed and measured heads. [WSRC-TR-2004-00106] Simulated flow directions vertically averaged over the entire thickness of the aquifer zones agree with conceptual models of groundwater flow.

Adequacy of GSAD Data Set for Groundwater Flow Simulation

The GSAD includes field data and interpretations collected in the GSA through 1996. Although characterization and monitoring have been ongoing, the additional data has not altered fundamental understanding of groundwater flow patterns and gradients in the GSA. The GSAD is a subset of site-wide data sets of soil lithology and groundwater information. These larger sets of data are captured in the Environmental Restoration Data Management System (ERDMS) database, ACP landmark database and other resources. The relationship between GSAD and the full set of data is pictured in Figure 4.2-18.

Figure 4.2-18: The GSAD Database Relationship

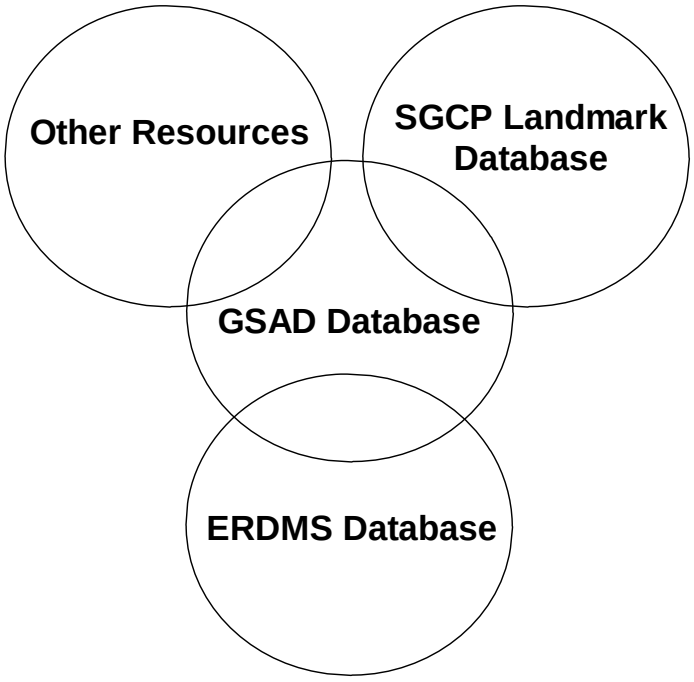

The more recent field data (i.e., 1996-2006) is limited to CPT picks and a few geophysical logs with no new HTF foot-by-foot core descriptions. During the 1980s and early 1990s, significant work was conducted within the GSA to better define the hydrogeology including installation of well clusters and continuous core descriptions and geophysical logs associated with the deepest well in the cluster. At that point, the hydrostratigraphy of the GSA was considered sufficiently defined, and no additional characterization was planned. Since the mid-1990s, wells have been installed to better define plumes and CPT logs have been generated for structural, seismic, and vadose zone monitoring purposes. Most of the new data are shallow and consist of CPT or geophysical logs. Most of the new data may provide picks for the top two aquifers surfaces only. [SRNL-STI-2010-00148]

In order to evaluate the need to update the original GSAD to incorporate new hydrogeologic information, two evaluations were identified. Figure 4.2-19 shows recent hand-drawn water table contour maps for the GSA based on water level data collected in 1995, 1998, and 2003. Contours were developed using mean water levels from SRS wells, field verification of perennial stream reaches, and the USGS 1:24000 scale topography data. [WSRC-MS-95-0524, WSRC-TR-98-00045, WSRC-TR-2003-00250] These contour maps are consistent with each other indicating that there has not been a significant change in our understanding of long-term average water table conditions in the GSA since the mid-1990s.

Figure 4.2-19: Water Table Contour Maps for GSA

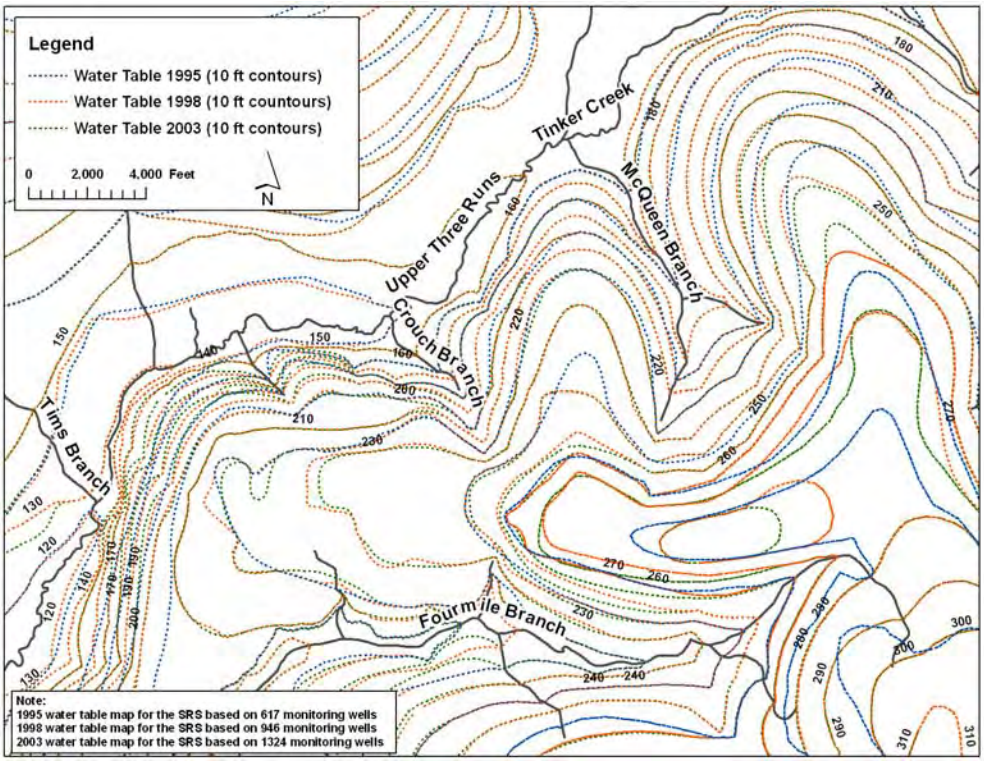

A report was prepared in 2010 (*Hydrogeologic Data Summary in Support of the H-Area Tank Farm Performance Assessment*) to provide a summary of recent available geotechnical data for the HTF vicinity. This report focused on sediment descriptions, geotechnical data (e.g., grain size analyses), and interpretations for the vadose zone from historical and recent studies. The report also included potentially significant findings regarding the saturated zone (e.g., existence/thickness of the TCCZ). Review of the data collected in SRNL-STI-2010-00148 showed that the available data is consistent with the assumptions made for vadose zone sediments in the HTF PA modeling effort. [SRNL-STI-2010-00148]

One area of particular interest in the SRNL-STI-2010-00148 data review was the TCCZ. Measurements of the TCCZ thickness were compared within the HTF to the TCCZ thickness as represented in the GSA/PORFLOW Model, which was developed from data lying outside the HTF. Generally, the two values are close, and uncertainty in data quality interpretation is not exceeded by the differences. The study indicates that the TCCZ exhibits spatial correlation across HTF, such that interpolation-using data outside the HTF produces reasonable estimates of actual thickness. The GSA/PORFLOW Model representation of the TCCZ is judged reasonable for HTF PA modeling.

Best-estimate predictions and field monitoring indicate that plume migration can be expected to occur through the UTR-UZ and UTR-LZ for travel distances through at least 100 meters. Contamination may or may not pass through the UTR TCCZ before reaching the 100-meter perimeter. In PORFLOW modeling, the TCCZ is assigned the same geochemical properties (distribution coefficient) as the aquifer zones for UTR-UZ and UTR-LZ (no credit is taken for the TCCZ as a potential chemical barrier to plume migration laterally and downward). Hydraulically, the TCCZ is assigned a vertical conductivity of 2.1E-06 cm/s (26 in/yr) in H Area. Thus, the confining zone is also relatively ineffective as a flow barrier.

Although the Gordon Confining Unit may not be completely continuous in all areas of the GSA, the formation has sufficient continuity to function as a significant flow barrier, and be classified as a "confining unit" as opposed to a "confining zone" (e.g., TCCZ). Variation in leakance through the Gordon Confining Unit would lead to somewhat faster and/or slower travel within the UTR Aquifer. Uncertainty in aquifer velocity/travel time is considered in GoldSim modeling. Higher leakance would increase peak concentration in the Gordon Aquifer, but decrease the overall peak, which occurs in the UTR Aquifer. The GSA/PORFLOW representation of the green clay as a confining unit is viewed as reasonable for HTF PA modeling.

Figure 4.2-20 provides a comparison of the GSA 2003 hand-contoured water table map (bottom) and the water table predicted by the GSA/PORFLOW 2008 model.

Figure 4.2-20: Comparison of (a) 2008 GSA/PORFLOW Model Predicted and (b) Hand-Contoured 2003 Water Table Maps

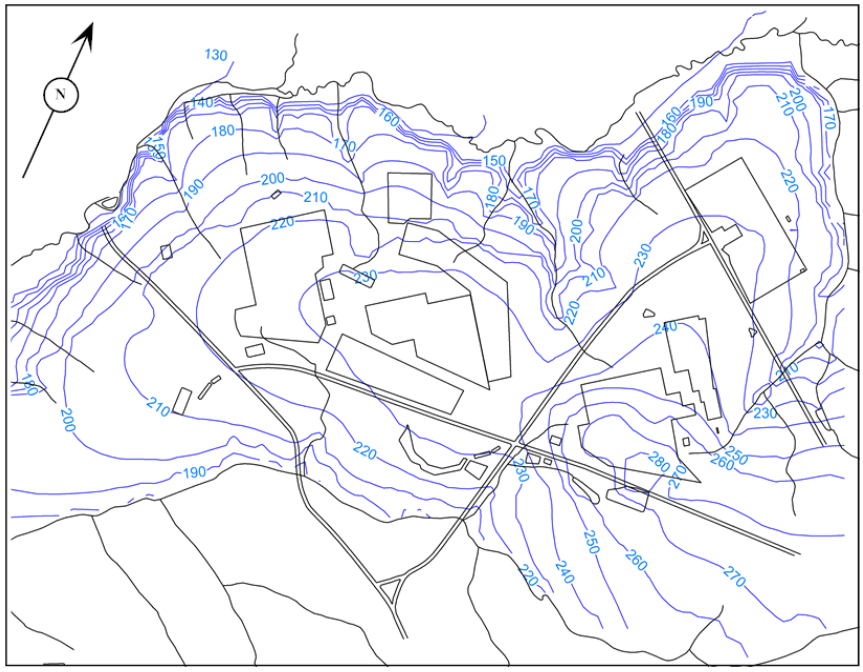

(a)

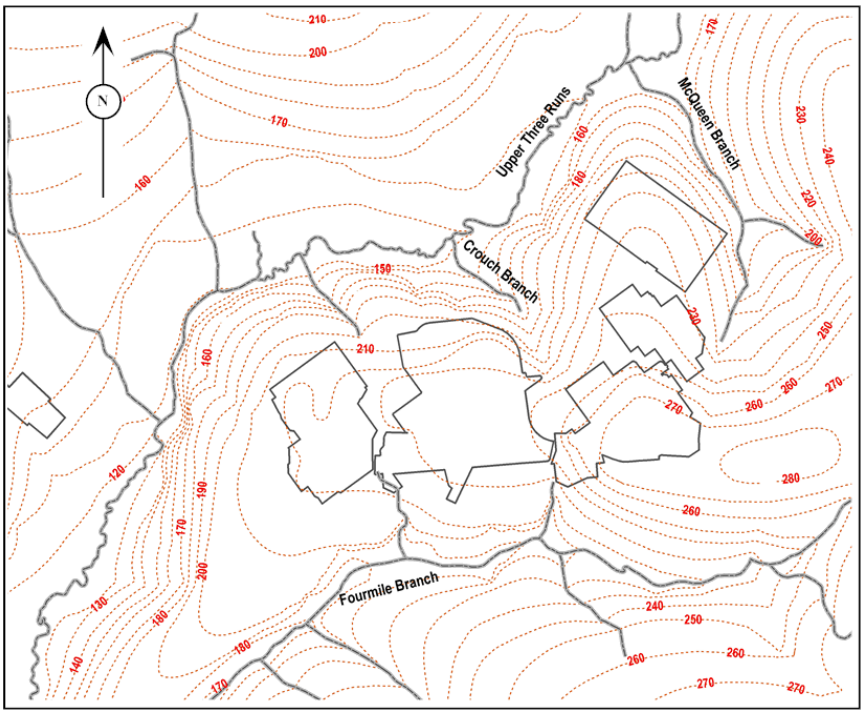

(b)

[SRNL-STI-2010-00148]

Table 4.2-21 summarizes hydraulic head residuals between the model and the field data. [WSRC-TR-2004-00106, Section 3.1] Table 4.2-21 also summarizes more recent well water level data through 2006 (available because of new well installations and continued monitoring). The agreement between the model and the data set through 2006 is similar to that of the original data set. [SRNL-STI-2010-00148]

Table 4.2-21: Hydraulic Head Residuals - GSA/PORFLOW Model and Field Data through 2006

Aquifer Zone	Number of Wells	Median Residual (ft)	Average Residual (ft)	Root-Mean-Square Residual (ft)	Minimum Residual (ft)	Maximum Residual (ft)
Up to 1995 Data	**638**					
Gordon	79	-0.0	-0.5	1.7	-4.7	2.5
UTR-LZ	173	+0.8	+0.6	4.6	-9.4	27.0
UTR-UZ	386	-0.1	-0.5	3.4	-15.2	10.0
Up to 2006 Data	**917**					
Gordon	94	+0.3	-0.0	1.5	-3.8	2.6
UTR-LZ	272	+1.1	+1.0	4.7	-11.9	27.0
UTR-UZ	551	+0.8	+0.1	3.5	-16.8	14.5

[SRNL-STI-2010-00148]

4.2.2.1.5 Transport Model Interfaces

As noted earlier, the ICM of subsurface water flow and contaminant transport comprises three principal elements, 1) the closure cap, 2) the vadose zone, and 3) the saturated aquifer zone, as illustrated in Figure 4.2-11.

The prescribed rainfall condition, in the form of daily rainfall values over an extended period, is the primary input or external boundary condition to the closure cap flow analysis. The closure cap model produces a net infiltration rate at the bottom of the closure cap that becomes a flow boundary condition to the adjoining vadose zone. The assumption is water infiltration to the closure cap is free of contaminants, so the concentration is set to zero at the top boundary of the vadose zone.

Groundwater flow in the much larger scale saturated zone, or aquifer model, is controlled by net infiltration or recharge over a broad area surrounding the HTF. Rather than using the flow exiting the vadose zone at the water table as a direct input to the aquifer model, an average recharge value is applied to the aquifer flow model based on field studies. [WSRC-TR-96-0399, Volume 2] For saturated zone contaminant transport, the contaminant flux leaving the bottom of the vadose zone model becomes the source of contamination entering the aquifer.

Each water table flux contribution from an individual waste tank is assigned to the aquifer transport grid by uniformly distributing the flux to those water table cells with centroids lying within the footprint of the waste tank. Each flux originating from discrete

ancillary equipment is assigned to the cell with the closest centroid. Flux from transfer lines is spread uniformly over the facility footprint.

4.2.2.2 Material Properties

Material properties of interest appear in technical reports including:

- The conceptual closure cap layers (SRNL-ESB-2008-00023)
- The vadose zone soil (SRNL-STI-2010-00148)
- The cementitious materials for example waste tank top and sides, basemat, and grout (WSRC-STI-2006-00198, WSRC-STI-2007-00369)
- The CZ (WSRC-STI-2007-00544)
- The carbon steel waste tank liner (WSRC-STI-2007-00061, SRNL-STI-2010-00047)
- The stainless steel ancillary equipment (WSRC-STI-2007-00460)
- The soil and groundwater in the saturated zone, for example the aquifers underlying the waste tank systems (SRNL-STI-2010-00148)

Because material properties form a key part of the ICM, some data from other technical reports identified above are duplicated in this section for completeness. Material properties for carbon steel, cementitious material, and stainless steel are also provided. The only relevant information for both carbon and stainless steel is the projected time of failure under different conditions. The assumption for this material is it is impermeable until the time of steel failure, and then becomes sufficiently permeable that it is not a barrier to contaminant migration.

4.2.2.2.1 Conceptual Closure Cap Material Properties

Preliminary values for conceptual closure cap layer thickness and infiltration rate changes with time from the predicted degradation of the conceptual closure cap are provided in SRNL-ESB-2008-00023.

Tables 4.2-22 and 4.2-23 provide the conceptual closure cap layer thicknesses and infiltration rates, respectively. These values are considered preliminary values for the HTF closure cap conceptual design.

Table 4.2-22: Conceptual Closure Cap Layers Top to Bottom

Layer	Layer Thickness (in)
Vegetative Cover	N/A
Topsoil	6
Upper Backfill	30
Erosion Barrier	12
Geotextile Fabric	NC
Middle Backfill	12
Geotextile Filter Fabric	NC
Lateral Drainage Layer	12
Geotextile Fabric	NC
HDPE Geomembrane	0.06 (60 mil)
GCL	0.2
Upper Foundation Layer	12
Lower Foundation Layer	72 (min.)

[SRNL-ESB-2008-00023, Table 1]
NC = Not Calculated

Table 4.2-23: Conceptual Closure Cap Infiltration Over Time

Time Interval (yr)	Average Annual Infiltration Through GCL (in/yr)
0	0.00088
100	0.010
180	0.17
290	0.37
300	0.50
340	1.00
380	1.46
560	3.23
1,000	7.01
1,800	10.65
2,623	11.47
3,200	11.53
5,600	11.63
10,000	11.67

[SRNL-ESB-2008-00023, Table 2]

4.2.2.2.2 Vadose Zone Material Properties

In this section, the focus of this portion of the overall HTF closure input conceptual model (Figure 4.2-11) is on the region between the existing grade (prior to closure cap installation) and the top of the water table, excluding the waste tanks themselves. This area (number 5 in Figure 4.2-11) includes the concrete working slab on which the waste tanks were built, the undisturbed, unsaturated soil under this slab, and the existing backfill soil around the waste tanks. Note that the modeling properties of procured sand used in the waste tank liner systems are also discussed herein. The parameters that comprise this section include:

- Vadose zone thickness under each of the 29 waste tanks
- Saturated effective diffusion coefficient
- Average total porosity
- Average dry bulk density
- Average particle density
- Saturated horizontal hydraulic conductivity
- Saturated vertical hydraulic conductivity
- Distribution coefficient values
- Characteristic curves (suction head, saturation, and relative permeability)

Vadose Zone Background

Section 3.2.1 provides a detailed description of the construction of the various waste tank groups situated in HTF. The general construction approach for each waste tank group involved four major steps:

1. Excavating an area below grade and stockpiling the excavated soil
2. Laying an non-reinforced concrete working slab at the bottom of the excavation to provide a stable platform for construction activities
3. Constructing the waste tanks
4. Backfilling around the waste tanks with the previously removed soil

A substantial body of vadose zone characterization data is available for the GSA, especially for the E-Area LLW Disposal Facilities, which are located approximately 3,000 feet northwest of the HTF. Available data show that the vadose zone at HTF is similar to the vadose zones in both E Area and F Area. [SRNL-STI-2010-00148] Figure 4.2-21 is a location map for borings across the GSA, including borings from F Area, E Area, and H Area. The GSA is located on a topographic high between two streams, UTR to the north and Fourmile Branch to the south. Figure 4.2-22 shows a geologic cross-section across the GSA, based on the core descriptions and gamma ray logs from seven boring locations (three from H Area, three from E Area, and one from F Area) specified on Figure 4.2-21. Across the GSA, marker bed relations (i.e., vertical occurrences of the TCCZ and Gordon Confining Unit), are identified and appear similar in nature. [SRNL-STI-2010-00148]

A review of the recent and historical water level data in the HTF indicates that the Type I tanks (Tanks 9 through 12) are submerged, Type II tanks (Tanks 13 through 16) are partially submerged, and all the remaining waste tanks have a negligible to relatively thin vadose zone (< 20 feet). The vadose zone is thickest beneath the northern Type IIIA tanks (Tanks 38 through 43). In the HTF, the undisturbed vadose zone beneath the waste tanks appears to correspond to the "Upland Unit" and Tobacco Road Sand Formation [SRNL-STI-2010-00148], according to existing hydrogeologic interpretations of CPT logs presented in Figure 4.2-23. The properties of this zone most likely represent the upper vadose zone properties as identified in WSRC-STI-2006-00198. [SRNL-STI-2010-00148]

Figure 4.2-21: The GSA Geologic Cross-Section Location Map

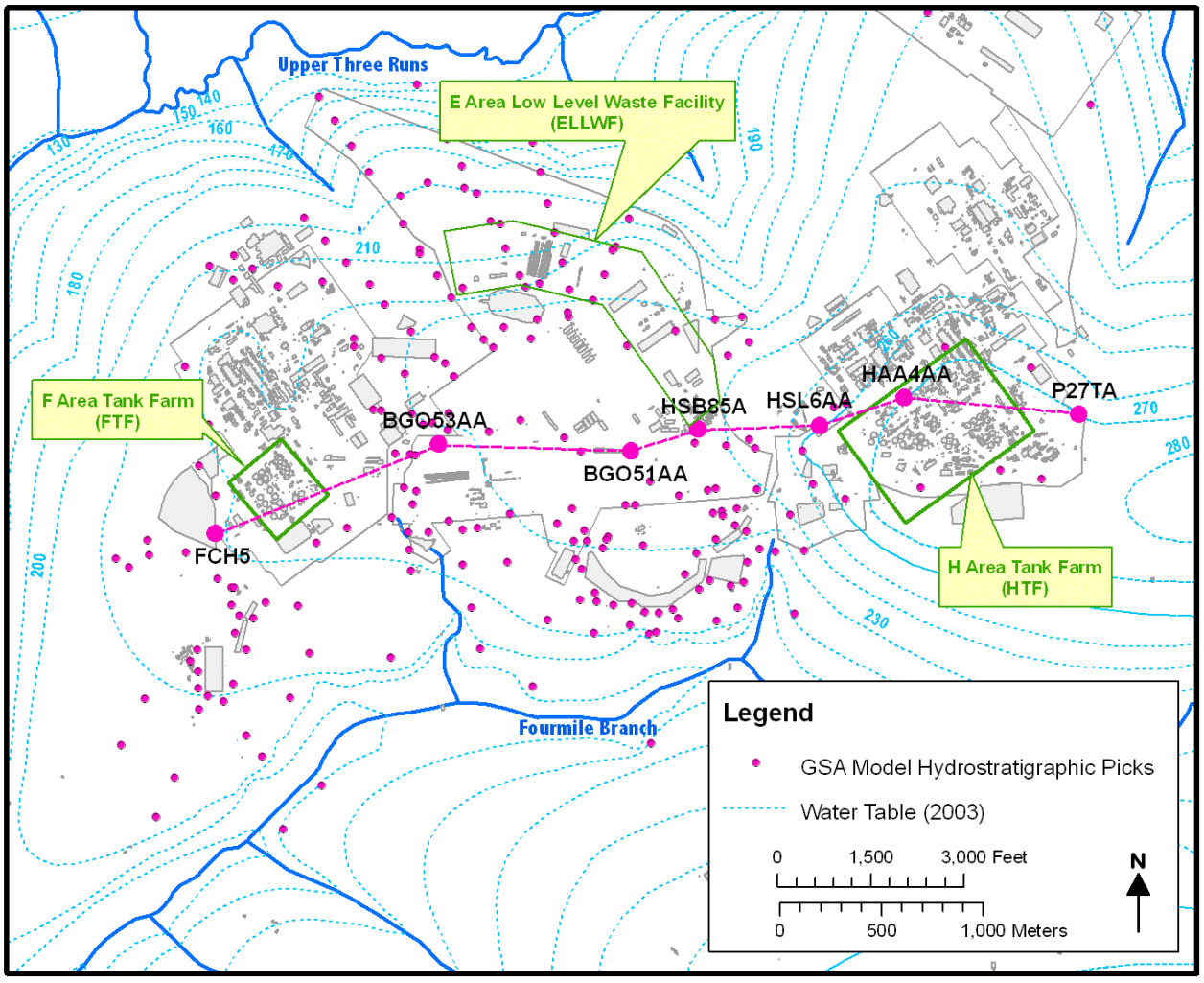

[SRNL-STI-2010-00148]

Figure 4.2-22: Comparison of E-Area, F-Area, and H-Area Vadose Zone Using Core Descriptions and Gamma Ray Logs

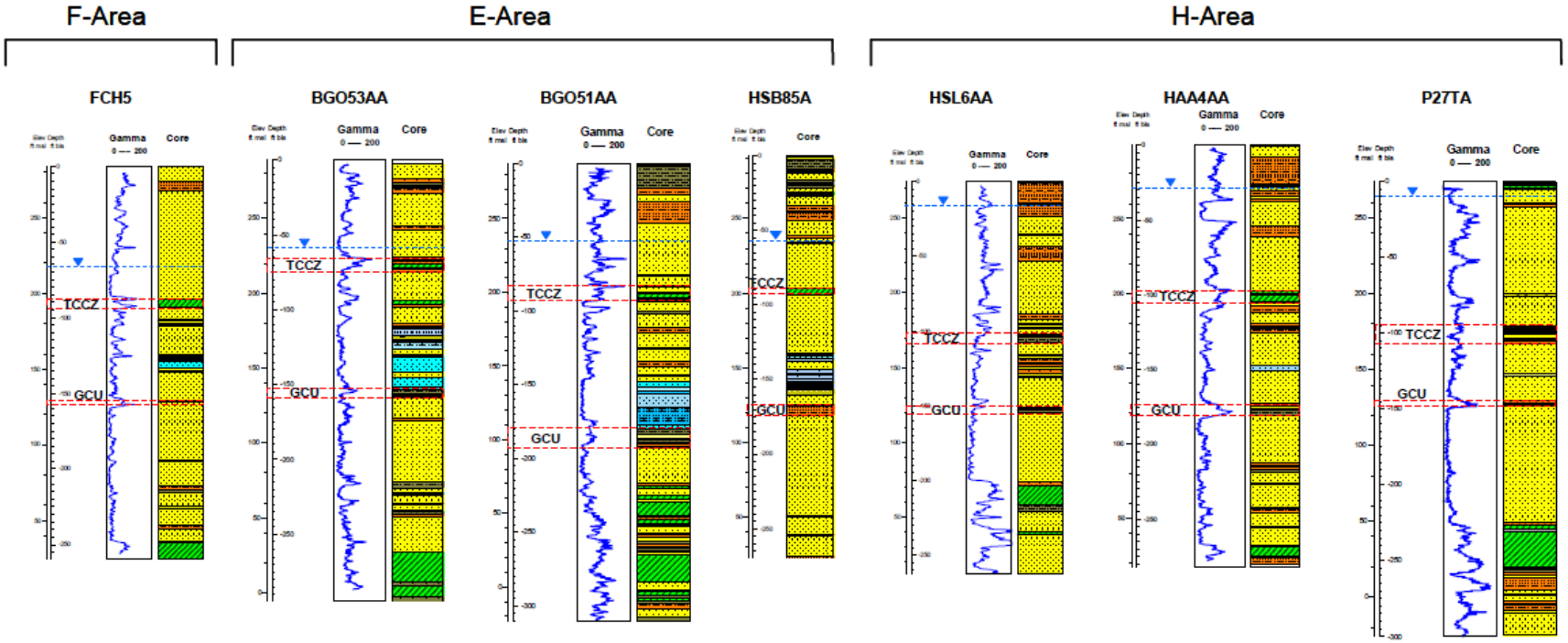

NOTES: MSL = mean sea level; bls = below land surface; ft = feet; Gamma is shown in API (American Petroleum Institute) units; TCCZ = Tan Clay Confining Zone as defined in the GSA/PORFLOW Model database; color coated lithology columns are based on foot by foot core descriptions; in general colors correspond to the following: yellows = sands, grays and greens = clays, oranges = clayey sands, blues = calcitic sections/limestones (SRNL-STI-2010-00148)

Figure 4.2-23: Comparison of H-Area Vadose Zone Using CPT Logs

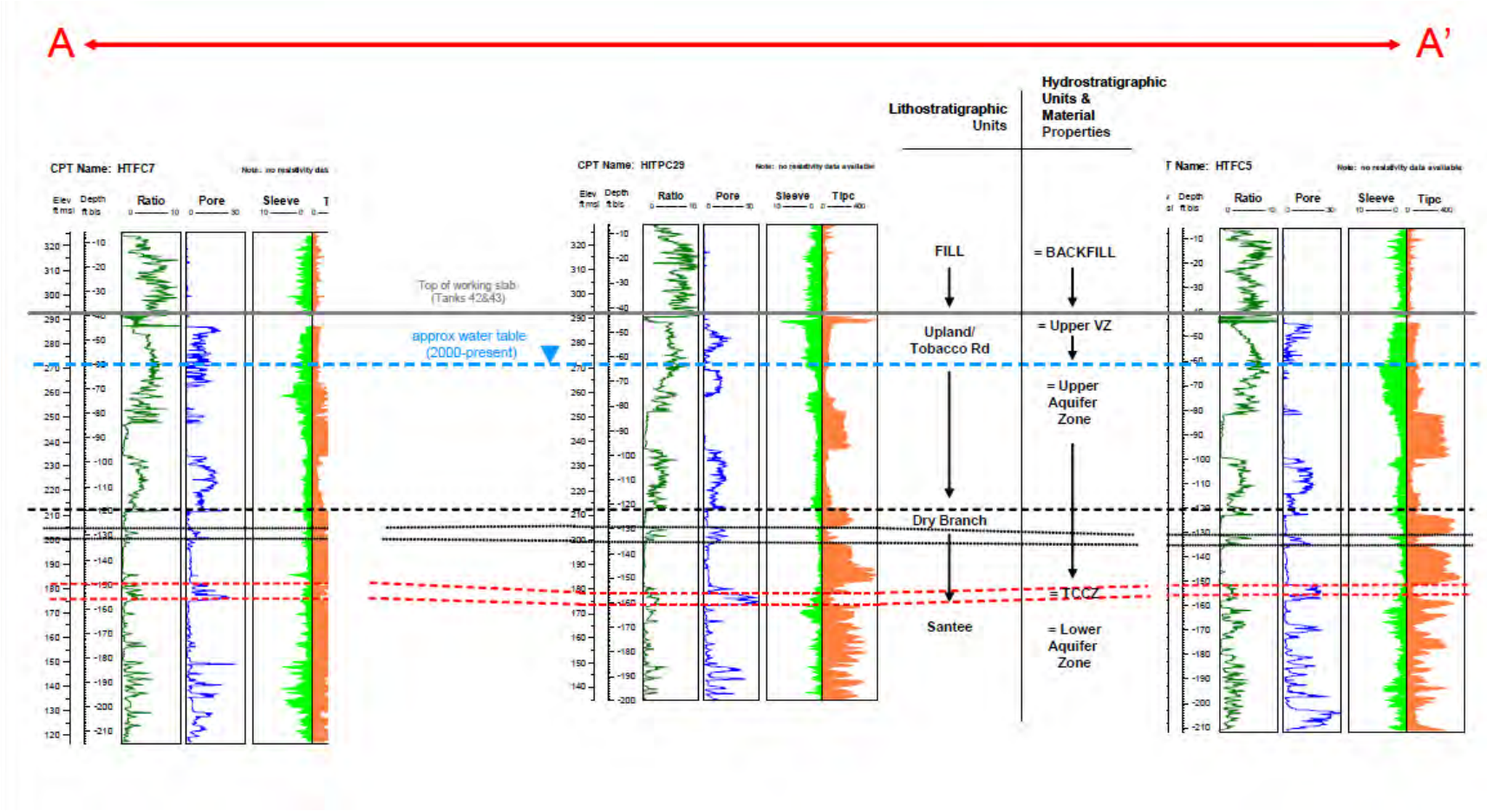

NOTES: msl = mean sea level; bls = below land surface; ft = feet; TCCZ = Tan Clay Confining Zone; Upper VZ = Upper Vadose Zone;
FOR CPT LOGS: sleeve = sleeve resistance (tsf); tipc = tip resistance (tsf); ratio = friction ratio (reflects sleeve/tip); pore = pore pressure (psi)
[SRNL-STI-2010-00148]

Concrete Working Slab

As described in Section 3.2.1, all the HTF waste tanks have a working slab below their basemat except the Type IV tanks (Tanks 21 through 24), which have a maintenance slab between them. Table 4.2-24 summarizes available information on the design of the working slabs for the different HTF waste tank types. Figure 4.2-24 shows a typical working slab under Tanks 13 through 16 (Type II tanks). The working slabs for the Type IIIA tanks were broken up or perforated with holes before backfilling, and this condition is assumed to exist between the waste tanks, but not underneath the waste tanks.

Table 4.2-24: Waste Tank Working Slab Information by Type

Tank Type	Working Slab Design
I	A 4 inches thick slab with a 42 foot 5-inch radius, and a wire mesh layered in the middle (W145225)
II	A 6 inches thick slab, with the four waste tanks placed within a 255 foot x 274 foot rectangle (W163048)
IV	A 3-inch drainage and maintenance slab between waste tanks (W230826)
III	A 6 inches thick slab that slopes away from the waste tanks extending at least 30 feet beyond waste tank vault (W236439)
IIIA	A minimum 4-inch thick working slab filling the entire excavation, extending at least 25 feet beyond the waste tank vaults and was either broken up or punched with holes (4-inch diameter on 18-inch center) prior to backfilling as shown in Figure 3.2-30 (W449843, W700834, W706301)

Figure 4.2-24: Working Slab for Tanks 13 through 16

Table 4.2-25 shows estimated material properties for the working slabs. Figure 4.2-25 provides the characteristic curves (suction head, and relative permeability) for the working slab.

Table 4.2-25: Estimated Working Slab Material Properties of Interest

Material	Saturated D_e (cm^2/sec)	η_e (%)	ρ_h (g/cm^3)	ρ_n (g/cm^3)	K_{sat} (cm/sec)
Low Quality Concrete	8.0E-07	21.1	2.06	2.61	1.0E-08

[WSRC-STI-2006-00198 for low quality concrete]
D_e = Effective Diffusion Coefficient
η_e = Effective Porosity
ρ_h = Dry Bulk Density
ρ_n = Particle Density
K_{sat} = Saturated Hydraulic Conductivity

Figure 4.2-25: Working Slab (Low Quality Concrete) Characteristic Curves

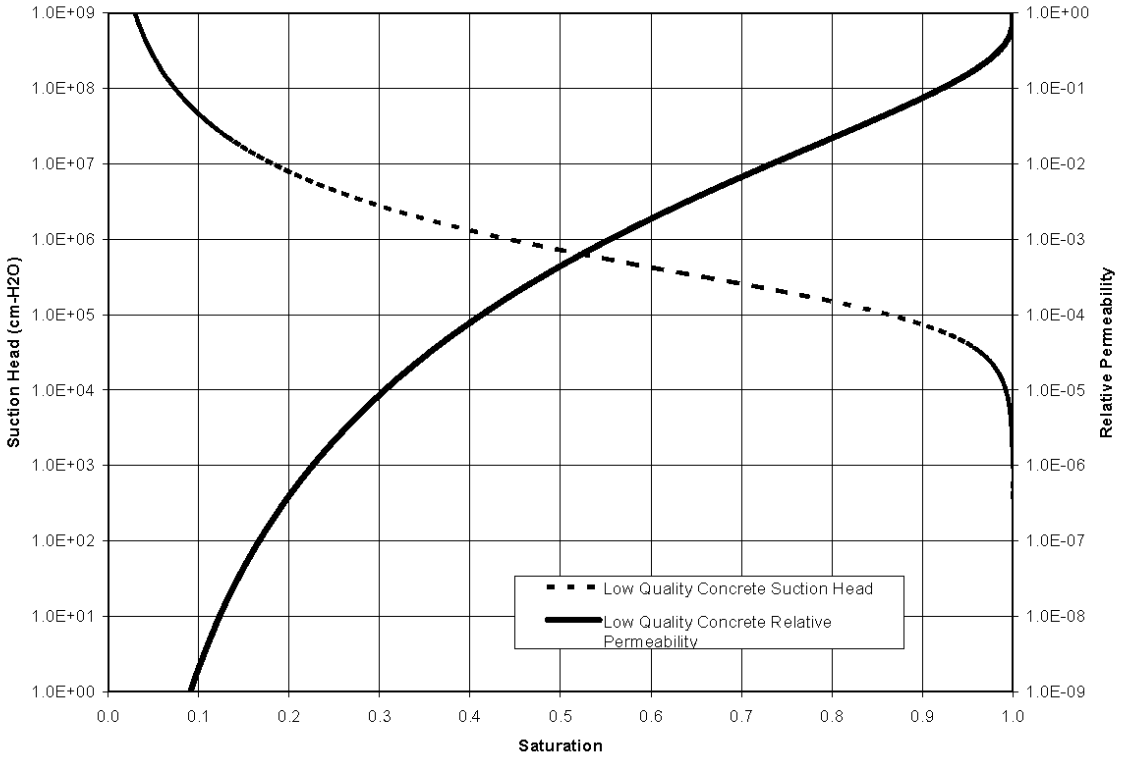

[WSRC-STI-2006-00198]

Given the minimal thickness of the working slabs compared to the waste tank basemats, the slabs were ignored in modeling contaminant transport through the waste tank bottom and basemat into the vadose zone for all waste tank types except for the Type II tanks. For the Type II tanks, there is inventory modeled in the sand pads and the working slab is 6 inches thick.

Vadose Zone and Backfill Material Properties

The physical and chemical properties of the vadose zone soils surrounding and below the contamination sources are needed for the ICM. Data tables are presented for several vadose zone material properties: saturated effective diffusion coefficients, average total porosity, average dry bulk density, saturated horizontal hydraulic conductivity, saturated vertical hydraulic conductivity, and distribution coefficient values. The properties are assumed not to change over time because of the stability of the soil and soil structure. These material properties are summarized in Tables 4.2-26, 4.2-27, and 4.2-28. Figures 4.2-26 and 4.2-27 illustrate the vadose zone and backfill characteristic curves, showing suction head, saturation, and relative permeability.

Table 4.2-26: Estimated Vadose Zone Material Properties of Interest

Material	Saturated D_e (cm^2/sec)	Average η_T (%)	Average ρ_h (g/cm^3)	Average ρ_n (g/cm^3)	Horizontal K_{sat} (cm/s)	Vertical K_{sat} (cm/s)
Upper Vadose Zone	5.3E-06	39	1.65	2.70	6.2E-05	8.7E-06
Lower Vadose Zone	5.3E-06	39	1.62	2.66	3.3E-04	9.1E-05

[WSRC-STI-2006-00198]
D_e = Effective Diffusion Coefficient
η_T = Total Porosity
ρ_h = Dry Bulk Density
ρ_n = Particle Density
K_{sat} = Saturated Hydraulic Conductivity

Figure 4.2-26: Upper and Lower Vadose Zone Characteristic Curves

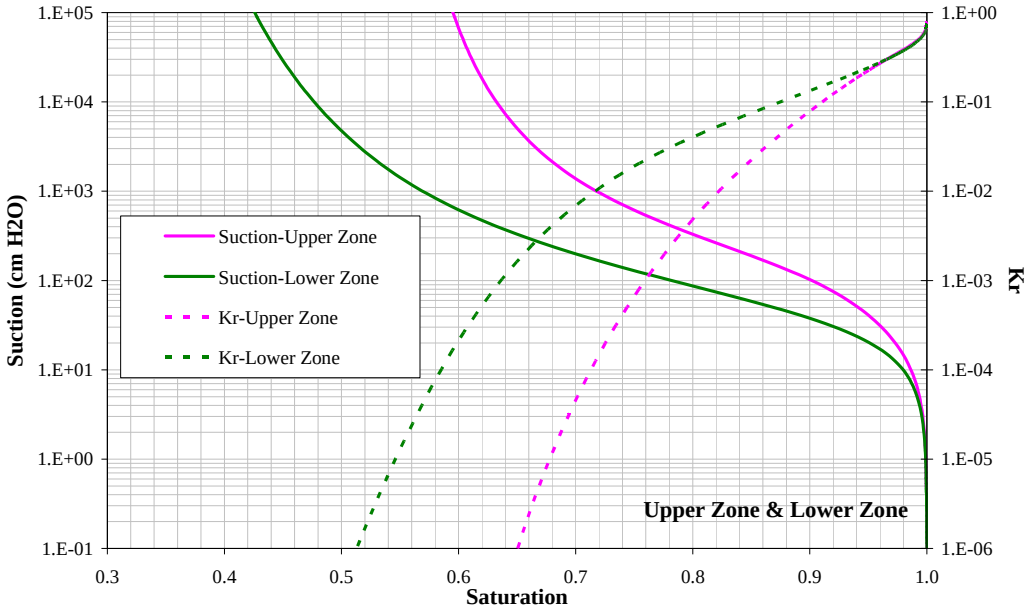

[WSRC-STI-2006-00198]

Table 4.2-27: Estimated Backfill Material Properties of Interest

Material	Saturated D_e (cm^2/sec)	Average η_T (%)	Average ρ_h (g/cm^3)	Average ρ_n (g/cm^3)	Horizontal K_{sat} (cm/s)	Vertical K_{sat} (cm/s)
Backfill	5.3E-06	35	1.71	2.63	7.6E-05	4.1E-05

Note For controlled compacted backfill; all property values except for saturated D_e are based on laboratory data for samples of similar backfill from the GSA; saturated D_e values are based on literature values.

[WSRC-STI-2006-00198, Table 5-18]

D_e = Effective Diffusion Coefficient

η_T = Total Porosity

ρ_h = Dry Bulk Density

ρ_n = Particle Density

K_{sat} = Saturated Hydraulic Conductivity

Figure 4.2-27: Backfill Characteristic Curves

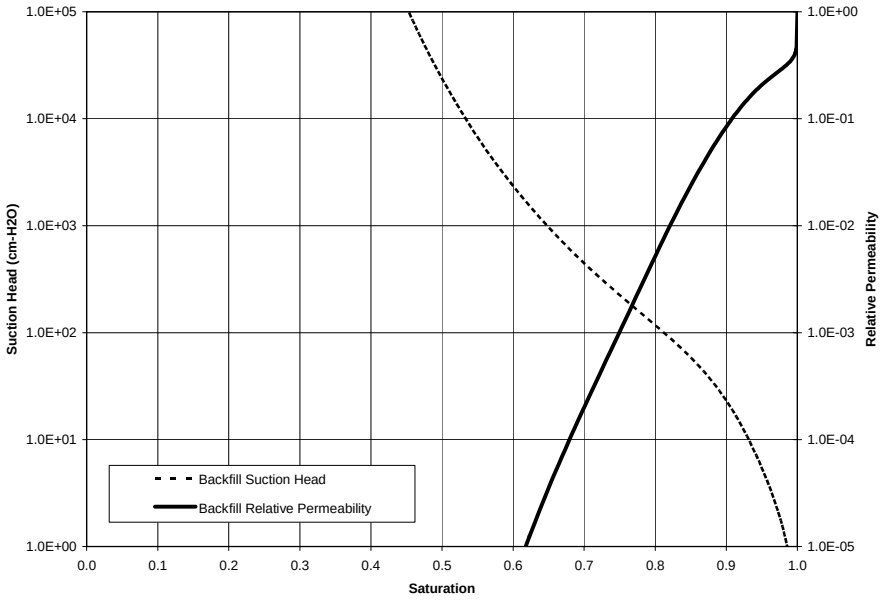

[WSRC-STI-2006-00198]

Table 4.2-28 summarizes available information about the backfill that is present around the waste tanks and, in some cases, also over the tanks.

Table 4.2-28: Waste Tank Backfill Information by Type

Tank Type	Backfill Information
I	Excavated soil was compacted around and over the waste tanks. The backfill was installed per W145225. Nine feet of backfill was emplaced over the waste tank tops extending to a finish grade of approximately 300 feet above MSL. [W146377]
II	Backfill around the waste tanks was installed per drawing W163048 specifications. The backfill below the working slab is test controlled compacted backfill not to contain more than 7% material passing through a #200 sieve (0.0029-inch sieve opening). The backfill around the waste tanks was placed in successive, uniform layers, with a compacted thickness no more than 12 inches. It was then brought to an elevation level with the top of the waste tanks (approximately 325 feet above MSL) and extended laterally for a minimum of 21 feet then sloped down at an angle less than 1:1 for a lateral distance of 31 feet, reaching final grade at an elevation of 300 feet above MSL. [W163048]
IV	Earth was excavated from the area surrounding the waste tanks to a depth of 17 feet below existing grade. [W230826] Vermiculite bags (minimum 8 inches thick) were installed immediately adjacent to the waste tank walls to provide cushion layer for expansion voids behind and between bags were filled with earth backfill. [DP-478] Standard compaction of excavated soil (sandy clay) was placed around and over waste tanks. [W231221, W230976, W231023]
III/IIIA	All areas receiving backfill (including sloped areas) were prepared per W700834. Excavated soil was compacted around and over the waste tanks. Prior to placing backfill, either the working slab was broken up or 4-inch holes, 18 inches on center were punched in the slab. In other areas receiving backfill, the soil cover (e.g., vegetation, top soil, soil-erosion protection layer) was removed and the ground scarified to a depth of 4 inches. Backfill with the amount (percent) of water most favorable to achieve not less than 95% of the maximum dry density was used. [W701036]. Backfill was placed to within 1 foot of the elevation of the top of the Type III/IIIA tanks. [W231220, W700242, W701036, W704700]

As indicated in Table 4.2-28, the excavated soil was used for backfilling around the waste tanks. Excavated soil was also used to cover the tops of the waste tanks, except for the Type IIIA tanks, as shown in this table. The cover soil consisted predominately of upper vadose zone soil (i.e., sand with a significant silt and clay content) with some lower vadose zone soil (i.e., a coarser-grained soil). Soil considered too sandy was not utilized as backfill. [WSRC-STI-2006-00198]

The backfill was placed either by standard compaction or by test-controlled compaction. Standard compaction consisted of rolling damp, maximum 12-inch lifts of soil with mechanical compaction equipment until a visually uniform compaction was obtained. Test-controlled compaction consisted of compacting moisture-conditioned soil with mechanical compaction equipment until densities greater than or equal to 95% of maximum dry soil density was obtained as determined by testing. One exception to this general rule was the use of bags of vermiculite around Tanks 21 through 24. It was assumed that the presence of the material would have an insignificant effect on modeling.

Recommended distribution coefficient values for the vadose zone and backfill soil are taken from recent compilation of geotechnical data prepared in support of site PA modeling. [SRNL-STI-2009-00473] Estimates of the distribution coefficient values were provided for each element and soil type. These values are based primarily on SRS site-specific experimental data, some central value of literature, or on expert judgment, with the site-specific experimental data being the preferred information

source. Table 4.2-29 identifies distribution coefficient values of the vadose zone and backfill soils. The distribution coefficient values for each radionuclide in Table 4.2-29 were used in deterministic, sensitivity, and uncertainty analyses in the PA. SRNL-STI-2009-00473 provides information for soil distribution coefficient values when influenced by the high pH of cementitious material leachate. The values are applicable to vadose (unsaturated) zone soils and are not applicable to waste tanks in the water table (Type I and II tanks). The transition to non-cement leachate impacted distribution coefficient value will coincide with the transition of the CZ to Oxidized Region III.

Table 4.2-29: Recommended K_d Values for the Vadose Zone

Element	Soils Media		Cement Leachate Impacted Soils Media	
	Backfill Soil (mL/g)*	Vadose Zone Soil (mL/g)**	Backfill Soil (mL/g)*	Vadose Zone Soil (mL/g)**
Ac	8,500	1,100	12,750	1,650
Ag	150	60	480	192
Al	1,300	1,300	1,950	1,950
Am	8,500	1,100	12,750	1,650
Ar	0	0	0	0
As	200	100	280	140
At	0.9	0.3	0.1	0
Ba[b]	101	15	303	45
Bi	8,500	1,100	12,750	1,650
Bk	8,500	1,100	12,750	1,650
C	400	10	2,000	50
Ca	17	5	51	15
Cd	30	15	90	45
Ce	8,500	1,100	12,750	1,650
Cf	8,500	1,100	12,750	1,650
Cl	0	0	0	0
Cm	8,500	1,100	12,750	1,650
Co	100	40	320	128
Cr	10	4	14	6
Cs	50	10	50	10
Cu	70	50	224	160
Eu	8,500	1,100	12,750	1,650
F	0	0	0	0
Fe	400	200	600	300
Fr	50	10	50	10
Gd	8,500	1,100	12,750	1,650
H	0	0	0	0
Hg	1,000	800	3,200	2,560
I	0.9	0.3	0.1	0
K	25	5	25	5
Lu	8,500	1,100	12,750	1,650

Table 4.2-29: Recommended K_d Values for the Vadose Zone (Continued)

Element	Soils Media		Cement Leachate Impacted Soils Media	
	Backfill Soil (mL/g)*	Vadose Zone Soil (mL/g)**	Backfill Soil (mL/g)*	Vadose Zone Soil (mL/g)**
Mn	200	15	280	21
Mo	1,000	1,000	1,400	1,400
N	0	0	0	0
Na	25	5	25	5
Nb	0	0	0	0
Ni	30	7	96	22
Np	9	3	14	5
Pa	9	3	14	5
Pb	5,000	2,000	16,000	6,400
Pd	30	7	96	22
Pm[a]	0	0	0	0
Po	5,000	2,000	10,000	4,000
Pr[a]	0	0	0	0
Pt	30	7	96	22
Pu	5,950	290	11,900	580
Ra[b]	185	25	555	75
Rb	50	10	50	10
Re	1.8	0.6	0.2	0.1
Rh[a]	0	0	0	0
Rn	0	0	0	0
Ru[a]	0	0	0	0
Sb	2,500	2,500	3,500	3,500
Se	1,000	1,000	1,400	1,400
Sm	8,500	1,100	12,750	1,650
Sn	5,000	2,000	15,000	6,000
Sr	17	5	51	15
Tc	1.8	0.6	0.2	0.1
Te	1,000	1,000	1,400	1,400
Th	2,000	900	4,000	1,800
U	300	200	900	600
V[a]	0	0	0	0
Y	8,500	1,100	12,750	1,650
Zn	30	15	90	45
Zr	2,000	900	4,000	1,800

* Backfill soil represented by clayey sediment

** Vadose zone soil represented by sandy sediment

Note: Values from SRNL-STI-2009-00473 unless otherwise noted

a Not included in SRNL-STI-2009-00473 so assigned a value of zero

b SRNL-STI-2010-00527

4.2.2.2.3 Procured Sands

Type II tanks were constructed above a 1-inch sand pad contained within a circular pan. An additional 1-inch sand pad is located under the secondary liner. In accordance with the requirements of site specifications, the consistency of sand in both of the 1 inch layers consists of clean, hard, durable, siliceous particles free from foreign material (i.e., procured and washed sand free of silt or clay), and uniformly graded from standard sieves #16 and #100. The size of the sand grain ranges from 0.15 mm (#100 sieve) to 1 mm (#16 sieve), and is classified as fine to medium sand per the Unified Soil Classification System (USCS), and fine to coarse per the USDA classification. [W163018]

Table 4.2-30 provides the estimated materials properties for the sand. Figure 4.2-28 provides the characteristic curves (suction head, and relative permeability) for the sand.

Table 4.2-30: Estimated Sand Material Properties of Interest

Material	Saturated D_e (cm^2/sec)	Average η_T (%)	Average ρ_h (g/cm^3)	Average ρ_n (g/cm^3)	Horizontal K_{sat} (cm/s)	Vertical K_{sat} (cm/s)
Sand	8E-06	38	1.65	2.66	5E-04	2.8E-04

[WSRC-STI-2006-00198, Table 5-18]
D_e = Effective Diffusion Coefficient
η_T = Total Porosity
ρ_h = Dry Bulk Density
ρ_n = Particle Density
K_{sat} = Saturated Hydraulic Conductivity

Figure 4.2-28: Procured Sand Characteristic Curves

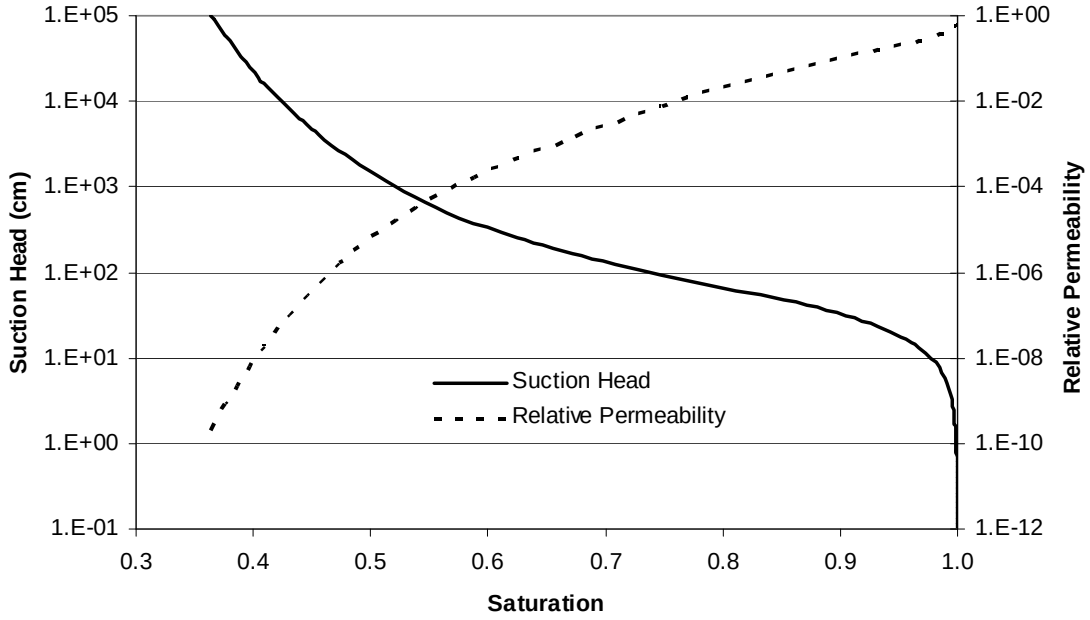

[WSRC-STI-2006-00198]

Table 4.2-31 presents the thickness of the vadose zone beneath each of the waste tanks. The thicknesses of the vadose zone below the different waste tanks range from approximately -35.5 to 18.2 feet with negative values indicating the base of the tank is below the water table.

Table 4.2-31: Vadose Zone Thickness for HTF

Tank Type	Waste Tank	Working Slab Top Elevation (ft above MSL)	Approximate Water Table Elevation (ft above MSL)	Vadose Zone Thickness (ft)
I	9	241.4	276.9	-35.5
	10	241.4	276.3	-35.5
	11	241.4	277.2	-35.5
	12	241.4	276.6	-35.5
II	13	270.3	276.9	-6.6
	14	270.3	276.9	-6.6
	15	270.3	276.9	-6.6
	16	270.3	276.9	-6.6
IV	21	281.8	274.7	7.1
	22	281.8	274.7	7.1
	23	281.8	274.7	7.1
	24	281.8	274.7	7.1
III	29	283.5	275.4	8.1
	30	283.5	275.4	8.1
	31	283.5	275.4	8.1
	32	283.5	275.4	8.1
IIIA	35	282.7	268.3	14.4
	36	283.7	269.3	14.4
	37	283.7	269.3	14.4
	38	291.1	272.9	18.2
	39	291.1	272.9	18.2
	40	291.1	272.9	18.2
	41	291.1	272.9	18.2
	42	291.1	272.9	18.2
	43	291.1	272.9	18.2
	48	288.1	275.6	12.5
	49	288.1	275.6	12.5
	50	288.1	275.6	12.5
	51	288.1	275.6	12.5

[SRNL-STI-2010-00148]

4.2.2.2.4 Cementitious Material Properties

The physical and chemical properties of the cementitious materials associated with the waste tanks after closure (i.e., waste tank top and sides, basemat, grout fill) are needed for the ICM. Property estimates for cementitious materials associated with the HTF will be utilized as input to deterministic, sensitivity, and uncertainty modeling. This section will provide initial properties, hydraulic conductivity, distribution coefficients, and degradation timing. Some properties are expected to remain constant over time. These include porosity, dry bulk density, particle density, and the water retention curves. Because the form of cementitious material degradation is cracking and not the dissolving the cement paste, the porosity, bulk density, and particle density of the cementitious material, a marginal impact is expected. While it is recognized that some variability exists, it was judged a reasonable modeling simplification to hold porosity, dry bulk density, particle density, and the water retention curves constant. Section 4.4.2 describes additional cases employed in the model, which include the existence of fast flow paths, which could be attributed to cracked cementitious materials.

Estimates for these properties for the cementitious materials associated with the HTF waste tanks have been provided in WSRC-STI-2007-00369. The cementitious materials in the HTF can be grouped into two types, 1) the grout used to fill the waste tanks when operationally closed, and 2) the concrete in the waste tank vault roof, basemat, and walls. The properties associated with the waste tank grout are taken from the specification fill grout properties in WSRC-STI-2007-00369, which are based on testing of the grout formula planned to be used for waste tank fill. The properties associated with the waste tank concrete are taken from the basemat surrogate properties in WSRC-STI-2007-00369, which are based on testing of similar vintage SRS concrete (concrete from a P-Area foundation slab that is over 30 years old). The properties from WSRC-STI-2007-00369 are shown in Table 4.2-32 and Figure 4.2-29

Table 4.2-32: Cementitious Material Initial Properties

Material	η (%)	ρ_h (g/cm^3)	ρ_n (g/cm^3)	D_e (cm^2/sec)	K (cm/sec)
Vault Concrete (Basemat, Roof and Walls)	16.8	2.06	2.51	8.0E-07	3.4E-08
Grout Fill	26.6	1.84[a]	2.51	8.0E-07	3.6E-08

[WSRC-STI-2007-00369]

a Calculated as (ρ_n) x (1-η)

D_e = Effective Diffusion Coefficient

η = Porosity

ρ_h = Dry Bulk Density

ρ_n = Particle Density

K = Hydraulic Conductivity

Figure 4.2-29: Recommended Characteristic Curves for Waste Tank Grout and Concrete

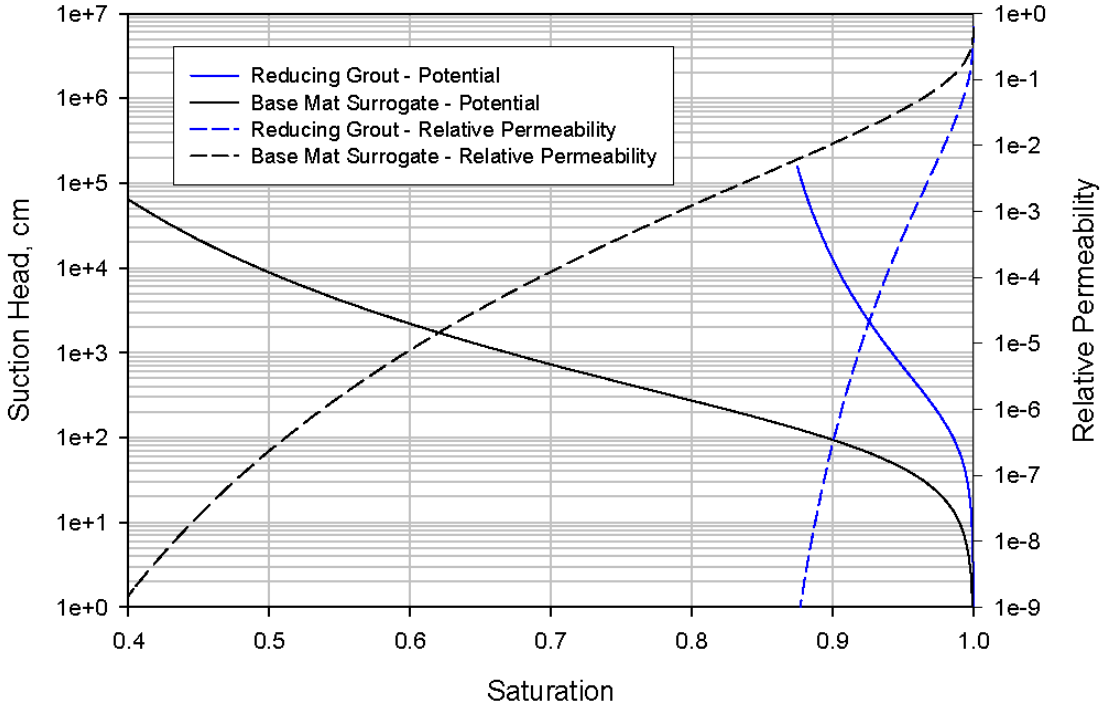

[WSRC-STI-2007-00369]

Cementitious Material Hydraulic Conductivity

The cementitious barriers identified in the HTF closure concept are either reinforced concrete (waste tank vault and basemat) or non-reinforced grout (annulus and waste tank grouts). The hydraulic conductivities of the initial state (non-degraded) materials were obtained from a concrete sample collected from a slab constructed in 1978 that was used as a surrogate for the vault and basemat concrete, and a laboratory sample of grout that was prepared by the current specification for waste tank operational closure. [WSRC-STI-2007-00369]

The saturated hydraulic conductivities of the concrete barriers after degradation by the various mechanisms were estimated. The discussion of the modeling approach and parameters will be detailed in Section 4.4.4.1.

Cementitious Materials Distribution Coefficients

The distribution coefficient values are necessary for cementitious materials through which contaminants have the potential to travel. Table 4.2-33, provides distribution coefficient values for cementitious materials as a function of aging. The distribution coefficient values in Table 4.2-33 are based on SRS site-specific data, values from literature, or on engineering judgment, with the site-specific data being the preferred information source. [SRNL-STI-2009-00473] The distribution coefficient for an element is dependent on the pH of the pore water, which in turn is dependent upon the amount of water (number of pore water volumes) that has passed through the

cementitious material over time. The water chemistry for the testing reported in SRNL-STI-2009-00473 is found in Table 9 of WSRC-STI-2007-00640. The experimental information for the aged concrete is used as the basemat surrogate. The experimental results are similar to the values for oxidized concrete contained in NUREG-CR-6377 except for a non-zero technetium distribution coefficient. The experimental values reported in SRNL-STI-2009-00473 are used in conjunction with like element experimental values and previously reported distribution coefficient work in WSRC-STI-2007-00640 in the determination of the recommended distribution coefficient values reported in Table 4.2-33.

Table 4.2-33: Recommended K_d Values for Cementitious Materials

	Oxidizing Cementitious Media			Reducing Cementitious Media		
Element	**Young-Age (mL/g)**	**Middle-Age (mL/g)**	**Old-Age (mL/g)**	**Young-Age (mL/g)**	**Middle-Age (mL/g)**	**Old-Age (mL/g)**
Ac	6,000	6,000	600	7,000	7,000	1,000
Ag	4,000	4,000	400	5,000	5,000	1,000
Al	6,000	6,000	600	7,000	7,000	1,000
Am	6,000	6,000	600	7,000	7,000	1,000
Ar	0	0	0	0	0	0
As	1,000	1,000	100	1,000	1,000	100
At	8	15	4	5	9	4
Au[a]	0	0	0	0	0	0
Ba	100	100	70	100	100	70
Be[a]	0	0	0	0	0	0
Bi	6,000	6,000	600	7,000	7,000	1,000
Bk	6,000	6,000	600	7,000	7,000	1,000
C	3,000	3,000	300	3,000	3,000	300
Ca	15	15	5	15	15	5
Cd	4,000	4,000	400	5,000	5,000	1,000
Ce	6,000	6,000	600	7,000	7,000	1,000
Cf	6,000	6,000	600	7,000	7,000	1,000
Cl	10	10	1	10	10	1
Cm	6,000	6,000	600	7,000	7,000	1,000
Co	4,000	4,000	400	5,000	5,000	2,000
Cr	10	10	1	1,000	1,000	1,000
Cs	2	20	10	2	20	10
Cu	4,000	4,000	400	5,000	5,000	2,000
Es[a]	0	0	0	0	0	0
Eu	6,000	6,000	600	7,000	7,000	1,000
F	10	10	1	10	10	1
Fe	6,000	6,000	600	7,000	7,000	1,000
Fr	2	20	10	2	20	10
Ga[a]	0	0	0	0	0	0
Gd	6,000	6,000	600	7,000	7,000	1,000
Ge[a]	0	0	0	0	0	0
H	0	0	0	0	0	0

Table 4.2-33: Recommended K_d Values for Cementitious Materials (Continued)

	Oxidizing Cementitious Media			Reducing Cementitious Media		
Element	**Young-Age (mL/g)**	**Middle-Age (mL/g)**	**Old-Age (mL/g)**	**Young-Age (mL/g)**	**Middle-Age (mL/g)**	**Old-Age (mL/g)**
Hf[a]	0	0	0	0	0	0
Hg	300	300	100	5,000	5000	2,000
Ho[a]	0	0	0	0	0	0
I	8	15	4	5	9	4
In[a]	0	0	0	0	0	0
Ir[a]	0	0	0	0	0	0
K	2	20	10	2	20	10
Kr	0	0	0	0	0	0
La[a]	0	0	0	0	0	0
Lu	6,000	6,000	600	7,000	7,000	1,000
Mn	100	100	10	100	100	10
Mo	300	300	150	300	300	150
N	10	10	1	10	10	1
Na	0.5	1	0.5	0.5	1	0.5
Nb	1,000	1,000	500	1,000	1,000	500
Ni	4,000	4,000	400	4,000	4,000	400
Np	10,000	10,000	5,000	10,000	10,000	5,000
P[a]	0	0	0	0	0	0
Pa	10,000	10,000	5,000	10,000	10,000	5,000
Pb	300	300	100	500	500	250
Pd	4,000	4,000	400	4,000	4,000	400
Pm[a]	0	0	0	0	0	0
Po	300	300	100	5,000	5,000	500
Pr[a]	0	0	0	0	0	0
Pt	4,000	4,000	400	5,000	5,000	2,000
Pu	10,000	10,000	2,000	10,000	10,000	2,000
Pu_4	10,000	10,000	2,000	10,000	10,000	2,000
Pu_5	1,000	1,000	100	1,000	1,000	100
Ra	100	100	70	100	100	70
Rb	2	20	10	2	20	10
Re	0.8	0.8	0.5	5,000	5,000	1,000
Rh[a]	0	0	0	0	0	0
Rn	0	0	0	0	0	0
Ru[a]	0	0	0	0	0	0
Sb	1,000	1,000	100	1,000	1,000	100
Sc[a]	0	0	0	0	0	0
Se	300	300	150	300	300	150

Table 4.2-33: Recommended K_d Values for Cementitious Materials (Continued)

Element	Oxidizing Cementitious Media			Reducing Cementitious Media		
	Young-Age (mL/g)	Middle-Age (mL/g)	Old-Age (mL/g)	Young-Age (mL/g)	Middle-Age (mL/g)	Old-Age (mL/g)
Si[a]	0	0	0	0	0	0
Sm	6,000	6,000	600	7,000	7,000	1,000
Sn	4,000	4,000	2,000	5,000	5,000	500
Sr	15	15	5	15	15	5
Ta[a]	0	0	0	0	0	0
Tc	0.8	0.8	0.5	5,000	5,000	1,000
Te	300	300	150	300	300	150
Th	10,000	10,000	2,000	5,000	5,000	500
Ti[a]	0	0	0	0	0	0
Tl	2	20	10	2	20	10
U	250	250	70	2,500	2,500	2,500
V[a]	0	0	0	0	0	0
Y	6,000	6,000	600	7,000	7,000	1,000
Zn	4,000	4,000	400	5,000	5,000	2,000
Zr	10,000	10,000	2,000	5,000	5,000	500

[SRNL-STI-2009-00473]

a Assigned a value of zero

The number of pore water volumes passing through the waste tank and the corresponding transitions to different waste tank chemistry conditions is included in the HTF modeling. As part of the waste release modeling (discussed in detail in Section 4.2.1), the estimated transition times between various chemical phases was calculated for the waste tank pore water. The waste tank pore water chemistry for non-submerged waste tanks was calculated to change from Region II Reduced conditions (Middle-Age Reducing) to Region II Oxidized conditions (Middle-Age Oxidizing) after 371 pore volumes pass through the grout. The change from Region II conditions (Middle Age) to Region III conditions (Old Age) was calculated to occur after 2,131 pore volumes. [ISSN 1019-0643, WSRC-STI-2007-00544]

The waste tank pore water chemistry for submerged waste tanks was calculated to change from Condition C to Condition D after 1,414 pore volumes pass through the grout. The change from Condition D to Oxidized Region III was calculated to occur after 2,383 pore volumes pass through the grout. [WSRC-STI-2007-00544]

As a modeling simplification, the pore volume transition times for the Base Case were determined assuming the representative grout formula was present throughout the waste tank interior.

As part of the UA/SA, the transition times between chemical states was varied in the stochastic analyses as described in Section 5.6.3.8.

Based on changes in the pH with aging, the distribution coefficient values for concrete have been divided into three stages as shown in Table 4.2-33. [SRNL-STI-2009-00473] The young, middle, and old ages correspond to Regions I, II, and III. Waste tank grout and concrete are initially characterized as middle aged (Region II)

and transition to Region III over time as the material properties change. Because the waste tank grout and cement in individual waste tanks will be aged at the time of overall HTF closure, none of the waste tank cementitious materials were characterized as young (Region I). [ISSN 1019-0643]

Grout and Concrete Degradation

The current SRS HTF disposal environment is very benign with respect to chemical degradation of the reinforced concrete vaults and the waste tank grout material. Consequently, the degradation due to chemical processes is expected to progress at a very slow rate. An evaluation of the HTF grout and concrete degradation is presented in more detail in SRNL-STI-2010-00035.

The most extensive cementitious material attack was found to be from carbonation on unsaturated concrete and grout. Carbonation was found to result in the greatest penetration as a function of time. For material with the porosity of the surrogate basemat concrete (16.8% v/v) the depth of penetration from carbonation was estimated to be 21 centimeters (8.27 inches) after 1,000 years. The estimated depth of penetration for the representative grout from carbonation reactions was 36 centimeters (14.17 inches) after 1,000 years. These values were applied to Type I, II, and III/IIIA tanks. Type IV tanks contain no cooling coils in the grout and are therefore not affected by steel expansive phase corrosion impacts, the estimated depth of penetration for the representative fill grout was 8.2 centimeters (3.23 inches) after 1,000 years. [SRNL-STI-2010-00035]

The penetration depth of the chemical species responsible for the degradation was assumed as equivalent to the depth of degradation. The consequences of the degradation depended on the material porosity and if the material contained steel reinforcement because carbon-steel rebar introduces an additional degradation process (i.e., concrete cracking due to formation of expansive metal corrosion products). [SRNL-STI-2010-00035]

Porosity and diffusion coefficient data for two representative materials were used in calculations to predict the depth of penetration of the various forms of chemical attack. These materials were a surrogate foundation slab of concrete (3,000 lb/in^2 of concrete from P Area that was poured in 1978) which represented the vault and basemat concrete and a waste tank grout that represented all of the grout in the waste tanks and the annulus spaces. For saturated concrete and grout, acid leaching (i.e., decalcification) was the most aggressive degradation mechanism. The depth of severe decalcification at 1,000-years exposure was 6.5 and 8.2 centimeters for the surrogate vault concrete and waste tank grout, respectively. The effect of decalcification is to increase porosity and permeability and to decrease the pH of the pore solution from approximately 12.5 to lower values depending on the evolution of the mineral phase assemblages as a function of calcium concentration in the pore solution. [SRNL-STI-2010-00035]

The effect of carbonation on the permeability of the cementitious barriers in the HTF closure concept depends on whether the barrier contains steel. Carbonation in itself

may actually reduce permeability by plugging pores with calcium carbonate. However, it will affect the permeability of reinforced concrete because the concrete will crack due to formation of expansive iron hydroxide phases that form when steel corrodes. Steel passivation is lost when the pH of the pore solution is in equilibrium with calcium carbonate (a pH of approximately 8.4) rather than calcium hydroxide (a pH of approximately 12.5). [SRNL-STI-2010-00035]

The consequences of carbonation with respect to the permeability of the cementitious barriers in the HTF depend on the assumptions made to link depth of penetration with formation of expansive iron hydroxide phase from associated rebar corrosion and the assumptions linking corrosion with concrete cracking. For the reinforced vault concrete, the assumption that cracking occurs simultaneously with carbonation is unrealistic. Cracking will lag the carbonation by a considerable time especially in the absence of other corrodents such as chloride ions. When cracking from expansion does occur, the permeability will increase.

Because the annulus grout and grout in the waste tanks without cooling coils do not contain rebar or steel, the overall effect of carbonation should be minimal regardless of the depth of penetration. The permeability of these materials is not expected to change significantly as the result of carbonation. This is the case even though the rate of carbonate penetration is faster due to the higher porosity of the fill grout (26.6% v/v). [SRNL-STI-2010-00035]

Carbonation of the grout will not commence until the waste tank is breached due to corrosion or development of a fast pathway. Based on calculated waste tank corrosion rates a lengthy lag time is anticipated before carbonate actually contacts the grout and the carbonation front advances to the cooling coils. The corrosion rate is expected to be very slow in the absence of additional corrodents. The effect of carbonation on cracking when it does occur is expected to be the same as described above. However, the possibility exists that expansive reactions occurring under the somewhat constrained conditions of the buried waste tank could result in very little change in permeability. [SRNL-STI-2010-00035]

The radiological effects on degradation of grouted waste tank residuals are estimated as bounded by the modeled degradation mechanism based on data from a study on solidification of SRS HLW sludge in Portland cement matrices. In this study, simulated high-level cementitious waste forms were gamma-irradiated to 1,010 radiation-absorbed doses. After irradiation, compressive strength and the strontium leachability of the cementitious waste forms were measured and compared to samples that were not irradiated. No significant reductions of compressive strength or increase in strontium leaching, which are degradation metrics, were attributed to the radiological exposure. [DP-1448] The effects of the alpha radiation on the degradation properties of grout are expected to be less than the effects of the gamma radiation because the alpha dose rates that the grout will be exposed to are lower than the gamma dose rates. [SRNL-PSE-2006-00097]

The timing of the degradation of the waste tank cementitious materials is detailed in Table 4.2-34 for the various waste tank types. The table provides the point in time

the applicable cementitious material (grout or concrete) transitions from the initial state, to a degrading state, to a fully degraded state.

Table 4.2-34: Cementitious Material Degradation Transition Times (Yrs) by Waste Tank Type

Cementitious Material Stages	Type I	Type II	Type III	Type IIIA	Type IV
HTF Fill Grout (Initial Properties)	0 - 2,700	0 - 5,100	0 - 5,100	0 - 5,000	0 - 800
Degrading HTF Fill Grout	2,700 - 13,200	5,100 - 16,700	5,100 - 19,200	5,000 - 19,100	800 - 64,400
Fully Degraded HTF Fill Grout	13,200	16,700	19,200	19,100	64,400
HTF Concrete (Initial Properties)	0 - 1,350	0 - 2,550	0 - 2,550	0 - 2,500	0 - 400
Degrading HTF Aged Concrete	1,350 - 2,700	2,550 - 5,100	2,550 - 5,100	2,500 - 5,000	400 - 800
Fully Degraded HTF Aged Concrete	2,700	5,100	5,100	5,000	800

[SRR-CWDA-2010-00019]

4.2.2.2.5 Contamination Zone Properties

A waste release study describing the component of the CZ conceptual model related to the waste release approach (i.e., contaminant leaching) was prepared for the HTF PA. [WSRC-STI-2007-00544] This study describes the methods used to estimate solubility and sorption controls on contaminant release, and provides specific calculations for uranium and technetium as examples of the process used. The approach is the same as conducted for the FTF PA and adjusted for HTF conditions. [WSRC-STI-2007-00544]

4.2.2.2.6 Carbon and Stainless Steel Material Properties

Material properties for carbon steel used in the liner and stainless steel used in the ancillary equipment are expressed as predicted times of failure due to corrosion under different conditions or as being initially failed based on current waste tank liner conditions. Prior to failure, steel is assumed as impermeable with respect to both advection and diffusion. After failure, steel is assumed to be absent, or otherwise not a hindrance to advection and diffusion (i.e., there would be no retardation). However, in the steel liner failure analyses there was not an independent assessment of the secondary steel liner is not independently assessed, it is explicitly modeled and fails at the same time as the primary steel liner.

Carbon Steel

Predictions for failure of the carbon steel liners are based on the results of two studies. [WSRC-STI-2007-00061, SRNL-STI-2010-00047] These studies developed

estimates for corrosion-induced failure of the steel liners. These estimates considered general and localized corrosion mechanisms of the waste tank steel exposed to the CZ, to grout, and to soil conditions for the Type I, Type II, Type III/IIIA, and Type IV tanks in HTF. SRNL-STI-2010-00047 focused specifically on the degradation of the Type I and II tanks and transfer lines in groundwater.

Degradation of the waste tank steel encased in grouted conditions was estimated due to carbonation of the concrete leading to low pH conditions, or the chloride-induced depassivation of the steel leading to accelerated corrosion. Chloride-induced corrosion was determined to be the more aggressive phenomenon.

The time of liner failure is calculated based on steel corrosion rates under different conditions (e.g., differing diffusion coefficients). These failure times vary with waste tank design, owing to differences in construction. The failure analyses consider general and localized corrosion mechanisms of the steel liner exposed to the CZ, grout, and SRS soil conditions. Consumption of the waste tank steel encased in grouted conditions is estimated due to carbonation of the concrete leading to low pH conditions, and the chloride-induced depassivation of the steel leading to accelerated corrosion.

The liner failure analyses considered the current condition of the HTF waste tanks, with the relevant parameters being known leak sites, their location, and whether they led to accumulation on the annulus floor. All HTF Type I and Type II tanks (Tanks 9 through 16) have documented leak sites. [SRNL-STI-2010-00047, C-ESR-G-00003] The Type III/IIIA and Type IV tanks have not experienced any service-induced pitting or cracking and are assumed in the same condition as when put into service. There are not any waste tanks believed to have experienced general corrosion based on the results of ultrasonic inspections. [WSRC-STI-2007-00061, page 16] The liner failure study considered the condition of the HTF waste tanks to be closed when determining the liner failure times. Since the transport model is most concerned with tank failures that could allow significant flow through and away from the CZ, the failure mechanisms of primary concern are those near or at the bottom of the waste tanks that cause significant through-wall flow. Data on waste tank conditions is compiled and updated annually through a waste tank inspection program. The leak site information in C-ESR-G-00003 is updated as needed to reflect any changes to conditions. C-ESR-G-00003 documents the number of leak sites and their location on the liner. As noted above, Tanks 9 through 16 have leak sites as documented in C-ESR-G-00003. Waste tanks with only a small number of leak sites that are located near the top of the liner and away from the CZ are modeled as failing per the information provided in SRNL-STI-2010-00047, which includes Tanks 9, 10, 11, and 13. Tanks 12, 14, 15, and 16 have either many leak sites and/or leak sites located near the bottom of the liner, thus near the CZ. Tanks 12, 14, 15, and 16 are therefore modeled with liner failure at the time of closure and the liner is assumed as not a barrier to flow.

The liner studies considered that the waste tank steel liner thicknesses at the time of closure maybe different from the nominal thicknesses per specifications used for this

analysis. Specifically, chemical cleaning utilizing OA has been proposed to remove the last remnants of waste in the waste tank prior to operational closure. An analysis of the waste tank chemical cleaning was completed to determine any major influence on the initial thickness. Corrosion testing has been done to determine the effects of the OA cleaning process on the carbon steel. The maximum metal loss due to the cleaning process is minimal (less than 10 millimeters), and does not affect the liner failure model. [SRNL-STI-2010-00047]

A stochastic approach is used to estimate the distributions of failures based upon the differing mechanisms of corrosion, but accounting for variances in each of the independent variables. It is assumed that life of the waste tank liners is a function of the time to corrosion initiation plus the time for corrosion to propagate through the liner. The corrosion proceeds under grouted conditions until chloride can induce depassivation of the surface or carbonation can reduce the pH of the surrounding concrete, thereby negating the high pH "protection" of the steel liner.

The failure time of the liner is defined to be:

$$t_{failure} = t_{initiation} + \frac{Thickness}{CorrosionRate}$$

where:

$t_{failure}$	=	time to complete consumption of the waste tank wall by general corrosion
$t_{tinitiation}$	=	time to chloride induced depassivation or carbonation front
Thickness	=	initial thickness of liner (millimeter)
CorrosionRate	=	dependent upon condition (i.e., chloride or carbonation in mm/yr)

The time to failure of the primary liner by general corrosion can be due to the following:

1. General corrosion in grouted conditions
2. Chloride induced depassivation, followed by general corrosion
3. Carbonation induced loss of protective capacity of the concrete
4. A combination of items 1 through 3

The corrosion rate, once chloride induced depassivation occurs, is calculated based upon oxygen diffusion through the concrete. The corrosion rate assumption once the carbonation front reaches the liner is 10 mm/yr. [SRNL-STI-2010-00047] Thus, the system is modeled as a competition between the initiation time to chloride-induced depassivation and the initiation time to carbonation induced corrosion rates. The system also addresses the issue of the carbonation front reaching the waste tank liner prior to complete failure by chloride-induced corrosion.

The stochastic analysis elucidated insights into the controlling mechanisms of failure for each of the tank types. The failure times, as presented in SRNL-STI-2010-00047, are a function of the diffusion coefficients, thereby controlling the failure times. The analyses are based upon the assumption that carbonation was the most aggressive mechanism of corrosion of the waste tank liner due to the loss of the high pH environment, and that chloride may induce depassivation on the steel surface, but is still dependent upon the oxygen diffusion to drive the corrosion reaction. The relative effects of carbonation and chloride induced corrosion as a function of diffusion coefficient can be examined by comparing the median values of failure for each of the conditions. The results suggest that the carbonation rates are the critical factor in controlling the life estimation. Once the carbonation front has reached the steel liner, the liner is essentially consumed within a nominal time of 50 years. As such, the recommendations for failure time used in stochastic modeling for contaminant escape are critically linked to the diffusion coefficients. The diffusion coefficient for oxygen through the concrete is not as critical.

The failure distributions for a diffusion coefficient of 1.0E-06 cm^2/sec are used in the stochastic modeling analyses. The distributions reflect the results of the statistical corrosion analysis using site-specific water and soil conditions. [WSRC-STI-2007-00061, SRNL-STI-2010-00047] These diffusion rates are considered bounding (i.e., faster than rates that are typically reported). Typically, the diffusion rates of each are calculated and/or measured to be approximately 1.0E-08 cm^2/sec. The results indicate that the majority of the statistical observations convert to carbonation related initiation/failure when carbonation diffusion coefficients are greater than 1.0E-05 cm^2/sec.

A failure analysis was performed to incorporate a diffusion coefficient distribution and a more bounding corrosion rate distribution into a single waste tank life, liner distribution. The additional waste tank liner failure analysis considers the passive current density along with other potential corrosion mechanisms with uncertainty included. The parameters included in the analysis take into account:

- Grout may provide less corrosion protection than high quality concrete
- Potential for galvanic corrosion with stainless steel
- Initial failures by stress corrosion cracking
- Variability in the passive current density
- Potential rapid gaseous transport pathways leading to small regions with carbonation reaching the tank liner at early periods
- Spatially variant corrosion rate at different locations on the same waste tank
- Potential for more rapid corrosion of welds

This analysis incorporated a wider range of outcomes into a single distribution, so that the possible liner failure dates and probabilities across the entire spectrum of scenarios could be observed at one time. The results of this sensitivity study are shown in Table 4.2-35. [WSRC-STI-2007-00061, SRNL-STI-2010-00047] The liner failure distributions can be interpreted in two ways, with the specified failure probability and calculated year representing either:

- The year in which the stated percentage of waste tanks will have their primary liners totally fail (e.g., 25% of all the Type IV tanks will have their primary waste tank liners completely fail at year 90)
- The year in which a given percentage of an individual waste tank primary liner fails (e.g., 25% of the Tank 21 primary liner will fail at year 90)

Table 4.2-35: Comprehensive Sensitivity Analysis of Carbon Steel Liner

Tank Type	Years Following HTF Tank Closure		
	25% Failure Probability	50% Failure Probability	75% Failure Probability
Type I	2,097	4,183	6,153
Type II	2,461	4,890	6,283
Type III/IIIA	3,397	8,272	15,289
Type IV	90	2,010	8,104

[WSRC-STI-2007-00061, SRNL-STI-2010-00047]

For the failure analysis presented in SRNL-STI-2010-00047, within HTF Type I and II tanks were exposed to soils with significant amounts of groundwater. The groundwater can increase the general corrosion rate due to higher electrolyte mobility and higher conductivity that can increase corrosion. Differences in oxygen concentration at the interface where soil with groundwater meets soil without groundwater can cause galvanic cells that increase the corrosion rate. The Type I tanks in the HTF are submerged more than 50% in groundwater. Type II tanks in the HTF have some exposure of the concrete vault bottom to soil with groundwater. The effect of groundwater on the waste tank corrosion can be seen by comparing this simulation with the simulation for Type I tanks in Table 40 of WSRC-STI-2007-00061 Revision 2. The median time to failure of the waste tank decreased to 4,183 years in the presence of groundwater from 7,630 years in soils with no significant groundwater. The decrease in the time to failure is mainly due to the higher corrosion rate of the waste tank liner after it has gone through depassivation from chloride attack. [SRNL-STI-2010-00047]

Although Type II tanks are primarily in soil without groundwater, some Type II tanks are partially submerged in groundwater. The median time to failure of the waste tank decreased to 4,890 years in the presence of groundwater from 13,600 years in soils with no significant groundwater. [SRNL-STI-2010-00047]

The cases are meant to represent conditions that may be present without regard to the mechanism that led to those conditions. There are a variety of mechanisms that can lead to earlier degradation times than those modeled in Case A (Base Case). In the closed HTF conditions, some mechanisms may be possible although not likely. The cases should not be interpreted as representing a specific mechanism for liner degradation. The liner failure times modeled in Cases B, C, D, and E are meant to encompass various mechanisms and provide information on the risk significance of earlier liner failure than that modeled in the Base Case.

This showed that if differences between expected waste tank modeling cases (Section 4.4.1) are disregarded, and all liner failure mechanisms are considered simultaneously, the liner life could be shortened. Utilizing different scenarios for

modeling is still preferred for the ICM Base Case since independently moving the liner failure date forward can decrease the peak dose within 20,000 years. Early liner failure tends to allow the closure cap to reduce infiltration into the waste tank during release of radionuclides that are not significantly affected by either the waste release solubility limits and/or concrete/soil retardation (e.g., with low soil/concrete distribution coefficient values). The early liner failure can, therefore spread the releases out over a longer period.

Table 4.2-36 presents a summary of the deterministic (i.e., single value) and probabilistic (i.e., distribution) values that are used to determine liner failure during modeling. The deterministic values utilize the median values from the stochastic analysis. The results corresponding to the reasonably bounding carbon dioxide diffusion rates (1.0E-06 cm^2/sec) were utilized for baseline modeling and a bounding oxygen diffusion rate of 1.0E-04 cm^2/sec for submerged waste tanks and 1.0E-06 cm^2/sec for non-submerged waste tanks. The results corresponding to the maximum evaluated carbon dioxide diffusion rates (1.0E-04 cm^2/sec) were utilized for fast flow case modeling and for the rising aquifer modeling case, where the loss of reducing capability for the cementitious materials might be expected to occur sooner but the oxygen diffusion rates are not changed from the Base Case. As discussed previously, Tanks 12, 14, 15, and 16 were modeled with a liner failure at the time of waste tank operational closure based on the number and/or location of existing leak sites.

Table 4.2-36: Carbon Steel Liner Life Estimates by Waste Tank Type

Waste Tank Type	Applicable Cases[a]	Grouted Waste Tank Liner Condition[f]	Liner Failure Year for Modeling	
			Deterministic	Probabilistic
Type I	A	D_i 1.0E-06 CO_2, 1.0E-04 O_2	11,397[b]	Figure 43[c]
	B, C, D, E	D_i 1.0E-04 CO_2, 1.0E-04 O_2	1,142[b]	Figure 44[c]
Type II	A	D_i 1.0E-06 CO_2, 1.0E-04 O_2	12,687[b]	Figure 46[c]
	B, C, D, E	D_i 1.0E-04 CO_2, 1.0E-04 O_2	2,506[b]	Figure 47[c]
Type III/IIIA	A	D_i 1.0E-06 CO_2, 1.0E-06 O_2	12,751[d]	Table 34[e]
	B, C, D, E	D_i 1.0E-04 CO_2, 1.0E-06 O_2	2,077[d]	Table 35[e]
Type IV	A	D_i 1.0E-06 CO_2, 1.0E-06 O_2	3,638[d]	Table 37[e]
	B, C, D, E	D_i 1.0E-04 CO_2, 1.0E-06 O_2	75[d]	Table 38[e]

a. Conditions are from Table 4.4-1.
b. Median value from same figures as (c) below $D_i(O_2)$ = 1.0E-04
c. Figures from SRNL-STI-2010-00047
d. Median value from same tables as (e) below $D_i(O_2)$ = 1.0E-06
e. Tables from WSRC-STI-2007-00061
f. Diffusion coefficient reported in cm^2/sec
D_i = Intrinsic diffusion coefficient

Prior to failure, the liner is assumed impermeable with respect to both advection and diffusion. After failure, the liner is assumed to not be a hindrance to advection and diffusion (i.e., retardation due to the presence of corrosion products is not included in the model).

The failure years associated with Table 4.2-36 represent median values used to represent failure, which as discussed previously, was modeled as the date from which

the steel liner is absent or otherwise not a hindrance to advection and diffusion. The conceptual model is a reasonable simplification, utilizing a "simultaneous" liner failure model, which assumes the entire liner fails in a given year. The simultaneous liner failure model was used instead of using a patch model, which would add percentages of each waste tank failing each year (i.e., leak sites in the liner appearing at different waste tank locations, percent of through wall leakage increasing, and the waste tank gradually failing over time). Although, an exact simulation of the expected primary liner failure mechanism, the conceptual model liner failure approach is reasonable for the following reasons:

- The CZ of concern is located essentially across the waste tank bottoms, making failure of most liner sections unimportant, since they would not result in flow through or contaminant release from the CZ.
- Modeling the entire primary liner to fail concurrently would have a tendency to maximize the flow path simultaneously into and away from the CZ, which would in turn has a tendency to maximize peak doses. Allowing the entire liner to fail early or allowing small flow paths through the CZ as the patch model approach would simulate, can have the tendency to decrease the resulting peak doses (as detailed in the Section 5.6.7 comprehensive sensitivity analysis discussion).
- Though not addressed independently in the carbon steel failure analysis, in addition to the primary liner, there is a full secondary steel liner for the Type III/IIIA tanks and a 5-foot high secondary liner near the CZ for the Type I and Type II tanks. In the analyses, these secondary liners are assumed to fail at the same time as the primary steel liner. If the patch model were used, failure of a single patch near the CZ might not result in contaminant release if the nearby secondary liner patches were still intact.

Stainless Steel

Two conditions were analyzed in WSRC-STI-2007-00460 for situations without significant groundwater, general corrosion, and pitting penetration. Table 4.2-37 presents the results of the study for these two conditions in soil for various stainless steel wall thicknesses. Pitting corrosion was found to be the controlling mechanism for the degradation of the stainless steel transfer line core piping and its consequent ability to maintain confinement of contaminants. It is assumed that if 75% of the transfer line is intact, the line is capable of providing this confinement function (i.e., once 25% of the line wall has been penetrated, the lines are considered incapable of confining contaminants). The probabilistic analysis for the HTF is discussed further in Section 4.4.2 of this PA.

Table 4.2-37: Corrosion Induced Failure Times for Stainless Steel Transfer Lines

SRS Soil Conditions	Years Following Waste Tank Closure		
	3-in dia (0.19-in min wall thickness)	2-in dia (0.14-in min wall thickness)	1-in dia (0.12-in min wall thickness)
Failure: steel consumption	4,725	3,375	2,900
Failure: 25% pitting penetration	532	515	510
First pit penetration	189	135	116

[WSRC-STI-2007-00460]

The lifetime of the transfer lines is shortened by both general corrosion and pitting corrosion. The life of the stainless steel transfer lines was estimated for general corrosion based upon 0.04 mm/yr bounding. Pitting of the stainless steel transfer lines starts faster than general corrosion, but the pitting rate decreases significantly and the pitting depth is less than the depth of general corrosion by 500 years after soil with groundwater exposure. The failures of the lines due to general corrosion are between 2,900 to 4,725 years for various diameter stainless steel pipes. [WSRC-STI-2007-00460]

These estimates considered general and localized corrosion mechanisms of the stainless steel exposed to SRS soil conditions for the stainless steel core transfer lines in HTF. Section 3.2.2.1 describes the different types of transfer lines used in the HTF. The vast majority of the piping is stainless steel, either encased in concrete, inside a carbon-steel jacket, or surrounded by a cement-asbestos jacket. The core pipe has a diameter ranging from 1 inch to 3 inches with minimum wall thicknesses from 0.12 inch to 0.19 inch (minimum wall thicknesses are 87.5% of nominal wall thicknesses). [WSRC-STI-2007-00460]

Within H Area, many transfer lines are exposed to soils with significant amounts of groundwater. Predictions for failure of the stainless steel transfer line core piping are based on the results of a recent study specific to HTF closure. [SRNL-STI-2010-00047]

The results of the stochastic failure analysis for the stainless steel transfer lines exposed to significant groundwater are presented in Table 4.2-38. Pitting corrosion was found to be the controlling mechanism for the degradation of the stainless steel transfer line core piping and its consequent ability to maintain confinement of contaminants. It is assumed that if 75% of the transfer line is intact, the line is capable of providing this confinement function (i.e., once 25% of the line wall has been penetrated, the lines are considered incapable of confining contaminants). The 25% time to failure for an H Area 1-inch diameter transfer line with a minimum thickness of 120 millimeters and has been exposed to soils with significant amount of water was 6,000 years. This failure probability represents the most conservative failure time for the HTF transfer lines. This long failure time (compared to the results in Table 4.2-37) is predicted due to the low rate of corrosion for stainless steel samples tested by the National Bureau of Standards. [SRNL-STI-2010-00047]

Table 4.2-38: Analysis of Stainless Steel Transfer Lines Submerged in Groundwater

Wall Thickness	Years Following HTF Waste Tank Closure		
	25% Failure Probability	50% Failure Probability	75% Failure Probability
3-in dia pipe (avg) 216 mm (0.216 in)	10,797	27,001	36,016
1-in. dia pipe (min) 120 mm (0.120 in)	5,999	15,001	20,009

[SRNL-STI-2010-00047]

The median time to failure predicted from stochastic simulations for the HTF transfer lines is significantly longer than for the transfer lines in the FTF. The difference in lifetime is due to different assumptions about the general corrosion and pitting rates for stainless steel. One of the primary causes for the shift in failures time is a change in the pitting rate equation to a power law expression from a constant rate. Due to this change, general corrosion has limited transfer line lifetime instead of pitting. [SRNL-STI-2010-00047]

Due to the varying degradation times calculated, a failure time of 510 years is assumed in modeling for all ancillary equipment to maximize the dose contributions of the ancillary inventory.

4.2.2.2.7 Saturated Zone Hydraulic Properties

Within the GSAD, soils with a saturated hydraulic conductivity greater than 1.0E-07 cm/sec are defined as sandy and those with a saturated hydraulic conductivity less than 1.0E-07 cm/sec are defined as clay when defining transport properties (i.e., distribution coefficient and effective diffusion coefficient). [WSRC-STI-2006-00198] For consistency with the vadose zone soils, the saturated zone soils within the GSA model that are defined as sandy are assigned the effective diffusion coefficient of the upper vadose zone (i.e., 5.3E-06 cm^2/sec) and those defined as clay are assigned that of the vadose zone clay (i.e., 4.0E-06 cm^2/sec).

Table 4.2-39 provides a summary of the saturated zone soils hydraulic properties (as represented by the vadose zone soil properties) and the model input used to represent these values. As indicated in Table 4.2-39, the properties of the upper vadose zone are representative of sandy soil and the saturated zone soil is representative of both sandy soil and clayey soil (dependent on location). Thus, the distribution coefficient values used for transport of contaminants through the upper vadose zone and the sandy soil regions of the saturated zone are assigned the distribution coefficient values for sandy soil that are presented in Table 4.2-29 for vadose zone soil. For those regions within the saturated zone that are representative of clayey soil, the distribution coefficient values used for transport of contaminants through these regions are assigned the distribution coefficient values for clayey soil that are presented in Table 4.2-29 for backfill soil.

Table 4.2-39: Upper Vadose Zone and Effective Saturated Zone Soil Properties

Actual/Model	η (%)	ρ_h (g/cm^3)	ρ_n (g/cm^3)	Saturated D_e (cm^2/sec)
Upper Vadose Zone	39 (total)	1.65	2.70	5.3E-06
Saturated Zone Soil (Effective Properties for Modeling Purposes)	25 (effective)	1.04 (effective)	1.39 (effective)	Sandy: 5.3E-06 Clay: 4.0E-06

[WSRC-STI-2006-00198, Section 5.6.1]
η = Porosity
ρ_h = Dry Bulk Density
ρ_n = Particle Density
D_e = Effective Diffusion Coefficient

4.2.3 Exposure Pathways and Scenarios

Intruder and MOP exposure pathways must be defined to calculate receptor doses. The primary mechanism for transport of radionuclides from the HTF is expected to be leaching to the groundwater, groundwater transport to the well and the stream, and subsequent human consumption or exposure. The scenarios are not assumed to occur until after the 100-year institutional control period ends, after which time it is assumed that no active HTF facility maintenance will be conducted. All potential exposure pathways are identified in Tables 4.2-40 and 4.2-41 for the MOP and intruder, respectively. Tables 4.2-40 and 4.2-41 identify the individual assumed pathways and whether quantified dose calculations are required for the individual pathways. Tables 4.2-40 and 4.2-41 also identify the individual pathways that are not assumed to occur. The consumption rates, bioaccumulation factors, transfer factors, and exposure times that are used in conjunction with the pathways are discussed in detail in Section 4.6. The DCFs used in conjunction with the pathways are discussed in detail in Section 4.7.

Table 4.2-40: Potential MOP Stabilized Contaminant Exposure Pathways

Primary Stabilized Contaminant Source	Stabilized Contaminant Release Mechanism	Primary Pathway	Secondary Pathway	Tertiary Pathway	Exposure Route	MOP at Well	MOP at Stream
Waste Tank & Ancillary Equipment	Groundwater release at Stream	Domestic Use of Stream water	Drinking Water	N/A	Ingestion	N/A	X
Waste Tank & Ancillary Equipment	Groundwater release at Stream	Domestic Use of Stream water	Showering	N/A	Dermal	N/A	O
Waste Tank & Ancillary Equipment	Groundwater release at Stream	Domestic Use of Stream water	Showering	N/A	Inhalation	N/A	X
Waste Tank & Ancillary Equipment	Groundwater release at Stream	Domestic Use of Stream water	Showering	N/A	Ingestion (incidental)	N/A	X
Waste Tank & Ancillary Equipment	Groundwater release at Stream	Stream water	Swimming	N/A	Inhalation	X	X
Waste Tank & Ancillary Equipment	Groundwater release at Stream	Stream water	Swimming	N/A	Dermal	O	O
Waste Tank & Ancillary Equipment	Groundwater release at Stream	Stream water	Swimming	N/A	Ingestion (incidental)	X	X
Waste Tank & Ancillary Equipment	Groundwater release at Stream	Stream water	Swimming	Direct Rad Emissions	External Exposure	X	X
Waste Tank & Ancillary Equipment	Groundwater release at Stream	Stream water	Fishing, Boating	Direct Rad Emissions	External Exposure	X	X
Waste Tank & Ancillary Equipment	Groundwater release at Stream	Stream water	Fishing, Boating	N/A	Dermal	O	O
Waste Tank & Ancillary Equipment	Groundwater release at Stream	Stream water	Fish Biotic Uptake	Fish	Ingestion	X	X
Waste Tank & Ancillary Equipment	Groundwater release at Stream	Stream water	Shellfish Biotic Uptake	Shellfish	Ingestion	O	O
Waste Tank & Ancillary Equipment	Groundwater release at Stream	Stream water to Livestock	Livestock Biotic Uptake	Meat	Ingestion	N/A	X

Table 4.2-40: Potential MOP Stabilized Contaminant Exposure Pathways (Continued)

Primary Stabilized Contaminant Source	Stabilized Contaminant Release Mechanism	Primary Pathway	Secondary Pathway	Tertiary Pathway	Exposure Route	MOP at Well	MOP at Stream
Waste Tank & Ancillary Equipment	Groundwater release at Stream	Stream water to Livestock	Livestock Biotic Uptake	Milk	Ingestion	N/A	X
Waste Tank & Ancillary Equipment	Groundwater release at Stream	Stream water to Poultry	Poultry Biotic Uptake	Meat	Ingestion	N/A	X
Waste Tank & Ancillary Equipment	Groundwater release at Stream	Stream water to Poultry	Poultry Biotic Uptake	Eggs	Ingestion	N/A	X
Waste Tank & Ancillary Equipment	Groundwater release at Stream	Stream Water Irrigation	Garden Vegetables Biotic Uptake	Vegetables	Ingestion	N/A	X
Waste Tank & Ancillary Equipment	Groundwater release at Stream	Stream Water Irrigation	Fodder Biotic Uptake	Livestock Biotic Uptake - Meat	Ingestion	N/A	X
Waste Tank & Ancillary Equipment	Groundwater release at Stream	Stream Water Irrigation	Fodder Biotic Uptake	Livestock Biotic Uptake - Milk	Ingestion	N/A	X
Waste Tank & Ancillary Equipment	Groundwater release at Stream	Stream Water Irrigation	Fodder Biotic Uptake	Poultry Biotic Uptake - Meat	Ingestion	N/A	X
Waste Tank & Ancillary Equipment	Groundwater release at Stream	Stream Water Irrigation	Fodder Biotic Uptake	Poultry Biotic Uptake - Eggs	Ingestion	N/A	X
Waste Tank & Ancillary Equipment	Groundwater release at Stream	Stream Water Irrigation	Fugitive Dust Generation during Irrigation	Ambient Air (particulates)	Inhalation	N/A	X
Waste Tank & Ancillary Equipment	Groundwater release at Stream	Stream Water Irrigation	Vapor Generation during Irrigation	Ambient Air (vapors)	Inhalation	N/A	X
Waste Tank & Ancillary Equipment	Groundwater release at Stream	Stream Water Irrigation	Direct Soil Contact	N/A	Ingestion (incidental)	N/A	X
Waste Tank & Ancillary Equipment	Groundwater release at Stream	Stream Water Irrigation	Direct Soil Contact	N/A	Dermal	N/A	O

Table 4.2-40: Potential MOP Stabilized Contaminant Exposure Pathways (Continued)

Primary Stabilized Contaminant Source	Stabilized Contaminant Release Mechanism	Primary Pathway	Secondary Pathway	Tertiary Pathway	Exposure Route	MOP at Well	MOP at Stream
Waste Tank & Ancillary Equipment	Groundwater release at Stream	Stream Water Irrigation	Direct Rad Emissions from soil	N/A	External Exposure	N/A	X
Waste Tank & Ancillary Equipment	Volatilization	Ambient Air (vapors)	N/A	N/A	Inhalation	X	X
Waste Tank & Ancillary Equipment	Volatilization	Ambient Air (vapors)	Plume Rad Exposure	N/A	External Exposure	X	X
Waste Tank & Ancillary Equipment	Volatilization	Ambient Air (vapors)	Livestock Biotic Uptake	Meat	Ingestion	X	X
Waste Tank & Ancillary Equipment	Volatilization	Ambient Air (vapors)	Livestock Biotic Uptake	Milk	Ingestion	X	X
Waste Tank & Ancillary Equipment	Volatilization	Ambient Air (vapors)	Poultry Biotic Uptake	Meat	Ingestion	X	X
Waste Tank & Ancillary Equipment	Volatilization	Ambient Air (vapors)	Poultry Biotic Uptake	Eggs	Ingestion	X	X
Waste Tank & Ancillary Equipment	Volatilization	Ambient Air (vapors)	Garden Vegetables Biotic Uptake	Vegetables	Ingestion	X	X
Waste Tank & Ancillary Equipment	Volatilization	Ambient Air (vapors)	Fodder Biotic Uptake	Livestock Biotic Uptake - Meat	Ingestion	X	X
Waste Tank & Ancillary Equipment	Volatilization	Ambient Air (vapors)	Fodder Biotic Uptake	Livestock Biotic Uptake - Milk	Ingestion	X	X
Waste Tank & Ancillary Equipment	Volatilization	Ambient Air (vapors)	Fodder Biotic Uptake	Poultry Biotic Uptake - Meat	Ingestion	X	X
Waste Tank & Ancillary Equipment	Volatilization	Ambient Air (vapors)	Fodder Biotic Uptake	Poultry Biotic Uptake - Eggs	Ingestion	X	X

Table 4.2-40: Potential MOP Stabilized Contaminant Exposure Pathways (Continued)

Primary Stabilized Contaminant Source	Stabilized Contaminant Release Mechanism	Primary Pathway	Secondary Pathway	Tertiary Pathway	Exposure Route	MOP at Well	MOP at Stream
Waste Tank & Ancillary Equipment	Groundwater Withdrawal at Well	Domestic Use of Well Water	Drinking Water	N/A	Ingestion	X	N/A
Waste Tank & Ancillary Equipment	Groundwater Withdrawal at Well	Domestic Use of Well Water	Showering	N/A	Dermal	O	N/A
Waste Tank & Ancillary Equipment	Groundwater Withdrawal at Well	Domestic Use of Well Water	Showering	N/A	Inhalation	X	N/A
Waste Tank & Ancillary Equipment	Groundwater Withdrawal at Well	Domestic Use of Well Water	Showering	N/A	Ingestion (incidental)	X	N/A
Waste Tank & Ancillary Equipment	Groundwater Withdrawal at Well	Well Water to Livestock	Livestock Biotic Uptake	Meat	Ingestion	X	N/A
Waste Tank & Ancillary Equipment	Groundwater Withdrawal at Well	Well Water to Livestock	Livestock Biotic Uptake	Milk	Ingestion	X	N/A
Waste Tank & Ancillary Equipment	Groundwater Withdrawal at Well	Well Water to Poultry	Poultry Biotic Uptake	Meat	Ingestion	X	N/A
Waste Tank & Ancillary Equipment	Groundwater Withdrawal at Well	Well Water to Poultry	Poultry Biotic Uptake	Eggs	Ingestion	X	N/A
Waste Tank & Ancillary Equipment	Groundwater Withdrawal at Well	Well Water Irrigation	Garden Vegetables Biotic Uptake	Vegetables	Ingestion	X	N/A

Table 4.2-40: Potential MOP Stabilized Contaminant Exposure Pathways (Continued)

Primary Stabilized Contaminant Source	Stabilized Contaminant Release Mechanism	Primary Pathway	Secondary Pathway	Tertiary Pathway	Exposure Route	MOP at Well	MOP at Stream
Waste Tank & Ancillary Equipment	Groundwater Withdrawal at Well	Well Water Irrigation	Fodder Biotic Uptake	Livestock Biotic Uptake - Meat	Ingestion	X	N/A
Waste Tank & Ancillary Equipment	Groundwater Withdrawal at Well	Well Water Irrigation	Fodder Biotic Uptake	Livestock Biotic Uptake - Milk	Ingestion	X	N/A
Waste Tank & Ancillary Equipment	Groundwater Withdrawal at Well	Well Water Irrigation	Fodder Biotic Uptake	Poultry Biotic Uptake - Meat	Ingestion	X	N/A
Waste Tank & Ancillary Equipment	Groundwater Withdrawal at Well	Well Water Irrigation	Fodder Biotic Uptake	Poultry Biotic Uptake - Eggs	Ingestion	X	N/A
Waste Tank & Ancillary Equipment	Groundwater Withdrawal at Well	Well Water Irrigation	Fugitive Dust Generation during Irrigation	Ambient Air (particulates)	Inhalation	X	N/A
Waste Tank & Ancillary Equipment	Groundwater Withdrawal at Well	Well Water Irrigation	Vapor Generation during Irrigation	Ambient Air (vapors)	Inhalation	X	N/A
Waste Tank & Ancillary Equipment	Groundwater Withdrawal at Well	Well Water Irrigation	Direct Soil Contact	N/A	Ingestion (incidental)	X	N/A
Waste Tank & Ancillary Equipment	Groundwater Withdrawal at Well	Well Water Irrigation	Direct Soil Contact	N/A	Dermal	O	N/A
Waste Tank & Ancillary Equipment	Groundwater Withdrawal at Well	Well Water Irrigation	Direct Rad Emissions from Soil	N/A	External Exposure	X	N/A

X = addressed quantitatively, O = addressed qualitatively, N/A = not applicable

Table 4.2-41: Potential Intruder Waste Exposure Pathways

Primary Stabilized Contaminant Source	Stabilized Contaminant Release Mechanism	Primary Pathway	Secondary Pathway	Tertiary Pathway	Exposure Route	Acute Intruder	Chronic Intruder
Ancillary Equipment	Drill Cuttings brought to Surface	Fugitive Dust Generation during drilling	Ambient Air (particulates)	N/A	Inhalation	X	N/A
Ancillary Equipment	Drill Cuttings brought to Surface	Drill Cuttings dropped on surface	Direct Soil Contact	N/A	Ingestion	X	N/A
Ancillary Equipment	Drill Cuttings brought to Surface	Drill Cuttings dropped on surface	Direct Soil Contact	N/A	Dermal	O	N/A
Ancillary Equipment	Drill Cuttings brought to Surface	Drill Cuttings dropped on surface	Direct Rad Emissions	N/A	External Exposure	X	N/A
Ancillary Equipment	Drill Cuttings brought to Surface	Drill Cuttings mixed in Garden	Garden Vegetables Biotic Uptake	Vegetables	Ingestion	N/A	X
Ancillary Equipment	Drill Cuttings brought to Surface	Drill Cuttings mixed in Garden	Fodder Biotic Uptake	Livestock Biotic Uptake - Meat	Ingestion	N/A	N/A
Ancillary Equipment	Drill Cuttings brought to Surface	Drill Cuttings mixed in Garden	Fodder Biotic Uptake	Livestock Biotic Uptake - Milk	Ingestion	N/A	N/A
Ancillary Equipment	Drill Cuttings brought to Surface	Drill Cuttings mixed in Garden	Fodder Biotic Uptake	Poultry Biotic Uptake - Meat	Ingestion	N/A	N/A
Ancillary Equipment	Drill Cuttings brought to Surface	Drill Cuttings mixed in Garden	Fodder Biotic Uptake	Poultry Biotic Uptake - Eggs	Ingestion	N/A	N/A
Ancillary Equipment	Drill Cuttings brought to Surface	Drill Cuttings mixed in Garden	Direct Soil Contact	N/A	Ingestion	N/A	X
Ancillary Equipment	Drill Cuttings brought to Surface	Drill Cuttings mixed in Garden	Direct Soil Contact	N/A	Dermal	N/A	O
Ancillary Equipment	Drill Cuttings brought to Surface	Drill Cuttings mixed in Garden	Direct Rad Emissions	N/A	External Exposure	N/A	X

Table 4.2-41: Potential Intruder Waste Exposure Pathways (Continued)

Primary Stabilized Contaminant Source	Stabilized Contaminant Release Mechanism	Primary Pathway	Secondary Pathway	Tertiary Pathway	Exposure Route	Acute Intruder	Chronic Intruder
Ancillary Equipment	Drill Cuttings brought to Surface	Drill Cuttings mixed in Garden	Fugitive Dust Generation during Irrigation	Ambient Air (particulates)	Inhalation	N/A	X
Waste Tank & Ancillary Equipment	Groundwater release at Stream	Domestic use of Stream water	Drinking Water	N/A	Ingestion	N/A	N/A
Waste Tank & Ancillary Equipment	Groundwater release at Stream	Domestic use of Stream water	Showering	N/A	Dermal	N/A	N/A
Waste Tank & Ancillary Equipment	Groundwater release at Stream	Domestic use of Stream water	Showering	N/A	Inhalation	N/A	N/A
Waste Tank & Ancillary Equipment	Groundwater release at Stream	Domestic use of Stream water	Showering	N/A	Ingestion (incidental)	N/A	N/A
Waste Tank & Ancillary Equipment	Groundwater release at Stream	Stream water	Swimming	N/A	Inhalation	N/A	X
Waste Tank & Ancillary Equipment	Groundwater release at Stream	Stream water	Swimming	N/A	Dermal	N/A	O
Waste Tank & Ancillary Equipment	Groundwater release at Stream	Stream water	Swimming	N/A	Ingestion (incidental)	N/A	X
Waste Tank & Ancillary Equipment	Groundwater release at Stream	Stream water	Swimming	Direct Rad Emissions	External Exposure	N/A	X

Table 4.2-41: Potential Intruder Waste Exposure Pathways (Continued)

Primary Stabilized Contaminant Source	Stabilized Contaminant Release Mechanism	Primary Pathway	Secondary Pathway	Tertiary Pathway	Exposure Route	Acute Intruder	Chronic Intruder
Waste Tank & Ancillary Equipment	Groundwater release at Stream	Stream water	Fishing, Boating	Direct Rad Emissions	External Exposure	N/A	X
Waste Tank & Ancillary Equipment	Groundwater release at Stream	Stream water	Fishing, Boating	N/A	Dermal	N/A	O
Waste Tank & Ancillary Equipment	Groundwater release at Stream	Stream water	Fish Biotic Uptake	Fish	Ingestion	N/A	X
Waste Tank & Ancillary Equipment	Groundwater release at Stream	Stream water	Shellfish Biotic Uptake	Shellfish	Ingestion	N/A	O
Waste Tank & Ancillary Equipment	Groundwater release at Stream	Stream water to Livestock	Livestock Biotic Uptake	Meat	Ingestion	N/A	N/A
Waste Tank & Ancillary Equipment	Groundwater release at Stream	Stream water to Livestock	Livestock Biotic Uptake	Milk	Ingestion	N/A	N/A
Waste Tank & Ancillary Equipment	Groundwater release at Stream	Stream water to Poultry	Poultry Biotic Uptake	Meat	Ingestion	N/A	N/A
Waste Tank & Ancillary Equipment	Groundwater release at Stream	Stream water to Poultry	Poultry Biotic Uptake	Eggs	Ingestion	N/A	N/A
Waste Tank & Ancillary Equipment	Groundwater release at Stream	Stream Water Irrigation	Garden Vegetables Biotic Uptake	Vegetables	Ingestion	N/A	N/A

Table 4.2-41: Potential Intruder Waste Exposure Pathways (Continued)

Primary Stabilized Contaminant Source	Stabilized Contaminant Release Mechanism	Primary Pathway	Secondary Pathway	Tertiary Pathway	Exposure Route	Acute Intruder	Chronic Intruder
Waste Tank & Ancillary Equipment	Groundwater release at Stream	Stream Water Irrigation	Fodder Biotic Uptake	Livestock Biotic Uptake - Meat	Ingestion	N/A	N/A
Waste Tank & Ancillary Equipment	Groundwater release at Stream	Stream Water Irrigation	Fodder Biotic Uptake	Livestock Biotic Uptake - Milk	Ingestion	N/A	N/A
Waste Tank & Ancillary Equipment	Groundwater release at Stream	Stream Water Irrigation	Fodder Biotic Uptake	Poultry Biotic Uptake - Meat	Ingestion	N/A	N/A
Waste Tank & Ancillary Equipment	Groundwater release at Stream	Stream Water Irrigation	Fodder Biotic Uptake	Poultry Biotic Uptake - Eggs	Ingestion	N/A	N/A
Waste Tank & Ancillary Equipment	Groundwater release at Stream	Stream Water Irrigation	Fugitive Dust Generation during Irrigation	Ambient Air (particulates)	Inhalation	N/A	N/A
Waste Tank & Ancillary Equipment	Groundwater release at Stream	Stream Water Irrigation	Vapor Generation during Irrigation	Ambient Air (vapors)	Inhalation	N/A	N/A
Waste Tank & Ancillary Equipment	Groundwater release at Stream	Stream Water Irrigation	Direct Soil Contact	N/A	Ingestion (incidental)	N/A	N/A
Waste Tank & Ancillary Equipment	Groundwater release at Stream	Stream Water Irrigation	Direct Soil Contact	N/A	Dermal	N/A	N/A
Waste Tank & Ancillary Equipment	Groundwater release at Stream	Stream Water Irrigation	Direct Rad Emissions from Soil	N/A	External Exposure	N/A	N/A

Table 4.2-41: Potential Intruder Waste Exposure Pathways (Continued)

Primary Stabilized Contaminant Source	Stabilized Contaminant Release Mechanism	Primary Pathway	Secondary Pathway	Tertiary Pathway	Exposure Route	Acute Intruder	Chronic Intruder
Waste Tank & Ancillary Equipment	Volatilization	Ambient Air (vapors)	N/A	N/A	Inhalation	N/A	X
Waste Tank & Ancillary Equipment	Volatilization	Ambient Air (vapors)	Plume Rad Exposure	N/A	External Exposure	N/A	X
Waste Tank & Ancillary Equipment	Volatilization	Ambient Air (vapors)	Livestock Biotic Uptake	Meat	Ingestion	N/A	O
Waste Tank & Ancillary Equipment	Volatilization	Ambient Air (vapors)	Livestock Biotic Uptake	Milk	Ingestion	N/A	O
Waste Tank & Ancillary Equipment	Volatilization	Ambient Air (vapors)	Poultry Biotic Uptake	Meat	Ingestion	N/A	O
Waste Tank & Ancillary Equipment	Volatilization	Ambient Air (vapors)	Poultry Biotic Uptake	Eggs	Ingestion	N/A	O
Waste Tank & Ancillary Equipment	Volatilization	Ambient Air (vapors)	Garden Vegetables Biotic Uptake	Vegetables	Ingestion	N/A	O
Waste Tank & Ancillary Equipment	Volatilization	Ambient Air (vapors)	Fodder Biotic Uptake	Livestock Biotic Uptake - Meat	Ingestion	N/A	O
Waste Tank & Ancillary Equipment	Volatilization	Ambient Air (vapors)	Fodder Biotic Uptake	Livestock Biotic Uptake - Milk	Ingestion	N/A	O

Table 4.2-41: Potential Intruder Waste Exposure Pathways (Continued)

Primary Stabilized Contaminant Source	Stabilized Contaminant Release Mechanism	Primary Pathway	Secondary Pathway	Tertiary Pathway	Exposure Route	Acute Intruder	Chronic Intruder
Waste Tank & Ancillary Equipment	Volatilization	Ambient Air (vapors)	Fodder Biotic Uptake	Poultry Biotic Uptake - Meat	Ingestion	N/A	O
Waste Tank & Ancillary Equipment	Volatilization	Ambient Air (vapors)	Fodder Biotic Uptake	Poultry Biotic Uptake - Eggs	Ingestion	N/A	O
Waste Tank & Ancillary Equipment	Groundwater Withdrawal at Well	Domestic Use of Well Water	Drinking Water	N/A	Ingestion	N/A	X
Waste Tank & Ancillary Equipment	Groundwater Withdrawal at Well	Domestic Use of Well Water	Showering	N/A	Dermal	N/A	O
Waste Tank & Ancillary Equipment	Groundwater Withdrawal at Well	Domestic Use of Well Water	Showering	N/A	Inhalation	N/A	X
Waste Tank & Ancillary Equipment	Groundwater Withdrawal at Well	Domestic Use of Well Water	Showering	N/A	Ingestion (incidental)	N/A	X
Waste Tank & Ancillary Equipment	Groundwater Withdrawal at Well	Well Water to Livestock	Livestock Biotic Uptake	Meat	Ingestion	N/A	X
Waste Tank & Ancillary Equipment	Groundwater Withdrawal at Well	Well Water to Livestock	Livestock Biotic Uptake	Milk	Ingestion	N/A	X
Waste Tank & Ancillary Equipment	Groundwater Withdrawal at Well	Well Water to Poultry	Poultry Biotic Uptake	Meat	Ingestion	N/A	X
Waste Tank & Ancillary Equipment	Groundwater Withdrawal at Well	Well Water to Poultry	Poultry Biotic Uptake	Eggs	Ingestion	N/A	X

Table 4.2-41: Potential Intruder Waste Exposure Pathways (Continued)

Primary Stabilized Contaminant Source	Stabilized Contaminant Release Mechanism	Primary Pathway	Secondary Pathway	Tertiary Pathway	Exposure Route	Acute Intruder	Chronic Intruder
Waste Tank & Ancillary Equipment	Groundwater Withdrawal at Well	Well Water Irrigation	Garden Vegetables Biotic Uptake	Vegetables	Ingestion	N/A	X
Waste Tank & Ancillary Equipment	Groundwater Withdrawal at Well	Well Water Irrigation	Fodder Biotic Uptake	Livestock Biotic Uptake - Meat	Ingestion	N/A	X
Waste Tank & Ancillary Equipment	Groundwater Withdrawal at Well	Well Water Irrigation	Fodder Biotic Uptake	Livestock Biotic Uptake - Milk	Ingestion	N/A	X
Waste Tank & Ancillary Equipment	Groundwater Withdrawal at Well	Well Water Irrigation	Fodder Biotic Uptake	Poultry Biotic Uptake - Meat	Ingestion	N/A	X
Waste Tank & Ancillary Equipment	Groundwater Withdrawal at Well	Well Water Irrigation	Fodder Biotic Uptake	Poultry Biotic Uptake - Eggs	Ingestion	N/A	X
Waste Tank & Ancillary Equipment	Groundwater Withdrawal at Well	Well Water Irrigation	Fugitive Dust Generation during Irrigation	Ambient Air (particulates)	Inhalation	N/A	X
Waste Tank & Ancillary Equipment	Groundwater Withdrawal at Well	Well Water Irrigation	Vapor Generation during Irrigation	Ambient Air (vapors)	Inhalation	N/A	X
Waste Tank & Ancillary Equipment	Groundwater Withdrawal at Well	Well Water Irrigation	Direct Soil Contact	N/A	Ingestion (incidental)	N/A	X
Waste Tank & Ancillary Equipment	Groundwater Withdrawal at Well	Well Water Irrigation	Direct Soil Contact	N/A	Dermal	N/A	O
Waste Tank & Ancillary Equipment	Groundwater Withdrawal at Well	Well Water Irrigation	Direct Rad Emissions from Soil	N/A	External Exposure	N/A	X

X = addressed quantitatively, O = addressed qualitatively, N/A = not applicable

4.2.3.1 Member of the Public Exposure Pathways

Table 4.2-40 presents and this section discusses the MOP exposure pathways used in the PA analyses. Table 4.2-40 also indicates whether quantitative dose calculations are included as part of the PA analyses. The assumption is that these scenarios occur after the end of the 100-year institutional control period and discontinuation of the active HTF facility maintenance. Section 4.6 discusses in detail the consumption rates and bioaccumulation factors used in conjunction with the pathways.

4.2.3.1.1 Scenario with Well Water as Primary Water Source

The primary water source for the MOP exposure pathways is a well drilled into the groundwater aquifers. A GSA stream is the secondary water source for recreational use pathways and the fish ingestion pathway.

In the groundwater well-dose analyses, doses are calculated using water from a well for domestic purposes (e.g., drinking water, irrigation). The following exposure pathways involving the use of contaminated well water are assumed to occur as presented in Table 4.2-40 and Figure 4.2-30.

- Direct ingestion of well water
- Ingestion of milk and meat from livestock (e.g., dairy and beef cattle) that drink well water
- Ingestion of meat and eggs from poultry that drink well water
- Ingestion of vegetables grown in garden soil irrigated with well water
- Ingestion of milk and meat from livestock (e.g., dairy and beef cattle) that eat fodder from pasture irrigated with well water
- Ingestion of meat and eggs from poultry that eat fodder from pasture irrigated with well water
- Ingestion and inhalation of well water while showering

Figure 4.2-30: Scenario with Well Water as Primary Water Source

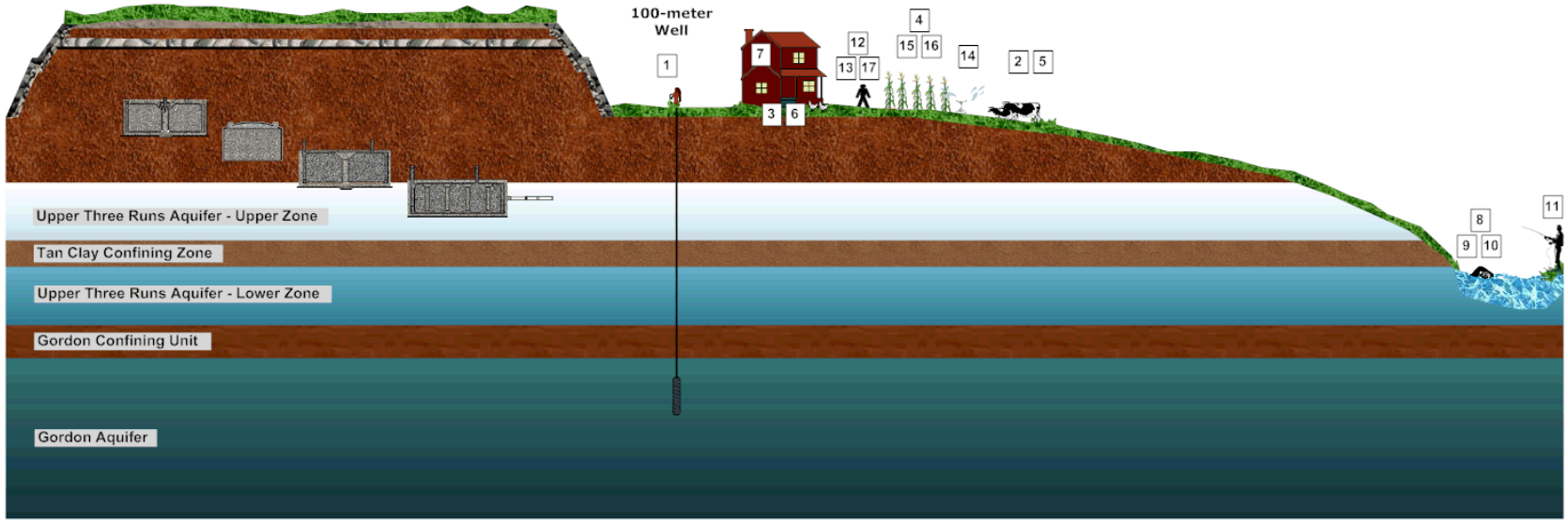

SCENARIO WITH WELL WATER AS PRIMARY WATER SOURCE

1. Direct ingestion of well water
2. Ingestion of milk and meat from livestock (e.g., dairy and beef cattle) that drink well water
3. Ingestion of meat and eggs from poultry that drink well water
4. Ingestion of vegetables grown in garden soil irrigated with well water
5. Ingestion of milk and meat from livestock (e.g., dairy and beef cattle) that eat fodder from a pasture irrigated with well water
6. Ingestion of meat and eggs from poultry that eat fodder from a pasture irrigated with well water
7. Ingestion and inhalation of well water while showing
8. Direct irradiation during recreational activities (e.g., swimming, fishing, boating) from stream water
9. Dermal contact with stream water during recreational activities (e.g., swimming, fishing)
10. Incidental ingestion and inhalation of stream water during recreational activities
11. Ingestion of fish from the stream water
12. Direct plume shine
13. Inhalation
14. Inhalation of well water used for irrigation
15. Inhalation of dust from the soil that was irrigated with well water
16. Ingestion of or dermal contact with soil that was irrigated with well water
17. Direct radiation exposure from radionuclides deposited on the soil that was irrigated with well water

The following exposure pathways involving the use of contaminated surface water (from the applicable stream) for recreational use are assumed to occur:

- Direct irradiation during recreational activities (e.g., swimming, fishing, boating) from stream water
- Dermal contact with stream water during recreational activities (e.g., swimming, fishing)
- Incidental ingestion and inhalation of stream water during recreational activities
- Ingestion of fish from the stream water

Additional exposure pathways could involve releases of radionuclides into the air from the water taken from the well (i.e., volatile radionuclides such as H-3, C-14, I-129). Exposures from the air pathway in this PA:

- Direct plume shine
- Inhalation

Other secondary and indirect pathways contribute relatively minor doses to a receptor (MOP) when compared to direct pathways such as ingestion of milk and meat. These pathways include:

- Inhalation of well water used for irrigation
- Inhalation of dust from the soil irrigated with well water
- Ingestion of or dermal contact with soil irrigated with well water
- Direct radiation exposure from radionuclides deposited on the soil irrigated with well water

4.2.3.1.2 Scenario with Stream Water as Primary Water Source

In the stream dose analyses, doses are calculated using water from the closest stream (Fourmile Branch or UTR) for domestic and recreational purposes. The following exposure pathways involving the use of surface water (from the applicable stream) are assumed to occur as presented in Table 4.2-40 and Figure 4.2-31.

- Direct ingestion of stream water
- Ingestion of milk and meat from livestock (e.g., dairy and beef cattle) that drink stream water
- Ingestion of meat and eggs from poultry that drink stream water
- Ingestion of vegetables grown in garden soil irrigated with stream water
- Ingestion of milk and meat from livestock (e.g., dairy and beef cattle) that eat fodder from pasture irrigated with stream water
- Ingestion of meat and eggs from poultry that eat fodder from pasture irrigated with stream water
- Ingestion and inhalation of stream water while showering

Figure 4.2-31: Scenario with Stream Water as Primary Water Source

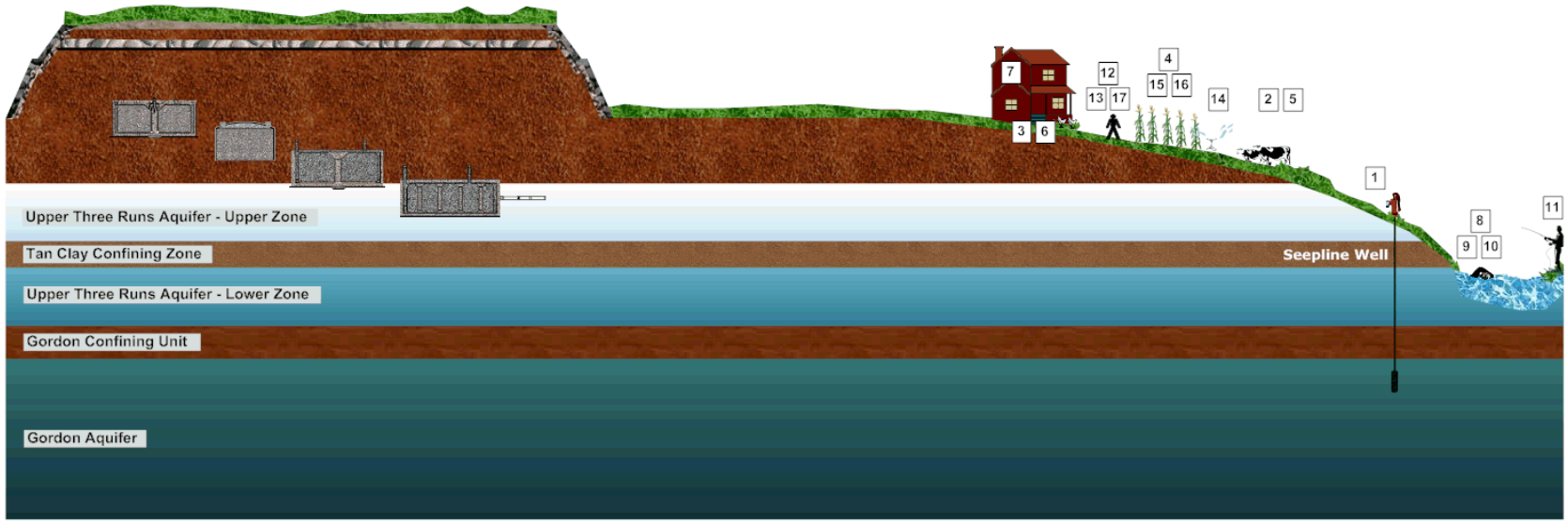

DOSE ANALYSES USING STREAM WATER AS PRIMARY WATER SOURCE

1. Direct ingestion of stream water
2. Ingestion of milk and meat from livestock (e.g., dairy and beef cattle) that drink stream water
3. Ingestion of meat and eggs from poultry that drink stream water
4. Ingestion of vegetables grown in garden soil irrigated with stream water
5. Ingestion of milk and meat from livestock (e.g., dairy and beef cattle) that eat fodder from a pasture irrigated with stream water
6. Ingestion of meat and eggs from poultry that eat fodder from a pasture irrigated with stream water
7. Ingestion and inhalation of stream water while showing
8. Direct irradiation during recreational activities (e.g., swimming, fishing, boating) from stream water
9. Dermal contact with stream water during recreational activities (e.g., swimming, fishing)
10. Incidental ingestion and inhalation of stream water during recreational activities
11. Ingestion of fish from the stream water
12. Direct plume shine
13. Inhalation
14. Inhalation of well water used for irrigation
15. Inhalation of dust from the soil that was irrigated with stream water
16. Ingestion of or dermal contact with soil that was irrigated with stream water
17. Direct radiation exposure from radionuclides deposited on the soil that was irrigated with stream water

The following exposure pathways involving the use of contaminated surface water (from the applicable stream) for recreational use are assumed to occur:

- Direct irradiation during recreational activities from stream water (e.g., swimming, fishing, boating)
- Dermal contact with stream water during recreational activities (e.g., swimming, fishing)
- Incidental ingestion and inhalation of stream water during recreational activities
- Ingestion of fish from the stream water

Additional exposure pathways could involve releases of radionuclides into the air from the water taken from the stream (i.e., volatile radionuclides such as H-3, C-14, I-129). Exposures from the air pathway in this PA:

- Direct plume shine
- Inhalation

Other secondary and indirect pathways contribute relatively minor doses to a receptor when compared to direct pathways such as ingestion of milk and meat. These pathways include:

- Inhalation of stream water used for irrigation
- Inhalation of dust from the soil that was irrigated with stream water
- Ingestion of or dermal contact with soil that was irrigated with stream water

Direct radiation exposure from radionuclides deposited on the soil that was irrigated with stream water

4.2.3.1.3 Basis for Public Release Pathways

Table 4.2-40 was prepared to provide a list of the HTF exposure pathways identified as candidates for detailed analyses. The list of candidates was developed based on a review of SRS PA analyses and NRC documents. [SRS-REG-2007-00002, SRR-CWDA-2009-00017, NUREG-0782, NUREG-0945, NUREG-1573] Those activities at SRS that could bring humans in contact with stabilized contaminants (e.g., water use, hunting, fishing, recreational activities such a swimming and boating, habitation in dwellings, other unique activities that involve water use or ground disturbance) were considered (with emphasis on local practices), to ensure that any pathways unique to SRS were taken into account. The *SRS Ecology Environmental Information Document* (WSRC-TR-2005-00201) was used as a source of relevant environmental information and conditions at SRS. For example, WSRC-TR-2005-00201 was used to identify potential wild game available on-site, potential bio-intrusion candidates (flora and fauna), and the potential for the presence of fish and/or shellfish in the creeks bordering the HTF.

Those potential pathways denoted with an "X" had quantified analysis for the various receptors. Potential pathways denoted with an "O" did not have quantified analysis performed based on the applicable justifications provided throughout this section (Table 4.2-40). The guidance found in NUREG-1854 indicates that transport pathways may be excluded from PA if it can be demonstrated that either there is limited potential for

radionuclide releases into a particular pathway, or the pathway is not viable (e.g., water is not potable). Other pathways were marked as "N/A" because of the nature of the scenario making the interaction of two or more pathways impossible (e.g., a garden that receives 100% of its irrigation water from a well cannot also receive water from a stream).

Pathways related to the MOP resident scenario using water from a well or stream had the following assumptions made:

- The stabilized contaminants release mechanisms to the MOP are leaching of stabilized contaminants to the groundwater and volatilization of the stabilized contaminants to the surface. Well drilling is not a release mechanism since any well drilling associated with the MOP scenarios would be outside the HTF buffer zone and therefore stabilized contaminants remain undisturbed.
- Bio-intrusion and/or erosion are not considered credible mechanisms for significant stabilized contaminant disturbance based on the depth and form of the stabilized contaminant. The stabilized contaminants will be significantly below ground, from at least 10 feet for ancillary equipment to approximately 40 feet for stabilized contaminant waste tank heels. Stabilized contaminants are contained within stainless steel or carbon steel equipment and stabilized via grouting as part of waste-tank system closures. No mechanism was identified that would result in stabilized contaminant disturbance and dispersal that would affect the dose to the MOP (outside the HTF buffer zone).
- In the well water as primary water source scenario, well water will be used as a primary potable water source for a residence near the well (e.g., drinking water, showering) and will be used by the resident as a primary water source for agriculture (e.g., irrigation, livestock water).
- In the MOP near a stream scenario, stream water will be used as a primary potable water source for a residence near the stream (e.g., drinking water, showering) and will be used by the resident as a primary water source for agriculture (e.g., irrigation, livestock water).
- In both MOP scenarios, the resident (near the well and/or near a stream) can use a stream for recreational activities (e.g., swimming, fishing, boating).
- Any wild game ingested (deer, wild pigs) would merely offset ingested livestock, and would result in a lower total dose since the livestock raised near HTF would be more affected by HTF stabilized contaminants than transient wild game.
- A survey of land and water usage characteristics within a 50-mile region of SRS was conducted and documented in WSRC-RP-91-17. The results of this study found that hogs are raised on farms within 50 miles of the SRS; however, hogs eat commercial feed. Thus, the consideration of local consumption of hogs is not in the determination of "meat" production or consumption.
- There are two streams (UTR and Fourmile Branch) from which ingestion of finfish with significant contamination is possible. The assumption for these streams as a source of dietary fish was conservative, and the two streams are not significant sources of edible shellfish, and shellfish play an insignificant role in

local diets in relation to other ingested dose contributors such as livestock, milk, and vegetables, thus shellfish were excluded (local invertebrate consumption total is 2 kg/yr). [WSRC-TR-2005-00201, WSRC-STI-2007-00004]

- Since there is no substantial water source at the well site, there was no consideration for pathways related to water-related commercial activities. Based on the relative proximity of a large, natural water source (i.e., the Savannah River), there is no assumption that a man-made body of water would be created at the MOP resident site.
- The consideration for the dose associated with dermal absorption of radionuclides is insignificant because, unlike some chemicals, radionuclides generally adsorb poorly into the body. The one exception is tritium, where the concentrations found are small enough in groundwater rendering it an insignificant contributor to dose.
- The quantities of water ingested during the relatively short activities of showering (10 min/d) and swimming (7 hr/yr) are negligible and not addressed independently. The impact of these activities is addressed with the "direct ingestion of well water" pathway (i.e., they are included in the 337 liters of water that is assumed to be ingested every year). [SRNL-STI-2010-00447]

4.2.3.2 Intruder Exposure Pathways

After HTF closure, the stabilized contaminant materials will be primarily located in material protected areas (e.g., grouted waste tanks, DB covers, and valve box shielding). These are clearly distinguishable from the surrounding soil and make drilling an impractical scenario based on regional drilling practices. Regional drilling conditions indicate that a barrier (closure-cap erosion barrier, waste tank top, or grout fill) would cause drillers to stop operations and move drilling location. Transfer lines containing stabilized contaminants are highly vulnerable to intrusion because they are near grade-level prior to facility closure and a size (typically 3-inch diameter or less) that will reduce detection capability and increases intruder drilling operation encounter potential. However, even with their increased risk of encroachment, the probability is low due to the minimal surface area of the transfer lines within the entire HTF footprint. The analysis in support of this considered 82% of the transfer line length having a 3-inch diameter, 0.24% with a 4-inch diameter, and the balance of the lines having a diameter less than 3 inches.

Table 4.2-41 presents the dose pathways for an inadvertent intruder and intruder scenarios are discussed in Section 4.2.3.2.1. Additionally, Table 4.2-41 indicates if detailed dose calculations are required. The assumption is that intruder release scenarios will occur after the 100-year institutional control period ends (after which active HTF facility maintenance has concluded). Because of the longevity of stainless steel transfer line integrity, (see Section 4.2.2.2.6) this is considered a conservative scenario. Natural processes such as erosion (addressed in Sections 3.2.4.4 and 3.2.4.5), seismic activity (addressed in Section 3.1.4.3), and flooding (addressed in Section 3.1.5.4) were considered and will not have an impact on the modeled intruder scenarios.

4.2.3.2.1 Intruder Release Scenarios

The consumption rates and bioaccumulation factors that were used in conjunction with the Table 4.2-41 proposed pathways are discussed in detail in Section 4.6. The following intruder scenarios were considered for the calculation of the dose to an inadvertent intruder.

- Acute Intruder-Drilling Scenario
- Acute Intruder-Construction Scenario
- Acute Intruder-Discovery Scenario
- Chronic Intruder-Agricultural (Post-Drilling) Scenario
- Chronic Intruder-Resident Scenario
- Chronic Intruder-Recreational Hunting Fishing Scenario
- Bio-intrusion Scenario

4.2.3.2.2 Acute Intruder-Drilling Scenario

The assumption in this scenario is that a well is drilled into the closure site sometime after the end of active institutional controls. The assumed well uses are domestic water and irrigation. Based on the geologic characterization data for the HTF area contained in the GSAD database, discussed in Section 3.1.4, there do not appear to be any unique geologic natural resources in the HTF area. Lacking identification of additional natural resources in the HTF, additional drilling scenarios are not considered. The person or persons who perform the well installation are the acute intruder in a drilling scenario and exposure to drill cuttings during installation is anticipated.

The assumption is that a drilling borehole will penetrate the closure site. This scenario involves stabilized contaminants below the depth of typical construction excavations. The acute drilling scenario assumes that an inadvertent intruder drills a well into a transfer line, but not into a waste tank. Although the probability of hitting a transfer line within the area may be small, it is assumed that this occurs for the drilling scenario. The intruder is exposed to contaminated drill cuttings spread over the ground and contaminated airborne dust.

Exposure of a resident or farmer to drill cuttings left on the land surface after the installation of a well was considered under the intruder-resident scenario or intruder-agricultural scenarios.

The exposure pathways for this acute drilling scenario include (Figure 4.2-32):

- Inhalation of re-suspended drill cuttings
- External exposure to the drill cuttings
- Inadvertent drill cuttings ingestion

Figure 4.2-32: Acute Intruder Drilling Scenario

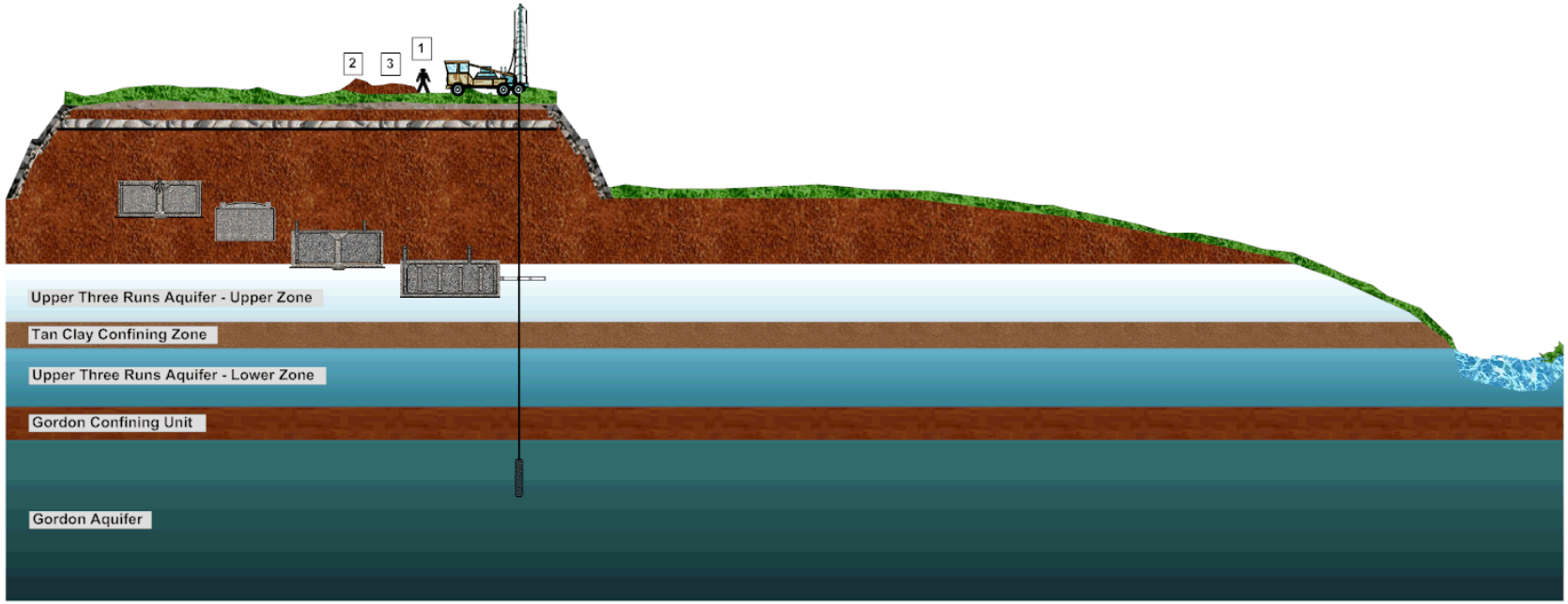

ACUTE INTRUDER-DRILLING SCENARIO

1. Inhalation of resuspended drill cuttings
2. External exposure to drill cuttings
3. Inadvertent drill cuttings ingestion

4.2.3.2.3 Acute Intruder-Construction Scenario

In this scenario, it is assumed that after the end of active institutional controls, a construction project begins at the site with associated earthmoving activities. The intruder-construction scenario involves an inadvertent intruder who chooses to excavate or construct a building on the closure site. The intruder is assumed to dig a basement excavation to a depth of approximately 10 feet. It is assumed that the intruder does not recognize the hazardous nature of the material excavated. During the excavation of the basement, the intruder is exposed to the exhumed stabilized contaminants by inhalation of re-suspended contaminated soil and external irradiation from contaminated soil. Due to the disposal depth of the stabilized contaminants in the waste tanks and in ancillary equipment (from a minimum of 10 feet to approximately 40 feet below the HTF closure cap), the intruder-construction scenario is not considered applicable. The intruder-construction scenario could also apply to an industrial facility that would require a deeper foundation excavation. While the *Savannah River Site Long Range Comprehensive Plan* (PIT-MISC-0041) and *Savannah River Site End State Vision* (PIT-MISC-0089) identify the GSA as an industrial zone, this is only in relation to future DOE activities. The institutional DOE knowledge would preclude building on top of the closed HTF. While the site is currently planned to be "federally owned, controlled, and maintained in perpetuity" (PIT-MISC-0089), the area surrounding the SRS in South Carolina do not currently support heavy industrial facilities. The main industrial resource would be the Savannah River and building an industrial facility miles away from the river is not expected. Due to these considerations, the intruder-construction scenario at the HTF is also not considered applicable for an industrial intruder.

4.2.3.2.4 Acute Intruder-Discovery Scenario

The intruder-discovery scenario is a modification of the intruder-construction scenario. The basis for the intruder-discovery scenario is the same as the intruder-construction scenario except that the exposure time is reduced. The scenario involves the intruder excavating a basement to a depth of approximately 10 feet. The intruder is assumed to recognize that he or she is digging into very unusual soil immediately upon encountering the waste tank/piping system and leaves the site. Consequently, the exposure time is reduced. Similar to the intruder-construction scenario, the intruder-discovery scenario was not considered for further analysis due to the disposal depth of the stabilized contaminants in the waste tanks and in ancillary equipment (from a minimum of 10 feet to approximately 40 feet below the HTF closure cap).

4.2.3.2.5 Chronic Intruder-Agricultural (Post-Drilling) Scenario

In the chronic intruder-agriculture scenario, it is assumed that after the end of active institutional controls, a farmer lives on, and consumes food crops grown and animals reared on the closure site, and performs recreational activities on the site. The chronic intruder-agriculture scenario is an extension of the Acute Intruder-Drilling Scenario. It is assumed, in this scenario, that an intruder lives in a building near the well drilled as part of the intruder-drilling scenario and engages in agricultural and recreational activities on

the contaminated site and stream. Excavation to the surface of the stabilized contaminants in the waste tanks was not considered credible due to its depth of more than 40 feet below the closure cap. Therefore, the chronic intruder-agriculture scenario was retained for the ancillary equipment inventory and specifically a waste transfer line because it is less protected than a DB, valve box, or PP (each shielded with thick shield covers of several feet of concrete as noted in Section 3.2.2).

The primary water source for the chronic intruder-agriculture scenario is a well drilled into the groundwater aquifers through a transfer line. The stream is the secondary water source for recreational use pathways and the fish ingestion pathway. The assumption for soil used for gardening purposes is that it is contaminated by both drill cuttings and irrigation well water. The intruder is exposed to (Figure 4.2-33):

- Direct ingestion of well water
- Ingestion and inhalation of well water while showering
- Ingestion of milk and meat from livestock (e.g., dairy and beef cattle) that drink well water
- Ingestion of meat and eggs from poultry that drink well water
- Ingestion of vegetables grown in garden soil irrigated with well water and containing contaminated drill cuttings
- Ingestion of milk and meat from livestock (e.g., dairy and beef cattle) that eat fodder from pasture irrigated with well water
- Ingestion of meat and eggs from poultry that eat fodder from pasture irrigated with well water
- Inhalation of well water used for irrigation
- Inhalation of dust from the soil that was contaminated by drill cuttings and irrigated with well water
- Ingestion of soil that was contaminated by drill cuttings and irrigated with well water
- Direct radiation exposure from radionuclides on the soil that was contaminated by drill cuttings and irrigated with well water

The following exposure pathways involving the use of contaminated surface water (from the applicable stream) for recreational use are assumed to occur:

- Direct irradiation during recreational activities (e.g., swimming, fishing, boating) from stream water
- Dermal contact with stream water during recreational activities (e.g., swimming, fishing)
- Incidental ingestion and inhalation of stream water during recreational activities
- Ingestion of fish from the stream water

The intruder may also be exposed to a release of volatile radionuclides (e.g., H-3, C-14, I-129) from the drill cuttings and contaminated well water. These pathways include:

- Direct plume shine
- Inhalation

Figure 4.2-33: Chronic Intruder Agricultural (Post-Drilling) Scenario

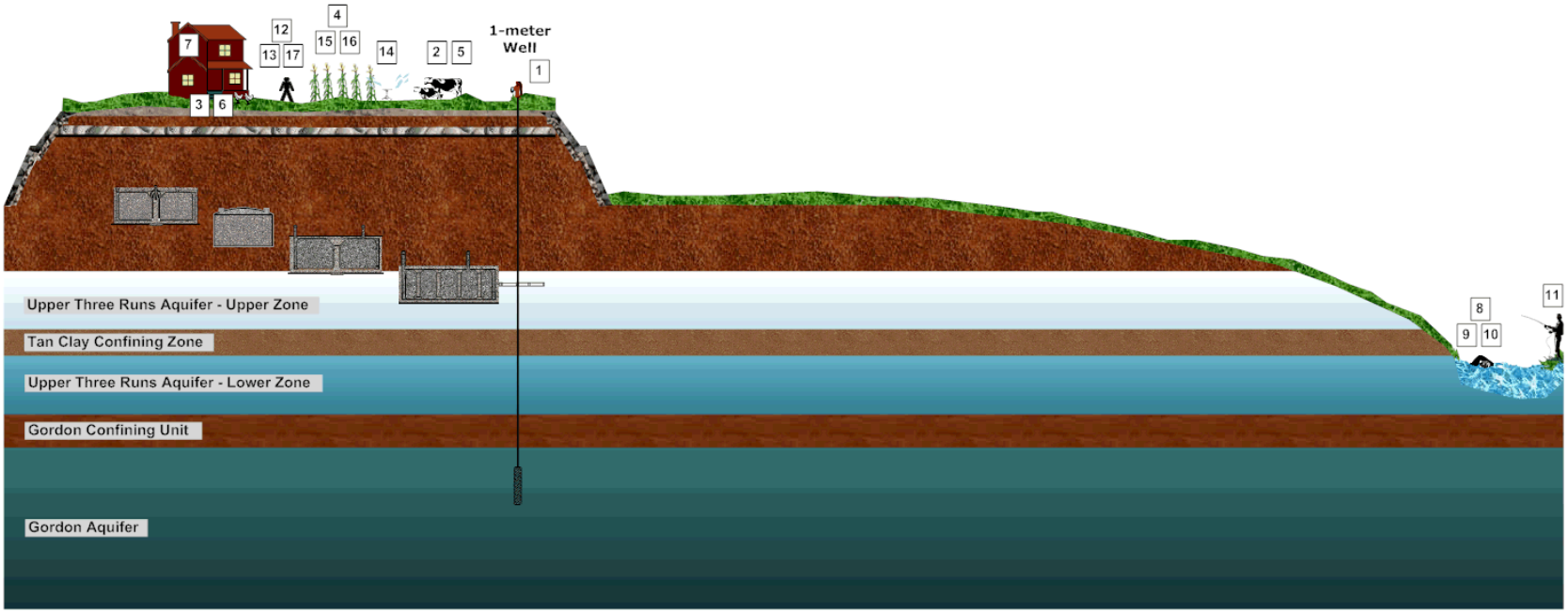

CHRONIC INTRUDER-AGRICULTURAL (POST-DRILLING) SCENARIO

1. Direct ingestion of well water
2. Ingestion of milk and meat from livestock (e.g., dairy and beef cattle) that drink well water
3. Ingestion of meat and eggs from poultry that drink well water
4. Ingestion of vegetables grown in garden soil irrigated with well water and containing contaminated drill cuttings
5. Ingestion of milk and meat from livestock (e.g., dairy and beef cattle) that eat fodder from a pasture irrigated with well water
6. Ingestion of meat and eggs from poultry that eat fodder from a pasture irrigated with well water
7. Ingestion and inhalation of well water while showing
8. Direct irradiation during recreation activities (e.g., swimming, fishing, boating) from stream water
9. Dermal contact with stream water during recreational activities (e.g., swimming, fishing)
10. Incidental ingestion and inhalation of stream water during recreational activities
11. Ingestion of fish from the stream water
12. Direct plume shine
13. Inhalation
14. Inhalation of well water used for irrigation
15. Inhalation of dust from the soil that was contaminated by drill cuttings and irrigated with well water
16. Ingestion of soil that was contaminated by drill cuttings and irrigated with well water
17. Direct radiation exposure from radionuclides on the soil that was contaminated by drill cuttings and irrigated with well water

4.2.3.2.6 Chronic Intruder-Resident Scenario

In this scenario, it is assumed that after the end of active institutional controls, an intruder (i.e., the resident intruder) inadvertently constructs a house at, and lives on, the closure site. The intruder-resident scenario involves the same pathways as the Chronic Intruder Agricultural (Post-Drilling) Scenario, with the potential for additional pathways associated with a house constructed over stabilized contaminants. The pathways uniquely associated with construction of a residence over stabilized contaminants were considered insignificant because of the depth of the stabilized contaminants under the closure cap and the shielding provided by the waste tank and ancillary equipment containment shielding. This shielding would reduce the external dose rates to very low levels. The intruder resident scenario did not require a unique analysis because it was addressed by the Chronic Intruder Agricultural (Post-Drilling) Scenario.

4.2.3.2.7 Chronic Intruder-Recreational Hunting/Fishing Scenario

In this scenario, the assumption is a hunter/fisher inadvertently visits the site, perhaps on a periodic basis, and consumes game and fish taken from the site. For the Chronic Intruder-Agricultural (Post-Drilling) Scenario, the intruder is assumed to perform similar recreational activities as the hunter/fisher who inadvertently visits the site, except for hunting wild game. As discussed in Section 4.2.3.3, the livestock raised near HTF would be more affected by HTF stabilized contaminants than transient wild game. Given the other significant exposure pathways the inadvertent intruder is considered to experience as part of the Chronic Intruder-Agricultural (Post-Drilling) Scenario (e.g., use of well water as potable water, ingestion of livestock and vegetables raised using well water), the intruder-recreational scenario is bounded by the Chronic Intruder Agricultural (Post-Drilling) Scenario and does not require unique analysis.

4.2.3.2.8 Bio-Intrusion Scenario

The bio-intrusion scenario assumes that an intruder moves onto the site but does not excavate into the stabilized contaminants. Rather, radioactivity is brought to the surface by plants through root uptake and by burrowing animals. Bio-intrusion is not considered a credible mechanism for significant stabilized contaminant disturbance, based on the stabilized contaminant depth and form. The stabilized contaminants will be significantly below ground, from at least 10 feet for ancillary equipment to at least 40 feet for stabilized contaminant tank heels. The stabilized contaminant is contained within closed waste tanks or equipment of either stainless steel or carbon steel and will be stabilized and/or grouted as part of the waste tank closure. Of the likely burrowing animal residents at SRS, only one burrower, the Florida Harvester Ant, is expected to burrow below 2 meters, and then, only 5% of its burrows are expected to be that deep. [WSRC-RP-92-1360] Assuming the HTF cover reverts to pine forest in the future, the pine trees could also pose a bio-intrusion risk, with a mature pine having roots from 6-feet to 12-feet deep. [WSRC-TR-2003-00436] These bio-intrusion depths are not deep enough to reach the principal HTF stabilized contaminant inventory at closure (stabilized contaminant tank heels), and are unlikely to reach any ancillary equipment inventory, which in almost

all cases will be more than 12-feet deep. Even if a pine tree root were to reach the ancillary equipment containment, no significant stabilized contaminant dispersal would be anticipated. The amount of contamination excavated from animal burrows or vegetative intrusion is far less than that involved in the agricultural (intruder-drilling) scenarios for drilling a domestic well into the underlying aquifers. Therefore, this scenario is bounded by the Chronic Intruder-Agricultural (Post-Drilling) Scenario and the bio-intrusion scenario does not require further analysis.

4.2.3.3 Basis for Intruder Pathways

Table 4.2-41 was prepared to provide a list of all the HTF exposure pathways identified as candidates for detailed analysis. The list of candidates was developed based on a review of SRS PA analyses and NRC documents. [SRS-REG-2007-00002, SRR-CWDA-2009-00017, NUREG-0782, NUREG-0945, NUREG-1573] Those human activities at SRS that could bring humans in contact with stabilized contaminants (e.g., water use, hunting, fishing, recreational activities such a swimming and boating, habitation in dwellings, other unique activities that involve water use or ground disturbance) were considered (with emphasis on local practices), to ensure that any pathways unique to SRS were taken into account. Those potential pathways that have quantitative analysis are denoted with an "X" for the various receptors. Quantitative analysis was not performed for potential pathways denoted with an "O", based on the applicable justifications provided throughout this section. NUREG-1854 states that transport pathways may be excluded from performance analysis if it can be demonstrated that either there is limited potential for radionuclides to be released into a particular pathway, or the pathway is not viable (e.g., water is not potable). Other pathways were excluded due to the nature of the scenario making them impossible (e.g., a garden that receives 100% irrigation from well water does not receive water from a stream).

The following inputs and assumptions were made regarding the intruder release pathways scenario using water from a well or stream.

- The stabilized contaminant release mechanisms to the intruder are well installation and inadvertent drilling into ancillary equipment, leaching of stabilized contaminants to the groundwater, and volatilization of the stabilized contaminants to the surface. Drilling a well into a waste tank is not considered a credible release mechanism, since local practices would cause a well driller to choose a new location before the stabilized contaminant waste tank inventory was disturbed. The local well drillers expect to reach good drinking water aquifers at 150 to 200 feet while drilling through sandy soil (no drilling through high-strength geologic materials). A driller would not expend the effort and equipment damage required to drill through the concrete/grout/steel covering the stabilized contaminant waste tank inventory. Even if the driller did not realize that he had struck a waste tank, and simply thought he had merely hit a layer of high-strength geologic materials, local experience would tell him that moving the drill site a short distance would avoid the impediment. Similarly, well drilling through a transfer line is also unlikely, especially while the line maintains some structural integrity. Nevertheless, as a bounding case for the purposes of this exercise, it has been assumed that a well

driller could drill through an intact transfer line immediately after the end of institutional control.

- Well water will be used by the inadvertent intruder as a primary potable water source (e.g., drinking water, showering) and is used as a primary water source for agriculture (e.g., irrigation, livestock water).
- The inadvertent intruder can use a nearby stream for recreational activities (e.g., swimming, fishing, and boating).
- Any wild game ingested (deer, wild pigs) would merely offset ingested livestock, and would result in a lower total dose since the livestock raised near HTF would be more affected by HTF stabilized contaminants than transient wild game.
- A survey of land and water usage characteristics within a 50-mile region of SRS was conducted and documented in WSRC-RP-91-17. The results of this study found that hogs are raised on farms within 50 miles of the SRS; however, hogs eat commercial feed. Thus, the local consumption of hogs is not considered in the determination of "meat" production or consumption.
- There are two streams (UTR and Fourmile Branch) from which ingestion of marine life with significant contamination is possible. These streams were conservatively assumed a source of dietary fish, excluding shellfish because the streams are not significant sources of edible shellfish and it plays an insignificant role in local diets when considered with other ingested contributors to dose (livestock, milk, and vegetables). [WSRC-TR-2005-00201, WSRC-STI-2007-00004]
- Since there is no substantive water source readily available at the well site, pathways related to water-related commercial activities were not considered. Based on the relative proximate of a large, natural water source (i.e., the Savannah River), it is not assumed that a man-made body of water would be created at the MOP resident site.
- The quantities of water ingested during the relatively short activities of showering (10 min/d) and swimming (7 hr/yr) are negligibly small and are not be addressed independently. The impact of these activities is addressed by the "direct ingestion of well water" pathway (i.e., they are included in the 337 liters of water that is assumed to be ingested every year). [SRNL-STI-2010-00447]
- The dose associated with dermal absorption of radionuclides is insignificant because, unlike some chemicals, radionuclides are generally adsorbed into the body very poorly. Tritium is an exception to this rule, but tritium is found in such relatively small concentrations in the groundwater that it would not be a significant contributor to dose.

4.2.4 Summary of Key Transport Assumptions

The following are the key transport analyses assumptions associated with contaminant release, groundwater transport, and dose.

4.2.4.1 Key Assumptions for Contaminant Release

- An independent conceptual waste release model was used to simulate stabilized contaminant release from the grouted tanks based on various chemical phases in the tank controlling solubility.

- Steel liner failure triggers contaminant release from the tanks. After failure, the carbon steel liner is assumed to be absent, or otherwise not a hindrance to advection and diffusion.
- The steel liner failure analyses considered general and localized corrosion mechanisms of the tank steel.
- Four waste tanks (Type I, Tank 12 and Type II, Tanks 14, 15, and 16) are assumed to have liner degradation at the time of HTF closure, based on present leak site numbers and physical locations.
- Tank concrete properties are originally characterized as Oxidizing Region II transitioning to Oxidizing Region III.
- The reducing grout properties are initially characterized as Reduced Region II, then transition to Oxidized Region II and Oxidized Region III.
- Transfer line inventory is modeled by distributing the assumed inventory over the HTF footprint. Other ancillary equipment is not modeled explicitly.
- Eight waste tanks, along with some ancillary equipment, are either fully submerged or partially submerged in the saturated zone.
- Leaching of contaminants is modeled as a non-uniform leaching process that depends on the chemical state of pore fluid contacting the stabilized contaminant at any given time.
- The calculation of radionuclide solubility in the CZs is done under the assumption of thermodynamic equilibrium using the geochemical modeling program, GWB.

In this analysis, the key conservatism introduced into the analysis was the decision to model only solubility controls to account for stabilized contaminant release in fate and transport models. Contaminant transport outside of the CZ was modeled using soil distribution coefficient values taken from compilations of geotechnical data in support of site PA modeling. The selection of solubility controlling phases is very conservative, meaning that where multiple phases of a radionuclide were possible, that with the highest solubility is selected. The process attempted to balance scientific knowledge with the need to be cautious and biased toward higher solubility. Some contaminants were simulated as having no identified solubility controls, with their releases modeled as instantaneous.

In an equilibrium model, the assumption that solubility rather than adsorption controls contaminant release results in faster overall release of radionuclides. This is because the maximum concentration that can desorb is controlled by solubility. In effect, if the distribution coefficient is low enough that a concentration is released that exceeds solubility, some of the radionuclide will precipitate bringing the concentration down to solubility. The stabilized contaminant release rate will drop below that dictated by solubility when the radionuclide inventory is depleted to where the concentration released is below solubility. At higher distribution coefficient values the concentration released at any given time will always be below the concentration dictated by solubility. Thus, time until complete release of a radionuclide using adsorption controls will always be longer than when only solubility controls are used.

4.2.4.2 Key Assumptions for Groundwater Transport

- HTF contaminant transport processes in cementitious materials and soils include advection, dispersion, and sorption, but not colloidal transport.
- Although the conceptual closure cap has a certain physical thickness (a minimum of 10 feet), the cap is viewed as a surface feature in the ICM and is simulated separately. The closure cap model produces a net infiltration rate at the bottom of the closure cap that becomes a flow boundary condition to the adjoining vadose zone.
- For saturated zone contaminant transport, the contaminant flux leaving the bottom of the vadose zone model becomes the source of contamination entering the aquifer.
- The aquifers of primary interest for HTF modeling are the UTR and Gordon Aquifers. Potential contamination from the HTF is not expected to enter the deeper Crouch Branch Aquifer.
- Because the HTF is located over a groundwater divide between UTR and Fourmile Branch, contaminants could eventually discharge to both streams, depending on the contaminant's origination point.
- The simulation model for groundwater flow constructed from the GSAD using the PORFLOW code is referred to as the GSA/PORFLOW Model. The 3-D grid comprises 102,295 active cells.
- Some cementitious properties are expected to remain constant over time. These include porosity, dry bulk density and particle density. Because the form of cementitious material degradation is cracking and not the dissolving the cement paste, the porosity, bulk density, and particle density of the cementitious material, a marginal impact is expected.
- The most extensive cementitious material attack was found to be from carbonation on unsaturated concrete and grout. Carbonation was found to result in the greatest penetration as a function of time. The effect of carbonation on the permeability of the cementitious barriers depends on whether the barrier contains steel.

In this analysis, several conditions introduce conservatism into the flow calculations. Of particular importance is the approach to handing loss of containment after failure of the steel liner. Immediately after failure, the liner is assumed as not a hindrance to advection or diffusion, which allows the immediate release of non-adsorbing contaminants and hastens the geochemical transition of the waste form from reducing to oxidizing conditions accompanied by a general increase in contaminant release rates.

4.2.4.3 Key Assumptions for Dose Calculations

- The primary mechanism for transport of radionuclides is expected to be leaching to the groundwater, groundwater transport to the well/stream, and subsequent human consumption or exposure.
- The scenarios are not assumed to occur until after the 100-year institutional control period ends, after which time it is assumed that no active HTF facility maintenance will be conducted.

- Pathways related to the MOP resident scenario using water from a well or stream incorporated the following key assumptions:
  - The stabilized contaminants release mechanisms to the MOP are leaching of stabilized contaminants to the groundwater and volatilization of the stabilized contaminants to the surface. Well drilling is not a release mechanism.
  - Bio-intrusion and/or erosion are not considered credible mechanisms. The stabilized contaminants will be significantly below ground, from at least 10 feet for ancillary equipment to approximately 40 feet for stabilized contaminants.
  - In the well water as primary water source scenario, well water will be used as a primary potable water source for a residence near the well.
  - In the MOP near a stream scenario, stream water will be used as a primary potable water source for a residence near the stream.
  - There are two streams (UTR and Fourmile Branch) from which ingestion of finfish with significant contamination is possible. The assumption for these streams as a source of dietary fish was conservative, and the two streams are not significant sources of edible shellfish.
- Since there is no substantial water source at the well site, there was no consideration for pathways related to water-related commercial activities.
- The quantities of water ingested during the relatively short activities of showering (10 min/d) and swimming (7 hr/yr) are negligible and not addressed independently.
- The scenario involves the intruder excavating a basement to a depth of approximately 10 feet. The intruder is assumed to recognize that he or she is digging into very unusual soil immediately upon encountering the waste tank/piping system and leaves the site.
- The chronic intruder-agriculture scenario is an extension of the Acute Intruder-Drilling Scenario. It is assumed in this scenario that an intruder lives in a building near the well drilled as part of the intruder-drilling scenario and engages in agricultural and recreational activities on the contaminated site and stream.

Key conservatisms incorporated into the calculation of dose include that all groundwater concentrations used for dose calculations are maximum values. For example, a dose computed for Sector A, at the maximum hypothetical 100-meter well location, uses for each contaminant the maximum concentration from any of the wells within the sector. This maximum is selected for each time step in the simulation. The dose provided is the maximum of the sectors, A through F.

For the chronic intruder dose calculations, the concentration released below the footprint of Tank 11 is used for the 1m well concentration, because this is the waste tank with the highest calculated concentration of Ra-226, the main dose driver over the performance period. Taking the concentration from the footprint cell of Tank 11 is a conservative assumption and should provide a maximum dose to the chronic intruder.

4.2.4.4 Key Assumptions for Air and Radon Pathways

The following are the key air and radon pathway analyses assumptions:

- The stabilized contaminant layer was represented as a 1-foot layer of material located at the bottom of the waste tank.
- The stabilized contaminant layer, reducing grout, and concrete roof were assumed saturated at 50%.
- The stabilized contaminant layer is assumed to have properties similar to reducing grout.
- Exclusion of the top soil, upper backfill, HDPE geomembrane, GCL, and primary steel liner of the waste tank make the model conservative.
- The final closure cap as outlined with exclusions was assumed to remain intact for the duration of the simulation.

In this analysis, several conditions introduce conservatism into the calculations. These include:

- Using boundary conditions that force all gaseous radionuclides to move upward from the stabilized CZ to the land surface - some gaseous radionuclides diffuse sideways and downward in air-filled pores surrounding the stabilized CZ; therefore, ignoring this has the effect of increasing flux at the land surface.
- Not taking credit for removal of radionuclides via pore water moving vertically downward through the model domain - this mechanism would likely remove some dissolved radionuclides therefore its omission had the effect of increasing the estimate of instantaneous radionuclide flux at the land surface in simulations.
- Exclusion of the HDPE geomembrane, GCL, and the primary steel liner of the waste tank - inclusion of these materials in the model would significantly reduce the gaseous flux at land surface due to material properties (i.e., low air-filled porosity).
- Excluding cover materials above the erosion barrier (i.e., top soil and upper backfill layers) - this material exclusion shortens the diffusion pathway and could increase flux at the land surface.
- Assuming stabilized contaminant layer, reducing grout and the concrete roof are only 50% saturated - these materials are likely at or near saturation making the air-filled porosity equal to one-half the total porosity and increasing diffusive transport through the materials since gaseous flux is through air-filled porosity.
- Using Type I and Type II tanks with minimum closure cap thickness.
- Concentrating entire estimated HTF residual inventory to a 1-foot stabilized contaminant layer to determine maximum dose and flux.

4.3 Modeling Codes

In the process of completing the PA for the HTF, a variety of modeling codes were utilized to perform various media transport, radiological dose, and groundwater concentrations calculations. The purpose of this section is to present the modeling codes used and describe the modeling code integration. A brief description is provided for each modeling code, which includes the function of the code, available code manuals or technical documents for the applicable code revision, reasons for selection of the particular code, and available QA documentation for the code. The results of the HTF PA will be used during the CERCLA closure process and complement any additional evaluations necessary using existing ACP modeling methods for residual materials other than those in the waste tanks and ancillary equipment.

4.3.1 Modeling Codes Used

Five modeling codes were used to support the HTF PA, as discussed below. These are HELP, PORFLOW, GoldSim, CAP88-PC (CAP-88 for Personal Computers), and GWB.

4.3.1.1 Hydrologic Evaluation of Landfill Performance Model

The HELP model is a quasi 2-D water balance model designed to conduct landfill-water balance analyses. The HELP model was used to generate water infiltration estimates through the closure cap, for use in PA calculations. HELP model infiltration estimates form the input to subsequent flow and contaminant transport models.

The HELP model requires the input of weather, soil, and design data. It provides estimates of runoff, evapotranspiration, lateral drainage, vertical percolation (i.e., infiltration), hydraulic head, and water storage for the evaluation of various landfill designs. U.S. Army Corps of Engineers (USACE) personnel at the Waterways Experiment Station (WES) in Vicksburg, Mississippi developed the HELP model, under an interagency agreement with the EPA. [EPA-600-R-94-168b] As such, the HELP model is an EPA sanctioned model for conducting landfill-water balance analyses. HELP model version 3.07, issued on March 1, 1997, is the latest version of the model and was the version used for the HTF PA calculations. The HELP model was used at SRS in the development of calculations supporting the SDF PA and was the code used by ACP during CERCLA closure evaluations. [CBU-PIT-2005-00146] While other codes for closure cap infiltration calculations exist, the HELP model is a proven code that is appropriate for use at SRS. It is public domain software available from the WES website at http://www.wes.army.mil/el/elmodels/helpinfo.html. EPA and the USACE have provided a user's guide that provides instruction documentation associated with the HELP model. [EPA-600-R-94-168a] Figures 4.3-1 and 4.3-2 illustrate the integration of the HELP model in HTF PA modeling.

Figure 4.3-1: Modeling Code Integration for HTF PA

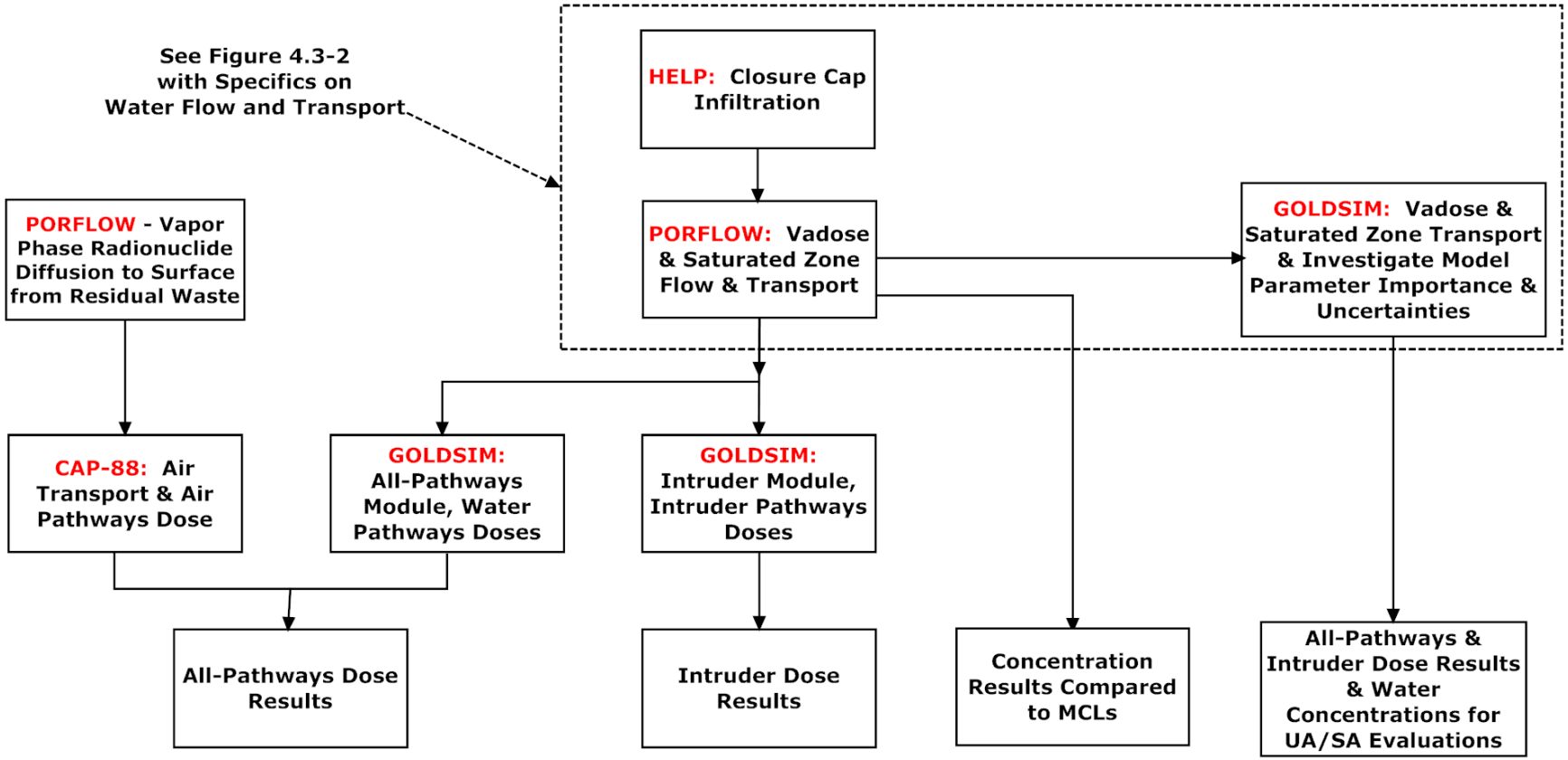

Figure 4.3-2: Modeling Code Integration (Details of Water Flow and Transport) for HTF PA

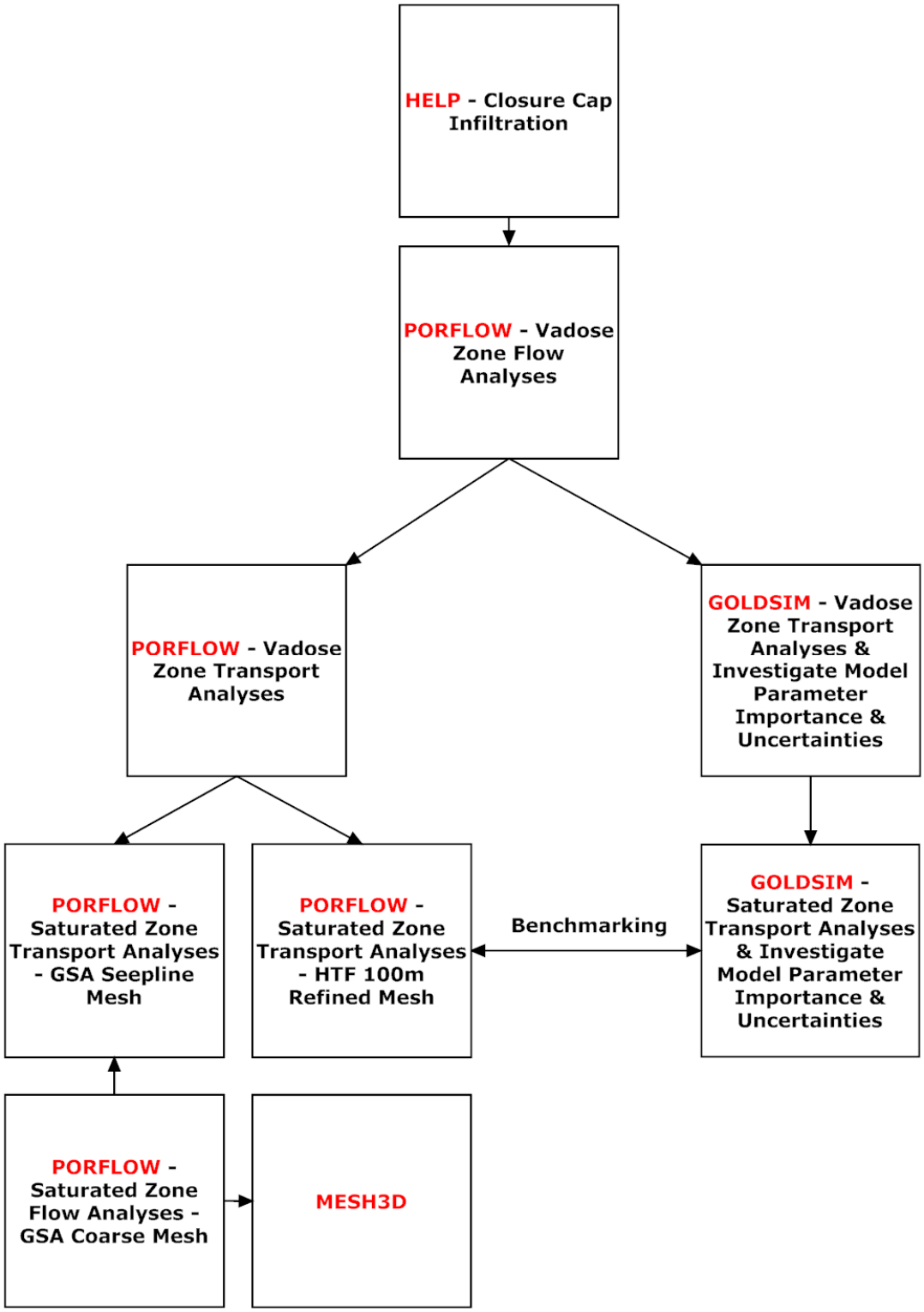

Engineering documentation provides information on the source language used to write the code, the hardware necessary to operate the code, data generation methodologies available for use, and the methods of solution. [EPA-600-R-94-168b]

HELP verification test reports exist which compare the model's drainage layer estimates to the results of large-scale physical models and compare the model's water balance estimates to "field data from 20 landfill cells at seven sites in the United States." [EPA-600-2-87-049, EPA-600-2-87-050]

The *FTF Closure Cap Concept and Infiltration Estimates* (WSRC-STI-2007-00184) report discusses eight water balance and infiltration studies that have been conducted in and around SRS by various organizations, including SRNL, USGS, State University of New York at Brockport, Pennsylvania State University, University of Arizona, and the Desert Research Institute. Findings from these studies are reported in the closure cap report. The HELP model results compare very well with the background water balance and infiltration studies, indicating that use of the HELP model produces reasonable and acceptable results. The closure cap report (WSRC-STI-2007-00184) shows that evapotranspiration dominates the water balance distribution of precipitation at SRS in both the background water balance and infiltration studies and in the results from the HELP model. Based upon these evaluations, use of the HELP model to establish the upper boundary condition infiltration for a 2-D PORFLOW vadose zone flow model is appropriate. [WSRC-STI-2007-00184]

The HELP model was used to evaluate seven closure cap infiltration cases. Case #6 is a soils only closure cap, with no barrier, drainage, or erosion control layers. As such, the HELP model water balance results from Case #6 are most applicable for comparison to the background water balance and infiltration studies. The average HELP model Case #6 infiltration (16.45 in/yr) is slightly greater than the median infiltration of the background studies (14.85 in/yr); indicating that the HELP model infiltration results are conservative.

In summary, additional studies for comparison to support HELP appropriateness in humid environments are not needed since the limitations of the software result in conservative infiltration estimates.

The Software Quality Assurance Plan (SQAP) for the HELP model version used for the HTF PA calculations is documented within Q-SQA-A-00005.

4.3.1.2 PORFLOW

PORFLOW is a commercial Computational Fluid Dynamics (CFD) tool developed by Analytic & Computational Research, Inc. PORFLOW numerically solves problems involving transient or steady state fluid flow, heat, salinity and mass transport in multi-phase, variably saturated, porous or fractured media with dynamic phase change. PORFLOW was used in the HTF PA modeling to calculate fluid flow and contaminant transport in the vadose and saturated zones. PORFLOW transport results were utilized by subsequent modeling codes to calculate radiological doses and perform human health and ecological risk evaluations. PORFLOW flow results were also used to conduct probabilistic simulations of contaminant transport via GoldSim, another computational tool. In addition, PORFLOW was use to calculate vapor phase radionuclide diffusion to the ground surface from stabilized contaminant material for use in air transport calculations. Figures 4.3-1 and 4.3-2 illustrate

the integration of PORFLOW in the HTF PA modeling and provide additional detail of the integration and steps of PORFLOW calculations for fluid flow and contaminant transport.

PORFLOW accommodates alternate fluid and media property relations, and complex and arbitrary boundary conditions. The geometry may be 2-D or 3-D, Cartesian, or cylindrical, and the mesh may be structured or unstructured, giving maximum flexibility to the user. PORFLOW version 6.10.3 was used for the HTF PA porous medium flow and transport analyses because its capabilities met program needs, core software functions have been verified through vendor and QA testing, and SRS personnel are experienced in applying PORFLOW in PA analyses. PORFLOW was used at SRS for calculations supporting the FTF and SDF PAs, and used by Idaho National Laboratory (INL) for analyses supporting closure of the tank farm facility. [SRS-REG-2007-00002, CBU-PIT-2005-00146, DOE-ID-10966] For the HTF PA, PORFLOW is an appropriate code because it can accommodate calculations in both the saturated and unsaturated zones and has the ability to simulate first-order decay and progeny in-growth associated with radionuclide chains, which is necessary for calculations involving radioactive stabilized contaminant disposal.

Analytic & Computational Research, Inc. has provided the following documentation for use the PORFLOW CFD tool:

- A user's guide (ACRi-2008)
- Validation data (ACRi-1994)
- Software verification for PORFLOW Versions 6.10.3 and 6.20.0 (ACRI-PORFLOW-QA-2008-1)

The SQAP for the PORFLOW version used for the HTF PA calculations is covered by WSRC-SQP-A-00028, G-TR-G-00002, SRNL-TR-2010-00023, and SRNL-TR-2010-00195.

MESH3D is a grid refinement tool developed by SRNL for extracting a portion of a PORFLOW model grid and flow solution, and optionally refining the cutout grid by subdividing cells. [Q-SQP-G-00003] The velocity and saturation fields are refined using a mass-conserving interpolation method. MESH3D is used to extract and refine a portion of the GSA/PORFLOW flow model of the vicinity of HTF for the purpose of performing higher resolution transport simulations of plume migration from waste tank sources out to 100 meters. Software design, use, testing, and QA plan for MESH3D are addressed by Q-SQP-G-00003.

The design check of the data used to perform the PORFLOW modeling is documented in SRR-CWDA-2010-00104 and SRNL-L6200-2010-00027, and all technical findings have been satisfactorily resolved. The scope of the design check includes

- Vadose zone flow input
- Vadose zone transport input
- Aquifer transport input

4.3.1.3 GoldSim

GoldSim is a commercial program developed by GoldSim Technology Group LLC (GTG). It is a user-friendly, graphical Windows-based program for carrying out dynamic

probabilistic simulations of complex systems to support management and decision-making in engineering, science, and business.

GoldSim was used to assist in developing uncertainty analyses for the HTF PA. The parameters modeled in GoldSim identified important input parameters in the groundwater transport model. GoldSim utilized the flow field outputs from PORFLOW to perform transport calculations and subsequent dose calculations for evaluation of input parameter importance and calculation uncertainties. GoldSim was used to evaluate parameter importance while developing the initial model for PORFLOW and provide feedback to the PORFLOW modelers on focus areas requiring additional attention. GoldSim was also employed for the performance of the all-pathways and intruder analyses by using the contaminant transport results from PORFLOW to calculate groundwater pathways and inadvertent intruder doses. Figures 4.3-1 and 4.3-2 illustrate the integration of GoldSim in the modeling efforts and provide additional detail of the integration and steps of GoldSim calculations for fluid flow and contaminant transport.

GoldSim was designed to facilitate the construction of large, complex models. The user can build a model of a system in a hierarchical, modular manner, such that the model can evolve and add detail as more knowledge regarding the system is obtained. Other features, such as the ability to manipulate arrays, the ability to "localize" parts of a model, and the ability to assign version numbers to a model that is constantly being modified and improved, further facilitate the construction and management of large models. GoldSim has an extensive internal database of units and conversion factors allowing the user to enter data and display results in any units and/or define customized units. GoldSim ensures dimensional consistency in models and carries out all of the unit conversions internally, eliminating the need to carry out (error-prone) unit conversions. The user can dynamically link external programs or spreadsheets directly into a HTF GoldSim Model. In addition, GoldSim was specifically designed to support the addition of customized modules (program extensions) to address specialized applications, such as contaminant transport.

GoldSim, version 10.11 Service Pack (SP) 3 is used for the PA porous medium transport and dose analyses because 1) its capabilities meet program needs, 2) it allows for ease of input changes and output visualization, and 3) it is used by other DOE sites (e.g., Nevada Test Site, Yucca Mountain Project) and the NRC.

The GTG provides a two-volume user's guide and a separate guide for data validation. [GTG-2009 for Vol.1 and Vol. 2, GTG-2010b] The SQAP for the HTF (PA) GoldSim Model is covered by SRR-CWDA-2010-00080.

4.3.1.4 CAP88-PC

The CAP-88 computer model is a set of computer programs, databases, and associated utility programs developed by the EPA for estimating dose and risk from radionuclide emissions to air. CAP-88 was used in the HTF PA to estimate annual dose to maximally exposed individuals (MEI) considering plume and ground gamma-shine, inhalation and foodstuff ingestion pathways using the vapor-phase radionuclide diffusion to the surface results from PORFLOW.

The CAP-88 was developed by the EPA and is used to demonstrate compliance with 40 CFR 61 *National Emissions Standards for Hazardous Air Pollutants (NESHAPs)*, Subpart H, *National Emission Standards for Emissions of Radionuclides other than Radon from Department of Energy Facilities*. The CAP-88 uses a modified Gaussian plume equation to estimate the average dispersion of radionuclides released from up to six sources at the same release location with different release heights. Assessments are done for a circular grid with a radius up to 50 miles. Figure 4.3-1 illustrates the integration of the CAP-88 in the HTF PA.

The original CAP-88 program was written in FORTRAN77 (Formula Translating System) and was compiled to run on an IBM (International Business Machine) 3090 mainframe under OS/VS2 (Operating System/Virtual Storage 2), using the IBM FORTRAN77 (1978 FORTRAN ANSI standard compliant revision) compiler (computer source code translator), at the EPA National Computer Center in the Research Triangle Park, North Carolina. The CAP88-PC software, released in 1992 allows the user to complete CAP-88 dose and risk assessment calculations in a personal computer environment. The CAP88-PC Version 1.0 is still in use today at SRS because prior personal computer versions of CAP-88 do not allow for adjustment of site-specific parameters of significance to the SRS, and CAP88-PC is an accepted model already being used at SRS for NESHAP compliance with the requirements in 40 CFR 61.93a for DOE facilities. CAP88-PC was used at SRS by ACP during CERCLA closure evaluations. In addition, CAP88-PC was used by INL during the development of calculations supporting their tank farm facility, and was used at SRS for development of calculations supporting the FTF PA. [CBU-PIT-2005-00146, DOE-ID-10966]

A user's guide for CAP88-PC Version 1.0 is available (EPA-402-B-92-001). The SQAP for the CAP88-PC version used for the HTF PA calculations is covered by Q-SQP-A-00002.

4.3.1.5 The Geochemist's Workbench

The GWB is a geochemical modeling software developed by the University of Illinois for manipulating chemical reactions, calculating stability diagrams and the equilibrium states of natural waters, tracing reaction processes, modeling reactive transport, plotting the results of these calculations, and storing the related data. The software contains tools for balancing reactions, calculating activity diagrams, computing speciation in aqueous solutions, plotting the results of these calculations, and storing the related data. [SRR-CWDA-2010-00105]

As described in Section 4.2.1.1, this code was used to estimate chemical conditions, such as the affects of the partial pressure of carbon dioxide. These calculations supported the conceptual model of contaminant releases from the CZ of the waste tanks. [WSRC-STI-2007-00544]

The user's guides for GWB are available online at the University of Illinois's website (http://www.geology.uiuc.edu/Hydrogeology/hydro_gwb.htm). The SQAP for GWB is covered by SRR-CWDA-2010-00154.

4.3.2 Software QA and Validation

General requirements for site QA are described in 1Q Manual, Procedure 2-1 *Quality Assurance Program*. The SQAP requirements are described in 1Q Manual, Procedure 20-1 *Software Quality Assurance*. The software QA implementation reports for the specific

software codes used in the HTF PA are identified in Section 4.3.1. The hierarchy of the SRS quality documents is described in this section.

Management Policies (MP), 1-01, Policy 4.2 contains the SRS policy statement regarding the company's commitment to provide products and services that meet or exceed the requirements and expectations of our customers. The MP is to be implemented in a manner to support implementation of the SRS imperatives of safety, disciplined operations, cost effectiveness, continuous improvement, and teamwork. The SRS has established and implemented an Integrated Safety Management System (ISMS). The QA program is consistent with, and an integral part, of the SRS ISMS. The MP requires the QA program to include appropriate quality procedures for compliance with legal, regulatory, contractual, and corporate quality requirements. The MP stipulates that the SRS QA program comply with DOE O 414.1C, 10 CFR 830, Subpart A, and the SRR *Quality Assurance Management Plan* (QAMP). Application of the QA program contributes to the safe, reliable, and environmentally sound operation of the SRS. It incorporates a graded approach commensurate QA/Quality Control (QC) risk definition and application requirements. Application of the QAMP enables error prevention, detection and correction of deficient conditions and the incorporation of an assessment process for identifying continuous improvement opportunities. The focus of quality improvement is to reduce the variability of every process that influences the quality and value of SRS products or services. [SRR-RP-2009-00764, MP 1-01, Policy 4.2]

***Savannah River Remediation, LLC Quality Assurance Management Plan*, SRR-RP-2009-00764,** describes the requirements and responsibilities for execution of the SRS QA program for implementing DOE O 414.1C, and 10 CFR 830, Subpart A. [MP 1-01, Policy 4.2] The *Quality Assurance Requirements for Nuclear Facility Applications* and other consensus standards are used in the development of the QAMP. [ASME NQA-1] The plan has been jointly approved by SRS and the Department of Energy - Savannah River Operations Office (DOE-SR) and serves as the basis for the establishment of the procedures. [SRR-RP-2009-00764]

Quality Assurance Manual* 1-Q, Procedure 2-1, *Quality Assurance Program provides the structure and procedures for achieving and verifying the SRS requirements for quality. The manual consists of a series of QA procedures that describe applicable QA requirements. Procedure 2-1, Section B states that the QA Program has been developed to be responsive to the requirements of DOE O 414.1C, and DOE *Nuclear Safety Management*, Title 10 CFR 830, Subpart A. Because of the size and complexity of SRS and its varied products, services, and missions, the program has been defined in a standard framework of company policy, procedures, and instructions to be used by the implementing organizations to perform quality-related activities. [1Q Manual, Procedure 2-1]

Conduct of Engineering Manual*, E7, Procedure 2.60, *Conduct of Engineering and Technical Support Procedure Manual is the QA implementing procedure for performing technical reviews. The end use of data drives the level of review required. Design Verification, the highest-level review, must be performed for work affecting Safety Significant (SS)/Safety Class (SC) systems. Design Check is the next lower level of

review and is required for all Production Support (PS) and General Service (GS) design output documents. Because the work associated with the PA and associated documents are not associated with SS or SC systems, the Design Check represents the appropriate level of rigor.

During a Design Check, the technical accuracy of the design document is assured by performing the following activities:

- A mathematical check, if appropriate
- A review for correct use of technical input, including quality requirements
- A review of the approach used and reasonableness of the output
- An administrative check (e.g., page numbers, format)

To perform a Design Check the following criteria must be met:

- Cannot be a participant in the development of the portion of the document being checked
- Must be knowledgeable in the area of the design or analysis for which they review
- Must be capable of performing similar design or analysis activities
- Must have the security clearance for access to sufficient information to perform the Design Check

Between 2002 and 2004 SRNL developed, piloted, and implemented technical review guidelines incorporating the E7 Manual, Procedure 2.60 requirements for performing Design Checks and Design Verification by document review. These guidelines also meet the requirements for review of Type 2 Calculations contained in E7 Manual, Procedure 2.31 *Engineering Calculations*. The guidelines provide a flowchart to map the SRNL technical review process, lines of inquiry for performing reviews, a checklist for communicating instructions, and best management practices to set a benchmark for management expectations.

Software QA is conducted in accordance with the requirements of the 1Q Manual, Procedure 20-1 through the development and execution of the SQAP. This procedure fulfills the requirements of DOE O 414.1C and 10 CFR 830, Subpart A. The QA plans and processes used by SRS to verify the inputs and outputs for the different modeling codes used are provided in the code specific descriptions in Section 4.3.1.

4.3.3 Modeling Codes Summary

Figures 4.3-1 and 4.3-2 present the approach to modeling code integration used for the HTF PA. Important to the implementation of the modeling integration shown in Figures 4.3-1 and 4.3-2 is assurance that the input data to the various codes is verified to be accurate. Documentation of the verification for the model input traced from source documents, to modeling input, and to appropriate sections within the PA has been performed and is described in *H-Area Tank Farm (HTF) Performance Assessment (PA) Model Quality Assurance (QA) Report*, SRR-CWDA-2010-00104. Model inputs are implemented as components to the model files (i.e., they are "hardwired" into the models). Consequently, inputs are controlled in accordance with the quality assurance requirements of the respective model(s) and any changes to the inputs result in a change to the model, thus requiring re-qualification of the affected model file(s).

4.4 Closure System Modeling

This section describes how the HTF design elements and their associated properties were represented in the computer modeling codes. The closed waste tank system conceptual design was an aphysical simplification of the actual waste tank system design, which is required for analytical modeling. Certain waste tank features and design elements are by necessity omitted in the conceptual model and are discussed in Section 4.4.1.

This section also describes how the HTF closure cap system is expected to behave in the future, and what modeling scenarios were used to depict system behavior over time. Because it is difficult to predict with a high level of certainty just what changes may occur to a closed, grouted waste tank system over the 10,000-year compliance period, this section describes a range of potential conditions that a closed waste tank or ancillary system may be subjected. While the baseline analysis (represented through the HTF PORFLOW Model) reflected the best estimate of future behavior of the closured system, the probabilistic analyses (represented through the HTF GoldSim Model) considered a variety of possible scenarios. In addition to analyzing differing scenarios in the 10,000-year compliance period, the transport models were all run to at least 20,000 years in order to determine peak concentrations that occur after the 10,000-year compliance period.

4.4.1 Individual Waste Tank Modeling

Certain waste tank features and design elements were omitted in the initial conceptual model. The waste tank design features not included in the initial conceptual design will be addressed in subsequent conceptual models (e.g., cooling coils and rebar as fast flow paths). A number of general modeling decision guidelines were followed for the initial design:

- The intent of the initial conceptual model was to capture waste tank dimensions and relative material differences for each discrete waste tank segment.
- Each discrete waste tank segment/area was represented as homogeneous, ignoring interior elements (e.g., rebar, cooling coils) and/or penetrations through the area (e.g., waste tank risers, transfer lines).

- Minimum segment thicknesses were used where an area had variable thickness (e.g., waste tank walls, waste tank tops).
- Grouting of void areas in the waste tanks (e.g., primary liner tank interior, waste tank annulus) was assumed to have occurred as planned.

4.4.1.1 Type I Tank Modeling

The Type I tank dimensions are presented in Figure 4.4-1. Specific areas where these modeling decisions are implemented for the Type I tanks are as follows:

- The basemat segment of the waste tank was derived from basemat thickness, without consideration for other material layers below the waste tank (i.e., concrete working slab, grout layer, lean concrete layer, and waterproofing layer).
- The primary liner and secondary liner are explicitly modeled.
- The primary and secondary liner assumed thicknesses were based on the minimum thicknesses only.
- The waste tank wall and liner penetrations (e.g., transfer lines) were not modeled.
- The waste tank primary liner, considered filled with grout, was treated as a discrete area.
- The 12 waste tank support columns and cooling coils were not modeled and not included in the primary liner waste tank interior. The waste tank annulus, assumed filled with grout, was treated as a discrete area.
- The roof penetrations of the waste tank (e.g., risers) were not modeled.
- Concrete supporting rebar in the waste tank top, walls, and basemat was not modeled, and concrete was considered a homogenous material.
- The waste tank underliner sump was not modeled.
- The waterproofing, brick wall, and bituminous grout layers outside the concrete vault were not modeled and considered as soil.

Figure 4.4-1: Typical Type I Tank Modeling Dimensions

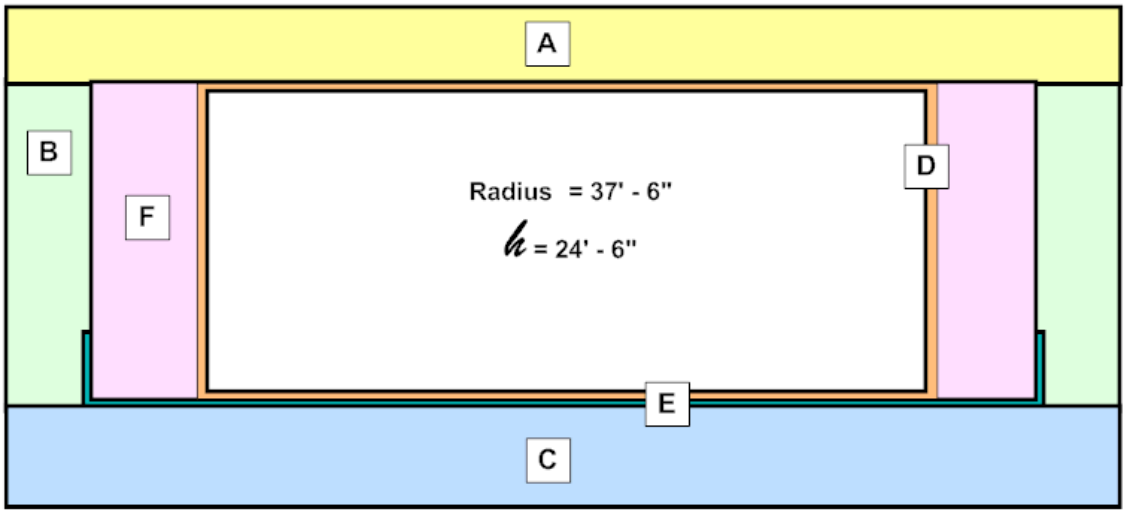

[NOT TO SCALE]

LABEL	THICKNESS	MATERIAL
A Concrete Roof	22"	Concrete
B Concrete Wall	22"	Concrete
C Concrete Basemat	30"	Concrete
D Primary Liner	0.5"	Carbon Steel
E Secondary Liner	5' high and 0.5" thick	Carbon Steel
F Grouted Annulus	30"	Tank Fill Grout

4.4.1.2 Type II Tank Modeling

The Type II tank dimensions are presented in Figure 4.4-2. Specific areas where these modeling decisions are implemented for the Type II tanks are highlighted below:

- The basemat segment was based on the basemat thickness disregarding other material layers below the waste tank (e.g., grout layer, and waterproofing layer).
- Primary and secondary liner assumed thicknesses were based on minimum thicknesses only.
- The waste tank wall and liner penetrations (e.g., transfer lines) were not modeled.
- The primary liner was considered as filled with grout and was treated as a discrete area.

- The support column and cooling coils were not modeled, and were not included in the primary liner. The waste tank annulus was treated as a discrete area because the assumption that it will be filled with grout.
- The roof penetrations (e.g., risers) were not modeled.
- Concrete rebar in the waste tank top, walls, and basemat was not modeled, such that concrete is considered a homogenous material.
- The soil hydration system was not modeled.

Figure 4.4-2: Typical Type II Tank Modeling Dimensions

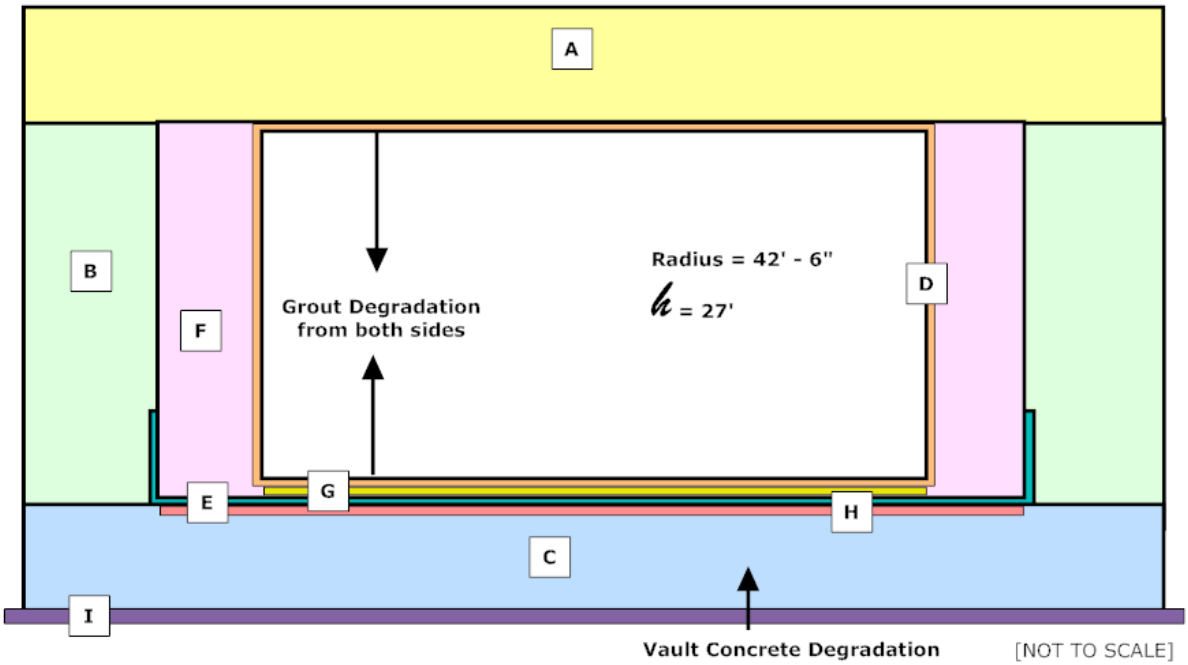

LABEL	THICKNESS
A Concrete Roof	45"
B Concrete Wall	33"
C Concrete Basemat	42"
D Primary Liner	0.5"
E Secondary Liner	5' high and 0.5" thick
F Grouted Annulus	30.625"
G Primary Liner Sand Bed	1"
H Secondary Liner Sand Bed	1"
I Concrete Working Slab	6"

4.4.1.3 Type III and IIIA Tank Modeling

The Type III and Type IIIA tank dimensions are presented in Figures 4.4-3 and 4.4-4, respectively. Specific areas where these modeling decisions are implemented for the Type III/IIIA tanks are highlighted below:

- Type IIIA basemat thickness has 2 inches subtracted to reflect the 2-inch leak detection slots cut into the basemat. [W701336, W707253]
- Thermocouple piping running through the waste tank walls and basemat was not modeled.
- The primary liner was considered as filled with grout and treated as a discrete area.
- The center column, center annulus, ventilation ductwork, and cooling coils were not modeled.
- The waste tank secondary liner was assumed as filled with grout and was treated as a discrete area.
- The primary liner and secondary liner assumed thicknesses were based on the minimum thicknesses only (e.g., extra thickness at knuckle not modeled).
- Penetrations through the waste tank wall and primary liner (e.g., transfer lines) were not modeled.
- The roof penetrations for the waste tanks (e.g., risers) were not modeled.
- Concrete rebar in the waste tank top, walls, and basemat were not modeled, such that concrete is considered a homogenous material.
- The underliner sump for the waste tank was not modeled.

Figure 4.4-3: Typical Type III Tank Modeling Dimensions

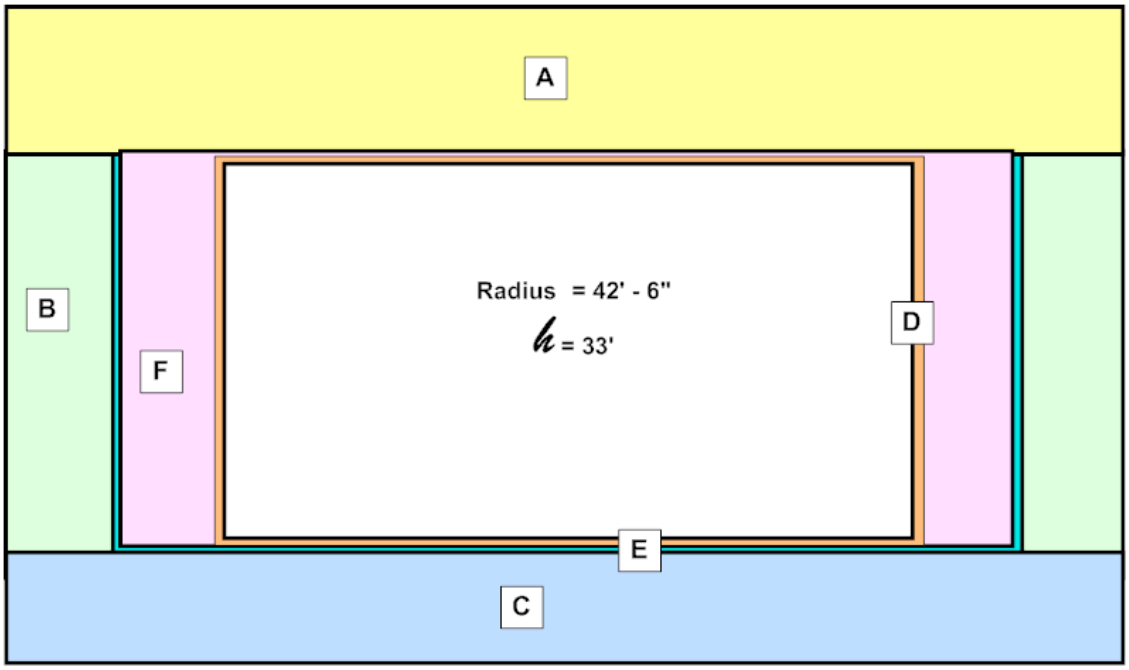

[NOT TO SCALE]

LABEL	THICKNESS	MATERIAL
A Concrete Roof	48"	Concrete
B Concrete Wall	30"	Concrete
C Concrete Basemat	42"	Concrete
D Primary Liner	0.5"	Carbon Steel
E Secondary Liner	0.375"	Carbon Steel
F Grouted Annulus	30"	Tank Fill Grout

Figure 4.4-4: Typical Type IIIA Tank Modeling Dimensions

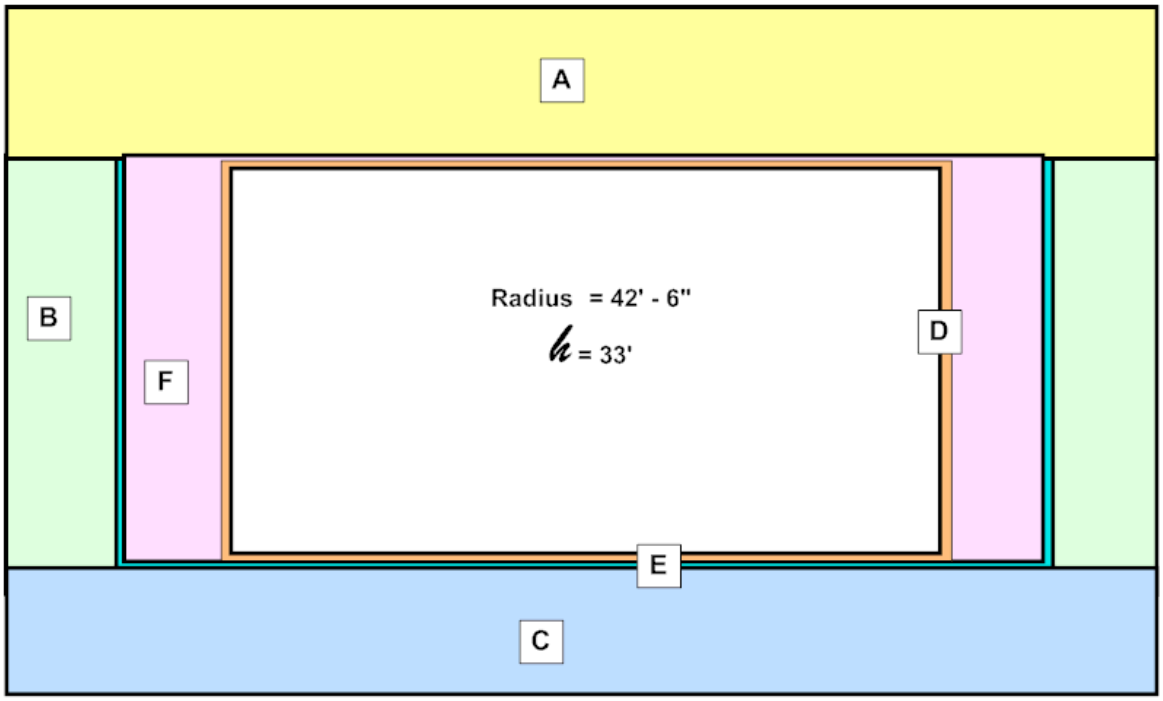

[NOT TO SCALE]

LABEL	THICKNESS	MATERIAL
A Concrete Roof	48"	Concrete
B Concrete Wall	30"	Concrete
C Concrete Basemat	41" (Typical) (43" - Tanks 35 - 37)	Concrete
D Primary Liner	0.5"	Carbon Steel
E Secondary Liner	0.375"	Carbon Steel
F Grouted Annulus	30"	Tank Fill Grout

4.4.1.4 Type IV Tank Modeling

The Type IV tank dimensions are presented in Figure 4.4-5. Specific areas where Type IV tank modeling decisions of interest are implemented are highlighted below:

- The basemat segment of the waste tank was based on the basemat thickness and the cement topping placed over the basemat. An approximately thickness of 0.1 inch was subtracted to account for the drainage grooves cut into the cement topping. The effective 0.1-inch groove thickness is based on the grooves being 1.625-inch deep and covering less than 6% of the waste tank footprint. The wall footing of the waste tank and the grouted segment between the wall footing and the basemat were not modeled.
- The primary liner waste tank cavity was assumed as filled with grout and treated as a discrete area.
- The primary liner assumed thickness was based on the minimum thicknesses only (e.g., extra thickness at knuckle not modeled).
- The waste tank wall and tank liner penetrations (e.g., transfer lines) were not modeled.
- The wall thickness of the waste tank is the minimum wall thickness and does not reflect the variable thickness of the wall.
- The thickness of the waste tank roof is the minimum thickness of the dome and does not reflect the variable thickness of the roof.
- The waste tank roof penetrations (e.g., risers) were not modeled.
- Concrete rebar in the waste tank top, wall, and basemat was not modeled such that concrete is considered a homogenous material.
- The waste tank underliner sump was not modeled.

Figure 4.4-5: Typical Tank IV Tank Modeling Dimensions

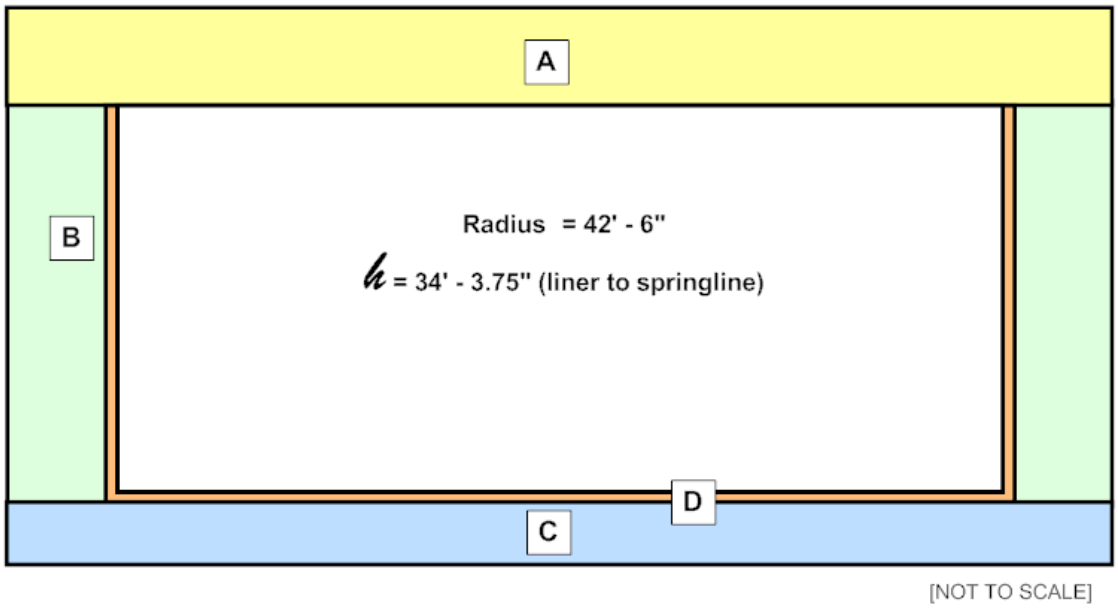

MATERIAL ZONE LABEL	THICKNESS	MATERIAL
A Concrete Roof	7"	Concrete
B Concrete Wall	7"	Concrete
C Concrete Basemat	6.9025"	Concrete
D Primary Liner	0.375"	Carbon Steel

4.4.2 Systems and Potential Degradation

There are 29 underground waste tanks and 10 (3 groups of pump tanks, 3 evaporators, and 4 groups of piping) ancillary systems identified and modeled in the closure of HTF. Each of these systems will initially be placed in a controlled condition at closure.

The HTF closure system is designed to contain the residual waste. However, the waste tanks themselves, the ancillary equipment, and the closure system will degrade over time, eventually releasing contaminants to the environment.

To simulate potential conditions in the HTF closure system over the modeling period, five waste tank cases have been identified for analyses. Each case starts out with the system closed as planned, with the waste tanks and ancillary equipment filled with grout and the closure cap in place. In the time frames discussed, year zero is taken to be the year during which the HTF is closed (current estimated closure date is 2032).

Waste tank Cases A through E begin with the engineered closure cap in place as planned. In the analyses of Cases A through E, expected degradation over time of the closure cap

materials was simulated using the increasing infiltration rates shown in Table 3.2-14. The waste release process described in Section 4.2.1 and the conceptual model material properties described in Section 4.2.2.2 were employed in each waste tank case evaluation. The differences between the five waste tank cases are summarized in Table 4.4-1 and are discussed in detail in the following sections.

Table 4.4-1: Waste Tank Case Summary

Case	Assumed Fast Flow Paths	Degradation of Cementitious Materials	Liner Failure Time[a]	CZ/Chemical Transition Driver
A	None	Degradation curve based on Table 4.2-34	Later failure date (based on grouted *D* of 1.0E-06 CO_2) in Table 4.2-36	Full Grout Capacity
B	Channel with no flow impedance through grout	Degradation assumed to be a step change at year 501	Early failure date (based on grouted *D* of 1.0E-04 CO_2) in Table 4.2-36	Full Grout Capacity
C	Channel with no flow impedance through grout	Degradation curve based on Table 4.2-34	Early failure date (based on grouted *D* of 1.0E-04 CO_2) in Table 4.2-36	CZ Reducing Capacity
D	Channel with no flow impedance through grout and basemat	Degradation assumed to be a step change at year 501	Early failure date (based on grouted *D* of 1.0E-04 CO_2) in Table 4.2-36	Full Grout Capacity
E	Channel with no flow impedance through grout and basemat	Degradation curve based on Table 4.2-34	Early failure date (based on grouted *D* of 1.0E-04 CO_2) in Table 4.2-36	CZ Reducing Capacity

Note Case E is a combination of Cases C and D. Case E uses flow path from Case D and remaining transitions from Case C.

D = diffusion coefficient

a Grouted *D* reported in cm^2/sec and Tanks 12, 14, 15, and 16 were modeled with a failed liner at the time of closure for all cases.

4.4.2.1 Waste Tank Case A

Figure 4.4-6 represents waste tank Case A. In Case A, no fast flow path exists from outside the waste tank system, through the waste tank, and exiting the system. In Case A, it was assumed that the cementitious material that makes up the walls, waste tank grout, and basemat concrete degrades over time (with these changes simulated by increasing hydraulic conductivity). Degradation of waste tank cementitious materials (degradation rate and timing) was based on SRNL-STI-2010-00035 and SRR-CWDA-2010-00019, and can vary dependant on waste tank type. The timing of the degradation of the waste tank cementitious materials is detailed in Table 4.2-34 for the various waste tank types. Case A was considered the HTF Base Case for waste tank operational closure.

Under Case A, the assumption for the entire primary (carbon steel) liner is impermeable, with the liner in direct contact with intact grout or concrete on all sides. Under these conditions, the liner was expected to remain impermeable until several thousand years after the waste tank operational closure as detailed in SRNL-STI-2010-00047, (except for Type I Tank 12 and Type II Tanks 14, 15, and 16, which have an assumed liner failure at HTF facility closure). After the liner fails, it was assumed, in Case A, that contaminants begin to leach from the degraded system based on changes to the pH and redox potential of the residual

contamination on the floor of the waste tank system. The reducing capacity of the full volume of grout is available to affect the infiltrating water. Individual radionuclide leach rates will vary over time based on solubility and adsorption controls. In this condition, it was assumed that no fast flow exits through the concrete basemat. Rather, it was assumed that contaminants were transported through the concrete basemat.

Figure 4.4-6: Case A

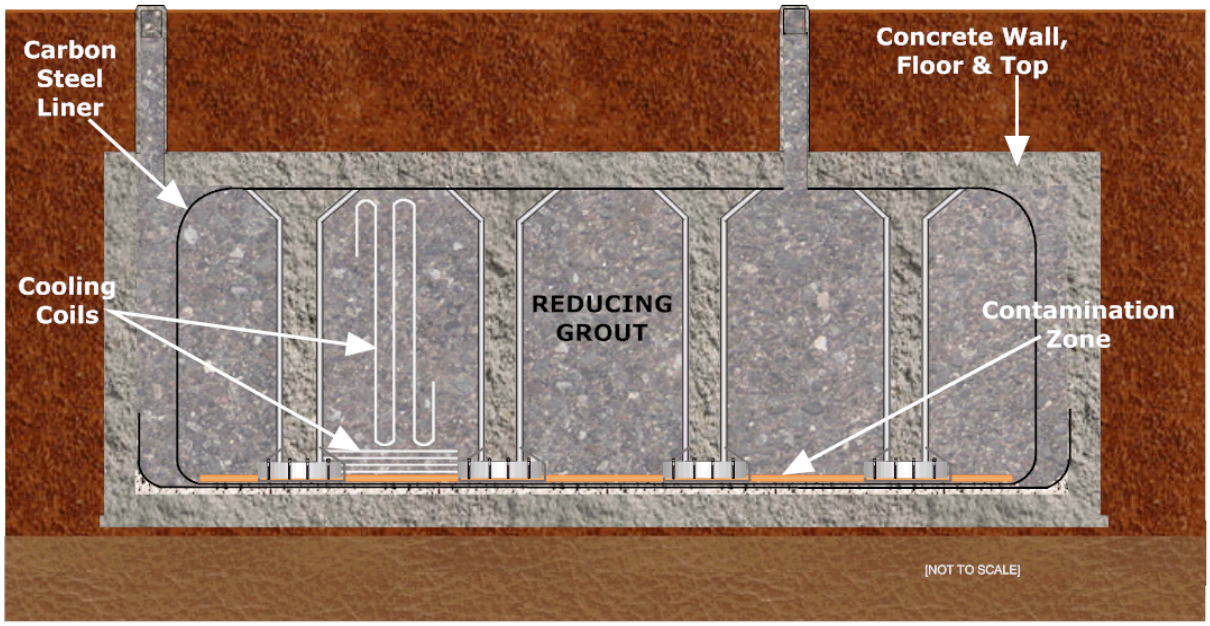

4.4.2.2 Waste Tank Case B

Figure 4.4-7 represents waste tank Case B. In waste tank Case B, it was assumed that a fast flow path exists between the waste tank top and CZ, (e.g., from riser through cooling coil) due to incomplete filling with grout during operational closure. The fast flow path through the grout was represented in the conceptual design by modeling a channel through the grout with full flow. The presence of the channel in the model is not ascribed to a particular cause, but is used to reflect the fact that various mechanisms have been postulated that could result in a significantly increased hydraulic conductivity (e.g., grout shrinkage, seismic induced fractures). The concrete walls, waste tank grout, and basemat degrade over time (as simulated by increasing hydraulic conductivity). The waste tank cementitious materials were assumed to begin to degrade at year 500, with degradation occurring essentially instantaneously.

It is assumed that concrete/grout pore water with relatively high oxygen concentration and low pH is in contact with the steel liner. In this condition, the diffusion coefficients (which control the failure times) are higher (1.0E-04 cm^2/sec) than in the Base Case (1.0E-06 cm^2/sec) and thus the steel liner will fail earlier than in the Base Case. Under these conditions, the steel liner was expected to remain impermeable until the analyzed failure times from SRNL-STI-2010-00047 were reached (Type I Tank 12 and Type II Tanks 14, 15, and 16, have an assumed steel liner failure at HTF facility closure).

After liner failure, it was assumed in Case B that contaminants begin to leach from the degraded system based on changes to the pH and redox potential of the residual contamination on the floor of the waste tank system. The reducing capacity of the full volume of grout is available to influence the infiltrating water. Individual radionuclide leach rates will vary over time based on solubility and adsorption controls. In Case B, it was assumed that no fast flow path exists through the concrete basemat. In fact, it was assumed that the concrete basemat had an increase in permeability based on concrete degradation. Whether the grout fast flow path is active during any period of time was dependent on the availability of sufficiently high infiltration through the conceptual closure cap.

Figure 4.4-7: Case B

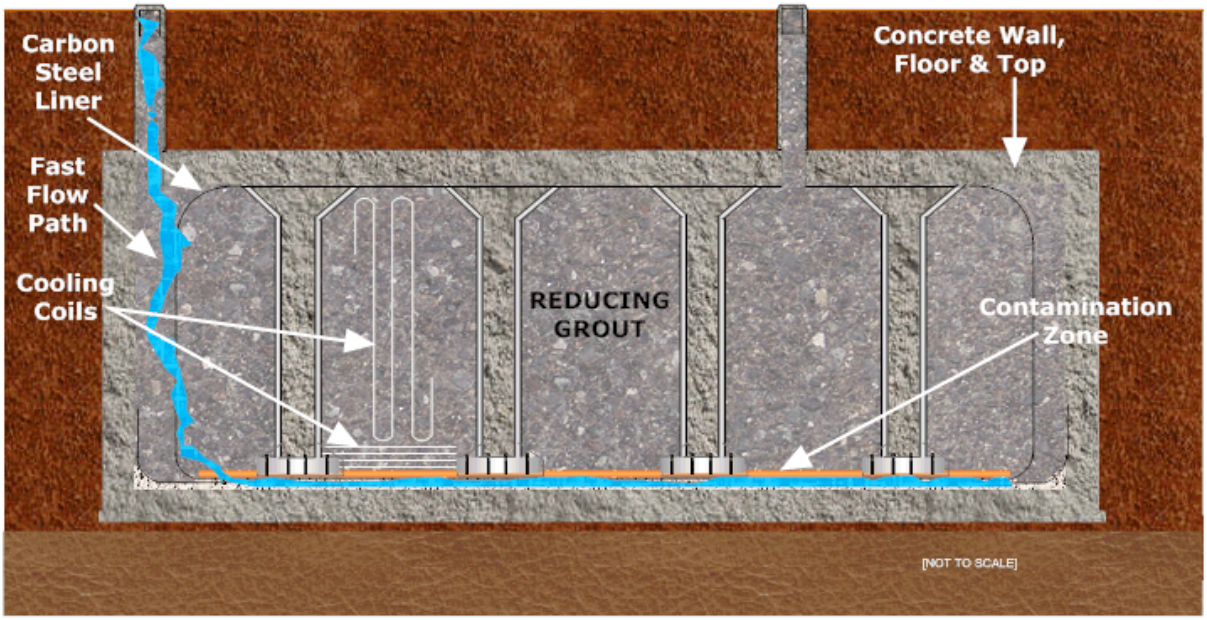

4.4.2.3 Waste Tank Case C

Figure 4.4-8 represents Case C. In Case C, it was assumed that a fast flow path exists between the waste tank top and CZ (e.g., from riser through cooling coil) due to incomplete filling with grout during closure. The fast flow path through the grout was represented in the conceptual design by modeling a channel through the grout with full flow. The presence of the channel in the model is not ascribed to a particular cause, but is used to reflect the fact that various mechanisms have been postulated that could result in a significantly increased hydraulic conductivity (e.g., grout shrinkage, seismic induced fractures). The concrete walls, waste tank grout, and basemat degrade over time (as simulated by increasing hydraulic conductivity). Degradation of waste tank cementitious materials (degradation rate and timing) was based on SRNL-STI-2010-00035 and SRR-CWDA-2010-00019, and can vary dependant on waste tank type. The timing of the degradation of the waste tank cementitious materials is detailed in Table 4.2-34 for the various waste tank types.

It is assumed that concrete/grout pore water with relatively high oxygen concentration and low pH is in contact with the steel liner. In this condition, the diffusion coefficients (which

control the failure times) are higher (1.0E-04 cm^2/sec) than in the Base Case (1.0E-06 cm^2/sec) and thus the liner will fail earlier than the Base Case. Under these conditions, the carbon steel liner was expected to remain impermeable until the analyzed failure times from SRNL-STI-2010-00047 are reached (Type I Tank 12 and Type II Tanks 14, 15, and 16 have an assumed carbon steel liner failure at HTF facility closure).

After the steel liner failure in Case C, it was assumed that contaminants began to leach from the degraded system based on changes to the pH and redox potential of the residual contamination on the floor of the waste tank system. The reducing capacity of the full volume of grout is not available to influence the infiltrating water. The infiltrating water chemistry is driven by the volume of the CZ due to the assumption that the fast flow bypasses the full grout volume and therefore the grout does not impart any chemistry changes to the water. Individual radionuclide leach rates will vary over time based on solubility and adsorption controls. In Case C, it was assumed that no fast flow path exists through the concrete basemat. Rather, the assumption was that the basemat has had an increase in permeability based on concrete degradation. Whether the grout fast flow path is active during any period was dependent on the availability of sufficiently high infiltration through the conceptual closure cap.

Figure 4.4-8: Case C

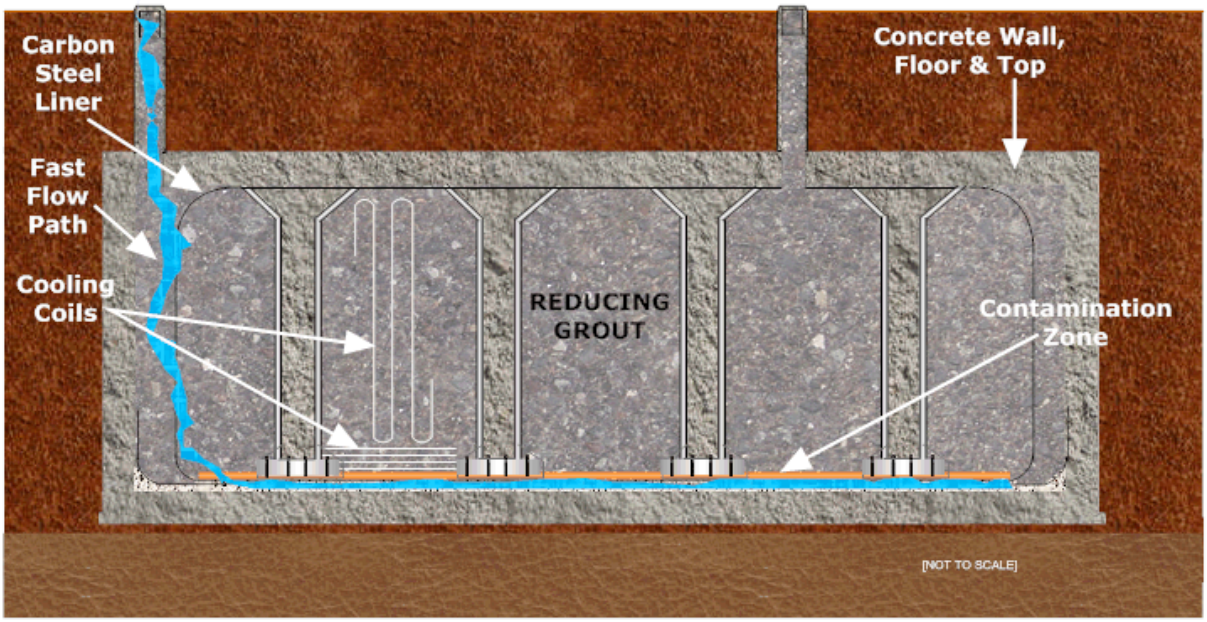

4.4.2.4 Waste Tank Case D

Figure 4.4-9 represents Case D. In Case D, it was assumed that a fast flow path exists through the entire operationally closed system (e.g., through a riser due to incomplete filling with grout during closure, through a cooling coil, through the waste tank grout, and through the basemat). The fast flow path through the grout and basemat was represented in the conceptual design by modeling a channel through the grout and basemat with full flow. The presence of the channel in the model is not ascribed to a particular cause, but is used to

reflect the fact that various mechanisms have been postulated that could result in a significantly increased hydraulic conductivity (e.g., grout shrinkage, seismic induced fractures). The concrete walls, waste tank grout, and basemat degrade over time (as simulated by increasing hydraulic conductivity). The waste tank cementitious materials were assumed to begin to degrade at year 500 with degradation occurring essentially instantaneously.

It is assumed that concrete/grout pore water with relatively high oxygen concentration and low pH is in contact with the steel liner. In this condition, the diffusion coefficients (which control the failure times) are higher (1E-04 cm^2/sec) than in the Base Case (1E-06 cm^2/sec) and thus the liner will fail earlier than the Base Case. In these conditions the steel liner was expected to remain impermeable until the analyzed failure times from SRNL-STI-2010-00047 are reached (Type I Tank 12 and Type II Tanks 14, 15, and 16, have an assumed liner failure at HTF facility closure).

After steel liner failure, it was assumed in Case D that contaminants begin to leach from the degraded system based on changes to the pH and redox potential of the residual contamination on the floor of the waste tank system. The reducing capacity of the full volume of grout is available to influence the infiltrating water. Individual radionuclide leach rates will vary over time based on solubility and adsorption controls. In Case D, it was assumed that a fast flow path exists through the concrete basemat. Whether the fast flow path is active during any period depended on the availability of sufficiently high infiltration through the closure cap.

Figure 4.4-9: Case D

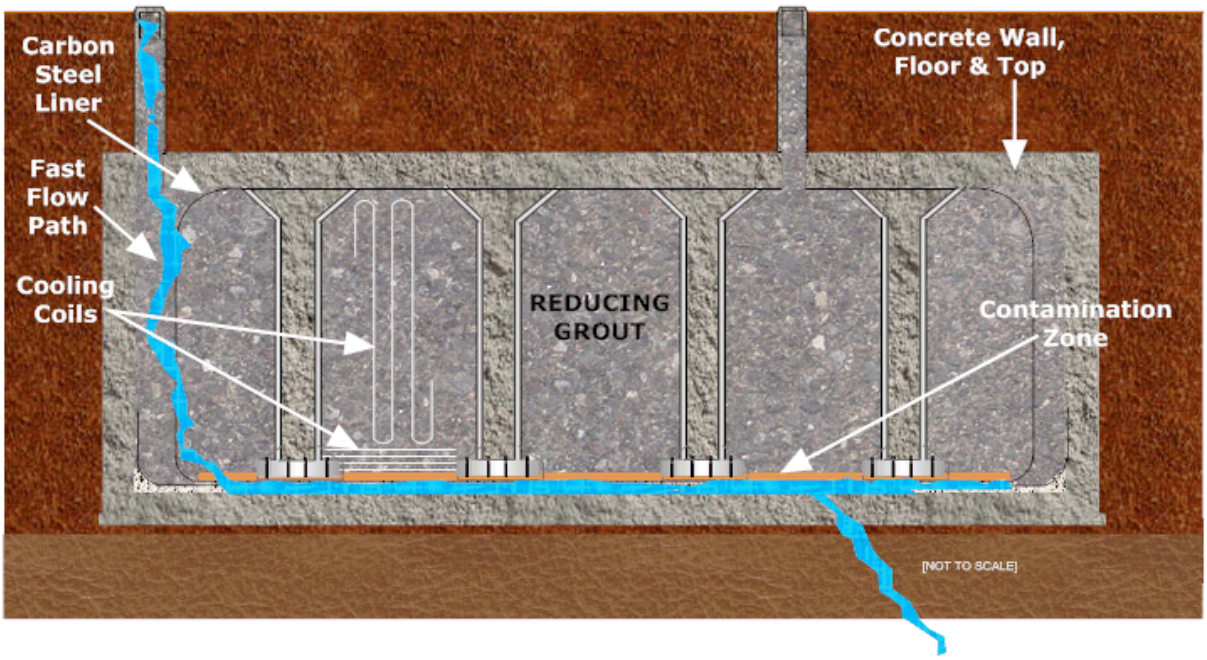

4.4.2.5 Waste Tank Case E

Figure 4.4-10 represents Case E. In Case E, it was assumed that a fast flow path exists though the entire operationally closed waste tank system (e.g., through riser due to incomplete filling with grout during operational closure, cooling coil, grout, and concrete basemat). The fast flow path through the grout and concrete basemat was represented in the conceptual design by modeling a channel through the grout and concrete basemat with full flow. The presence of the channel in the model is not ascribed to a particular cause, but is used to reflect the fact that various mechanisms have been postulated that could result in a significantly increased hydraulic conductivity (e.g., grout shrinkage, seismic induced fractures). The cementitious materials that make up the walls (grout and concrete basemat) degrade over time (as simulated by increasing hydraulic conductivity). The degradation of waste tank cementitious material (degradation rate and timing) was based on SRNL-STI-2010-00035 and SRR-CWDA-2010-00019, and varied depending on waste tank type. The timing of the degradation of waste tank cementitious materials is detailed in Table 4.2-34 for the various waste tank types.

It is assumed that concrete/grout pore water with relatively high oxygen concentration and low pH is in contact with the carbon steel liner. In this condition, the diffusion coefficients (which control failure times) are higher (1.0E-04 cm^2/sec) than in the Base Case (1.0E-06 cm^2/sec) and thus the liner will fail earlier than in the Base Case. Under these conditions, the carbon steel liner was expected to remain impermeable until the analyzed failure times from SRNL-STI-2010-00047 are reached (Type I Tank 12 and Type II Tanks 14, 15, and 16 have an assumed primary steel liner failure at HTF facility closure).

After liner failure, it was assumed in Case E that contaminants begin to leach from the degraded system based on changes to the pH and redox potential of the residual contamination on the floor of the waste tank system. The reducing capacity of the full volume of the grout is not available to influence the infiltrating water. The infiltrating water chemistry is driven by the volume of the CZ due to the assumption that the fast flow bypasses the full grout volume and therefore the grout does not impart any chemistry changes to the water. Individual radionuclide leach rates will vary over time based on solubility and adsorption controls. In Case E, it was assumed that a fast flow path exists through the concrete basemat. Whether the fast flow path is active during any period is dependent on the availability of sufficiently high infiltration through the conceptual closure cap.

Figure 4.4-10: Case E

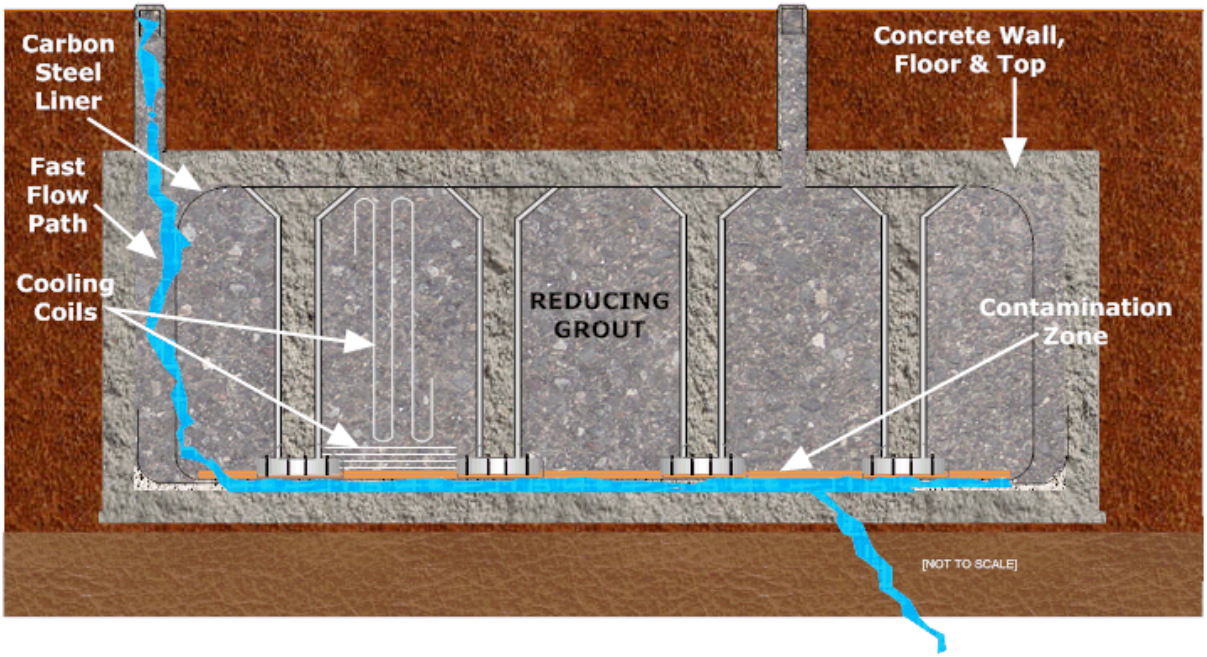

4.4.2.6 Ancillary Equipment Case

In the Ancillary Equipment Case (Figure 4.4-11) the conceptual closure cap degradation occurs as shown in Table 3.2-13. The ancillary equipment was located below grade in HTF (Section 3.2.2 provides details on HTF ancillary equipment) and was covered by the conceptual closure cap. Modeling consisted of source geometry of 19 separate point sources (HPT-2 through HPT-10, Old and New CTS pump tanks, Evaporators 242-H, 242-16H, and 242-25H) and a network of waste transfer lines represented by stabilized contaminants distributed over the entire HTF facility.

Figure 4.4-11: Ancillary Equipment Case

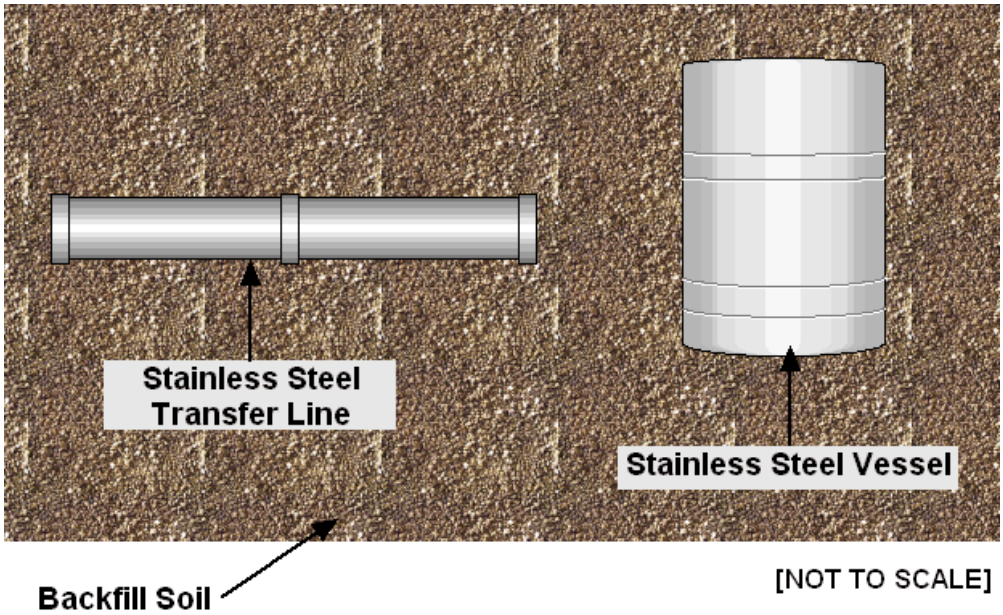

At the time of closure, it is assumed that the ancillary equipment will be intact. Contaminant release for this case was assumed to occur when the stainless steel fails. As discussed in Section 4.2.2.2, predictions for failure of the stainless steel transfer line core piping were based on results of recent studies specific to the application of the HTF closure PA. [WSRC-STI-2007-00460, SRNL-STI-2010-00047] These estimates considered general and localized corrosion mechanisms of the stainless steel exposed to SRS soil conditions for the stainless steel core transfer lines in HTF. The results of these studies were incorporated by assuming that the applicable ancillary equipment containment (e.g., pump tanks, evaporators, and transfer line core pipe) failed and released the associated inventory into the surrounding soil at year 510 (the earliest time of 25% pitting penetration for "in soil" 0.116-inch thick stainless steel). This simplification of the modeling was considered reasonable for all ancillary equipment containment because at closure, the ancillary equipment containments will not be directly in soil, (the pump tanks and evaporators are in concrete cells that will be filled with grout, and the transfer lines are typically contained within a secondary jacket). Additionally, only insignificant quantities of the HTF transfer lines are carbon steel rather than stainless steel (six carbon-steel lines equal to 1,313 feet out of the facility total 74,800 feet). This simplification was important for transfer line modeling since the transfer line inventory was not modeled as point sources but spread throughout the entire HTF modeling area. The transfer line inventory is minor relative to the waste tank inventories. Once the stainless steel containment for ancillary equipment fails, the associated source term was assumed available for release directly into the soil surrounding the ancillary equipment. It is assumed that no hold up or containment of the source term is provided by any of the cementitious materials surrounding the vessels, pits, and waste lines (such as the secondary containment structures). After container failure for ancillary equipment, the flow through the CZ was set equal to the conceptual closure cap driven infiltration rate.

For the probabilistic HTF analyses, each piece of ancillary equipment (with the transfer lines being treated as collective inventory) was assumed to fail independently with failure time occurring between the first pit penetration (116 years) and 100% pitting penetration (approximately 1,000 years). The most probable time of ancillary equipment failure in the probabilistic HTF analyses was assumed at the time of 25% pitting penetration (510 years).

4.4.3 Evaluation of Integrated System Behavior

Upon closure of the HTF, it is necessary to evaluate the integrated system behavior. The various individual system behaviors that are evaluated have been presented for waste tank Cases A through E (Figures 4.4-6 through 4.4-10) and the Ancillary Equipment Case (Figure 4.4-11). The analysis of the Base Case HTF PORFLOW Model results reflected the best estimate of closure system behavior. These independent modeling scenarios for the HTF waste tanks and ancillary equipment are melded together in the probabilistic analysis to produce integrated results.

The saturated zone is laid out on a grid so that individual waste tanks and ancillary equipment point sources can be individually resolved. Explicit representation of individual sources enables investigation of potential plume overlap from separate sources. Integrated system behavior, as measured by concentration at exposure points, was simulated by applying contaminant flux transients for various inventory sources and cases to appropriately located grid cells.

Provided below is a short description of the ICM process flow for the conceptual closure cap and vadose zone. The ICM consists of different segments, some represented by independent sub-models. For example, the waste release model developed different solubility limits for different chemical states; the chemical state used in the model was determined in PORFLOW based on the calculated pore volumes. It should be noted that since the sub-models were developed independently and may have different levels of conservatism, some shared input parameters might have different values from sub-model to sub-model. For example, the diffusion coefficient is different between the concrete degradation evaluation and waste tank liner failure evaluation. While the coefficient in the Base Case waste tank liner evaluation (Section 4.2.2.2.6) is a more expected value, the concrete degradation evaluation (Section 4.2.2.2.4) chose a high coefficient to estimate degradation rates conservatively. Emphasis was placed on ensuring that individual sub-models are defensible, and the fact that two model segments may assume different values for the same parameter was not considered significant if the sub-models are valid and defensible.

The model process flow explanation below describes how each individual model segment is integrated into the entire model and how its behavior is depicted. Timelines for the Base Case (Case A) and alternate cases (Case B through E) associated with the various model segments for the different waste tank types are provided in Tables 4.4-2 through 4.4-9.

The simplified model flow process for a single waste tank is provided in the following sections.

Table 4.4-2: Type I Tank Process Change Timeline

Change in Model Parameters	Year of Occurrence				
	(Base Case) Case A	Case B	Case C	Case D	Case E
Concrete (waste tank top, sides, basemat, etc.) starts to degrade hydraulically	1,350	500	1,350	500	1,350
Waste tank wall concrete transitions from Oxidized Region II to Oxidized Region III	2,139	528	2,361	528	2,373
Waste tank basemat concrete transitions from Oxidized Region II to Oxidized Region III	2,211	556	1,741	556	1,734
Waste tank roof concrete transitions from Oxidized Region II to Oxidized Region III	2,237	544	2,057	544	2,043
Closure cap reaches approximate steady state infiltration rate (11.5 in/yr)	2,625	2,625	2,625	2,625	2,625
Concrete fully degraded hydraulically	2,700	528	2,700	528	2,700
Waste tank grout starts to degrade hydraulically	2,700	500	2,700	500	2,700
Waste tank annulus grout transitions from Reducing Region II to Oxidized Region II	7,453	562	6,703	562	6,730
Waste tank annulus grout transitions from Oxidized Region II to Oxidized Region III	8,075	605	7,168	605	7,181
Waste tank steel liner fails hydraulically	11,397	1,142	1,142	1,142	1,142
Waste tank grout transitions from Reducing Region II to Oxidized Region II	11,760	1,561	8,497	1,561	8,496
CZ transitions from Reducing Region II to Oxidized Region II	11,760	1,561	1,172	1,561	1,144
Waste tank grout transitions from Oxidized Region II to Oxidized Region III	12,009	1,846	9,178	1,847	9,177
CZ transitions from Oxidized Region II to Oxidized Region III	12,009	1,846	1,193	1,847	1,146
Waste tank grout fully degraded hydraulically	13,200	528	13,200	528	13,200

Table 4.4-3: Type I Tank (No Liner) Process Change Timeline

Change in Model Parameters	Year of Occurrence				
	(Base Case) Case A	Case B	Case C	Case D	Case E
Waste tank steel liner fails hydraulically	0	0	0	0	0
Concrete (waste tank top, sides, basemat, etc.) starts to degrade hydraulically	1,350	500	1,350	500	1,350
Waste tank wall concrete transitions from Oxidized Region II to Oxidized Region III	2,135	543	2,318	544	2,348
Waste tank basemat concrete transitions from Oxidized Region II to Oxidized Region III	2,190	537	1,703	531	1,327
Waste tank roof concrete transitions from Oxidized Region II to Oxidized Region III	2,206	540	2,049	540	2,028
Closure cap reaches approximate steady state infiltration rate (11.5 in/yr)	2,625	2,625	2,625	2,625	2,625
Concrete fully degraded hydraulically	2,700	537	2,700	531	2,700
Waste tank grout starts to degrade hydraulically	2,700	500	2,700	500	2,700
Waste tank annulus grout transitions from Reducing Region II to Oxidized Region II	6,549	542	6,571	544	6,646
Waste tank annulus grout transitions from Oxidized Region II to Oxidized Region III	7,062	574	7,102	575	7,140
Waste tank grout transitions from Reducing Region II to Oxidized Region II	7,690	928	8,494	928	8,492
CZ transitions from Reducing Region II to Oxidized Region II	7,690	928	31	928	2
Waste tank grout transitions from Oxidized Region II to Oxidized Region III	8,381	1,217	9,176	1,217	9,175
CZ transitions from Oxidized Region II to Oxidized Region III	8,381	1,217	53	1,217	4
Waste tank grout fully degraded hydraulically	13,200	537	13,200	531	13,200

Table 4.4-4: Type II Tank Process Change Timeline

Change in Model Parameters	Year of Occurrence				
	(Base Case) Case A	Case B	Case C	Case D	Case E
Concrete (waste tank top, sides, basemat, etc.) starts to degrade hydraulically	2,550	500	2,550	500	2,550
Closure cap reaches approximate steady state infiltration rate (11.5 in/yr)	2,625	2,625	2,625	2,625	2,625
Waste tank basemat concrete transitions from Oxidized Region II to Oxidized Region III	3,778	585	2,719	588	3,101
Waste tank wall concrete transitions from Oxidized Region II to Oxidized Region III[a]	4,558	1,939	7,744	1,939	8,019
Waste tank roof concrete transitions from Oxidized Region II to Oxidized Region III	5,007	2,465	4,724	2,465	4,708
Concrete fully degraded hydraulically	5,100	585	5,100	588	5,100
Waste tank grout starts to degrade hydraulically	5,100	500	5,100	500	5,100
Waste tank annulus grout transitions from Reducing Region II to Oxidized Region II	9,126	1,143	10,805	1,143	11,940
Waste tank annulus grout transitions from Oxidized Region II to Oxidized Region III	11,291	3,788	20,000+	3,789	20,000+
Waste tank steel liner fails hydraulically	12,687	2,506	2,506	2,506	2,506
Waste tank grout transitions from Reducing Region II to Oxidized Region II	15,418	4,990	9,993	4,989	9,978
CZ transitions from Reducing Region II to Oxidized Region II	15,418	4,990	2,518	4,989	2,510
Waste tank grout fully degraded hydraulically	16,700	585	16,700	588	16,700
Waste tank grout transitions from Oxidized Region II to Oxidized Region III	20,000+	17,323	20,000+	17,321	20,000+
CZ transitions from Oxidized Region II to Oxidized Region III	20,000+	17,323	2,575	17,321	2,532

a Includes basemat concrete under wall

Table 4.4-5: Type II Tank (No Liner) Process Change Timeline

Change in Model Parameters	Year of Occurrence				
	(Base Case) Case A	Case B	Case C	Case D	Case E
Waste tank steel liner fails hydraulically	0	0	0	0	0
Waste tank basemat concrete transitions from Oxidized Region II to Oxidized Region III	109	89	89	561	1,849
Concrete (waste tank top, sides, basemat, etc.) starts to degrade hydraulically	2,550	500	2,550	500	2,550
Closure cap reaches approximate steady state infiltration rate (11.5 in/yr)	2,625	2,625	2,625	2,625	2,625
Waste tank wall concrete transitions from Oxidized Region II to Oxidized Region III[a]	4,551	5,733	6,794	5,757	8,033
Waste tank roof concrete transitions from Oxidized Region II to Oxidized Region III	4,849	2,461	4,688	2,459	4,569
Concrete fully degraded hydraulically	5,100	500	5,100	561	5,100
Waste tank grout starts to degrade hydraulically	5,100	500	5,100	500	5,100
Waste tank annulus grout transitions from Reducing Region II to Oxidized Region II	8,392	2,530	2,657	2,555	11,832
Waste tank grout transitions from Reducing Region II to Oxidized Region II	9,615	3,625	9,965	3,623	9,863
CZ transitions from Reducing Region II to Oxidized Region II	9,615	3,625	309	3,623	299
Waste tank grout fully degraded hydraulically	16,700	600	16,700	561	16,700
Waste tank annulus grout transitions from Oxidized Region II to Oxidized Region III	17,949	9,803	19,399	9,829	20,000+
Waste tank grout transitions from Oxidized Region II to Oxidized Region III	20,000+	15,969	20,000+	15,965	20,000+
CZ transitions from Oxidized Region II to Oxidized Region III	20,000+	15,969	493	15,965	463

a Includes basemat concrete under wall

Table 4.4-6: Type III Tank Process Change Timeline

Change in Model Parameters	Year of Occurrence				
	(Base Case) Case A	Case B	Case C	Case D	Case E
Concrete (waste tank top, sides, basemat, etc.) starts to degrade hydraulically	2,550	500	2,550	500	2,550
Closure cap reaches approximate steady state infiltration rate (11.5 in/yr)	2,625	2,625	2,625	2,625	2,625
Waste tank wall concrete transitions from Oxidized Region II to Oxidized Region III[a]	4,782	5,850	20,000+	5,850	20,000+
Waste tank roof concrete transitions from Oxidized Region II to Oxidized Region III	5,072	2,566	4,801	2,566	4,758
Concrete fully degraded hydraulically	5,100	600	5,100	600	5,100
Waste tank grout starts to degrade hydraulically	5,100	500	5,100	500	5,100
Waste tank steel liner fails hydraulically	12,751	2,077	2,077	2,077	2,077
Waste tank basemat concrete transitions from Oxidized Region II to Oxidized Region III	13,937	3,416	3,746	3,458	4,864
Waste tank annulus grout transitions from Reducing Region II to Oxidized Region II	14,762	1,263	9,142	1,263	13,455
Waste tank grout transitions from Reducing Region II to Oxidized Region II	16,092	5,719	10,383	5,719	10,343
CZ transitions from Reducing Region II to Oxidized Region II	16,092	5,719	2,087	5,719	2,081
Waste tank grout fully degraded hydraulically	19,200	600	19,200	600	19,200
Waste tank annulus grout transitions from Oxidized Region II to Oxidized Region III	20,000+	12,551	20,000+	12,551	20,000+
Waste tank grout transitions from Oxidized Region II to Oxidized Region III	20,000+	20,000+	20,000+	20,000+	20,000+
CZ transitions from Oxidized Region II to Oxidized Region III	20,000+	20,000+	2,134	20,000+	2,104

a Includes basemat concrete under wall

Table 4.4-7: Type IIIA Tank Process Change Timeline

Change in Model Parameters	Year of Occurrence				
	(Base Case) Case A	Case B	Case C	Case D	Case E
Concrete (waste tank top, sides, basemat, etc.) starts to degrade hydraulically	2,500	500	2,500	500	2,500
Closure cap reaches approximate steady state infiltration rate (11.5 in/yr)	2,625	2,625	2,625	2,625	2,625
Waste tank wall concrete transitions from Oxidized Region II to Oxidized Region III[a]	4,759	5,836	19,819	5,836	20,000+
Concrete fully degraded hydraulically	5,000	600	5,000	600	5,000
Waste tank grout starts to degrade hydraulically	5,000	500	5,000	500	5,000
Waste tank roof concrete transitions from Oxidized Region II to Oxidized Region III	5,173	2,741	4,947	2,741	4,904
Waste tank steel liner fails hydraulically	12,751	2,077	2,077	2,077	2,077
Waste tank basemat concrete transitions from Oxidized Region II to Oxidized Region III	13,914	3,389	3,729	3,431	4,891
Waste tank annulus grout transitions from Reducing Region II to Oxidized Region II	14,577	1,268	9,049	1,267	13,270
Waste tank grout transitions from Reducing Region II to Oxidized Region II	16,131	5,667	10,320	5,667	10,281
CZ transitions from Reducing Region II to Oxidized Region II	16,131	5,667	2,086	5,667	2,081
Waste tank grout fully degraded hydraulically	19,100	600	19,100	600	19,100
Waste tank annulus grout transitions from Oxidized Region II to Oxidized Region III	20,000+	12,112	20,000+	12,108	20,000+
Waste tank grout transitions from Oxidized Region II to Oxidized Region III	20,000+	20,000+	20,000+	20,000+	20,000+
CZ transitions from Oxidized Region II to Oxidized Region III	20,000+	20,000+	2,134	20,000+	2,104

a Includes basemat concrete under wall

Table 4.4-8: Type IIIA Tank (West) Process Change Timeline

Change in Model Parameters	Year of Occurrence				
	(Base Case) Case A	Case B	Case C	Case D	Case E
Concrete (waste tank top, sides, basemat, etc.) starts to degrade hydraulically	2,500	500	2,500	500	2,500
Closure cap reaches approximate steady state infiltration rate (11.5 in/yr)	2,625	2,625	2,625	2,625	2,625
Waste tank wall concrete transitions from Oxidized Region II to Oxidized Region III[a]	4,752	5,833	20,000+	5,833	20,000+
Concrete fully degraded hydraulically	5,000	600	5,000	600	5,000
Waste tank grout starts to degrade hydraulically	5,000	500	5,000	500	5,000
Waste tank roof concrete transitions from Oxidized Region II to Oxidized Region III	5,018	2,565	4,778	2,565	4,735
Waste tank steel liner fails hydraulically	12,751	2,077	2,077	2,077	2,077
Waste tank basemat concrete transitions from Oxidized Region II to Oxidized Region III	13,958	3,441	3,811	3,485	5,056
Waste tank annulus grout transitions from Reducing Region II to Oxidized Region II	14,582	1,264	9,059	1,263	13,335
Waste tank grout transitions from Reducing Region II to Oxidized Region II	16,085	5,630	10,287	5,630	10,247
CZ transitions from Reducing Region II to Oxidized Region II	16,085	5,630	2,087	5,630	2,081
Waste tank grout fully degraded hydraulically	19,100	600	19,100	600	19,100
Waste tank annulus grout transitions from Oxidized Region II to Oxidized Region III	20,000+	12,130	20,000+	12,126	20,000+
Waste tank grout transitions from Oxidized Region II to Oxidized Region III	20,000+	20,000+	20,000+	20,000+	20,000+
CZ transitions from Oxidized Region II to Oxidized Region III	20,000+	20,000+	2,136	20,000+	2,104

a Includes basemat concrete under wall

Table 4.4-9: Type IV Tank Process Change Timeline

Change in Model Parameters	Year of Occurrence				
	(Base Case) Case A	Case B	Case C	Case D	Case E
Concrete (waste tank top, sides, basemat, etc.) starts to degrade hydraulically	400	500	400	500	400
Waste tank roof concrete transitions from Oxidized Region II to Oxidized Region III	687	1,002	695	1,002	695
Concrete fully degraded hydraulically	800	600	800	600	800
Waste tank grout starts to degrade hydraulically	800	500	800	500	800
Waste tank wall concrete transitions from Oxidized Region II to Oxidized Region III	1,391	2,716	3,200	2,716	3,200
Closure cap reaches approximate steady state infiltration rate (11.5 in/yr)	2,625	2,625	2,625	2,625	2,625
Waste tank basemat concrete transitions from Oxidized Region II to Oxidized Region III	3,936	988	1,350	994	1,352
Waste tank steel liner fails hydraulically	3,638	75	75	75	75
Waste tank grout transitions from Reducing Region II to Oxidized Region II	7,491	5,346	6,896	5,346	6,896
CZ transitions from Reducing Region II to Oxidized Region II	7,491	5,346	302	5,346	301
Waste tank grout transitions from Oxidized Region II to Oxidized Region III	20,000+	20,000+	20,000+	20,000+	20,000+
CZ transitions from Oxidized Region II to Oxidized Region III	20,000+	20,000+	501	20,000+	501
Waste tank grout fully degraded hydraulically	20,000+	600	20,000+	600	20,000+

4.4.3.1 Closure Cap

A flow rate leaving the closure cap over time was determined in the closure cap sub-model. The infiltration rate into the closure cap top was based on the rainfall rates and the closure cap material properties (which are discussed in detail in Section 4.2.2.2.1). The flow rate out of the closure cap was calculated using the HELP code, with the closure cap modeled as degrading over time. The flow rate through the closure cap reached a steady state value at approximately year 2,600. Table 3.2-14 provides the time-variant infiltration rates based on the closure cap analysis presented in Section 3.2.4.

4.4.3.2 Waste Tank Top

The flow leaving the closure cap will travel to the waste tank, with the flow rate being affected by the concrete waste tank top. Based on the relative hydraulic properties of the two materials (soil vs. concrete), some flow will be directed around the waste tank into the surrounding soil, while some flow will travel downward through the concrete. The concrete material properties (which are discussed in detail in Section 4.2.2.2.4) were modeled as changing over time. The only waste tank top material properties of concern was the hydraulic properties, since the waste tank top impacts flow but will not retard contaminant transport (since no inventory was modeled at the top). The waste tank top hydraulic properties were defined initially and in a fully degraded state, and cementitious materials degradation analysis was performed to determine the time it would take to reach the fully degraded state (Table 4.2-34). Once the initial and end state times were set, the model assumed linear degradation of the hydraulic properties over time.

4.4.3.3 Waste Tank Liner Top

After passing through the concrete waste tank top, flow leaving the cap will travel into the grout (for Type IV tanks and after liner failure for Type I/II/III/IIIA tanks) or reach the top of the steel liner (for Type I/II/III/IIIA tanks before liner failure) and be deflected away from the waste tank. The liner failure time was determined by an independent sub-model analysis (described in Section 4.2.2.2.6) for each waste tank type except for the Type IV tanks (Type IV tanks do not have a top liner). Tank 12 (Type I) and Tanks 14, 15, and 16 (Type II) have liner failure at the time of closure. Prior to failure, the liner was modeled as being impermeable to both advection and diffusion. After failure, the liner was not a hindrance to flow and transport.

4.4.3.4 Waste Tank Grout

Water will enter the top of the waste tank grout and travels downward to the CZ at the bottom of the waste tank. The waste tank grout material properties (e.g., hydraulic conductivity, distribution coefficients, which are discussed in detail in Section 4.2.2.2.4) were modeled as changing over time. Some scenarios used in the sensitivity analyses (Section 4.4.2), fast flow paths through the grout were modeled resulting in a higher flow rate around the grout. The hydraulic properties were defined initially and in fully degraded state, and a cementitious materials degradation analysis was performed to determine the time it would take to reach the fully degraded state (Table 4.2-34). Once the initial and end state times were set, the model assumed linear degradation of the grout hydraulic properties over time.

Table 4.2-33, provides distribution coefficient values for cementitious materials as a function of chemical reduction ability and aging, with the grout "age" dependent on the pH of the concrete pore water, which in turn, is dependent upon the amount of water (number of pore volumes) that has passed through the concrete over time. A description of pore water chemistry modeling is provided in the Section 4.4.3.5.

The waste tank grout material properties of principal concern are the hydraulic properties, but the distribution coefficients, which control the waste tank grout radionuclide storage capacity, may also play a role in the release of radionuclides over time. Radionuclides may diffuse from the CZ upwards into the waste tank grout and be released over time after liner failure. In addition, because the Type IV tanks do not have a liner at the top, a circulation pattern with upward flow at the outer edge of the waste tank may occur in the waste tank grout and CZ prior to liner failure. The storage of radionuclides in the waste tank grout can delay the release of radionuclides after liner failure due to sorption. Also changes in distribution coefficients associated with chemistry changes can be reflected in radionuclide release rates from the grout. The grout hydraulic properties influence the water flow rate through the waste tank. The earlier the grout degrades, the earlier the flow rate through the waste tank reaches a steady state maximum flow.

4.4.3.5 Contamination Zone

In the model, the assumption for the waste tank residual inventory was that it is contained within a thin layer (i.e., the CZ) at the bottom of the waste tank. The release rate of contaminants from the CZ is solubility controlled, and is tied to the chemical properties (e.g., oxidation potential, pH) of the waste tank pore water. The release rate from the CZ is independent of the grout or CZ distribution coefficients. The assumed solubility limit varies depending on waste tank pore water chemistry and the controlling phase of the radionuclide being released. Different solubility limits for different waste tank chemistries were derived for the radionuclides in the CZ (as discussed in Section 4.2.1). Additional emphasis was placed on those radionuclides shown during initial modeling to have the most impact on peak dose (plutonium, neptunium, uranium, technetium), including an uncertainty study and development of stochastic distributions for alternative controlling phases (Section 4.2.1.3).

As pore volumes pass through the waste tank, the pH and reducing capability of the grout will be affected. The number of pore water volumes passing through the waste tank and the corresponding transitions to different waste tank chemistry conditions was included in the HTF modeling. As part of the waste release modeling (discussed in detail in Section 4.2.1), the estimated transition times between various chemical phases was calculated for the waste tank pore water. The waste tank pore water chemistry was calculated to change from Reducing Region II conditions (middle age reducing) to Oxidizing Region II conditions (middle age oxidizing) after 371 pore volumes had passed through the grout. The change from Oxidizing Region II conditions (middle age oxidizing) to Oxidizing Region III conditions (old age oxidizing) was calculated to occur after 2,131 pore volumes (Table 4.2-18). For submerged waste tanks, pore water chemistry was calculated to change from Reducing Region II conditions (middle age reducing) to Oxidizing Region II conditions (middle age oxidizing) after 1,414 pore volumes passed through the grout. The change from

Oxidizing Region II conditions (middle age oxidizing) to Oxidizing Region III conditions (old age oxidizing) was calculated to occur after 2,383 pore volumes (Table 4.2-18).

4.4.3.6 Waste Tank Liner Sides and Floor

After leaving the CZ and entering the waste tank pore water, the contaminants will not leave the waste tank until the steel liner fails (with the exception of liners of Tank 12 (Type I) and Tanks 14, 15, and 16 (Type II), which are assumed to fail at the time of HTF closure). For the Type IV tanks (which do not have a top liner) waste leaving the CZ can migrate into the waste tank grout and transport upward. The liner failure time was determined by analyses for each waste tank type, with both the primary and secondary liner (where applicable) failing at the same time. While it utilizes many of the same assumptions, the waste tank liner analyses calculate failure times independent of the flow and transport models. As discussed in Section 4.4.3.3, when the liner fails, it is assumed to fail completely with the modeled, failed liner having no further impact to flow and transport.

4.4.3.7 Basemat

After contaminants exit the waste tank liner, they are expected to enter the concrete waste tank basemat located directly below the liner. The waste tank grout material properties (which are discussed in detail in Section 4.2.2.2.4) were modeled as changing over time. The material properties of the concrete affect both the flow rate through the basemat and the distribution coefficient value. The hydraulic properties were defined initially, in a fully degraded state, and a cementitious materials degradation analysis was performed to determine the time it would take to reach the fully degraded state (Table 4.2-34). Once the initial and end state times were set, the model assumed linear degradation of the basemat hydraulic properties over time. In some sensitivity scenarios, fast flow paths through the basemat were modeled resulting in a higher flow rate through the basemat concrete.

Contaminant transport is retarded by basemat concrete with some radionuclides slowing greatly depending on their distribution coefficients. Table 4.2-33, provides distribution coefficient values for cementitious materials as a function of aging, with the grout "age" dependent on the pH of the concrete pore water, which in turn is dependent upon the amount of water (number of pore water volumes) that has passed through the concrete over time. A description of pore water chemistry modeling is provided in the Section 4.4.3.5. As the waste tank chemistry changes, the concrete transitions from Oxidizing Region II conditions (middle age oxidizing) to Oxidizing Region III conditions (old age oxidizing), and the associated material properties were modeled as changing (Region I is not considered because the waste tanks would have already reached Region II by the time of HTF closure).

4.4.3.8 Vadose Zone beneath the Waste Tank

After contaminants exit the basemat, they will enter the vadose zone (e.g., soil) beneath the waste tank (with the exception of the submerged waste tanks where contaminants would pass directly into the saturated zone, which is discussed in detail in Section 4.2.2.2.2). The vadose zone material properties affect both the flow rate through the soil and the associated distribution coefficient values, with both being important to the model. The vadose zone distribution coefficients can vary over time as a function of the redox state of the water coming from the grout. When the CZ water chemistry (based upon the grout water chemistry) is considered a function of Reducing Region II or Oxidizing Region II conditions (see Section 4.4.3.5), the vadose zone uses the leachate influenced values presented in Table 4.2-29. After the grout water chemistry was considered a function of Oxidizing Region III conditions, the non-impacted distribution coefficient values were used. Note that the leachate affected distribution coefficients were not used in Cases C and E, where a fast flow path that bypasses the grout at its outer edge of the grout was assumed to supply much of the water entering the vadose zone. The vadose zone depth below each waste tank can vary depending on the waste tank involved, as shown in Table 4.2-31. In the probabilistic model, the vadose zone thickness was allowed to vary, which did affect transport time through the soil. The working slabs under waste tank basemats were not explicitly modeled but were modeled as soil. Given the minimal thickness of the working slabs relative to the waste tank basemats, as well as the possibility of cracks in the working slabs, it was appropriate to disregard the working slabs in modeling contaminant transport through the waste tank bottom and basemat into the vadose zone.

4.4.4 Modeling Process

Figure 4.4-12 illustrates the general process to be followed in implementing the ICM. This figure shows the three component models and their key inputs.

Some inputs involve fixed parameters that do not change over time. These are generally shown on the left side of the figure. The inputs on the right side of the figure do change over time.

Figure 4.4-12: Model Process Flow

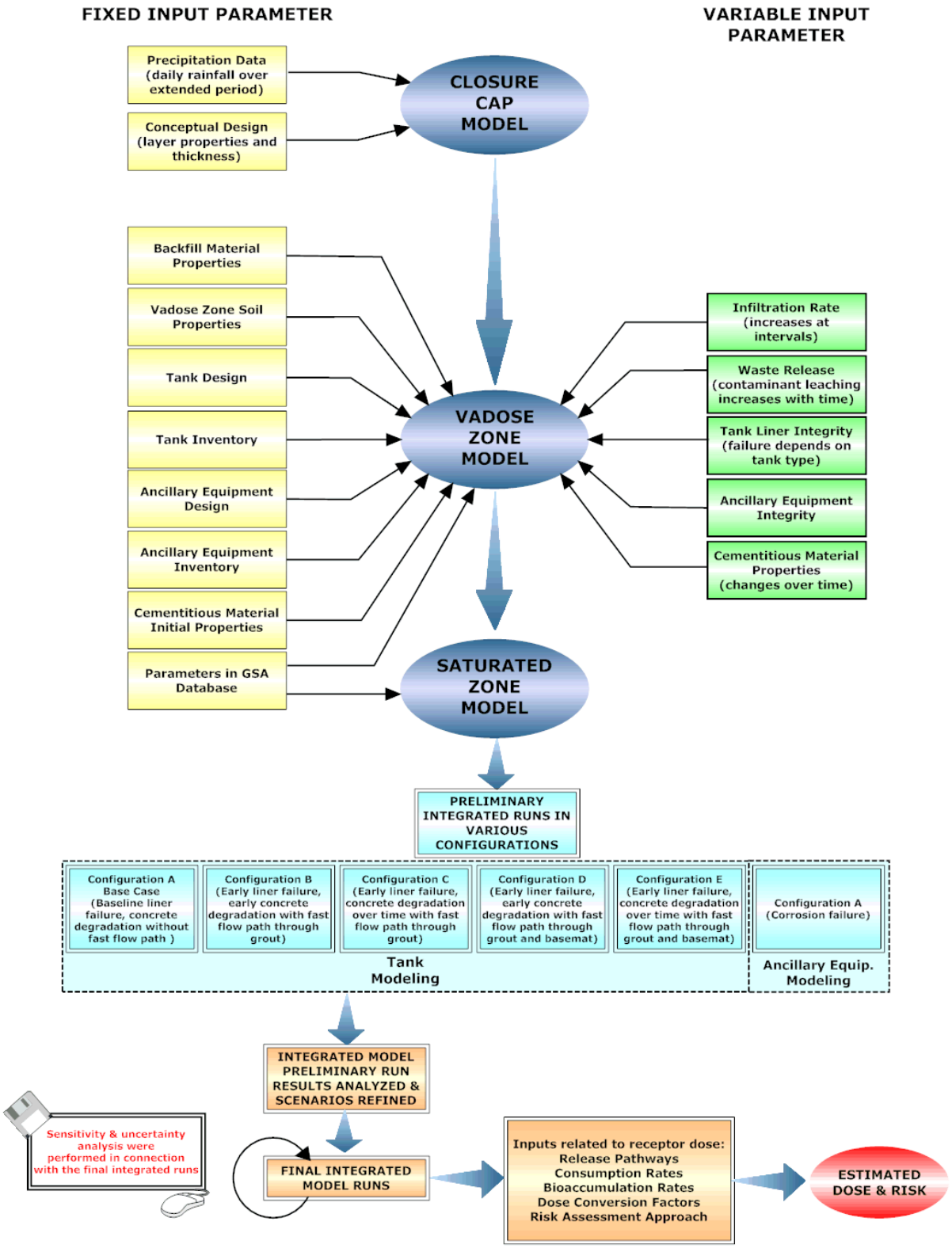

As shown in Figure 4.4-12, and as explained previously, five waste tank cases were identified for the preliminary model runs, which were accomplished using the applicable computer codes. These cases were analyzed by running the model using different combinations as discussed above.

The results of the preliminary model runs were analyzed. Based on analysis results the model was refined as indicated. Such refinements could involve eliminating one or more waste tank cases used in the preliminary analyses or the revision of a waste tank case.

After refinements were made, the final model runs were performed. The UA/SA were performed in connection with the final model runs, with results being assessed with the last of the final model runs.

The result of this process provided the predicted contaminant concentrations in groundwater and surface water. The data for radiological contaminants was then used in combination with the inputs related to receptor dose shown on Figure 4.4-12.

4.4.4.1 PORFLOW Modeling Process

A description of the HTF GoldSim Model is contained in SRNL-L6200-2010-00026.

4.4.4.1.1 Regional GSA and Local HTF Modeling in PORFLOW

The PORFLOW computer code was used to model HTF flow and transport for all cases. Regional GSA modeling in PORFLOW was developed using a 200 foot x 200-foot grid with primary focus on seepline concentration (Figure 4.4-13). Most of the groundwater flow paths discharge to UTR, which more deeply incises the terrain in comparison to Fourmile Branch. The abrupt counter-clockwise turn in some pathlines coincides with passage through the Gordon Confining Unit from the UTR Aquifer to the Gordon Aquifer. The two aquifers exhibit different flow directions in this area.

Figure 4.4-13: PORFLOW GSA Modeling

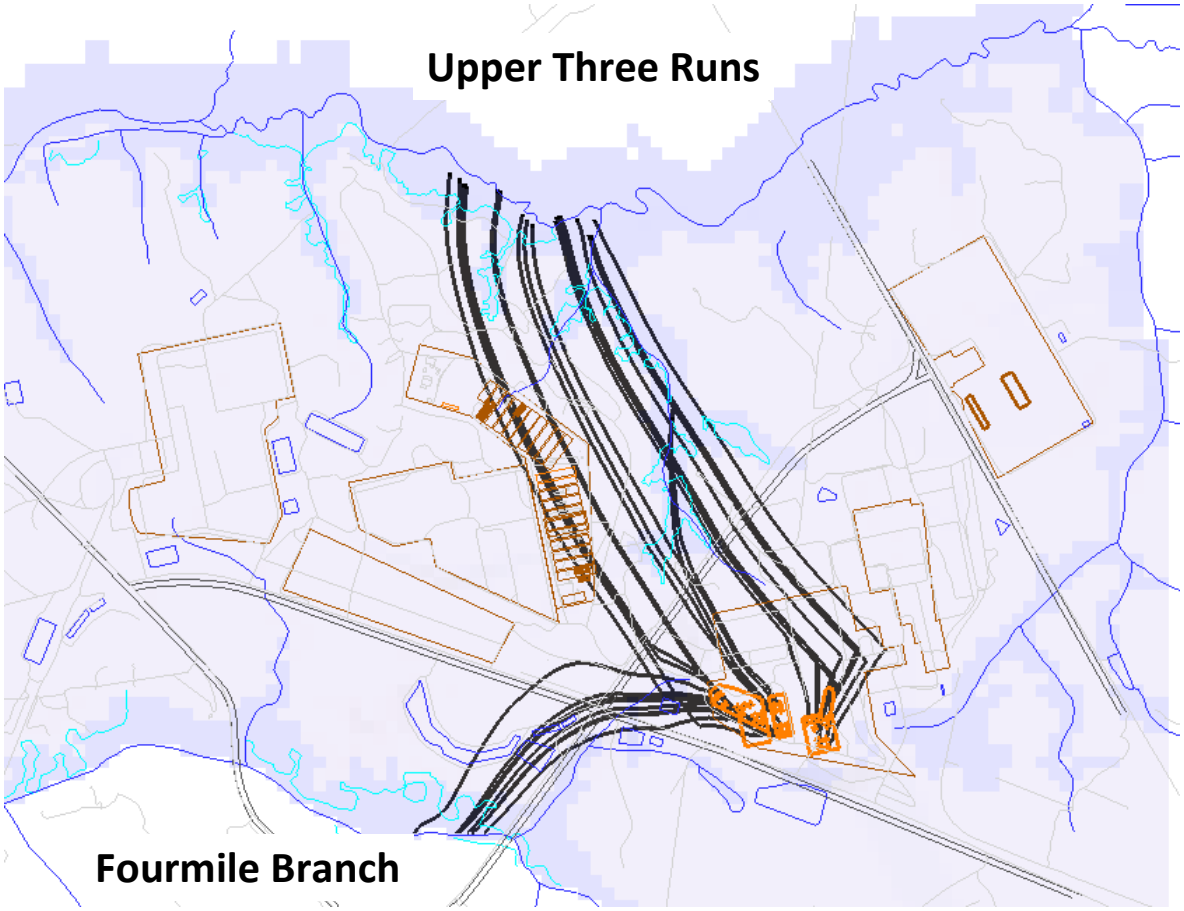

The HTF modeling was developed from the GSA scale model using a 50 foot x 50-foot grid refinement, with the primary focus being on the 1 meter and 100-meter concentrations (Figure 4.4-14). To avoid excessive numerical dispersion at the 100-meter scale, a grid resolution finer than 200 feet x 200 feet was required. The HTF velocity field was generated directly from the coarser scale GSA velocity model using a mass-conserving linear interpolation scheme, rather than a separate flow model requiring its own boundary conditions and properties. This approach ensured strict consistency between the two-aquifer flow fields, apart from resolution. The HTF velocity field includes the entire vertical extent of the GSA model within the horizontal confines of the HTF domain. The streamtraces from the HTF waste tanks are shown in Figure 4.4-14 as blue lines emanating from the waste tank centerlines (red dots). Twenty-year time markers (red dots located along the stream traces) indicate travel time in the saturated zone between waste tanks and the 100-meter perimeter (dash-dot line). In aquifer transport modeling, hydrodynamic dispersion is represented by longitudinal, transverse horizontal and transverse vertical dispersivities of 10 meter, 1 meter, and 0.1 meter, respectively, which are 10%, 1%, and 0.1% of a nominal 100-meter plume travel distance. Both the GSA and HTF scale models have been shown to preserve mass to adequate tolerances. [WSRC-TR-2004-00106, Q-SQP-G-00003] The approach used to

address numerical dispersion in the HTF PORFLOW Model is the same approach addressed in Section 4.3 of SRNL-STI-2009-00115 for the SDF PA model. [SRR-CWDA-2009-00017] The relevant discussion from SRNL-STI-2009-00115 is as follows:

> "*A grid resolution finer than 200 ft. x 200 ft. is required to avoid excessive numerical dispersion at the 100m plume scale. The amount of numerical dispersion depends on the numerical algorithm, grid spacing, and time stepping. For one-dimensional finite difference simulation using upstream spatial weighting and central temporal differencing, the effective dispersivity arising from numerical dispersion alone is equal to Δx/2, where Δx is the grid resolution. Typical modeling practice, arising from field scale tracer tests, is to assume a longitudinal dispersivity that is 10% of the plume travel distance. For SDF aquifer simulations, the length scale is taken as 100m and an appropriate physical dispersivity is 10m. An adequate grid resolution for 100m plume simulations is 50 ft. or 15m. Numerical dispersion associated with this resolution is thus equivalent to a dispersivity less than 8m. Therefore, a fifty mesh spacing does not introduce excessive numerical dispersion. This conclusion is supported by numerical studies presented in Section 6 of WSRC-STI-2007-00150.*"

Figure 4.4-14: HTF PORFLOW Model Streamtraces and 100m Boundary

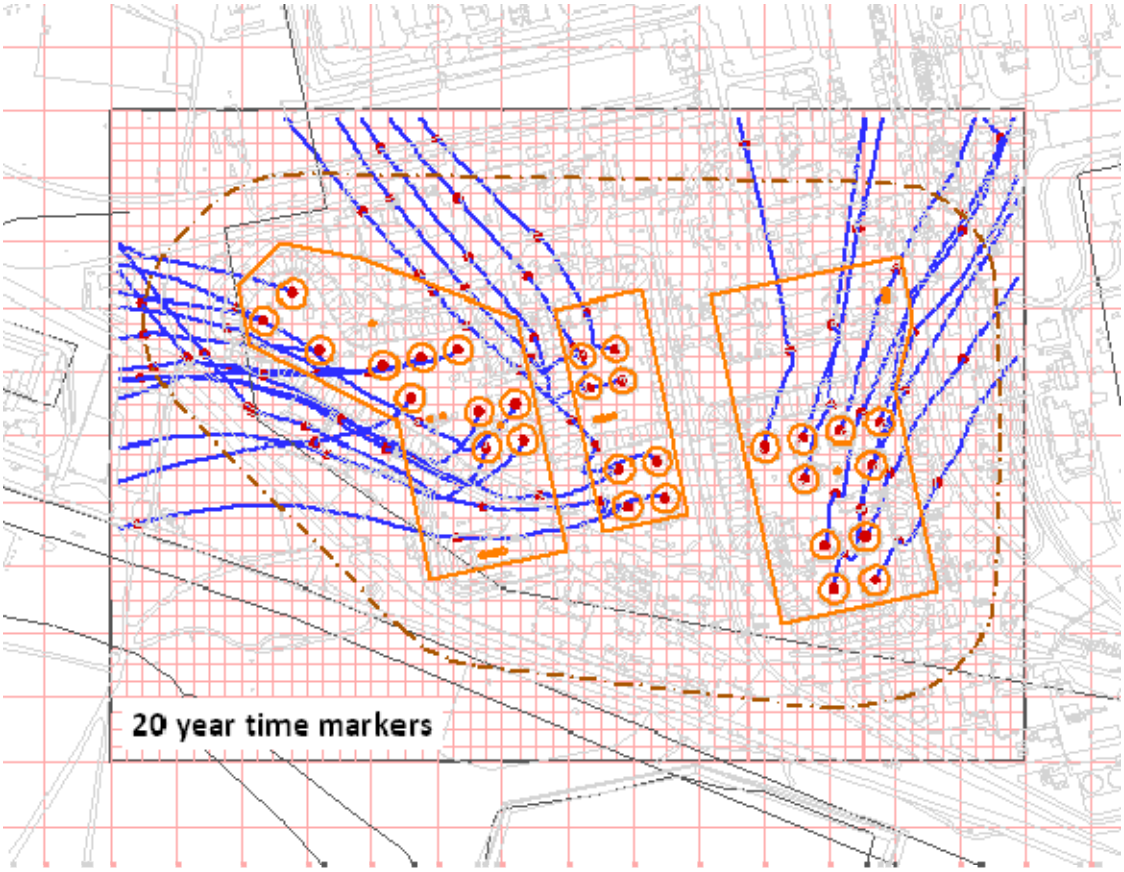

4.4.4.1.2 General Vadose Zone Waste Tank Modeling in PORFLOW

The waste tanks, surrounding vadose zone soils, and any saturated soils at or above the waste tank bottom were modeled in PORFLOW using an axi-symmetric, 2-D, radial slice (unit radian pie wedge). For waste tanks above the water table, the bottom boundary of the modeling domain coincides with the water table, and the contaminant flux leaving the model domain is the aquifer transport source term. For submerged or partially submerged waste tanks, the modeling domain extends below the water table, and the contaminant flux leaving the waste tank boundary becomes the aquifer source term. In the flow model, infiltration from the HELP cover system model was prescribed along the top boundary, a fixed pressure head consistent with the water table elevation was imposed along the bottom boundary, and no flow was allowed to cross the waste tank centerline or the outer radius of the model domain. In transport simulations, zero concentration was prescribed at the top boundary, zero diffusive flux along the bottom boundary, and no flux along the sides.

Because no flow/flux boundary conditions were applied to the sides of the model domain, lateral flow and transport in the saturated zone was not explicitly addressed in near-field PORFLOW simulations for submerged and partially submerged waste tanks. A modeling experiment conducted during the conceptual model development phase indicated that lateral flow has a negligible impact on advective contaminant release from the CZ (because of its minimal thickness) provided the later flow does not exceed roughly 100 times the downward flow. [SRNL-L6200-2010-00026] Prior modeling (PORTAGE-08-022) indicates generally smaller lateral to downward flow ratios in HTF (around ten times). Aquifer crossflow in near-field modeling could thus be neglected. Another consideration for submerged and partially submerged waste tanks is the effect of lateral flow in the aquifer on the chemical state of components, such as the waste tank grout, specifically oxidation potential, and the pH transition times, which are a function of pore volume counts. For an approximately account of aquifer crossflow, pore volume counts from the near-field flow model were inflated using a "crossflow factor" for the purpose of computing chemical transitions, as further discussed later in this section.

Up to 25 distinct material zones were used in PORFLOW to represent different materials and to reflect different flow scenarios (e.g., fast flow paths) for a given waste tank type. Approximately 5,000 to 7,000 grid blocks were used to represent each of the four different waste tank types (grid varies with waste tank type). A graphic depiction of the PORFLOW modeling grids for the various waste tank types, including a lower corner detail, is provided in Figures 4.4-15 through 4.4-22 (the Type IIIA tanks are similar to the Type III tanks, so no separate graphic is shown). It should be noted that the color variations within Figures 4.4-15 through 4.4-22 denote different modeling segments. Figure 4.4-23 shows a portion of the fast flow path (when activated) for a Type IV tank. Waste tank depth to the vadose zone was modeled as uniform for a particular waste tank type (i.e., one depth for all Type I tanks) using an average of the values in Table 4.2-31 for the associated waste tank type. The chosen grid resolution was a compromise between two competing objectives, 1) resolution of thin geometric features (e.g., CZ, waste tank liners) and sharp flow field transitions (e.g., pooled water flowing over roof

edge), and 2) achieving reasonable computer storage and runtimes. Each grid extends 30 feet beyond the outside radius of a waste tank to represent average conditions. At certain angles, obstructions such as adjacent waste tanks are present at shorter distances. A sensitivity study indicated insignificant impact on water table flux for a grid extending to the shorter half-distance between waste tanks. PORFLOW material properties for native soil utilize Section 4.2.2.2.2 parameters for vadose zone soil and for backfill utilize Section 4.2.2.2.2 parameters for backfill soil. Figures 4.4-24 through 4.4-39 display the flow fields for the various waste tank types over time. The figures are color coded to show the areas of highest saturation (dark blue) and have arrows, which denote the flow magnitude. The figures show how PORFLOW simulated flow, and how flow changes over time due to waste tank changes (e.g., cap degradation, grout degradation, liner failure).

Figure 4.4-15: PORFLOW Type I Tank Model

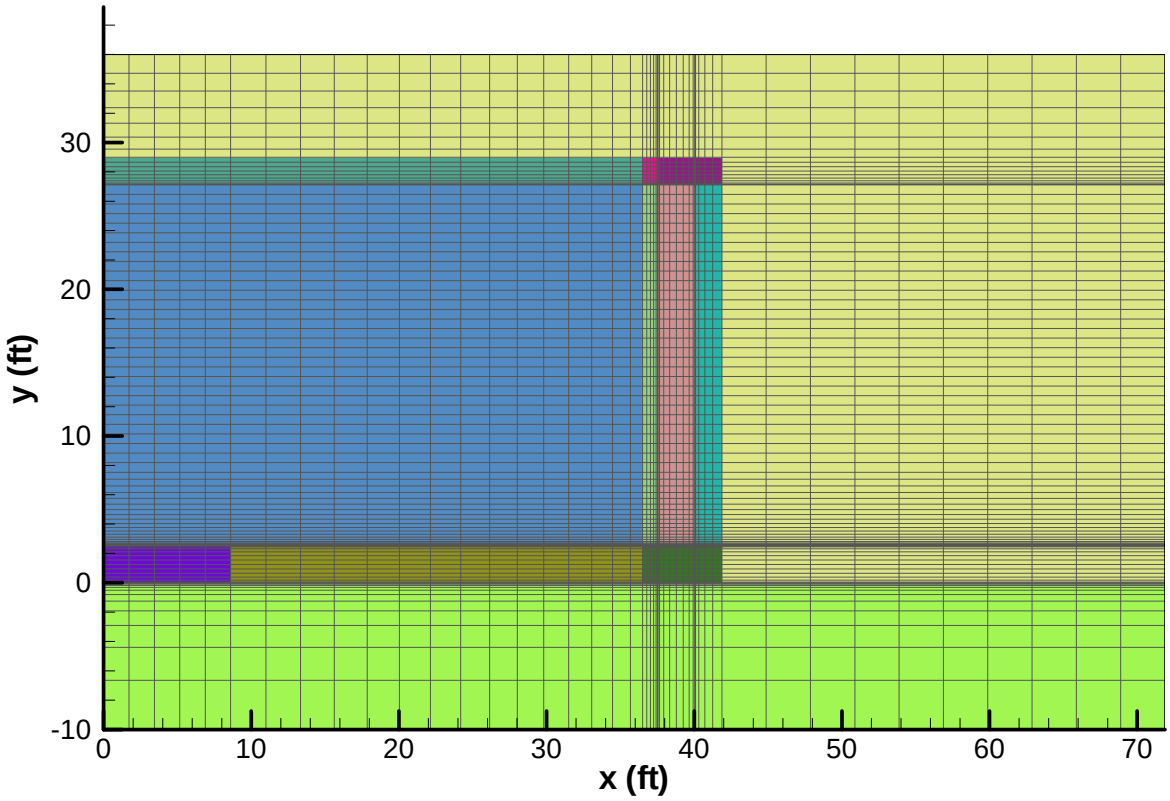

Figure 4.4-16: PORFLOW Type I Tank Model, Lower Corner Detail

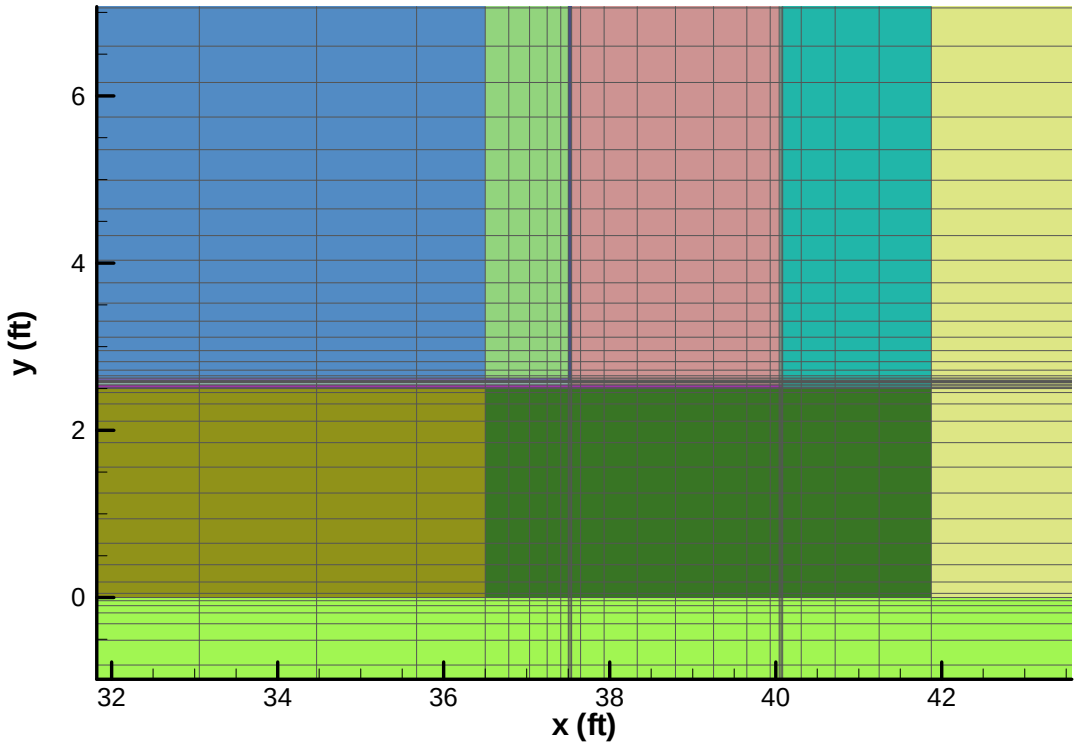

Figure 4.4-17: PORFLOW Type II Tank Model

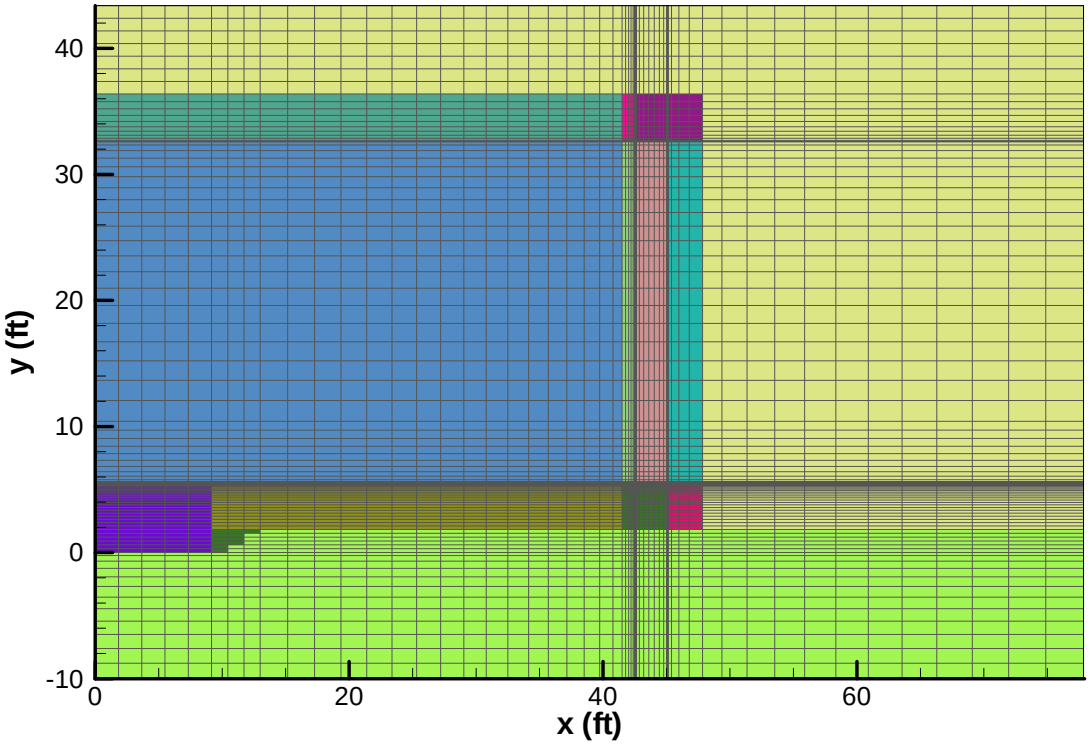

Figure 4.4-18: PORFLOW Type II Tank Model, Lower Corner Detail

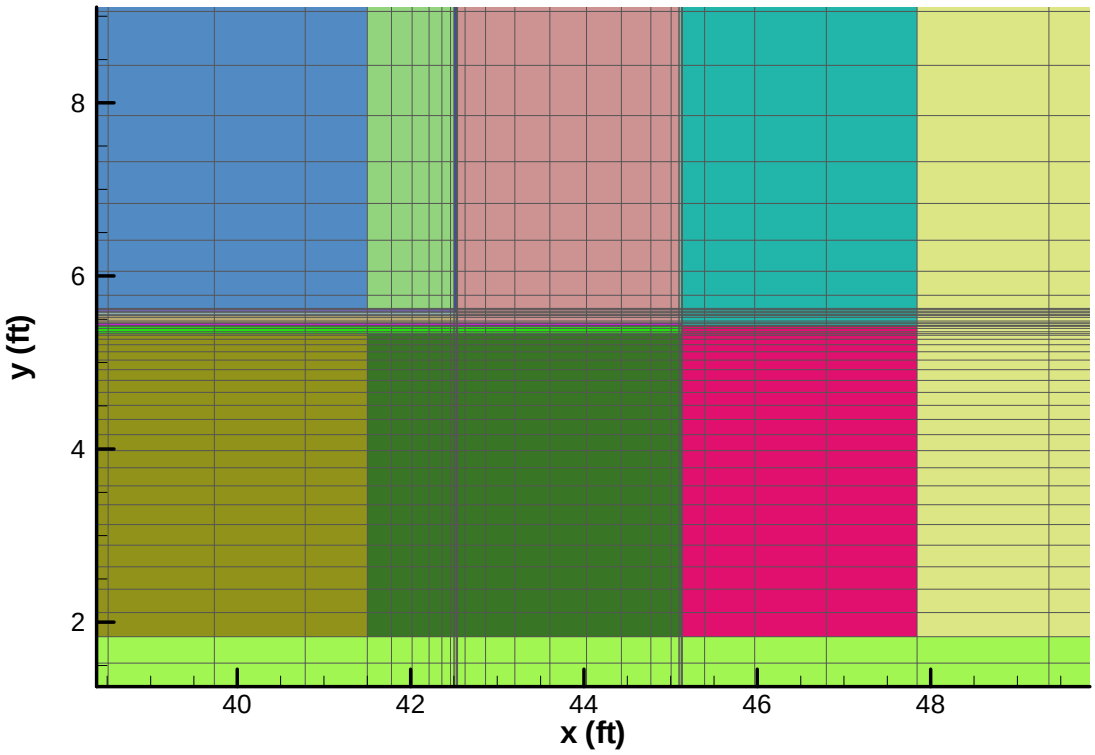

Figure 4.4-19: PORFLOW Type III Tank Model Detail

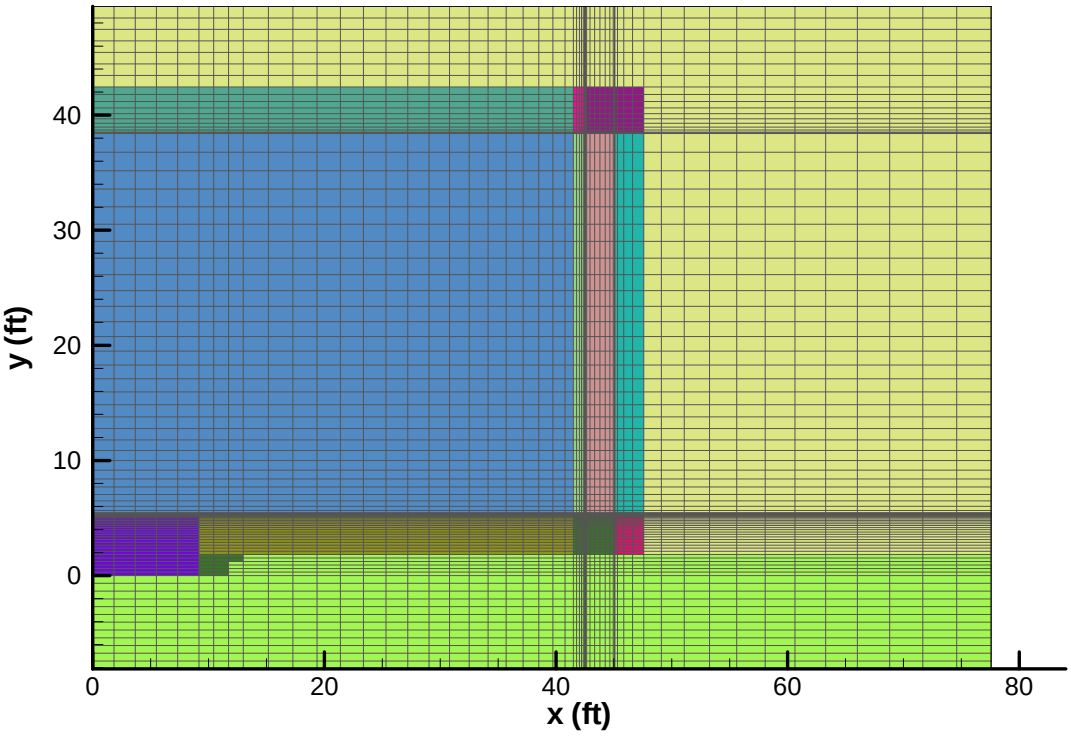

Figure 4.4-20: PORFLOW Type III Tank Model, Lower Corner Detail

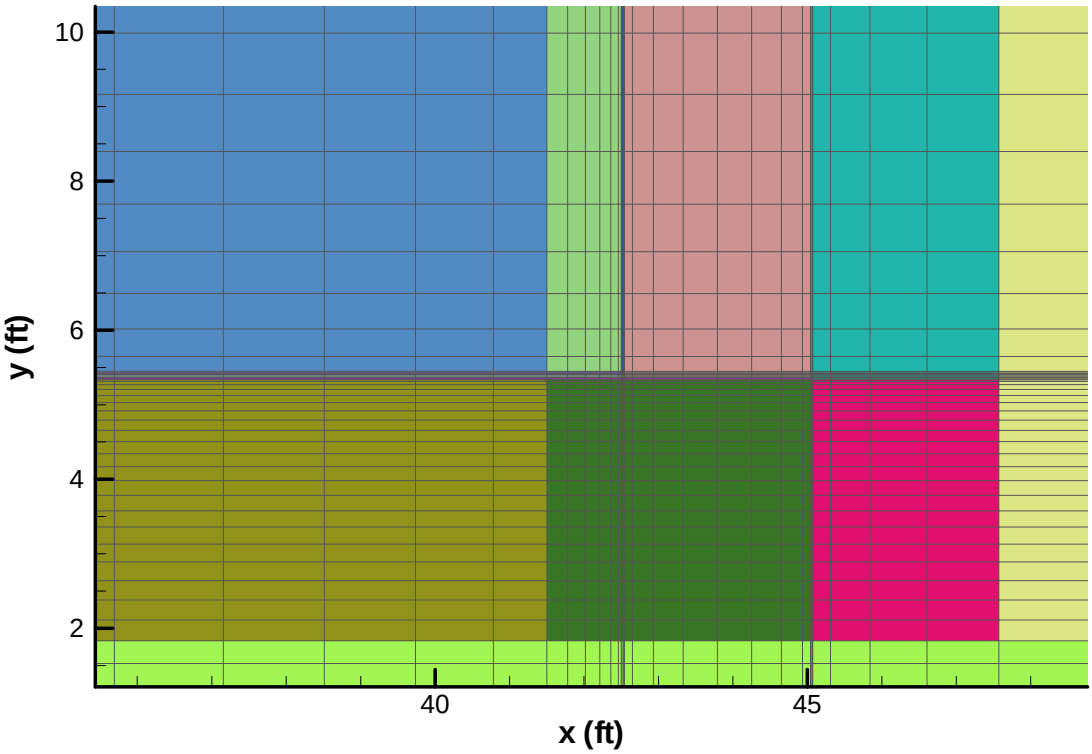

Figure 4.4-21: PORFLOW Type IV Tank Model, Domed Roof Explicitly Modeled

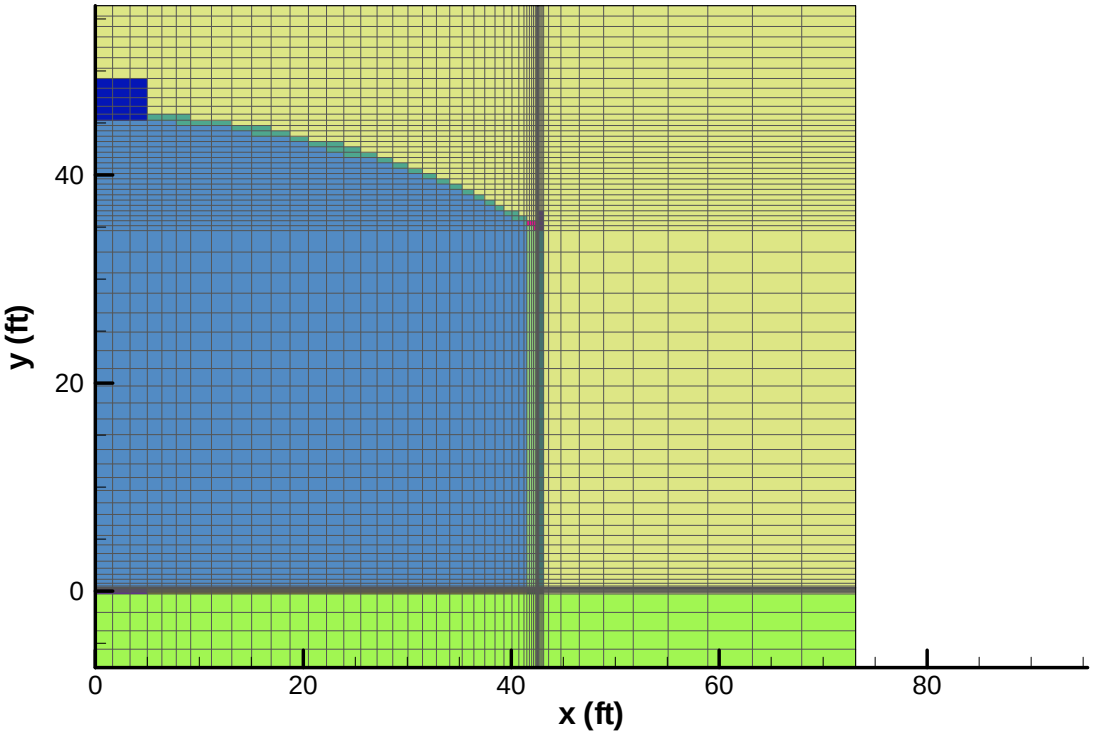

Figure 4.4-22: PORFLOW Type IV Tank Model, Lower Corner Detail

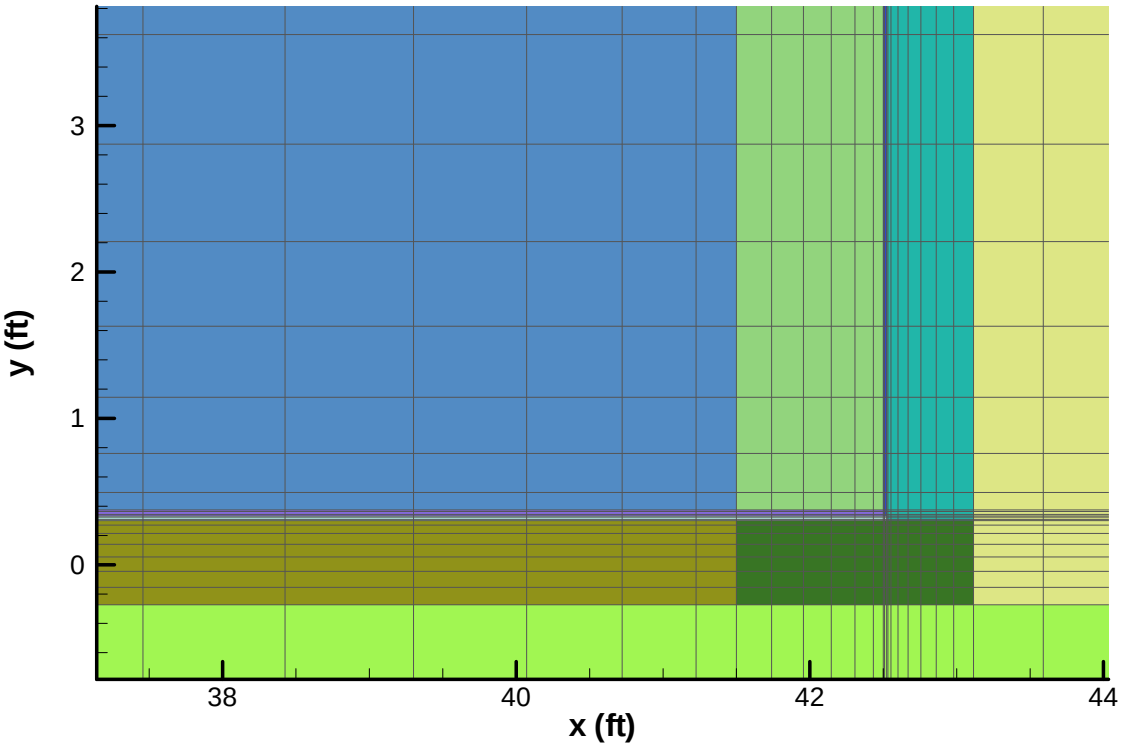

Figure 4.4-23: PORFLOW Type IV Tank Model, Tank Top Corner Detail

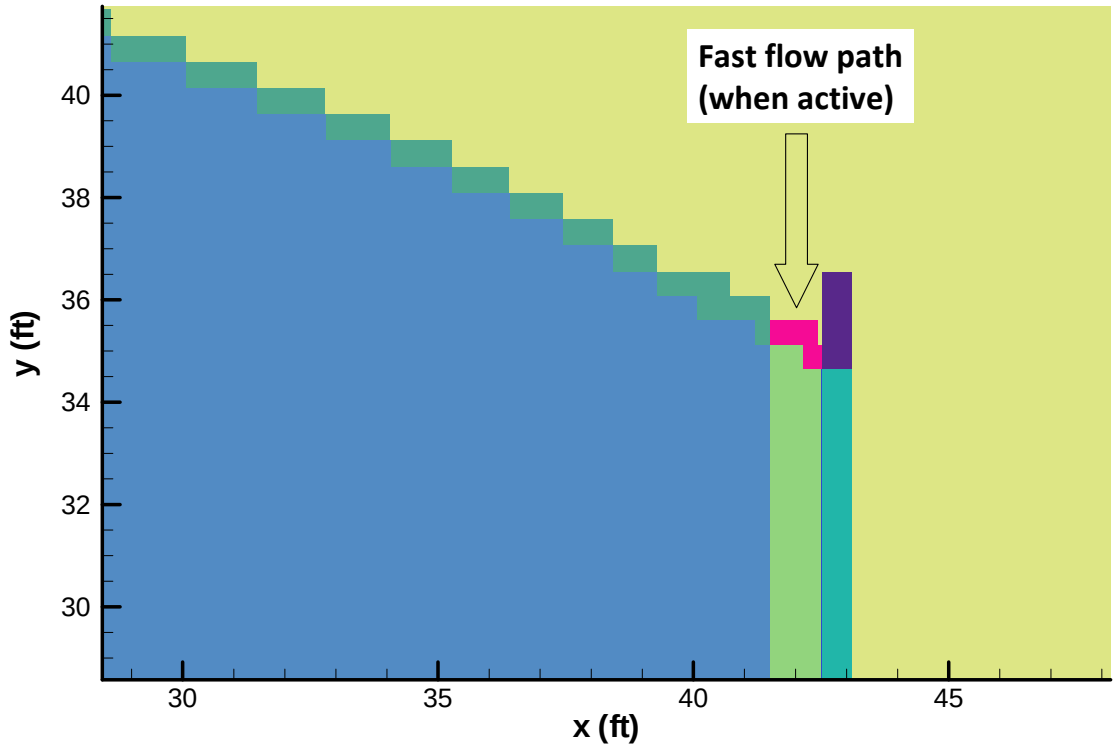

Figure 4.4-24: Type I Tank Flow Field - Year 100

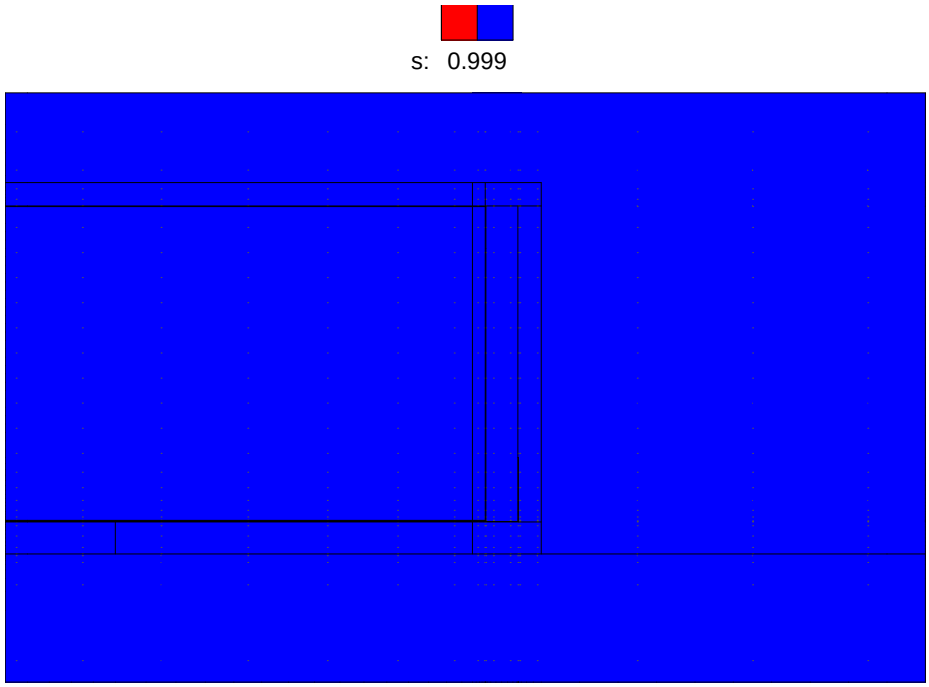

(s: = saturation)

Figure 4.4-25: Type I Tank Flow Field - Year 10,000

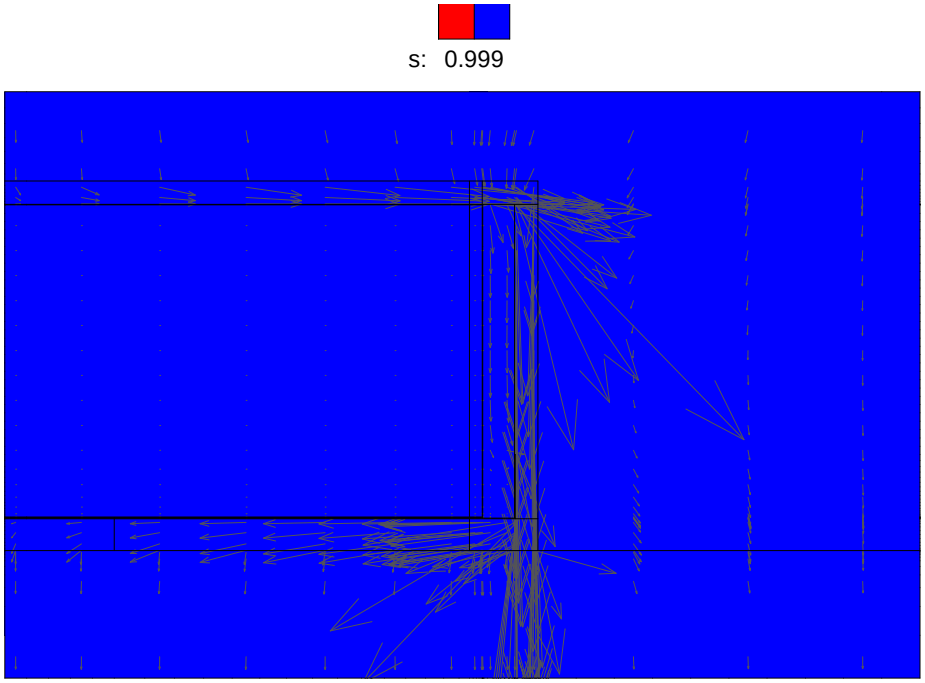

(s: = saturation)

Figure 4.4-26: Type I Tank Flow Field (Immediately Prior to Liner Failure) - Year 11,397

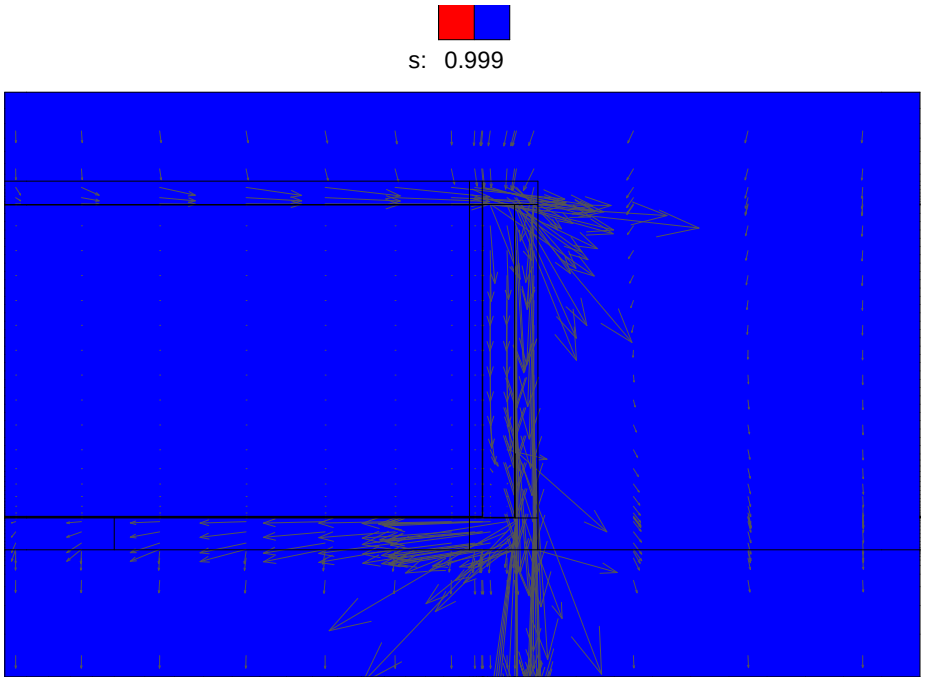

(s: = saturation)

Figure 4.4-27: Type I Tank Flow Field - Year 20,000

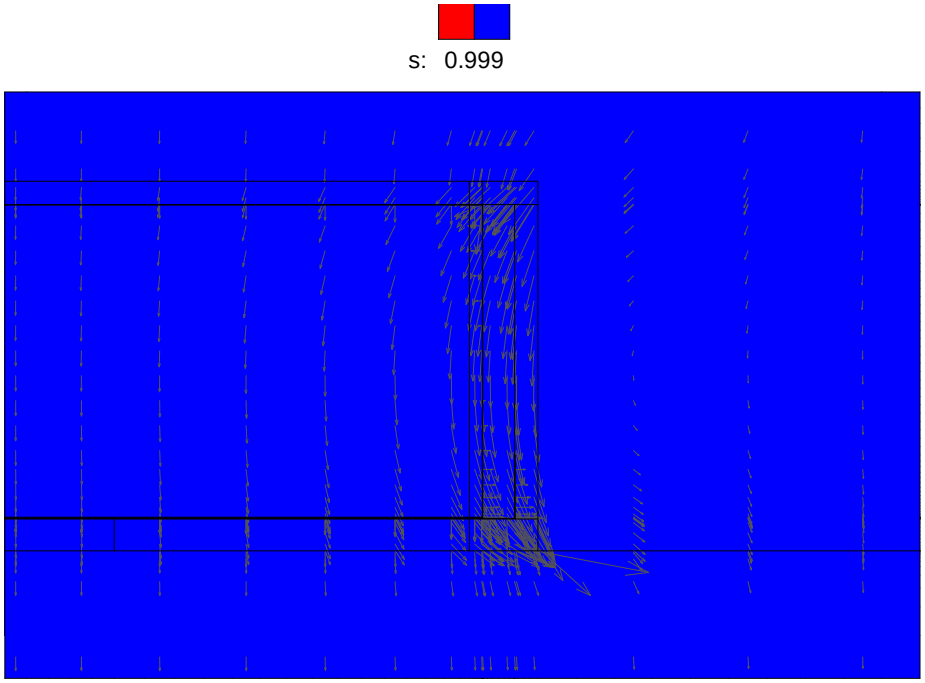

(s: = saturation)

Figure 4.4-28: Type II Tank Flow Field - Year 100

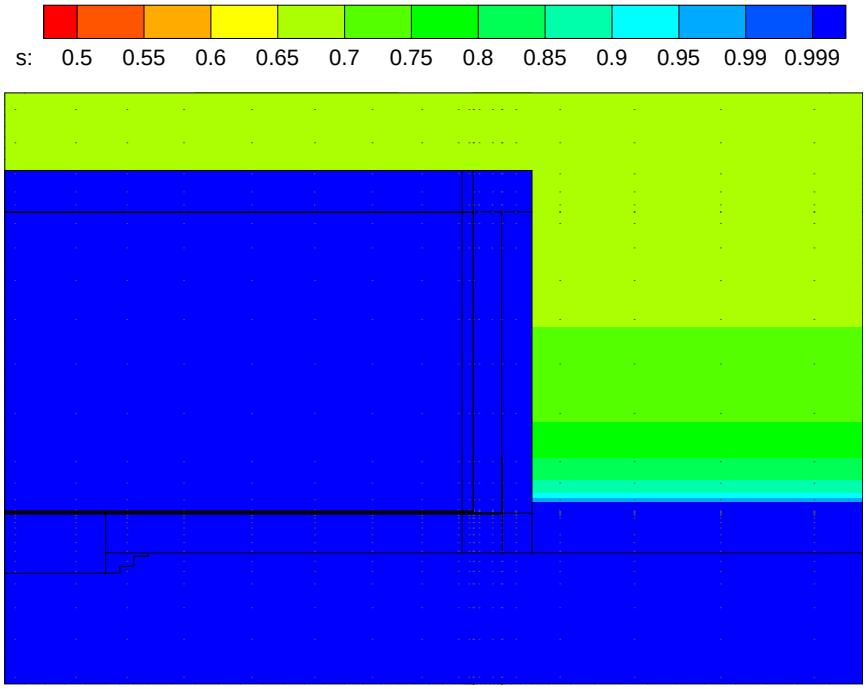

(s: = saturation)

Figure 4.4-29: Type II Tank Flow Field - Year 10,000

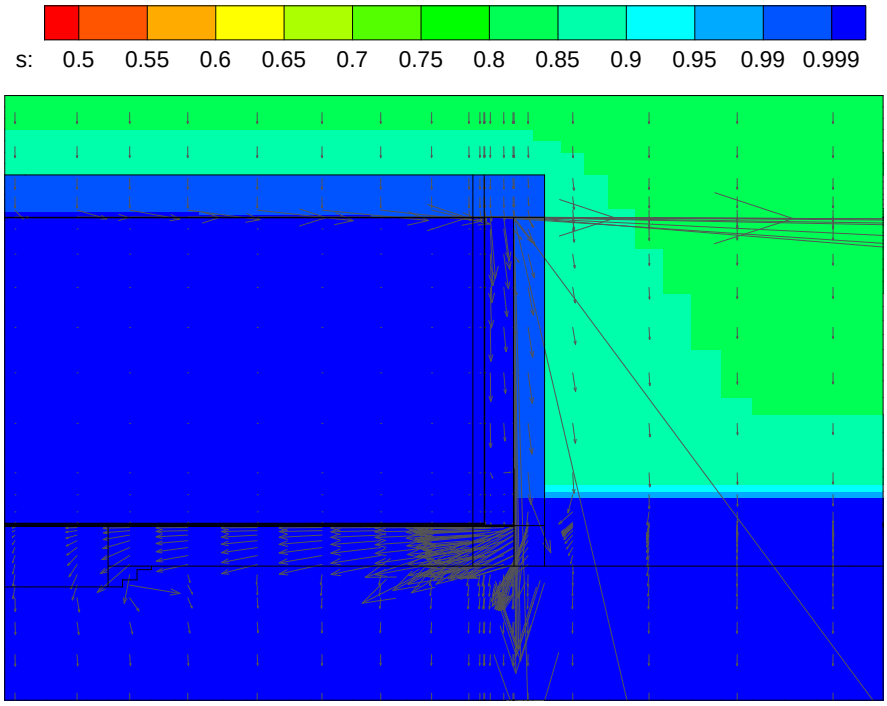

(s: = saturation)

Figure 4.4-30: Type II Tank Flow Field (Immediately Prior to Liner Failure) - Year 12,687

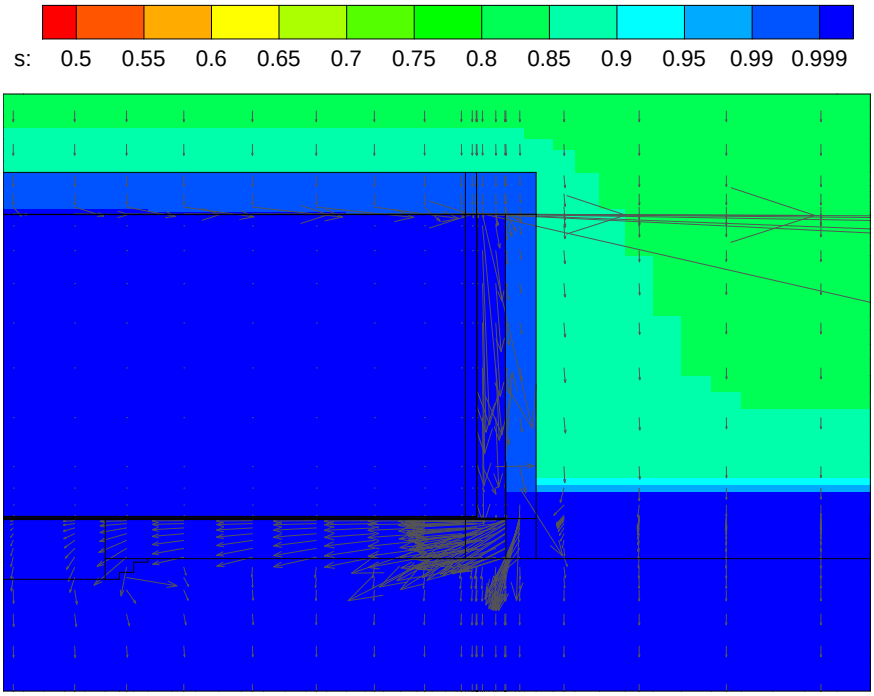

(s: = saturation)

Figure 4.4-31: Type II Tank Flow Field - Year 20,000

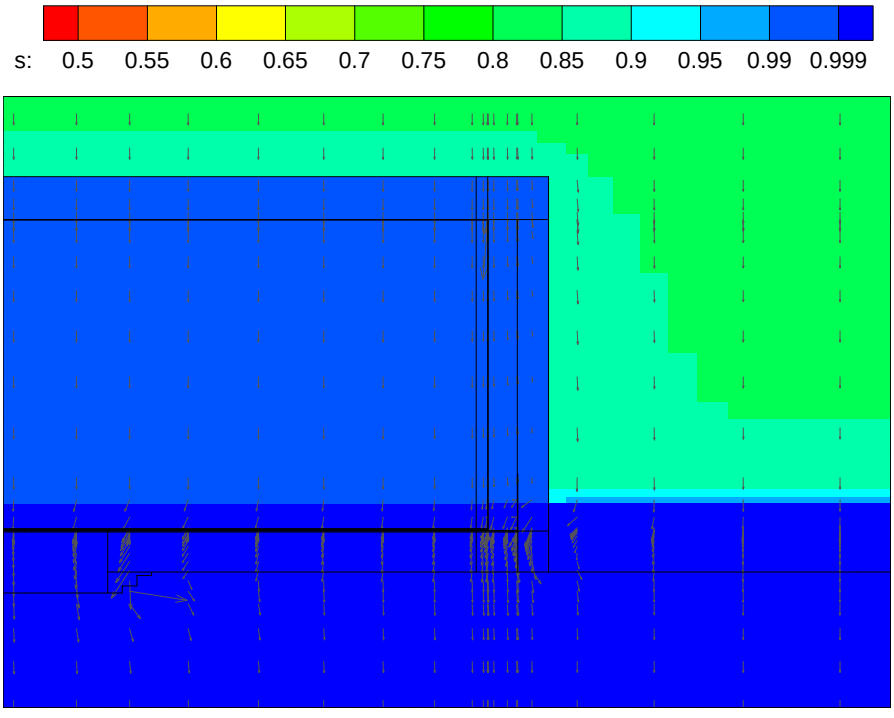

(s: = saturation)

Figure 4.4-32: Type III Tank Flow Field - Year 100

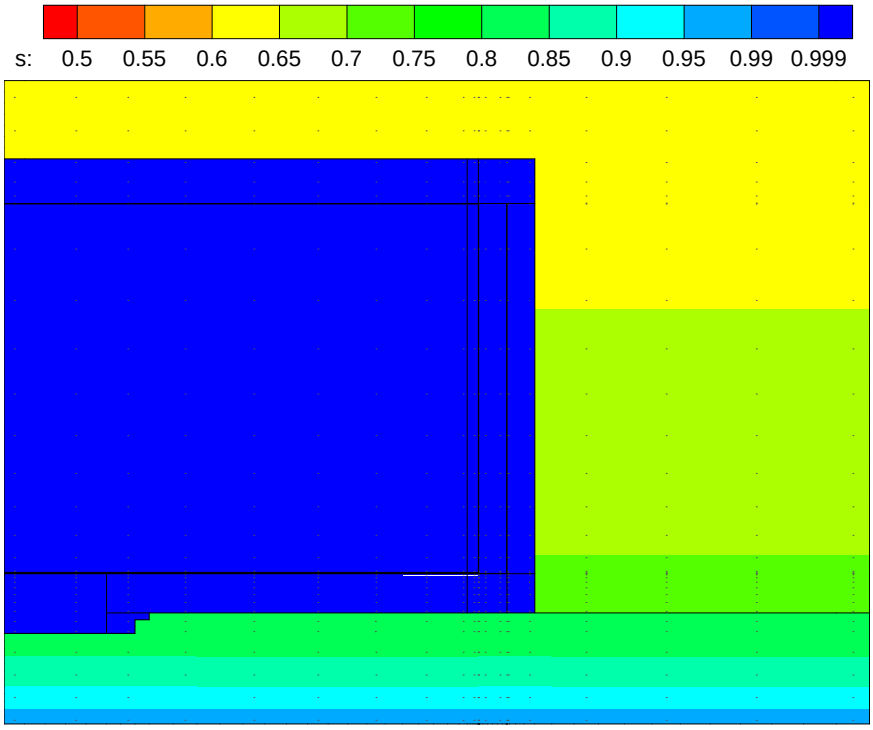

(s: = saturation)

Figure 4.4-33: Type III Tank Flow Field - Year 10,000

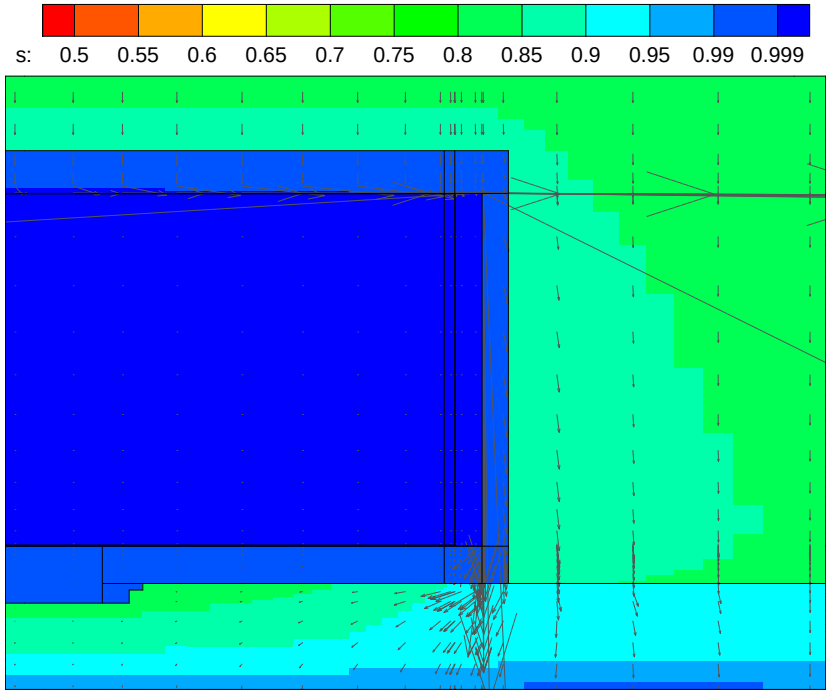

(s: = saturation)

Figure 4.4-34: Type III Tank Flow Field (Immediately Prior to Liner Failure) - Year 12,751

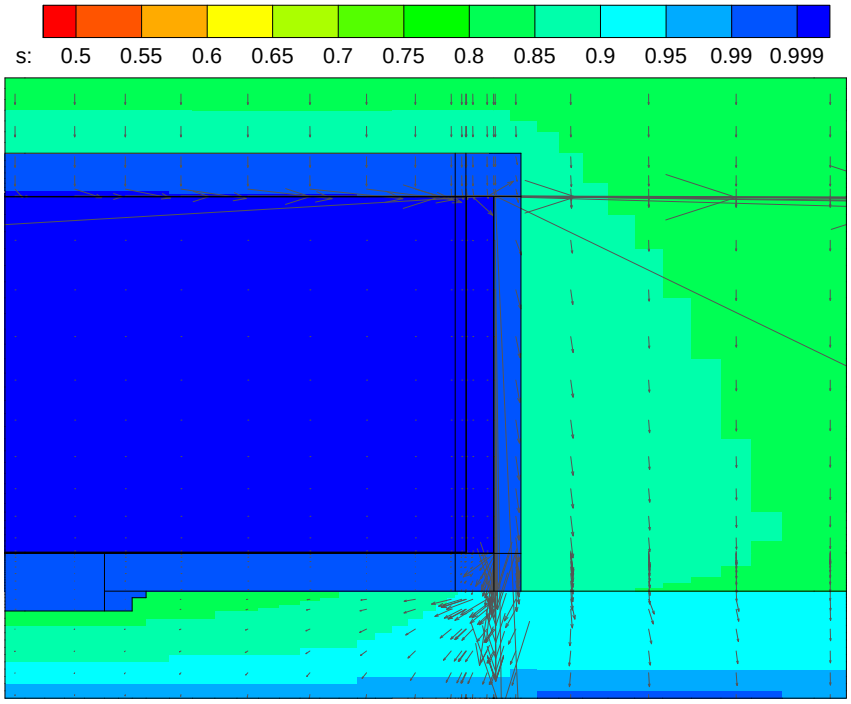

(s: = saturation)

Figure 4.4-35: Type III Tank Flow Field - Year 20,000

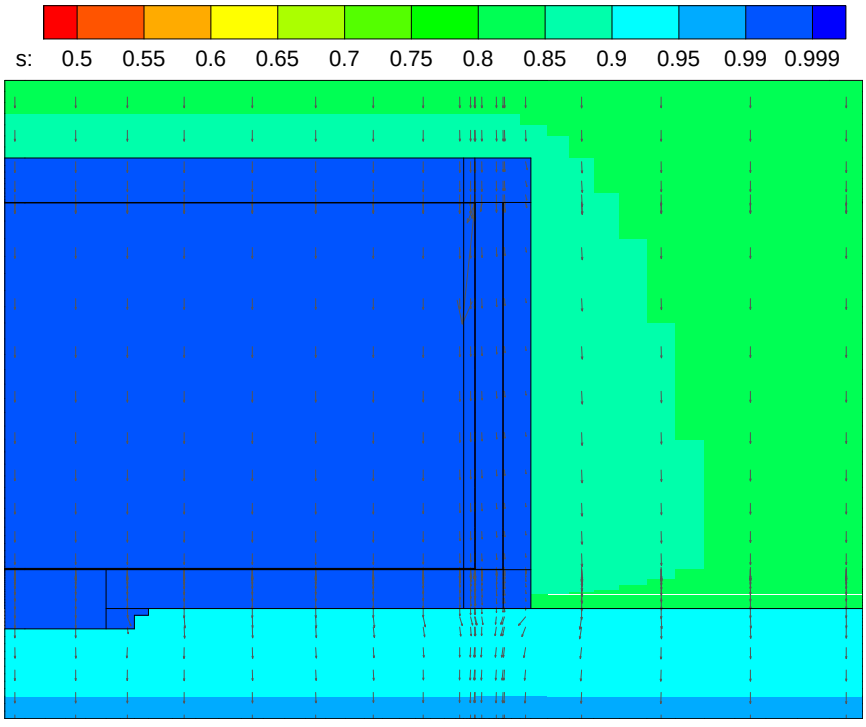

(s: = saturation)

Figure 4.4-36: Type IV Tank Flow Field - Year 100

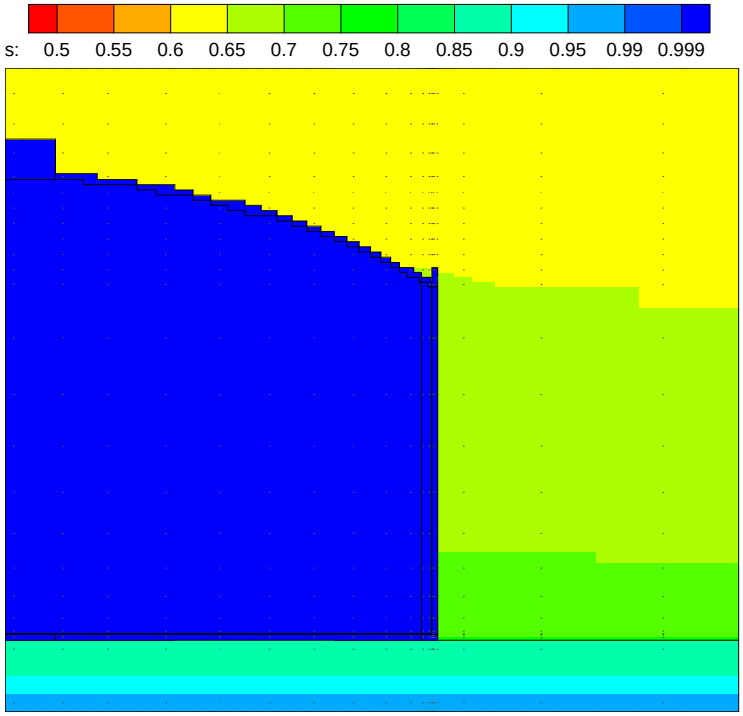

(s: = saturation)

Figure 4.4-37: Type IV Tank Flow Field (Immediately Prior to Liner Failure) - Year 3,638

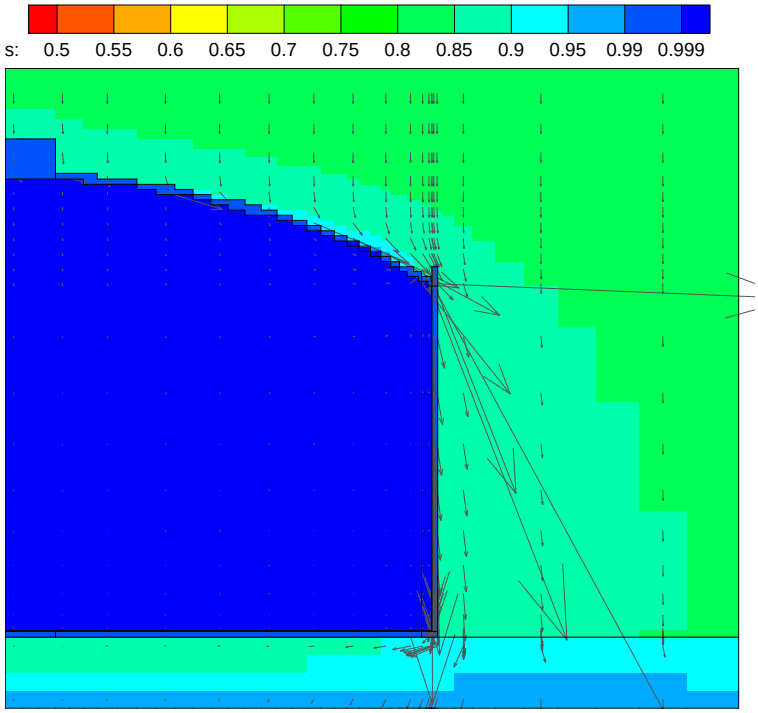

(s: = saturation)

Figure 4.4-38: Type IV Tank Flow Field - Year 10,000

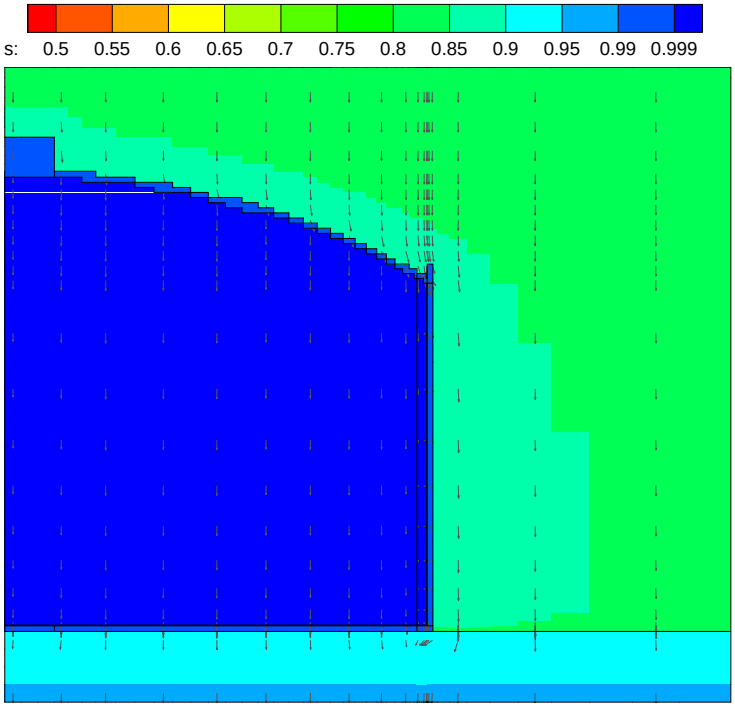

(s: = saturation)

Figure 4.4-39: Type IV Tank Flow Field - Year 20,000

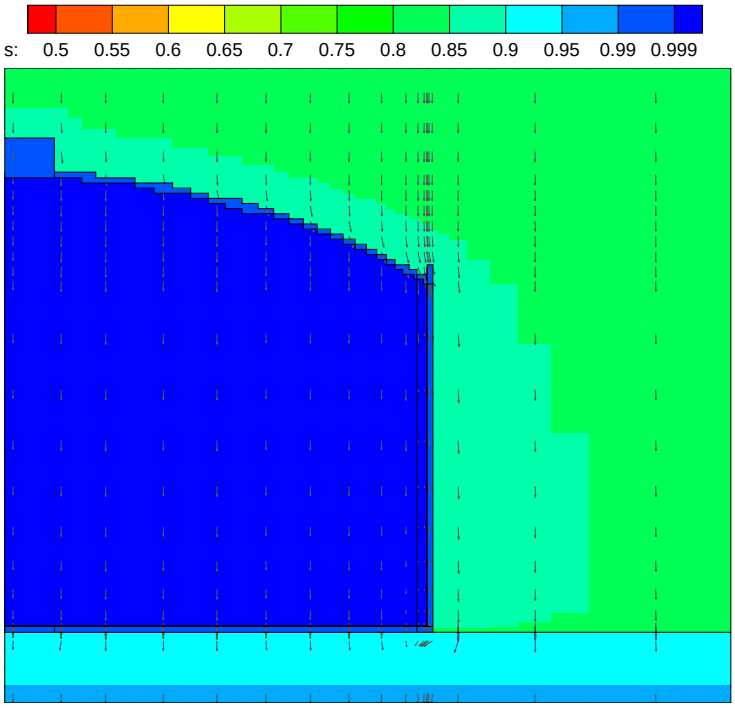

(s: = saturation)

Hydrodynamic dispersion was neglected in vadose transport modeling because most materials are homogeneous (e.g., concrete) or relatively so (e.g., backfilled soil). Preferential flow pathways through cracks, fractures, or other discrete features were modeled using one of two methods, depending on scale. Even though there is an increase in saturated hydraulic conductivity and modified characteristic curves, small-scale features are implicitly represented within a porous medium formulation. Large-scale features are explicitly represented in a porous medium formulation as discrete zones of high permeability (e.g., sand seam). A porous, rather than fractured, medium approach was preferred for smaller scale fracture scenarios because, 1) smaller scale crack/fracture geometry and other properties have not been defined for the degraded material of interest and 2) the scenarios of interest for the HTF PA can be adequately represented in the simpler porous medium approach.

Material properties are independently defined for each grid zone, but are not necessarily different (depending on the scenario). Properties are defined as the product of these factors:

- Base value from a materials palette, a time-invariant constant
- Time-dependent factor #1, intended to represent baseline physical changes
- Time-dependent factor #2, intended for UA/SA perturbations

The latter two factors defining the properties can be arbitrary piecewise-linear functions. They are functionally identical and differ only in intended usage. Material properties can change in the HTF GoldSim Model over time. In PORFLOW modeling, infiltrate pore volume as a function of time is calculated outside of PORFLOW after flow simulations have been completed. Chemical transitions in subsequent transport modeling are based on these calculations, oxidation potential, and pH transitions as a function of pore volumes from WSRC-STI-2007-00544. In general, chemical transitions for a material zone are based on infiltrate pore volumes for that same zone. For example, at the time when the calculated volume of pore water flowing through the grout zone equals the transition volume, the materials in the grout zone are subsequently modeled as having the properties associated with the new chemical phase (Table 4.2-1).

For some materials and cases, chemical transitions for a particular zone are tied to the transition in another zone. For example, the basemat of Type II tanks is divided into three sub-zones, 1) a thicker disk at the waste tank centerline, 2) an outer ring beneath the walls and annulus space, and 3) the remaining center ring. The transition times for all three regions are tied to the pore volume count through the center ring. Thus, no credit is taken for the thicker inner disk, nor is the pore volume count biased by faster flows rounding the outside corner of the overall basemat.

A second example of the chemical transition for a particular zone being tied to the transition is the CZ in the Base Case (Case A). In this case, infiltrate flowed downward through the waste tank grout and the pore water chemistry of the overlying grout is assumed imparted on the very thin CZ in intimate contact with grout. Therefore, the chemical transition times are considered identical for the two materials. Cases B and D initially had a fast flow path around the grout, but the grout degraded hydraulically at

year 501, after which infiltrate flowed downward through the grout. In these cases, the chemical transition of the CZ is also based on the overlying grout. For Cases C and E, a fast flow path through the grout existed, but the grout failed hydraulically as it did in the Base Case. Since the overlying grout remains intact longer, the infiltrate was able to bypass the waste tank grout (via the fast flow path) and flow through the CZ. For these cases, the CZ is based on its own pore water count.

Chemical degradation is indirectly coupled to hydraulic degradation through infiltrate pore volumes. Chemical transitions are a function of infiltrate pore volumes. Hydraulic degradation that alters the flow field may affect the infiltrate pore volume count, and thus oxidation potential and pH transitions occur in time.

For submerged and partially submerged waste tanks, the raw pore volume counts from near-field PORFLOW modeling were inflated for material zones to account for aquifer crossflow by using a 'crossflow factor' defined as:

$$\frac{F}{D} = 1 + \frac{C}{I}$$

Where F = total flow considering crossflow, D = downward flow from near-field PORFLOW modeling, C = crossflow rate, I = infiltration rate in near-field PORFLOW modeling. The adjusted total flow is used to count pore volumes flushed through a material zone. The crossflow rate is assumed to be C = 480 cm/yr, which corresponds to a crossflow ratio of ten times based on simulations in PORTAGE-08-022, and a nominal present day infiltration rate of 48 cm/yr. The crossflow factor is generally applied to waste tank components that are fully submerged. Further information is provided in SRNL-l6200-2010-00026.

For transport modeling, a fixed time step of 1 year was chosen for the vadose (and saturated) zone. The selected step size was compromised between two competing objectives, 1) resolution of concentration peaks from relatively mobile species that migrate as a pulse, and 2) achieving reasonable computer runtimes. A sensitivity study using the Base Case from the closely related FTF PA indicated good accuracy in general, the exception being nitrate, for which the reported results may be low by roughly one-third. [SRS-REG-2007-00002] However, nitrate results are well below performance objectives so the modeling bias was acceptable.

The materials palette used in HTF PORFLOW modeling is provided in Table 4.4-10.

Table 4.4-10: PORFLOW Materials Palette

Material ID	K_{sat} Horizontal (cm/sec)	K_{sat} Horizontal (cm/yr)	K_{sat} Vertical (cm/sec)	K_{sat} Vertical (cm/yr)	Saturated D_e (cm2/sec)	Saturated D_e (cm2/yr)	η_T (unitless)	ρ_h (g/cm^3)	ρ_n (g/cm^3)	Characteristic Curve
native_soil	6.2E-05	2.0E+03	8.7E-06	2.7E+02	5.3E-06	167.26	0.39	1.65	2.70	UpperVz
LowerVz	3.3E-04	1.0E+04	9.1E-05	2.9E+03	5.3E-06	167.26	0.39	1.62	2.66	LowerVz
OscBefore	1.2E-04	3.8E+03	1.2E-04	3.8E+03	5.3E-06	167.26	0.46	1.44	2.65	OscBefore
OscAfter	1.4E-05	4.4E+02	1.4E-05	4.4E+02	4.0E-06	126.23	0.27	1.92	2.65	OscAfter
backfill	7.6E-05	2.4E+03	4.1E-05	1.3E+03	5.3E-06	167.26	0.35	1.71	2.63	CcBackfill
IlvPermeable Backfill	1.4E-03	4.4E+04	7.6E-04	2.4E+04	8.0E-06	252.46	0.41	1.56	2.64	IlvPermeableBackfill
SingleVadose Zone	1.9E-04	6.0E+03	3.0E-05	9.5E+02	5.3E-06	167.26	0.39	1.63	2.67	SingleVadoseZone
Sand	5.0E-04	1.6E+04	2.8E-04	8.8E+03	8.0E-06	252.46	0.38	1.65	2.66	Sand
ClaySand	8.3E-05	2.6E+03	2.1E-05	6.6E+02	5.3E-06	167.26	0.37	1.68	2.67	ClaySand
Clay	2.0E-06	6.3E+01	9.5E-07	3.0E+01	4.0E-06	126.23	0.43	1.52	2.67	Clay
Gravel	1.5E-01	4.7E+06	1.5E-01	4.7E+06	9.4E-06	296.64	0.30	1.82	2.60	Gravel
basemat	3.5E-08	1.10E+00	3.5E-08	1.10E+00	8.0E-07	25.25	0.168	2.06	2.51	fractured_basemat
grout	3.6E-08	1.14E+00	3.6E-08	1.14E+00	8.0E-07	25.25	0.266	1.84	2.51	fractured_grout
wall_roof	3.5E-08	1.10E+00	3.5E-08	1.10E+00	8.0E-07	25.25	0.168	2.06	2.51	fractured_basemat
contaminated_zone	3.6E-08	1.14E+00	3.6E-08	1.14E+00	8.0E-07	25.25	0.266	1.84	2.51	fractured_grout
liner	5.0E-15	1.6E-07	5.0E-15	1.6E-07	1.0E-13	3.16E-06	0.39	N/A	2.70	Concrete_Qlow_NewCig Grout
vertical_liner	5.0E-15	1.6E-07	5.0E-15	1.6E-07	1.0E-13	3.16E-06	0.39	N/A	2.70	Concrete_Qlow_NewCig Grout
fast_flow	1.5E-01	4.7E+06	1.5E-01	4.7E+06	9.4E-06	296.64	0.30	1.82	2.60	Gravel

K_{sat}= Saturated Hydraulic Conductivity
η_T = Total Porosity
ρ_h = Dry Bulk Density
ρ_n = Particle Density
D_e = Effective Diffusion Coefficient

4.4.4.1.3 Fast Flow Path Modeling in PORFLOW

PORFLOW was used early in the analysis process to do scoping runs for the various cases described in Section 4.4.2. To represent the effect of a hypothetical fast flow path through a waste tank (Figure 4.4-40), the HTF PORFLOW Model assumed all water being shed from the tank roof was intercepted by a high conductivity vertical leg encircling the waste tank perimeter just inside the primary liner. Horizontal flow then takes place through the CZ, which was also assigned a large conductivity, with the entire CZ allowed to contact infiltrating water. Contaminant transport was then assumed to take place through a high conductivity center "donut" hole in the waste tank basemat. The hole was sized to allow high flow through the fast flow path and contamination layer in particular. The materials occupying the fast flow zones were assumed to have high conductivity and diffusion coefficient relative to backfilled and native soils, but no adsorption was assumed (i.e., $K_d = 0$ for all radiological and chemical transport).

Figure 4.4-40: PORFLOW Type IV Tank Fast Flow Path Model

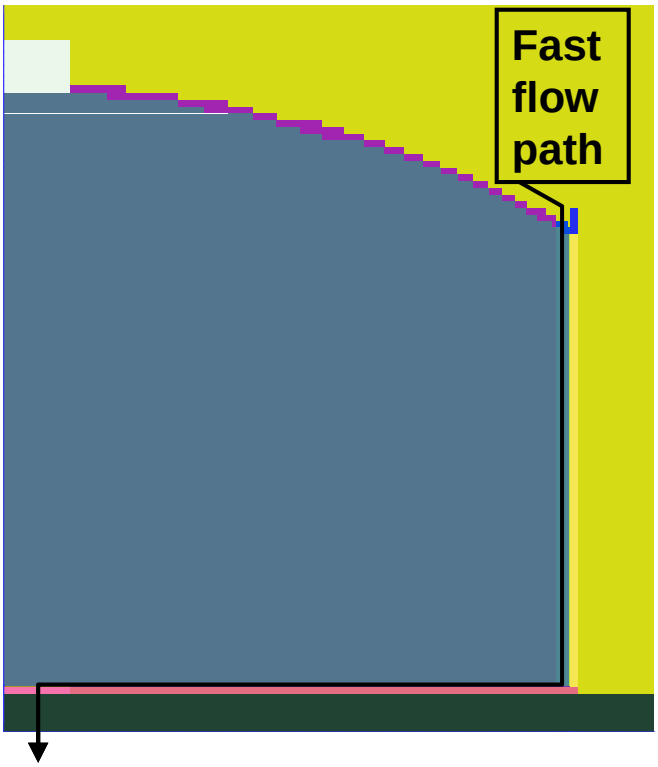

4.4.4.1.4 Vadose and Aquifer Model Validation in PORFLOW

Additional PORFLOW validation was performed beyond code verification exercises and GSA/HTF model development. Using characterization and monitoring data, aspects of the PORFLOW vadose zone and aquifer models have been compared to independent field data, as identified below. Additional detail can be obtained in the associated references.

Vadose Zone

- Soil suction and water content from Vadose Zone Monitoring System (VZMS) in E Area (WSRC-STI-2006-00198, Section 5.8)
- Tracer test pore velocity (WSRC-TR-2007-00283, Section 4.0)
- Tritium migration beneath the E-Area Slit Trenches (herein)

Aquifer

- Surveyed seeplines (WSRC-TR-2004-00106)
- Pathline comparisons to existing plumes (herein)

The VZMS monitors soil conditions beneath and alongside the solid waste disposal trenches (slit trenches) in E Area under uncapped infiltration conditions (Figure 4.4-41). E Area is located in the GSA adjacent to H Area. Field measurements using tensiometers and neutron probes indicate that soil suction ranges from approximately 50 to 200 centimeters, while water content varies between about 0.15 and 0.30. The latter values suggest water saturation between 35% and 75%. Infiltration over the affected area is estimated to be 30 cm/yr (12 in/yr). Using the upper vadose zone and lower vadose zone soil properties recommended in WSRC-STI-2006-00198 and adopted for HTF PA modeling, a PORFLOW representation of E-Area conditions produced suction head and saturation values of 83 centimeters and 91% in the upper vadose zone, and 170 centimeters and 72% in the lower vadose zone.

Figure 4.4-41: Layout and Instrumentation for VZMS at Slit Trenches

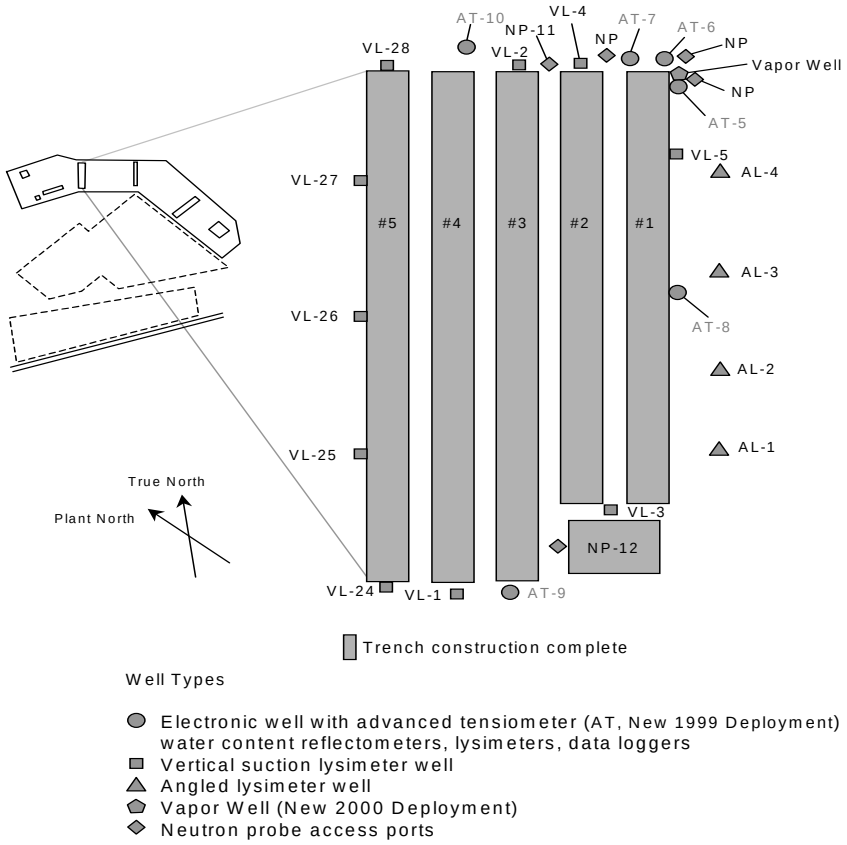

A series of field and laboratory tracer experiments have been conducted at SRS under uncapped (normal infiltration) conditions. The HTF GoldSim Model described above produced pore velocities of approximately 34 in/yr and 43 in/yr for upper and lower vadose zones, respectively. Together, the tracer test data indicate a pore velocity of about 45 in/yr for the same infiltration, which is similar to the model simulations.

A PORFLOW vadose zone model, similar to that used for HTF PA simulations was compared to tritium concentration data from the VZMS (Figure 4.4-41). Concentration data was grouped according to elevation (high/low) and location (center/edge) relative to a disposal trench (Figure 4.4-42). The concentration data exhibits large variability, as is commonly observed with point measurements (Figure 4.4-43). The "Generic" and "Concrete" labels in Figure 4.4-43 refer to the waste form(s) containing tritium contamination. "Generic" designates general waste of a variety of forms, whereas "Concrete" is reserved for concrete rubble waste generated from demolition of Building 232-F. In model simulations, tritium in "Generic" waste is immediately available for transport. Tritium embedded in concrete is released more slowly by diffusion. The HTF GoldSim Model has a homogeneous conductivity field and no dispersion was prescribed during transport simulations. Thus, the simulations may have under-predicted lateral plume spreading compared to actual conditions. For example, sediment layering can cause contamination to migrate outside the footprint of the trench. Small changes in the

degree of lateral plume dispersion can lead to large changes in "Edge" concentration, whereas the "Center" (plume centerline) concentration would be less affected. Given uncertainty in the tritium source strength and distribution, and PORFLOW simplification of natural subsurface heterogeneity, close agreement between the data and model was not expected. Rather than representing a definitive validation of the model, DOE believes the comparison does not provide evidence of model invalidation. Being equivalent to a spatial average representation, the PORFLOW predictions do not reflect the data scatter, but do appear to be generally consistent with the measurement trends.

Figure 4.4-42: Basis for HTF GoldSim Model and VZMS Data Comparison

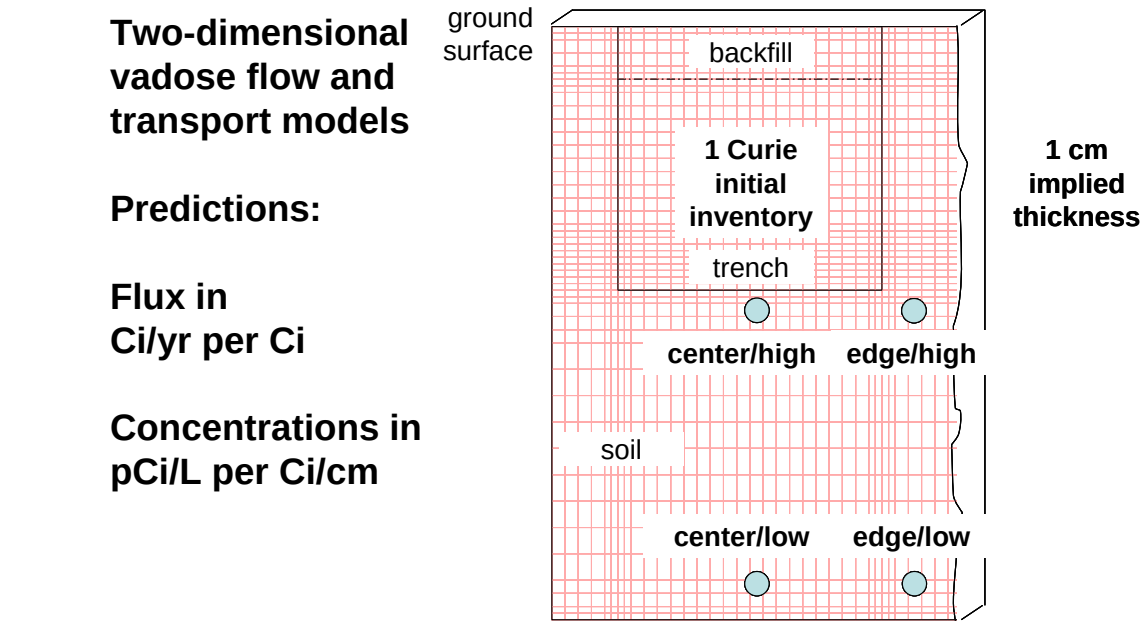

Figure 4.4-43: HTF GoldSim Model and VZMS Tritium Data Comparison

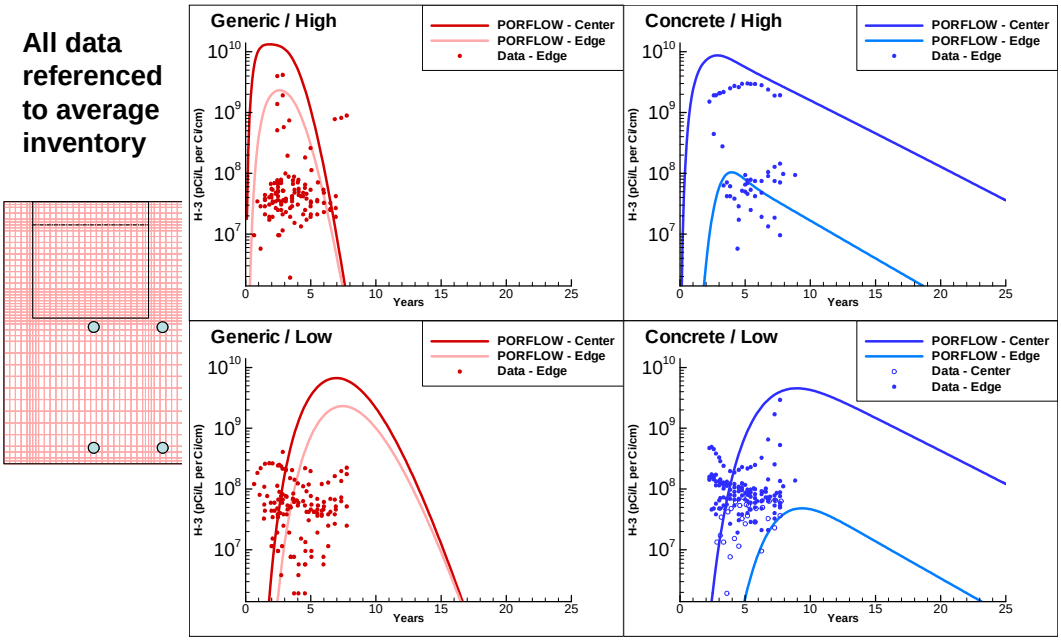

The GSA/PORFLOW Model predictions of seeplines bordering the GSA have been compared to field surveys (Figure 4.4-44). [WSRC-TR-2004-00106] The seepline data was not used in model development or calibration. The simulated seepage faces are generally consistent with the field observations.

Figure 4.4-44: Surveyed Seeplines Compared to GSA/PORFLOW Model Simulation

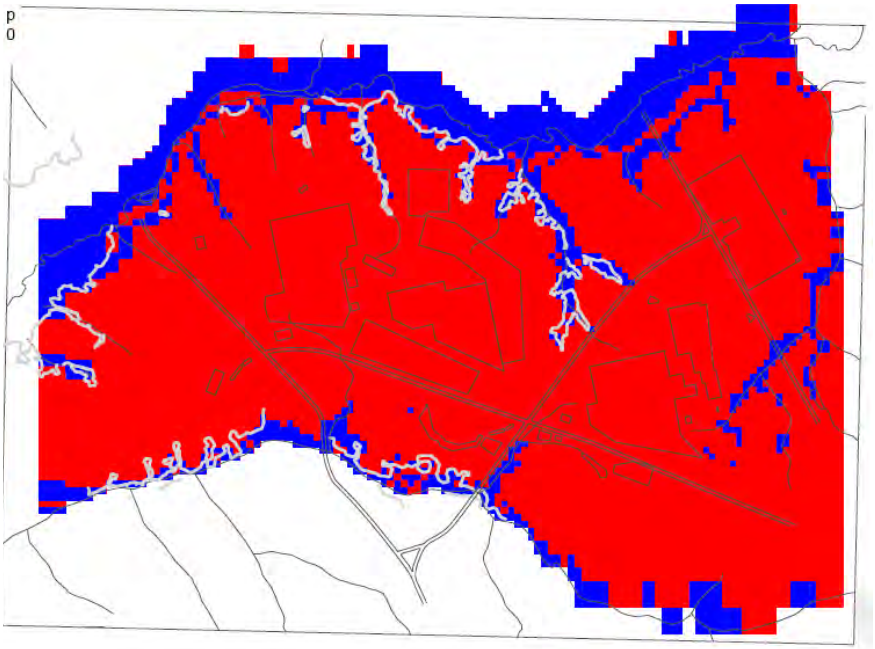

Note: Seepline predicted at interface of recharge (red) areas and discharge (blue) areas with surveyed seepline location shown in white trace lines. [WSRC-TR-2004-00106, Figure 3-6]

The GSA contains a number of tritium plumes, typically associated with E-Area solid waste disposal facilities. Being un-retarded, tritium is an ideal tracer of groundwater flow. Groundwater pathlines from the GSA/PORFLOW Model were compared to an existing tritium plume map. The model pathlines were observed to be consistent with plume trajectory deduced from monitoring well data (Figure 4.4-45). Simulated pathlines have also been compared to F-Area plumes, with good agreement (Figure 4.4-46). The plume distributions depicted in Figures 4.4-45 and 4.4-46 were generated from field measurements. Simulated pathlines are also compared to an H-Area plume in Figure 4.4-47 with similar paths although the plume data is limited. The plume distribution depicted in Figure 4.4-47 was generated from field measurements. The GSA/PORFLOW Model was not calibrated to these data.

Figure 4.4-45: Comparison of GSA/PORFLOW Groundwater Pathlines to a Tritium Plume Emanating from the E-Area Mixed Waste Management Facility

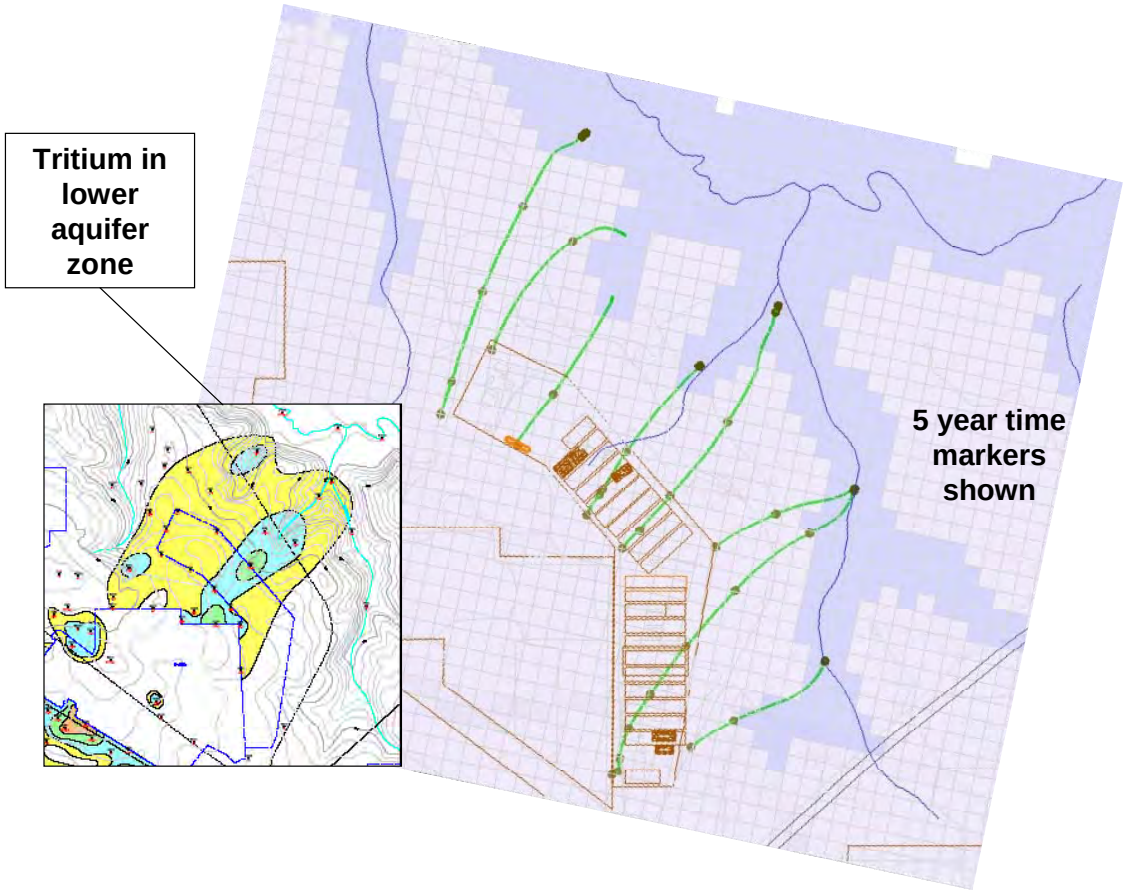

Figure 4.4-46: Comparison of GSA/PORFLOW Groundwater Pathlines to Contaminant Plumes Emanating from F Area

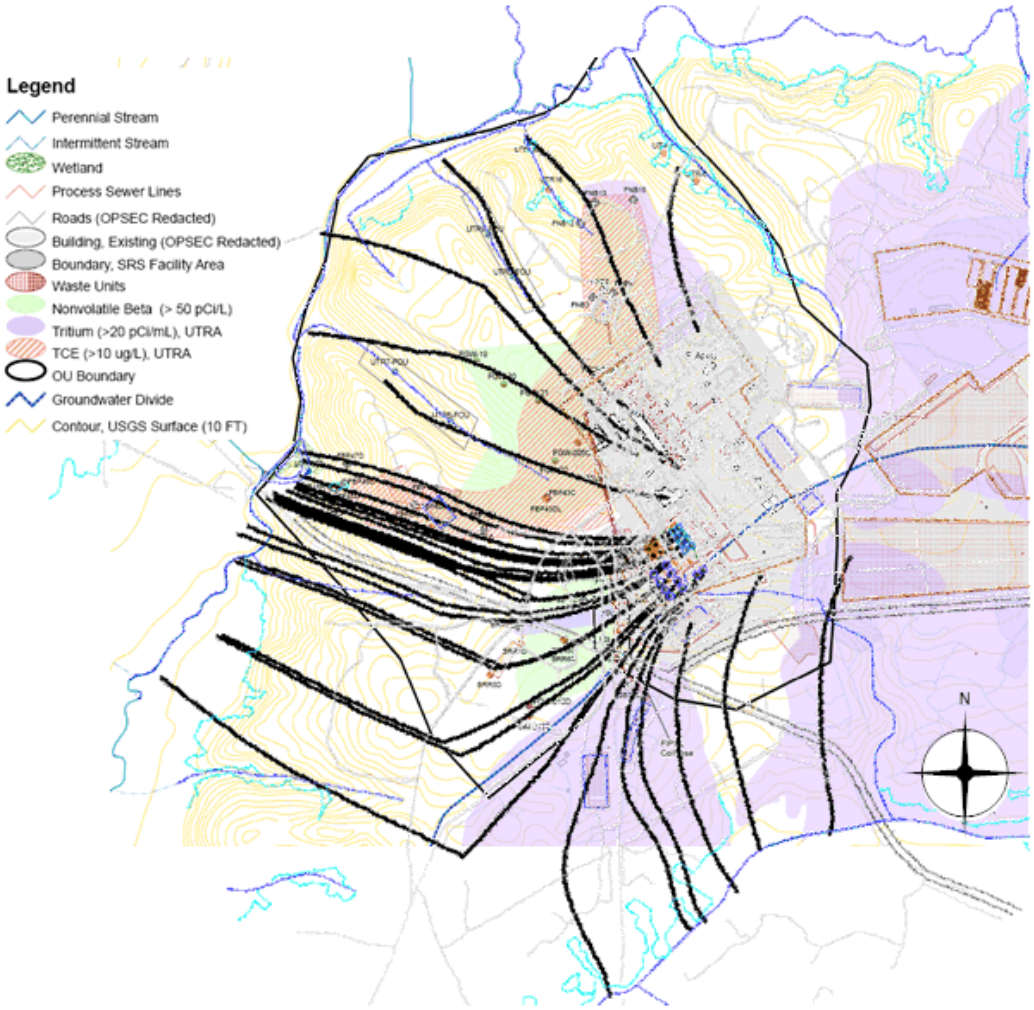

Figure 4.4-47: Comparison of GSA/PORFLOW Groundwater Pathlines to Contaminant Plume Emanating from H Area

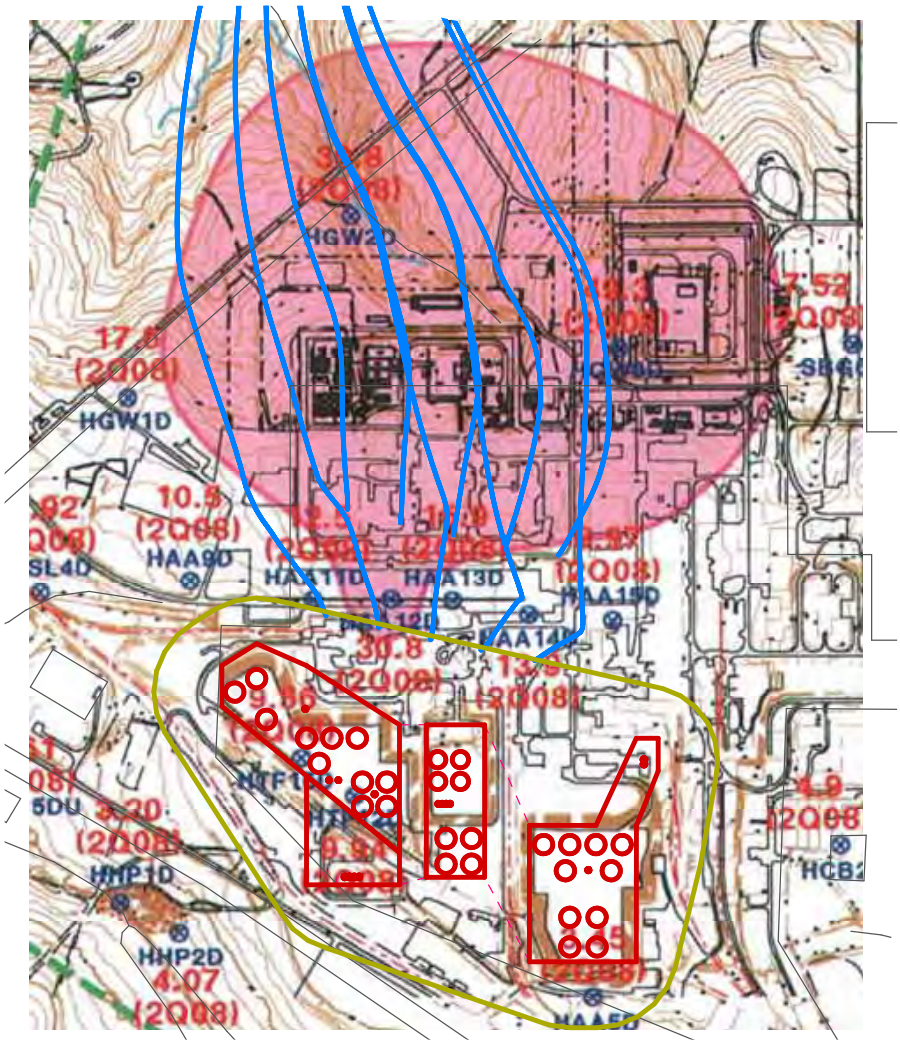

The simulated groundwater pathlines are compared to plumes deduced from field measurements as evidence that the GSA/PORFLOW Model reproduces plume trajectory in map view. The DOE recognizes that the figures do not address other relevant points of comparison, such as travel time and concentration. Such a comparison would require substantially more effort to reconstruct contaminant sources (amount, location, and release history) and interpret plume-monitoring data.

4.4.4.2 GoldSim Modeling Process

The H-Area Tank Farm Stochastic Fate and Transport Model (referred to as the HTF stochastic model, or simply the HTF GoldSim Model) is an object-oriented probabilistic model (as opposed to the PORFLOW deterministic model). The HTF GoldSim Model is designed to evaluate parameter sensitivity and the influence of parameter uncertainty on the migration of radionuclides from the closed HTF facility to the accessible environment. The following sections describe the stochastic modeling process. A detailed description of the HTF stochastic model development and input parameters can be found in the *H-Area Tank Farm Stochastic Fate and Transport Model* (SRR-CWDA-2010-00093). While discussing the GoldSim modeling process, the PORFLOW deterministic model is frequently referenced for comparison purposes. Please refer to Section 4.4.4.1 for an expanded explanation of the PORFLOW deterministic implementation.

The stochastic model is, by necessity, simpler than the PORFLOW groundwater model in its environmental transport calculations, but includes additional calculations that cannot be performed in PORFLOW. The HTF GoldSim Model is a 1-D model as opposed to the 3-D HTF GoldSim Model. Therefore, to replicate the 3-D processes represented in PORFLOW, some additional tasks, such as implementing a plume function, were required during GoldSim modeling. In addition, the HTF GoldSim Model does not independently model flow velocity, but uses input flow profiles generated by PORFLOW (see SRR-CWDA-2010-00093 for the input flow profiles used in the HTF GoldSim Model). Ultimately, to use the stochastic model with confidence, validation of the 1-D HTF GoldSim Model versus the 3-D HTF GoldSim Model is required and this validation has been explicitly addressed in the GoldSim benchmarking discussion (Section 5.6.2).

The stochastic model is comprised of two sub-models, 1) an abstraction of the HTF PORFLOW Model and 2) a dose calculator. Where necessary, the HTF GoldSim Model discussion will differentiate these two sub-models as the transport sub-model and the dose calculator sub-model. The abstraction is specifically designed to approximate the process of radionuclide transport from tanks and ancillary equipment sources in a manner that would allow for UA/SA to be performed in a time-efficient manner, while still allowing the influence of parameters on the transport processes to be examined.

The HTF GoldSim Model also includes a dose calculator, which can be used to evaluate dose at points of compliance based on the concentrations generated by the transport abstraction sub-model or generated by the HTF PORFLOW Model. The dose calculator sub-model will be discussed in Section 4.4.4.2.3, while the description below pertains to the GoldSim HTF transport sub-model.

4.4.4.2.1 HTF GoldSim Model Features

The HTF stochastic model was developed using GoldSim (Version 10.11, SP3), which is a graphics based object-oriented computer program designed to carry out dynamic, probabilistic simulations. [GTG-2010] In addition to its use as a generalized stochastic analysis program, GoldSim contains contaminant and radionuclide transport modules that can be used to develop probabilistic simulations of the release of contaminants from engineered barriers, and the fate and transport of contaminants through natural barriers.

GoldSim contaminant and radionuclide transport modules approximate contaminant or radionuclide transport processes analytically (or semi-analytically) using pipe elements (or networks of pipe elements) or numerically using networks of mixing cells (cell pathway elements). [GTG-2010]

To minimize computation time, the 3-D conceptual model simulated by the HTF PORFLOW Model is compartmentalized into simplified 1-D legs comprised of GoldSim cell pathway elements in the HTF transport model. Each leg is comprised of one or more mixing cells linked in series. When needed to reproduce specific effects in specific waste tank types (Tank Types II and IV), communication between parallel strings of cells was allowed.

In the GoldSim transport model, the waste tank structure was divided into several groups of cells, representing the various components of the waste tank structure (e.g., grout, CZ, steel liners, concrete basemat, sand pads, and the annulus grout). Figures 4.4-1 through 4.4-5 display a simplification of the various components that exist for each waste tank type. PORFLOW discretely represents these components, as illustrated in Figures 4.4-15 through 4.4-22. In contrast to the HTF GoldSim Model, certain design elements, such as the concrete roof, and for some waste tanks (Tank Types I and III/IIIA) the concrete wall, were not represented in the GoldSim HTF transport model.

The unsaturated zone (for non-submerged waste tanks), the saturated zone beneath the contaminant sources (waste tanks and ancillary equipment), and the saturated zone, downgradient from the contaminant sources were also simulated using sets of linked mixing cells.

Cell Pathway

As noted in the *GoldSim Contaminant Transport Module User's Guide* (GTG-2010), the cell pathway elements represent discrete, well-mixed environmental compartments or "mixing cells" that can be used to describe the environmental system being simulated. A cell pathway element represents a specific volume of reference fluid (water for the HTF model) and mass of solid(s). Within the cell, complete mixing takes place so there is no spatial differentiation of concentration within any phase. The dissolved species migrate between cells via advection or diffusion.

The GoldSim cell-pathway elements can simulate the transport processes within the waste tanks because the HTF GoldSim Model is designed to evaluate the fate and transport of radionuclide decay chains and can consider the influence of solubility controls on isotopes as well as sorption on the radionuclide transport process. GoldSim allows for two types of mass links between cells, advective links, and diffusive links.

Sub-Models and Looping Structure

The transport module takes advantage of GoldSim sub-model elements to define the transport abstraction as a separate "inner model" which was fed data from the main model. The sub-model can be switched on when performing GoldSim transport

simulations and switched off when using PORFLOW concentration results. In addition, the transport module takes advantage of GoldSim Looping Containers to allow the sub-model to be run in a looping mode for the 47 different contaminant sources (29 waste tanks and 18 ancillary equipment sources). For additional information regarding the looping architecture implemented in the HTF transport model, refer to Section 3.2 of SRR-CWDA-2010-00093.

Plume Function

The GoldSim transport sub-model provides a built-in function that can be used to impose the influence of horizontal transverse (lateral) and vertical transverse dispersion on the results generated by a 1-D transport analysis. Designed for use as a multiplier of concentration (or fluxes) at the end of pipe pathway elements to reflect the influence of transverse dispersion on the results, the plume function returns a value between zero and one. It was used in the transport sub-model of the HTF stochastic model to account for the influence of lateral and vertical dispersion on the 1-D transport analysis through the chain of cells representing the saturated zone.

For additional details regarding the analytical solutions used in the plume function, see Section 3.1 of SRR-CWDA-2010-00093.

Monte Carlo Method and Stochastic Elements

The HTF GoldSim Model uses a Latin Hypercube sampling (LHS) method and stochastic elements to propagate uncertainty in the future performance of the HTF as a barrier to contaminant transport. GoldSim stochastic elements are designed explicitly to represent uncertainty in input parameters within a model. Each uncertain parameter is represented by a range of possible values. The traditional Monte-Carlo method randomly samples the data over the complete probabilistic range at each realization. The LHS approach divides each stochastic element's distribution P{0,1} into up to 10,000 strata of equal probability. The actual number used is the smaller of the number of realizations and 10,000 strata. The strata are then randomly "shuffled" into a new order and a random value is then picked from each stratum. The application of the LHS process ensures that a uniform spanning of sampling occurs. [GTG-2009]

The stochastic parameters implemented within the HTF stochastic model are presented in Section 5.6.3, while a discussion of the UA/SA analyses is provided in Sections 5.6.4 and 5.6.5.

4.4.4.2.2 Transport Model Layout and Structure

Upper Level Model Organization

The HTF stochastic model was comprised of two sub-models; the first is the abstraction of the HTF PORFLOW Model and the second is the dose calculator. Figure 4.4-48 displays the upper level HTF GoldSim Model organization.

Figure 4.4-48: Top Level of the HTF Stochastic Model

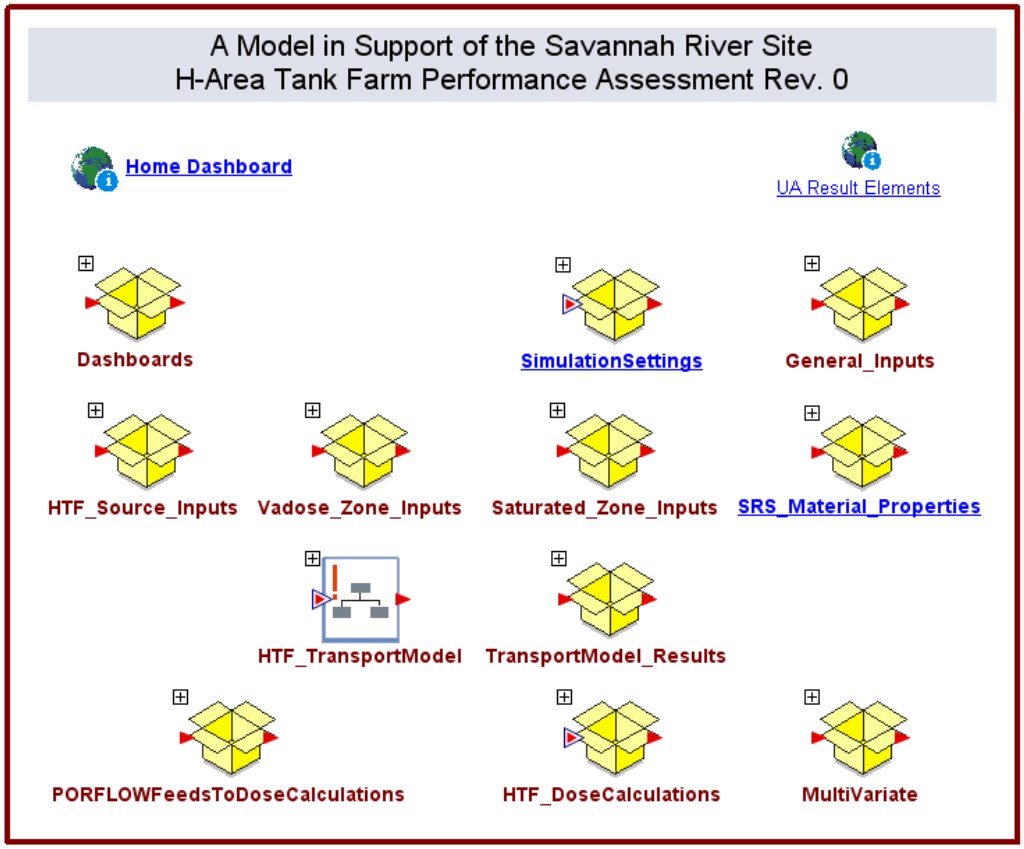

The dose calculator sub-model consisted of the following containers:

- *HTF_DoseCalculations*
- *PORFLOWFeedsToDoseCalculations*

The content of the dose calculator sub-model will be discussed in more detail in Section 4.4.4.2.3.

The following describes the contents of the transport sub-model. As shown in Figure 4.4-48, the static "outer" portion of the transport sub-model, in which all of the control elements and data input elements are assembled, was comprised of the following GoldSim containers:

- *General_Inputs* - contains globally used parameters, such as constants
- *HTF_Source_Inputs* - contains waste tank and ancillary equipment initial inventories
- *Vadose_Zone_Inputs* - contains vadose zone flow and geometry input parameters
- *Saturated_Zone_Inputs* - contains saturated zone properties
- *SRS_Material_Properties* - contains soil, cementitious, and liner material properties

These static "outer" model containers include parameters describing the model domain, (i.e. physical and chemical properties, the model flow system, and model geometry). The deterministic values assigned to the physical and chemical properties were set equal to the values used in the PORFLOW deterministic model. These properties are described in Section 4.2. Stochastic ranges applied to these parameters when the model was simulated in the probabilistic mode are presented in Section 5.6.3. Additional details on the HTF GoldSim Model inputs are included in SRR-CWDA-2010-00093.

The "inner" portion of the model was defined in:

- *HTF_TransportModel*
- *TransportModel_Results*

The "inner model," or sub-model, performs all of the dynamic transport calculations for mass transport associated with contaminant source releases. The sub-model was embedded within a series of containers, the uppermost being the *HTF_TransportModel* container (Figure 4.4-48), which deactivates when the time stepping begins for the dose calculator sub-model.

The *TransportModel_Results* container passed results from *HTF_Transport Model* to the main model. Details regarding the internal looping structure of the sub-models are provided in SRR-CWDA-2010-00093.

The upper level container *MultiVariate* included elements used specifically for the UA/SA, the results of which are discussed in Section 5.6.4 and Section 5.6.5.

The remaining upper level container *Dashboards* provided user controls for users viewing the model with a GoldSim Player.

Transport Model Overview

Transport for waste tanks and ancillary equipment are performed separately. Embedded within the *HTF_TransportModel* container (Figure 4.4-48) are the containers, *HTFTanks_Transport_Model* (HTF Tank transport sub-model) and *HTFAncillary_Equipment_Model* (HTF Ancillary Equipment transport sub-model). Figure 4.4-49 displays the contents of *HTFTanks_Transport_Model*.

Figure 4.4-49: Contents of the Container *HTFTanks_Transport_Model*

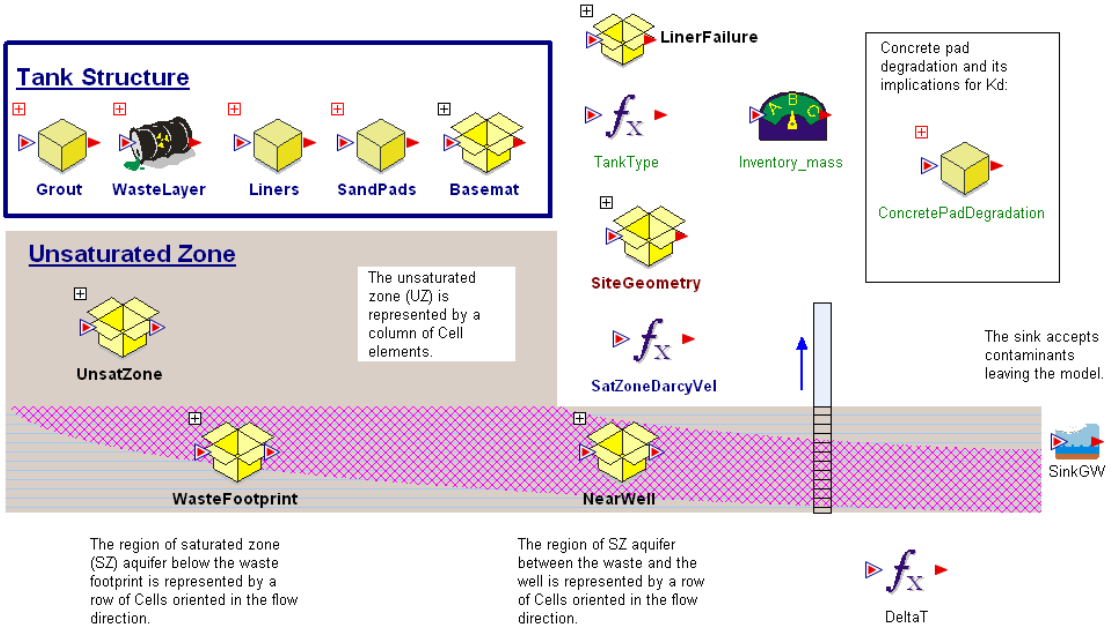

Waste Tank Transport

Below is a general overview of the components explicitly modeled in the HTF Tank transport sub-model.

In the HTF Tank transport sub-model, the cell networks are distributed within five upper level containers and a source element. The source element is a specialized type of container that is capable of performing functions associated with engineered barrier capabilities. Based upon these functions, this container executes a controlled release into associated cells, which are defined by inserting them into the source element. [GTG-2010] In the waste tank model, the cell associated with the source element (i.e. *WasteLayer*) represents the CZ in the engineered waste tank structure. In the ancillary equipment model, the cell associated with the source element represents the contaminated soil at the ancillary equipment location.

The upper level containers in the HTF Tank transport sub-model (*HTFTanks_Transport_Model)* that contain segments of the cell network are:

- *Grout*
- *WasteLayer*
- *Liners*
- *SandPads* (for Type II Tanks)
- *Basemat* (concrete)
- *UnsatZone*
- *WasteFootprint*
- *NearWell*

The transport relationships between these components are simplified in schematic diagrams, presented in Figures 4.4-50 and 4.4.-51. Although each waste tank type (Type I, II, III, IIIA, and IV) were modeled explicitly in the transport model, for simplicity, the multiple waste tank types in the HTF are identified in the schematic as Type II or non-Type II tanks (Figure 4.4-50 and 4.4-51, respectively). Type II tanks are identified separately because only Type II tanks have sand pads. Also included in the schematics are the unsaturated and saturated zone model components and the outputs used for dose calculations. Each cell in the diagrams presented in Figures 4.4-50 and 4.4-51 represent a separate domain in the HTF Tank transport sub-model. The arrows indicate the direction of transport and the type of transport, advective or diffusive. The numbered arrows indicate the points at which PORFLOW generated flow fields were used as input to calculate movement of the radionuclides from one domain to another. The thick arrows indicate HTF Tank transport sub-model output that fed the dose calculator sub-model. Specifically, radionuclide concentrations calculated in the Footprint Cell network and the *NearWell* network were output to the dose calculator sub-model (Section 4.4.4.2.3)

Figure 4.4-50: Schematic of Modeled Components for Type II Tanks

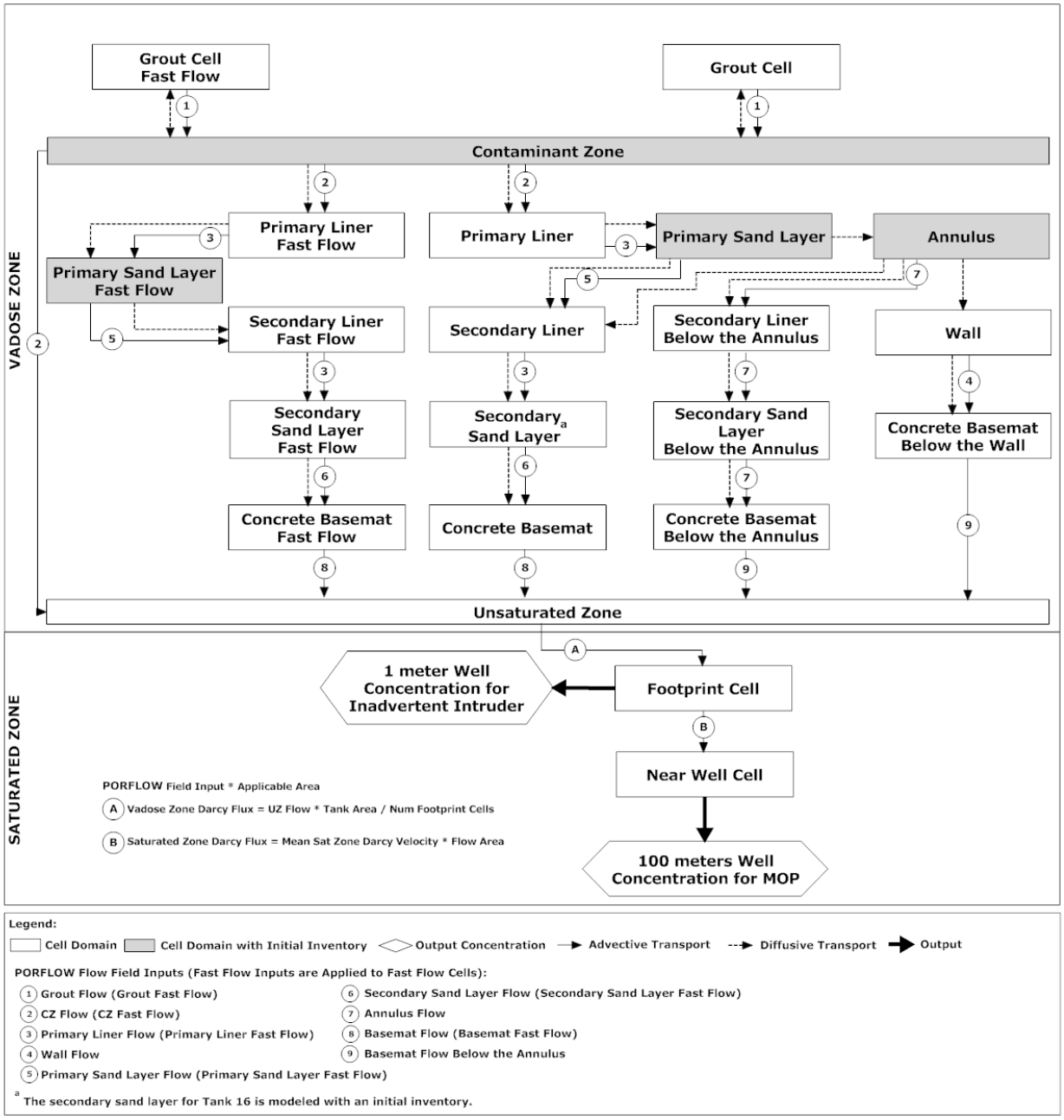

Figure 4.4-51: Schematic of Modeled Components for Non-Type II Tanks

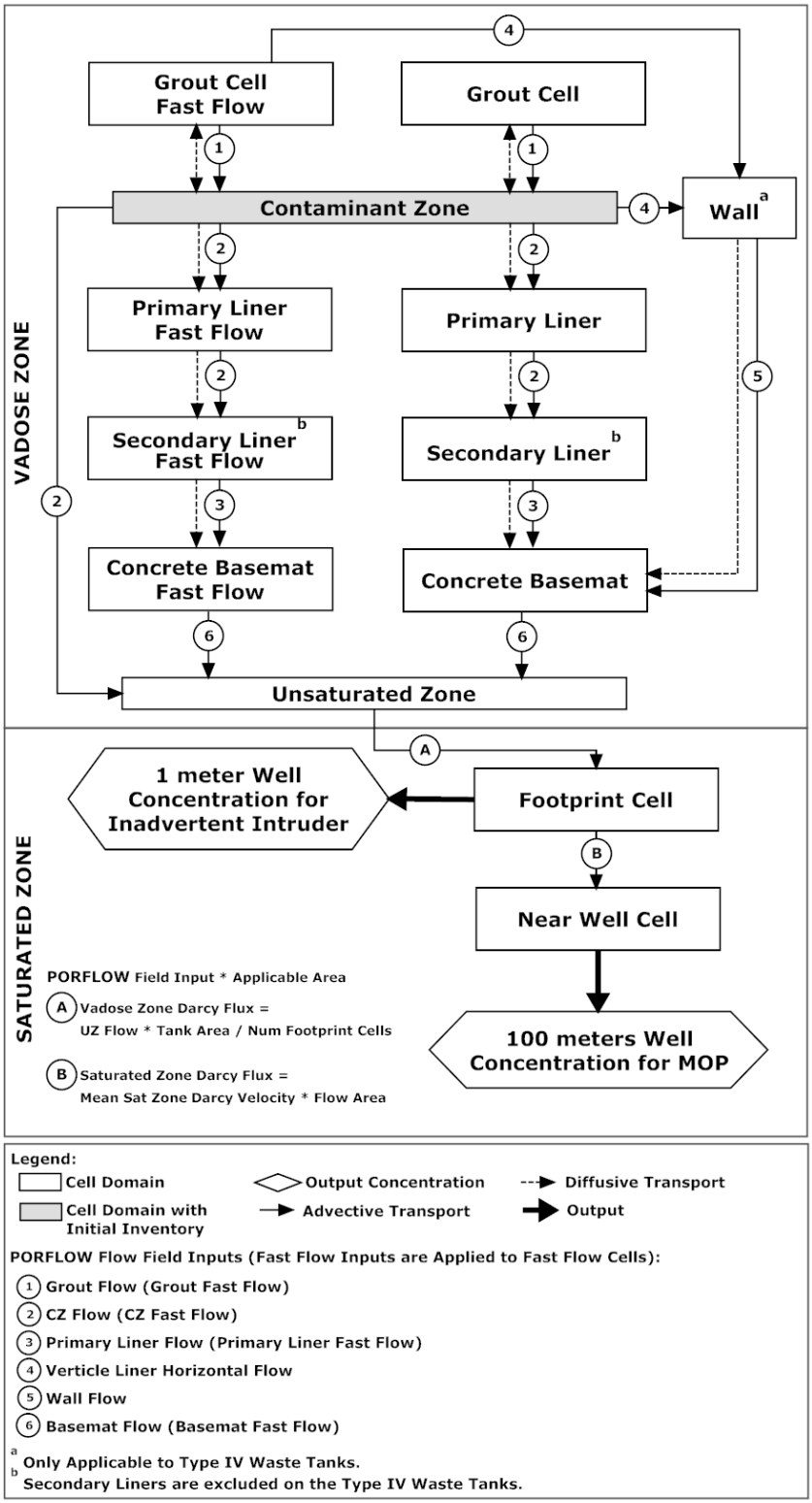

Separate cells were used to model the fast flow through the grout, liners (and for Type II tanks, the sand pads and secondary liners), and concrete basemat. These fast flow cells are represented in Figure 4.4-50 and 4.4-51 with the suffix, "fast flow". The fast flow cells are similar in construct to their nominal transport cell counterpart; however, the fast flow area is a fraction of the area of the normal transport cell (set based on the geometry of the different waste tank types). Additionally, a separate PORFLOW generated fast-flow flow field was applied to the fast flow cells. Transport through these cells was enabled during simulation of the alternative Cases B through E (see Table 4.4-1 for the Waste Tank Case Summary). The Base Case, Case A, does not allow transport through the fast flow cells. As implemented in the PORFLOW and HTF GoldSim Models, but not evident in the schematics (Figures 4.4-50 and 4.4-51), the fast flow path through the grout is located on the outer ring of the grout. However, upon entering the CZ, the fast flow moved laterally (Figures 4.4-8 through Figure 4.4-10) and then vertically downward through a fast flow path in the basemat in Cases D and E.

Grout

The grout, which fills the space overlying the CZ, was included in the model to simulate the effects of early time diffusion of radionuclides and non-radioactive species from the CZ upwards into the grout. This process can be important at early times prior to liner failure when the downward flow in the grout and CZ is very low. Diffusion of mass upwards into the grout allows for a delaying of the mass released from the grout. The grout was represented by 10 cell pathway elements connected in series. All mass that enters the grout originate in the CZ.

Also considered in the model was the influence of water leaching from the grout on the chemistry within the grout, the CZ, and the unsaturated zone. The distribution coefficients within the grout were modeled as a function of the number of pore volumes of water that passed through the grout. The relationship between the number of pore volumes flushed through the grout and the chemistry of the water passing through the grout is discussed in Section 4.2.1 and 5.6.3. Table 5.6-11 (Section 5.6.3) summarizes the number of pore water volumes (deterministic and stochastic ranges) required to flush through the grout before the chemical transition is achieved. The chemical transition times for each waste tank are provided in Tables 4.4-2 through 4.4-9 (Section 4.4.3). The timing of physical degradation of the grout and cementitious materials for each tank type is given in Table 4.2-34 (Section 4.2.2).

Cases A, B, and D having distribution coefficients in the unsaturated zone are a function of the number of pore volumes of water that have passed through the grout (see Table 4.4-1 for a summary of the different waste tank cases). Cases C and E having the reducing capacity of the full volume of grout are not considered to be available to affect the infiltrating water and therefore the distribution coefficients in the unsaturated zone are not a function of the number of pore volumes of water that have passed through the grout but through the CZ.

Waste Layer/CZ

In the HTF Tank transport sub-model (*HTFTanks_Transport_Model)*, the CZ was simulated using the source element, *WasteLayer*. The only barrier considered in the source element, the outer-barrier, failed immediately. Although the steel liner failure may not have occurred yet, the mass was released so that processes, such as upward diffusion from the CZ into the grout and minor leakage through the steel liner, could be considered. Two sources were defined in the source element, *WasteLayer*, the first source term was comprised of the radionuclide species, and the second source term was comprised of the non-radioactive species. A baseline inventory of radionuclides and non-radioactive contaminants were developed for each waste tank and component of ancillary equipment and a detailed description is presented in Sections 3.3.2 and 3.3.3. The source terms represent the median inventory multiplied by a factor that was set to one for deterministic runs and defines the influence of uncertainty for stochastic runs (See Section 5.6.3 for the inventory uncertainty distributions). The source element *WasteLayer* executes a controlled release into the associated cell *WasteCell*, which is located in the source element and represents the CZ in the engineered waste tank structure.

Liners (and where applicable Sand Pads, Lower Annulus, and Wall)

The timing of contaminant release below the waste tanks is largely a function of the effectiveness of the steel liners. The GoldSim transport model used the PORFLOW generated primary liner flow field as input. Prior to liner failure, the flow fields generated by PORFLOW indicate very little flow, in general. Type IV tanks, however, have a relatively thin primary liner (0.375 inch compared to 0.5 inch for Type I, II, and III/IIIA tanks, see Figures 4.4-1 through 4.4-5, Section 4.4.1) and no secondary liner. As a result, prior to liner failure, flow through the Type IV liner was greater relative to the other waste tank types.

In contrast, in the HTF GoldSim Model, the onset of diffusive transport through the liners for all waste tank types occurred only after liner failure. This was accomplished by setting the area of diffusion to zero prior to liner failure. Setting the diffusive area to zero is consistent with the HTF GoldSim Model, which multiplied the liner diffusion coefficient by a factor of 1.0E-6 prior to liner failure. The timing of liner failure for each waste tank type is listed in Table 5.6-10 (Section 5.6.3). The deterministic value (or baseline value) is equal to the median probability value.

Although the liners are thin, relative to the other waste tank components, and do not represent a zone with sorptive capacity, they are very important in limiting diffusive transport. For instance, in Type II tanks, the primary liner limits upward diffusion from the primary sand pad (which has an initial inventory) to the CZ. This is significant because the addition of solubility-limited radionuclides, such as Tc-99, to the CZ could result in underestimated releases of the solubility controlled species. This was avoided by explicitly modeling the diffusive term in the liners. The liner (for Type IV tanks) or liners (primary and secondary for Type I, II, III, and IIIA tanks) were each accounted for by a single cell pathway element. Additional

complexity was added in the GoldSim transport model for Type II tanks for adequate replication of the transport results from PORFLOW. For these waste tanks, a portion of the annulus and wall were also simulated.

When simulating releases from Type II tanks, sand pads were represented by two cell pathway elements, the *PrimarySandLayer* and *SecondarySandLayer* (and their fast flow counterparts). These sand pads are separated by the cell pathway *SecondaryLiner*. At the time of operational closure, the primary sand pad in the four Type II tanks (Tanks 13 through 16) are considered to have an initial inventory. In addition, the annulus in the four Type II tanks and the secondary sand pad in Tank 16 were assigned an initial inventory. For a description of the initial inventory estimates used in the HTF GoldSim Model for the Type II sand pads and annuli, refer to Section 3.4.2 (Table 3.4-1 and 3.4-2).

In addition to explicit representation of the Type II sand pads and liners, the lower portion (up to the height of the secondary liner) of the grouted annulus and the concrete wall were also modeled for this waste tank type (Figure 4.4-50). The six cells representing the lower portion of the grouted annulus were located within the *AnnulusModel* sub-container, and the six cells representing the lower portion of the wall were located within the *WallModel* sub-container. Both sub-containers were located within the *SandPads* container.

The grouted annulus and wall were important to transport because inventory within the sand pads and build up in the annulus from diffusion beginning at time zero. In addition, certain chemical species have extremely different distribution coefficients under various chemical conditions in these cementitious barriers. Radionuclides controlled by high distribution coefficients under Reducing Region II conditions in the annulus and relatively low distribution coefficients under Oxidizing Region II conditions, such as Tc-99 will rapidly move out of the annulus upon the annulus chemical transition, potentially leading to a pulse in dose. The chemical transition times in the annulus is controlled by the number of pore volumes that will have flushed through the annulus. The chemical transition times for the annulus in GoldSim were based on PORFLOW transition time inputs. Radionuclide transport in the wall was also controlled by sorption onto concrete for the different species, however, the initial chemical state of the wall material is Oxidizing Region II, and therefore had less impact on the overall transport as compared to the grouted annulus.

Basemat (Concrete)

The concrete basemat was represented by a series of five cell pathway elements. Mass entered the concrete at the *ConcretePadin* cell pathway element from the secondary liner for Type I, III, and IIIA, tanks, and from the single liner of the Type IV tanks whereas it entered the Type II tanks from the secondary sand pad. The mass moved downwards through the series of five cell pathway elements representing the basemat, exiting the basemat from *ConcretePadOut*. As with the rest of the waste tank structure mixing cells, transport through the basemat cells is a function of advection and diffusion. Note that because diffusion is simulated, the mass can also diffuse back upwards if the concentration gradient dictates. Similar to the other

cementitious barriers, radionuclide transport in the basemat concrete is controlled by sorption and is species and chemical environment dependent.

Type II tanks required additional cells to model the section of the concrete basemat below the annulus and wall. The concrete basemat below the annulus (*Basemat_np*), and concrete basemat below the wall (*Basemat_npw*) were each represented by five cell pathway elements. These containers can be found in *SandPads* container (Figure 4.4-49), under *Basemat2*. As with the nominal basemat cells that were discussed in the preceding paragraph, mass transport is a function of advection and diffusion, and is controlled via distribution coefficients under the various chemical environments. The chemical transition times were based on the PORFLOW transition times. The distribution coefficients in the basemat beneath the annulus were controlled by the general basemat transition times and the distribution coefficients beneath the wall were controlled by the wall transition times.

Unsaturated Zone

The unsaturated zone, labeled *UnsatZone* in the model, was simulated using a set of 10 cell pathway elements linked in series. Unlike the sets of cell pathway elements used to simulate the waste tank-structure components, the unsaturated zone cells were not linked in a coupled manner and the process of molecular diffusion was not considered. This change was implemented to minimize the computational effort in areas where matrix diffusion is not considered important.

For any waste tanks where the unsaturated zone does not exist, the total thickness of the unsaturated zone was set to a minimal value of 0.001 foot. This includes submerged waste tanks (in the saturated zone) and any stochastic realizations, where the sampling of saturated zone thickness updated the value of the unsaturated zone thickness to a value that is less than or equal to 0.001 foot.

Saturated Zone - Footprint

The saturated zone was simulated in the HTF transport model consisting of two segments. The first segment, *WasteFootprint*, was a series of cells representing the saturated zone beneath the footprint of the waste tank structure. The second segment, *NearWell*, was a series of cells representing the saturated zone beyond the footprint of the waste tank structure.

The footprint cells represented the saturated zone found beneath the waste tank footprint. A set of 10 cell pathway elements connected in series approximated this zone (Figure 4.4-52). One-tenth of the mass released by the unsaturated zone cell was assigned to each of the footprint cells. The footprint cells were linked together in a series (Figure 4.4-52) and a single volumetric flux rate defined the outflow from one cell to the next. Note that because the volumetric water flux from the unsaturated zone cell to each footprint cell was not explicitly added to the outflow term for each footprint cell, GoldSim indicated that there is a flow imbalance for these cells. This approximation assumes that the flow from the unsaturated zone was implicit to the volumetric flow rate approximation used for the footprint cell outflows.

Figure 4.4-52: GoldSim Cell Pathway Elements Used to Simulate the Saturated Zone beneath Waste Tank Footprint

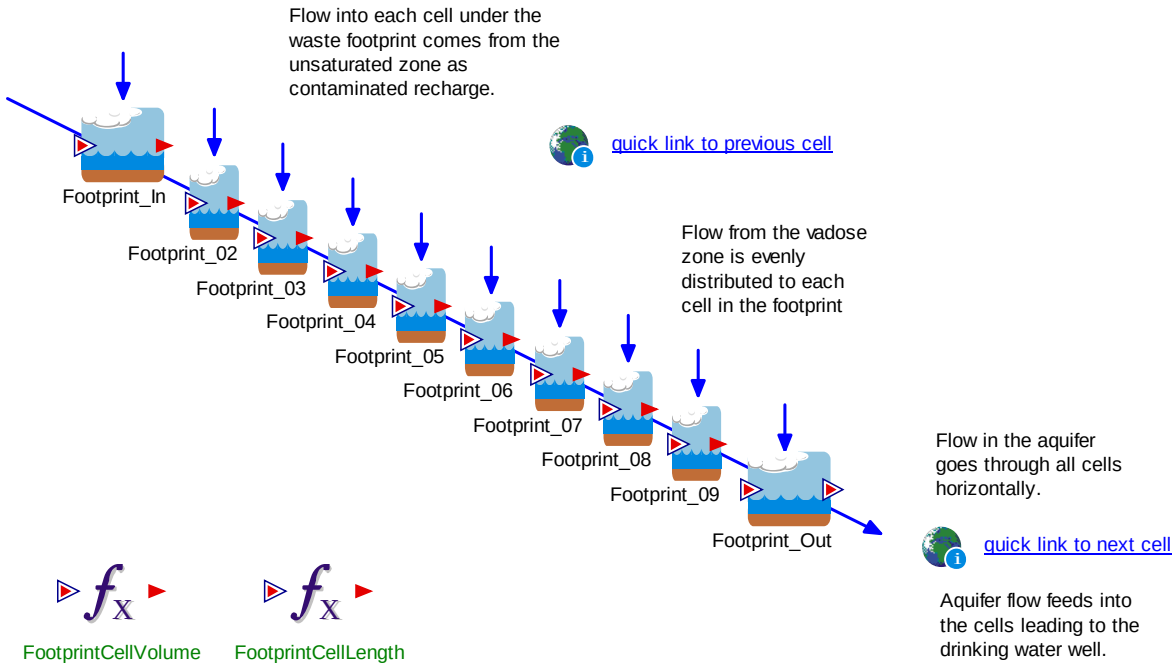

Saturated Zone -Near Well

The mass released from the cell pathway element *Footprint_Out* was applied to the cell pathway element *NearWell_In*. *NearWell_In* was the first (and most up gradient) well in a set of up to 50 wells linked together in series (Figure 4.4-53). The cells depicted in Figure 4.4-53 are just 10 of the cells that this section of the saturated zone was comprised. An additional 40 cells were in the container *NearWell*.

Figure 4.4-53: GoldSim Cell Pathway Elements Used to Simulate the Saturated Zone Found Outside Waste Tank Footprint

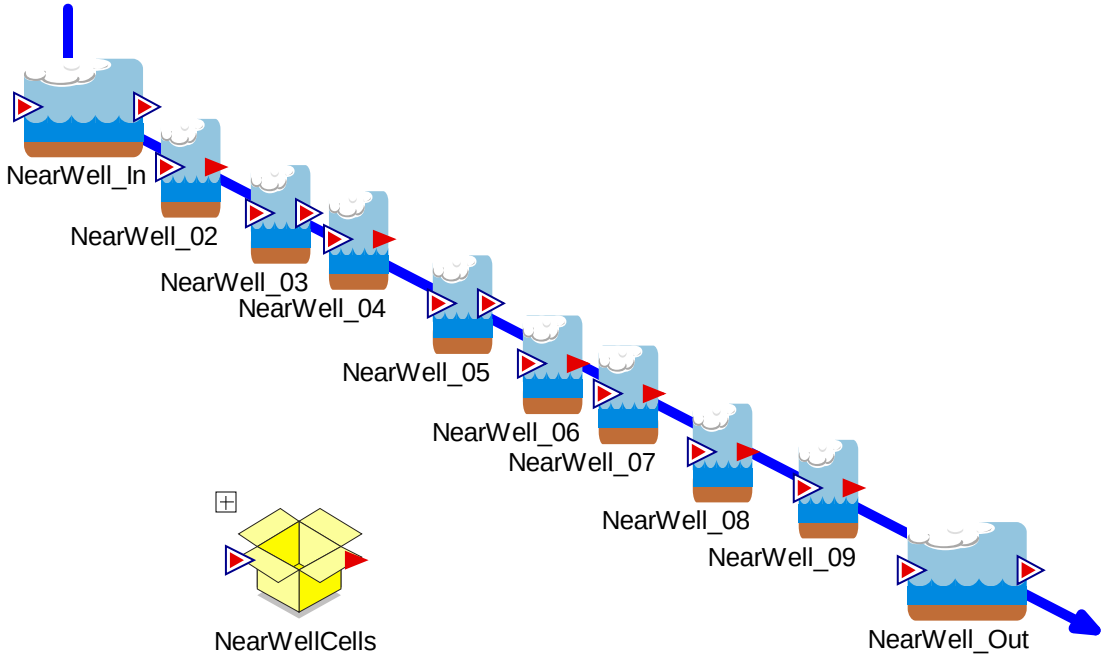

These cells were arranged in four sets of 10 cells, each set found in one of four containers found in *NearWell*. The actual number of wells used to represent the saturated zone outside the waste tank footprint was dependent on the user's choice of longitudinal dispersivity or local Peclet number (see Section 3.4 of SRR-CWDA-2010-00093).

Ancillary Equipment Transport

In contrast to the HTF Tank transport sub-model, which discretely modeled the grout, liners, sand pads, and concrete basemat components of the containment structure, the HTF Ancillary Equipment transport sub-model applied PORFLOW input flow fields through a waste layer and sets the ancillary equipment to fail at 510 years. Evidence discussed in Section 4.4.2.6 indicates this is a conservative (and simplifying) assumption.

Figure 4.4-54 displays the components of the HTF Ancillary Equipment transport sub-model. The unsaturated zone beneath the ancillary equipment is the same as that below the waste tanks. The saturated zone is also implemented in the same manner as the HTF Tank transport sub-model, and is comprised of the *WasteFootprint* and *NearWell* networks (e.g. Figure 4.4-52 and 4.4-53). Radionuclide concentrations calculated in the *NearWell* network are also output to the dose calculator sub-model (Section 4.4.4.2.3).

Figure 4.4-54: Contents of the Container *HTFAncillary_Equipment_Model*

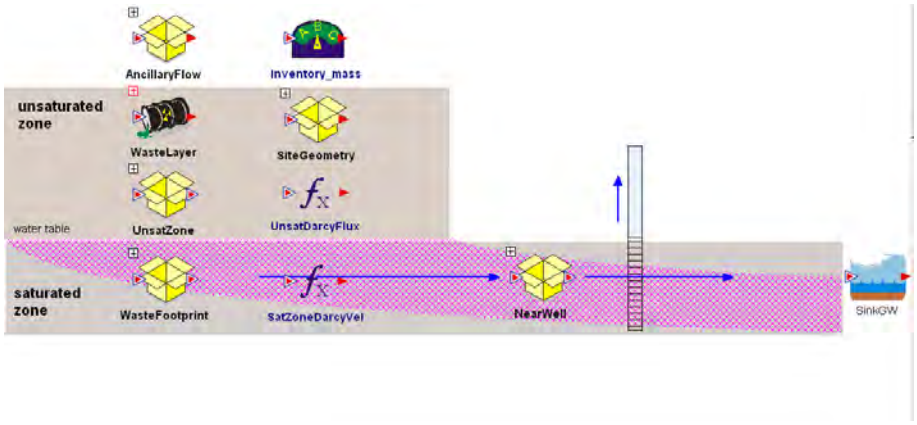

4.4.4.2.3 GoldSim Dose Calculator Sub-Model

Because of residual waste in HTF, contaminants may be released to the environment and in turn provide a dose to a potential receptor. Section 4.2.3 identifies the different exposure pathways that contaminants may travel to reach each receptor and Sections 4.6 and 4.7 provide the parameters used to estimate the dose to the receptors. The dose calculator sub-model calculates the dose to each of these receptors via the identified biotic pathways. Table 4.4-11 links the different biotic pathways contributing to the dose to each receptor with the contaminant source. The dose calculator applies an effective dose factor for a given biotic pathway to the identified contaminant concentration in order to calculate the dose to the receptor. The equations defining the dose to each receptor, which is equal to the product of the effective dose factor and the appropriate water or soil contaminant concentration, are detailed in Section 5.4 or Section 6.2 and 6.3 for the intruder. The dose calculator was used to calculate dose for all modeling cases.

Table 4.4-11: Summary of Biotic Pathways by Receptor

Receptor	Path	Biotic Pathway	Contaminant Concentration Source
MOP - Well	Ingestion	Drinking Water	100m water well
		Eating Chicken	100m water well
		Eating Chicken	Fodder (calculated from 100m water well)
		Eating Egg	100m water well
		Eating Egg	Fodder (calculated from 100m water well)
		Eating Beef	100m water well
		Eating Beef	Fodder (calculated from 100m water well)
		Drinking Milk	100m water well
		Drinking Milk	Fodder (calculated from 100m water well)
		Eating Vegetables	Leaf (calculated from 100m water well)
		Eating Vegetables	Root (calculated from 100m water well)
		Eating Fish	Stream (Seepline)
		Eating Soil	Irrigated Soil (calculated from 100m water well)
	Exposure	Irrigated Soil	Irrigated Soil (calculated from 100m water well)
		Swimming	Stream (Seepline)
		Boating	Stream (Seepline)
	Inhalation	Irrigation Water	100m water well
		Showering	100m water well
		Dust	Irrigated Soil (calculated from Seepline)
		Swimming	Stream (Seepline)
MOP - Stream	Ingestion	Drinking Water	100m water well
		Eating Chicken	100m water well
		Eating Chicken	Fodder (calculated from Seepline)
		Eating Egg	100m water well
		Eating Egg	Fodder (calculated from Seepline)
		Eating Beef	100m water well
		Eating Beef	Fodder (calculated from Seepline)
		Drinking Milk	100m water well
		Drinking Milk	Fodder (calculated from Seepline)
		Eating Vegetables	Leaf (calculated from Seepline)
		Eating Vegetables	Root (calculated from Seepline)
		Eating Fish	Stream (Seepline)
		Eating Soil	Irrigated Soil (calculated from Seepline)
	Exposure	Irrigated Soil	Irrigated Soil (calculated from Seepline)
		Swimming	Stream (Seepline)
		Boating	Stream (Seepline)
	Inhalation	Irrigated Soil	Stream (Seepline)
		Showering	Stream (Seepline)
		Dust	Irrigated Soil (calculated from stream)
		Swimming	Stream (Seepline)

Table 4.4-11: Summary of Biotic Pathways by Receptor (Continued)

Receptor	Path	Biotic Pathway	Contaminant Concentration Source
Acute - Intruder	Ingestion	Drill Cuttings	Drill Cuttings (calculated from transfer line source)*
	Exposure	Drill Cuttings	Drill Cuttings (calculated from transfer line source)*
	Inhalation	Drill Cuttings	Drill Cuttings (calculated from transfer line source)*
Chronic - Intruder	Ingestion	Drinking Water	1m water well
		Eating Chicken	1m water well
		Eating Chicken	Fodder (calculated from 1m water well)
		Eating Egg	1m water well
		Eating Egg	Fodder (calculated from 1m water well)
		Eating Beef	1m water well
		Eating Beef	Fodder (calculated from 1m water well)
		Drinking Milk	1m water well
		Drinking Milk	Fodder (calculated from 1m water well)
		Eating Vegetables	Leaf (calculated from 1m water well)
		Eating Vegetables	Root (calculated from 1m water well)
		Eating Vegetables	Root (calculated from Drill Cuttings spread around a garden)*
		Eating Fish	Stream (Seepline)
		Eating Soil	Irrigated Soil (calculated from 1m water well)
		Eating Soil	Drill Cuttings spread around garden*
	Exposure	Irrigated Soil	Irrigated Soil (calculated from 1m water well)
		Soil	Drill Cuttings spread around garden*
		Swimming	Stream (Seepline)
		Boating	Stream (Seepline)
	Inhalation	Irrigated Soil	1m water well
		Showering	1m water well
		Dust	Irrigated Soil (calculated from 1m water well)
		Dust	Drill Cuttings spread around garden*
		Swimming	Stream (Seepline)

* Indicates unique contaminant concentration source-specific to the intruder receptor.

Dose Calculator Organization

The HTF dose calculator sub-model contains the calculations used to estimate receptor doses to the MOP or to the inadvertent intruder, at points of compliance based on 1) the results from the transport abstraction sub-model, 2) output from the HTF PORFLOW transport model, or 3) estimated soil concentrations. The dose calculations were abstracted from conceptualizations of the possible exposure pathways identified in Table 4.4-11.

The container, *HTF_DoseCalculations*, which is found at the upper level of the model, distinguishes the dose-specific calculations from the HTF transport calculations. Brief descriptions of the different components within the dose calculator model are provided below.

The *Parameters* sub-container houses all of the inputs, deterministic and stochastic, used to calculate the effective dose factors for the pathways identified in Table 4.4-11. Within the *Parameters* sub-container are containers organized by the various biotic pathways (e.g., Beef, Milk, Water, Egg, etc.) identified in Table 4.4-11. The sub-container name reflects the inputs used in the biotic pathway. These biotic pathway sub-containers are displayed in Figure 4.4-55. The values used as inputs to the deterministic model are presented in Section 4.6 and Section 5.6.3 for stochastic parameters. Additional documentation regarding HTF GoldSim Model inputs is located in Section 6.0 of SRR-CWDA-2010-00093.

Figure 4.4-55: Contents of the Sub-Container *Parameters*

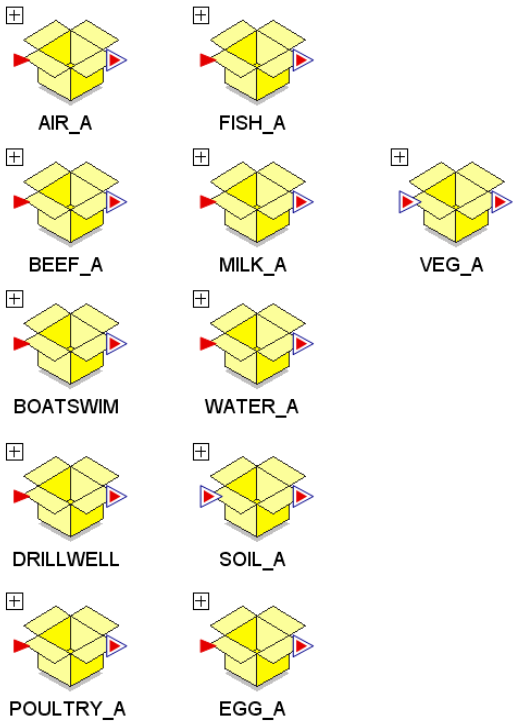

ExposureMediaConc contains the outputs of the GoldSim HTF transport calculations used by the GoldSim dose calculator. The outputs include aqueous radionuclide concentrations in the 100-meter well water. The concentrations are tracked by sector location, well location, and by contributing waste tank.

The sub-containers *GoldSimModel* and *PorflowModel* differentiate between dose calculations based on GoldSim transport model output and dose calculations based on the HTF PORFLOW output. Within these containers are the effective dose factor calculations organized by receptor, including the MOP dose from well pathways, MOP dose from stream pathways, and intruder pathways. For a more detailed description of the contents of these two sub-containers, see Section 5.1.1 and 5.1.2 of SRR-CWDA-2010-00093.

The Intruder Source Model, which calculates the contaminated soil concentrations used in the acute and chronic intruder dose calculations, is captured in, *Intruder_Drilling_Source*.

In both the acute and chronic intruder scenarios, the conceptual model assumes a transfer line is penetrated during the installation of a drinking water well. The contamination inside the transfer line is mixed with the volume of the drill cuttings and brought to the surface. The acute intruder receives a dose resulting from exposure to these drill cuttings. The chronic intruder is assumed to receive a dose resulting from spending time in a garden that has been contaminated with the drill cuttings mixed with a known volume of garden soil. The *Intruder_Drilling_Source* container provides the two separate contaminant soil concentration calculations.

By default, the intruder dose calculator is set to use the inventory associated with a 3-inch diameter transfer line. SRR-CWDA-2010-00023 provides documentation of the method used to estimate the 3-inch diameter transfer line inventory, which is an input to the dose calculator (see data element, *TransLineInventory_3in*). Additionally, the data elements, *TransLineInventory_4in*, *Tank13Inventory_Intr*, and *Tank24Inventory_Intr* contain the estimated inventory for a 4-inch transfer line, Tank 13, and Tank 24. Documentation of these estimated inventories are also provided in SRR-CWDA-2010-00023. The selector switch, *IntruderInventorySwitch*, is by default set to use the 3-inch diameter transfer line inventory, but by changing the switch to 2, 3, or 4, the user can simulate the intruder drilling into a 4-inch transfer line, Tank 13, or Tank 24, respectively. These alternative intruder scenarios were simulated and the results discussed in Section 6.5.

Because the acute intruder calculations are solely a function of contaminated soil concentrations not calculated in PORFLOW, these calculations are kept separate from the PORFLOW and the GoldSim calculations. They are contained in *AcuteIntruderCalcs*. The chronic and acute intruder exposure scenarios and the equations defining the dose to these receptors are described in detail in Sections 6.2 and 6.3.

Dose results are shown in container *DoseResults* and are organized by transport model (PORFLOW or GoldSim) and by receptor.

The GoldSim transport model dose results were calculated for benchmarking purposes and for UA/SA. The benchmarking process is discussed in Section 5.6.2, while the stochastic model is discussed in Section 5.6.3 and used for UA/SA presented in Sections 5.6.4 and 5.6.5. The dose results computed based on the PORFLOW generated concentrations were used for performance compliance and are presented in Section 5.5.

GoldSim Calculated Sources by Receptor

MOP Dose from Well Pathways - The MOP is assumed to have access to groundwater via a drinking water well located approximately 100 meters from the HTF boundary. In order to estimate the location that could result in the highest dose, a line of hypothetical wells were placed at the intersection of the 100-meter boundary and the PORFLOW generated stream traces (Figure 4.4-56). The projected dose estimate incurred by the MOP was calculated using groundwater from each well. (Note: HTF GoldSim Model concentrations were evaluated at these same hypothetical 100-meter well locations.)

Figure 4.4-56: HTF Waste Tank Sources with Hypothetical 100m Well Location

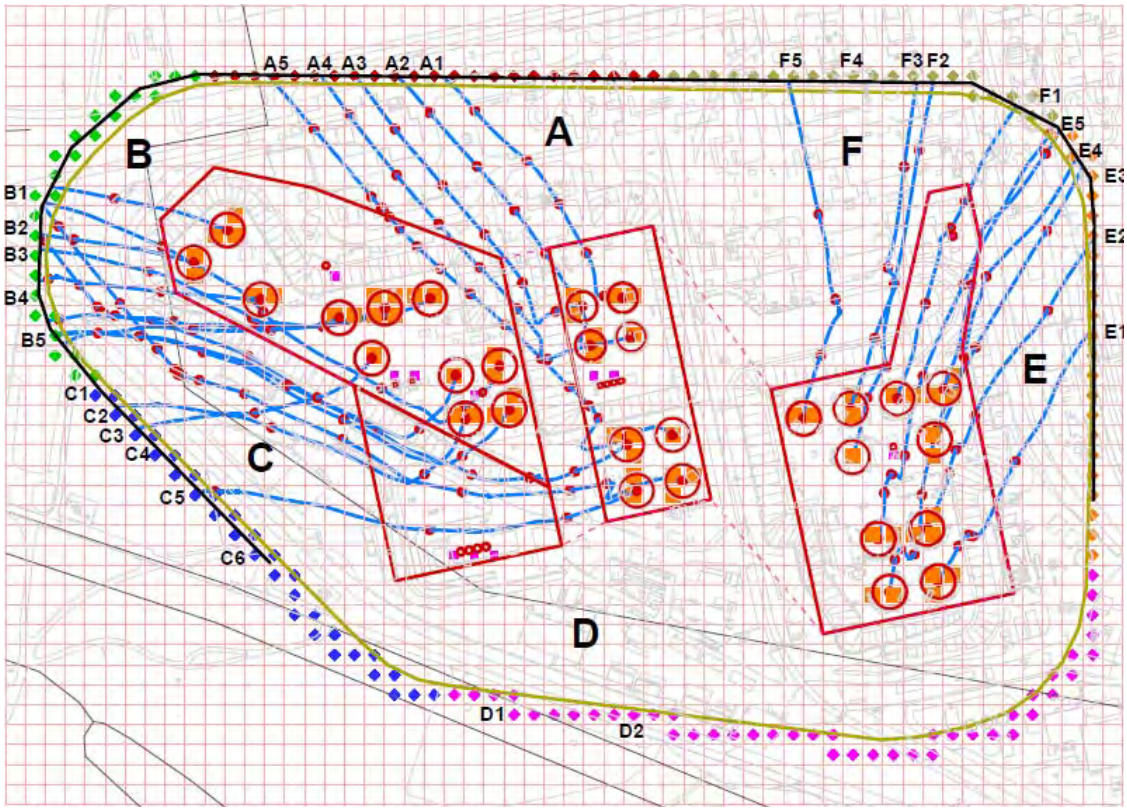

Light blue lines = PORFLOW generated stream traces from waste tank sources (circles)
Colored stipple = 100-meter boundary, colored by Sector A through E
A1 through A5, etc = hypothetical 100-meter well location

Figure 4.4-56 illustrates the hypothetical 100-meter well locations. A centerline distance and an offset distance along the PORFLOW stream trace was measured from each of the waste tanks to each of the hypothetical wells, and these lengths were input into the GoldSim transport model (see Section 4.4 of SRR-CWDA-2010-00093). Each well receives contaminant contributions from each waste tank (and ancillary equipment), depending on its proximity to the plume emanating from each contaminant source. For a discussion of the plume function, which is used in the calculation of the concentration at each well, see Section 4.4.4.2.1. The GoldSim calculated well concentrations were taken from the container, *ExposureMediaConc*.

MOP Dose from Stream Pathways - Transport assumptions for mobile contaminants are from the HTF area by groundwater through the aquifers underlying the HTF to the outcrops at Fourmile Branch and UTR. Upon reaching the surface water, the contaminants could be present at the seepline, in sediments at the bottom of streams, and at the shoreline. Human receptors could be exposed to contaminants through various pathways associated with the aquifers.

The transport sub-model estimates the concentration of contaminants at the seepline by applying a species dependent ratio ranging from 1% and 10% to the GoldSim calculated concentration at the 100-meter well. The data element, *SeeptoWellRatio_vec* contains the individual ratios applied to the 100-meter concentration in order to estimate the seepline concentration for each radionuclide. Although the ratios could have been assigned by element, it was more conservative to evaluate the ratio for the individual radionuclide. Table 4.4-12 displays the ratios used as input to the HTF GoldSim Model. The ratios were based on an analysis documented in Appendix F.

Table 4.4-12: Rad-Specific 100m Concentration to Seepline Concentration Ratio

Radionuclide	Ratio	Radionuclide	Ratio
Ac-227	0.1	Nb-93m	0.1
Ag	0.1	Nb-94	0.1
Ag-108m	0.1	Ni	0.1
Al-26	0.1	Ni-59	0.02
Am-241	0.01	Ni-63	0.1
Am-242m	0.1	NO2	0.1
Am-243	0.01	NO3	0.1
As	0.1	Np-237	0.1
Ba	0.1	Pa-231	0.1
Bi-210m	0.1	Pb	0.1
C-14	0.1	Pb-210	0.1
Ca-41	0.1	Pd-107	0.1
Cd	0.1	Pt-193	0.1
Cf-249	0.1	Pu-238	0.01
Cf-251	0.1	Pu-239	0.01
Cl-36	0.1	Pu-240	0.1
Cm-243	0.1	Pu-241	0.1
Cm-244	0.1	Pu-242	0.1
Cm-245	0.1	Pu-244	0.1
Cm-246	0.1	Ra-226	0.05
Cm-247	0.1	Ra-228	0.1
Cm-248	0.1	Sb	0.1
Co-60	0.1	Se	0.1
Cr	0.1	Se-79	0.1
Cs-135	0.02	Sm-147	0.1
Cs-137	0.1	Sm-151	0.1
Cu	0.1	Sn-126	0.1
Eu-152	0.1	Sr-90	0.1
Eu-154	0.1	Tc-99	0.06
Eu-155	0.1	Th-229	0.1
F	0.1	Th-230	0.02
Fe	0.1	Th-232	0.1
Gd-152	0.1	U-232	0.1
H-3	0.1	U-233	0.1
Hg	0.1	U-234	0.03
I-129	0.02	U-234	0.1
K-40	0.1	U-236	0.1
Lu-174	0.1	U-238	0.1
Mn	0.1	Zn	0.1
Mo-93	0.1	Zr-93	0.1

The individual radionuclide ratio (Table 4.4-12) was estimated using PORFLOW Case A (Base Case) simulated concentrations and was assumed to be the same for the alternative Cases B through E. Because the alternative cases only change the time of the waste release from the engineered barrier, it was assumed the physical processes within the vadose and saturated zones remain unchanged; therefore using the same ratio for the alternative cases is justified.

Chronic Intruder - The chronic intruder is exposed to contaminants in a drinking water well located 1 meter from a waste tank and from contaminated soil in a garden. For the GoldSim chronic intruder dose calculations, the concentration released below the footprint of Tank 11 was used for the 1-meter well concentration because this is the waste tank with the highest calculated concentration of Ra-226, the main dose driver over the performance period. Taking the concentration from the footprint cell of Tank 11 (*Footprint_Out*) is a conservative assumption and expected to provide a maximum dose for the chronic intruder. This concentration is passed to the element contained in, *GoldSimInput1mWell*.

For certain pathways, the chronic intruder obtains the additional dose from exposure to contaminated soil (See Table 4.4-11) calculated in the *Intruder_Drilling_Source* container.

Acute Intruder - The acute intruder is exposed to contaminated drill cuttings brought to the surface at the time of drilling. *DrillCuttings_Conc*, also located within *Intruder_Drilling_Source* container, calculates the concentration in the discrete amount of soil brought up during drilling. This concentration was applied to the effective dose factors to calculate the dose to the acute intruder only, while the *CuriesinGarden* represents the drill cuttings spread across a garden of a known volume, and was only applied to the dose of the chronic intruder.

PORFLOW Input Concentrations

The dose calculator sub-model has the functionality of either calculating dose based on concentrations calculated in the GoldSim transport model or from concentrations calculated in the PORFLOW transport model. The concentrations used for PORFLOW dose calculations are housed in container *PORFLOWFeedstoDoseCalculations*. These concentrations are case dependent, and were replaced when calculating PORFLOW dose for the alternative cases, Cases B through E.

Similar to the GoldSim concentrations, the PORFLOW concentrations are evaluated for each sector at the 100-meter water well (Figure 4.4-56) and at the 1-meter water well. A single seepline concentration is used, as opposed to individual sector concentrations. The seepline concentration used here is the maximum radionuclide concentration of the Fourmile Branch or the UTR Aquifer at each time step.

4.5 Airborne and Radon Analyses

The air and radon pathway analysis was conducted for the 10,000-year post-closure compliance period. The analytical method chosen was an approach where most parameters were set to their

best estimate values (i.e., based on available site-specific measurements or engineering judgment), while other parameters were set to conservative/bounding values. The conceptual PORFLOW transport model used for the air and radon pathway analysis had imbedded biases that where possible were conservative in intent. The same conceptual model was used for the air and radon pathways analyses and the PORFLOW transport model utilized the same input files for both pathways.

Of the available four waste tank types, the Type I and Type II tanks were chosen for this analysis. This analysis did not consider any associated piping or ancillary equipment. The two waste tank types (out of the four types) chosen were selected because they will have the least grout and concrete thickness above the stabilized CZ (which is located at the bottom of the waste tank). Additionally, for conservatism the minimum closure cap thickness over the waste tanks was assumed. These assumptions were anticipated to produce the maximum flux of gaseous radionuclides at the ground surface.

4.5.1 Air and Radon Pathway Conceptual Model

The approach taken focused primarily on a Base Case where nominal settings for many of the input parameters were conservatively chosen. The main analysis tool employed was the PORFLOW code that simulates the transport of radionuclide chains (i.e., parents and daughters) in porous media. The flux of radioactive gasses at the land surface above the HTF was evaluated for the assumed closure scenarios. [SRNL-ESB-2008-00023] Gaseous radionuclides within the CZ diffuse outward into the air-filled pore space of the overlying materials. Ultimately, some of the radionuclides emanate at the land surface. As such, air is the medium through which they diffuse. It was assumed that fluctuations in atmospheric pressure at the land surface that are capable of inducing small pulses of air movement into and out of the shallow soil profile over relatively short periods would have a net zero effect when averaged over longer periods. Thus, advective transport of radionuclides in air-filled soil pores was not considered a significant process when compared to the rate of air diffusion.

The closure cap, as described in SRNL-ESB-2008-00023, consists of a top soil layer, an upper backfill layer, an erosion barrier layer, middle backfill layer, lateral drainage layer, a HDPE geomembrane, a GCL, an upper foundation layer, and a lower foundation layer. The HDPE geomembrane and the GCL are excluded from these analyses. By excluding these materials, the baseline air analysis was more conservative as these materials have the expectation of significantly reducing the gaseous flux at the land surface. The HDPE geomembrane would have very low water vapor transmission; the GCL would have high porosity, low hydraulic conductivity, and swell when wet hydraulically plugging any holes that may develop in the HDPE membrane. [WSRC-STI-2007-00184] The top soil layer and the upper backfill layer were also excluded from the baseline analysis, since they are located above the erosion barrier and are therefore subject to erosion. The assumption for this analysis was that the components situated below the top of the erosion barrier (soil layers) remain intact for the duration of the simulation (10,000 years).

The Type I and Type II tanks include primary and secondary steel liners situated above a layer of basemat concrete. The top of the waste tank is covered with a concrete roof. For the baseline analysis, the model domain begins at the top surface of the lower primary liner and

extends through the stabilized contaminants to the top of the erosion barrier. The baseline model excluded the upper primary steel liner. As with the exclusion of the geomembrane and GCL, excluding the steel liner would make the model more conservative because if included, the expectation is the steel liner would significantly reduce the gaseous flux at the land surface.

The total thickness for a Type I tank waste tank and cover materials (excluding the top soil, upper backfill, geomembrane, GCL, and steel liner), including a 1.0-foot (0.3 meter) modeled, stabilized contaminant layer thickness, is 36.33 feet (11.07 meters). Total thickness for the Type II tank waste tank and cover materials (excluding the top soil, upper backfill, geomembrane, GCL, and steel liner), including a 1.0-foot (0.3 meter) thick modeled, stabilized contaminant layer is 41.75 feet (12.73 meters).

The stabilized contaminant layer thickness in this model differs from the groundwater model to provide additional conservatism providing a shorter pathway to the surface. Table 4.5-1 lists the analysis individual components for the Type I and Type II tanks (closure cap included). Materials are indicated with the associated thickness in inches, feet, and meters.

Table 4.5-1: Layers and Thicknesses for Type I and II Tanks and Cover Material

Layer	Thickness (in)	Thickness (ft)	Thickness (m)
Erosion Barrier	12	1.00	0.30
Middle Backfill	12	1.00	0.30
Lateral Drainage	12	1.00	0.30
Upper Foundation	12	1.00	0.30
Lower Foundation	72 (min)	6.00	1.83
Type I Concrete Roof	22	1.83	0.56
Type I Grout	282	23.5	7.16
Type II Concrete Roof	45	3.75	1.14
Type II Grout	324	27.00	8.23
Modeled Stabilized Contaminants Layer	12	1.00	0.30

[SRNL-STI-2010-00135]

4.5.2 Air and Radon Pathway Diffusive Transport Model

A 1-D PORFLOW based diffusive transport model Base Case was created for the HTF Type I and Type II tanks.

The governing equation for mass transport of species *k* in the fluid phase is given by:

$$\frac{\partial C_k}{\partial t} + \frac{\partial}{\partial x_i}\left(\frac{V_i}{R_f} C_k\right) = \frac{\partial}{\partial x_i}\left(\frac{D_{ij}}{R_f}\frac{\partial C_k}{\partial x_j}\right) + \gamma_k$$

Where:

C_k = concentration of species *k*, Ci/m^3

V_i = fluid velocity in the i^{th} direction, m/yr

D_{ij} = effective diffusion coefficient for the species, m^2/yr

R_f = retardation factor

γ_k = net decay of species *k*, Ci/m^3 yr

i, j = direction index

t = time, yr

x = distance coordinate, m

This equation is solved within PORFLOW to evaluate transient radionuclide transport above the waste tank and to determine gaseous radionuclide flux at the land surface over time. For this analysis, the advection term was disabled within PORFLOW and only the diffusive and net decay terms were evaluated.

The boundary conditions imposed on the entire model domain included:

- No-flux specified for all radionuclides along sides and bottom
  ($\partial C/\partial X = 0$ at $x = 0$, $x = 1$ and $\partial C/\partial Y = 0$ at $y = 0$)
- Species concentration set to zero at land surface (top of erosion barrier)
  ($C = 0$ at $y = y_{max}$)

These boundary conditions force all of the gaseous radionuclides to move upward from the stabilized CZ to the land surface. In reality, some lateral and downward diffusion occurs in the air-filled pores surrounding the stabilized CZ; hence ignoring this lateral and downward movement has the effect of increasing the flux at the land surface. This introduced some conservatism in the calculated results. Simulations were conducted in transient mode for diffusive transport in air, with results being obtained over 10,000 years.

The initial condition imposed on the domain, except for the stabilized CZ, included:

- Species concentration set to zero at time = 0

  ($C = 0$ for $0 \le x \le 1$ at $t = 0$ and $C = 0$ for $0 \le y \le y_{max}$ at $t = 0$)

For the air pathway analysis, the initial conditions for the model assumed a 1-curie inventory uniformly spread over the stabilized CZ for each radionuclide. The radon pathway analysis had an emanation factor of 0.25 applied resulting in an initial inventory of 0.25 curie uniformly spread over the stabilized CZ for each parent radionuclide. The emanation factor for the radon pathway analysis is explained more detail in Section 4.5.6.

4.5.2.1 Grid Construction

The model grid for the waste tank and overlying cover materials was constructed as a node mesh. This mesh creates a vertical stack of 78 model elements. Figure 4.5-1 shows a schematic of the PORFLOW Type I tank model grid. Figure 4.5-2 shows a schematic of the PORFLOW Type II tank model grid. The minimum possible cover thickness that could exist during the simulation period, the grid extends upward to the top of the erosion barrier. A set of consistent units was employed in the simulations for length, mass, and time, these being meters, grams and years, respectively.

Figure 4.5-1: Schematic of HTF GoldSim Model Grid for Air and Radon Pathway Analyses for Type I Tank

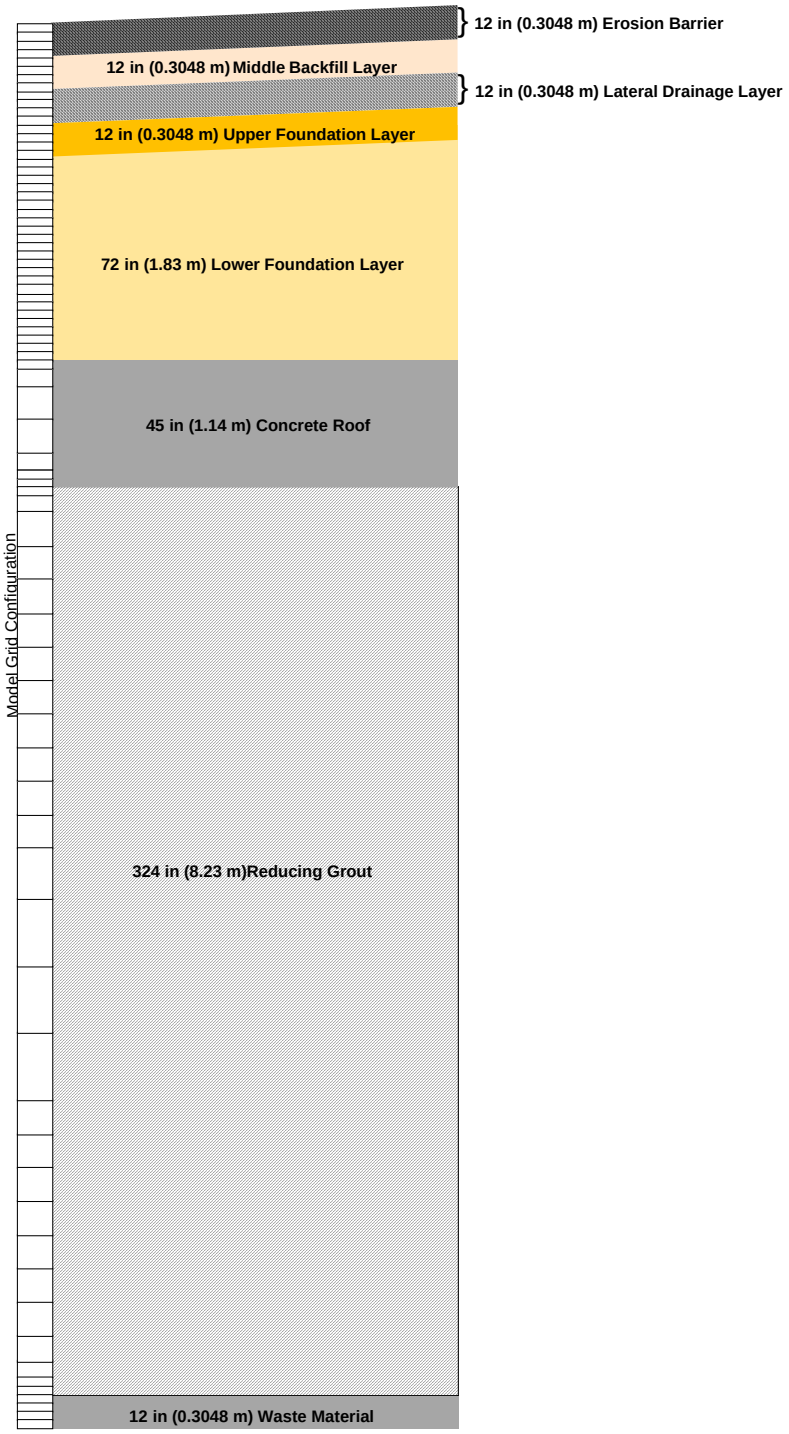

Note For conservatism, the model grid does not include the following layers: topsoil, upper backfill, HPDE geomembrane, and GCL.

Figure 4.5-2: Schematic of HTF GoldSim Model Grid for the Air and Radon Pathway Analyses for Type II Tank

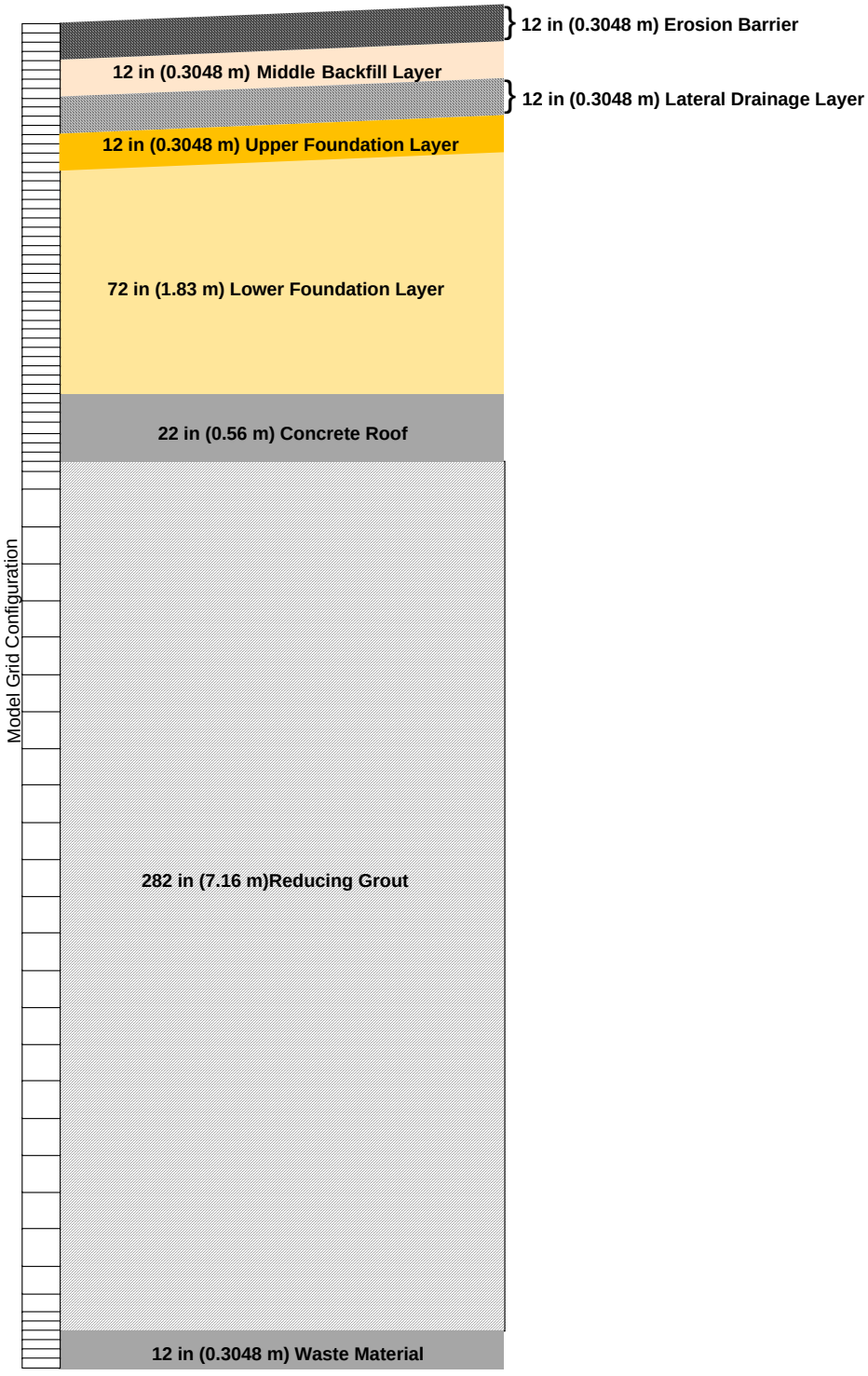

Note For conservatism, the model grid does not include the following layers: topsoil, upper backfill, HPDE geomembrane, and GCL.

4.5.2.2 Material Zone Properties and Other Input Parameters

Material properties utilized within the 1-D numerical model were specified for eight material zones defined within the model domain. Each material zone was assigned values of particle density, total porosity, average saturation, air-filled porosity, air density, and an effective air diffusion coefficient for each source element or compound. An effective air diffusion coefficient was used for each radionuclide and material layer, therefore tortuosity was assigned a unit value in each material zone. An air fluid density of 1.24E+3.0 g/m^3 at standard atmospheric conditions was used in the transport simulations. [SRNL-STI-2010-00135]

The stabilized contaminant layer was assumed 1 foot thick and confined to the bottom of the waste tank. The waste tank is to be filled with a grout from the existing specification, and it was assumed that the stabilized contaminant layer would have similar properties as the grout. The hydraulic and physical properties of this mix are reported in WSRC-STI-2007-00369. Based on the results of this testing, the stabilized contaminant layer and the grout layer were assigned a particle density of 2.51 g/cm^3 and a total and air-filled porosity of 0.266. The concrete roof layer was assumed similar to the basemat surrogate tested and reported in WSRC-STI-2007-00369. This layer was assigned a particle density of 2.51 g/cm^3 and a total air-filled porosity of 0.168. The stabilized contaminant layer and grout were expected to be at or near saturation due to short curing time and material water retention properties. [WSRC-STI-2007-00369] The concrete roof layer is likely to be at or near saturation due to infiltration through the closure cap materials over time as the closure cap degrades. [WSRC-STI-2007-00184] For this analysis, a saturation of 50% was conservatively assumed. Therefore, the air-filled porosity was set equal to 50% for the total porosity for the waste layer, grout, and concrete roof.

The foundation layer was divided into the upper and lower foundation layers. [WSRC-STI-2007-00184] It is anticipated that the lower foundation layer will need to promote drainage of infiltrating water away from and around the waste tanks, requiring a relatively high-saturated conductivity such as 1.0E-03 cm/sec. It is anticipated that the upper foundation layer will consist of soil with a moderately low permeability (i.e., $\leq$ 1.0E-06 cm/sec) produced by blending typical SRS backfill with a small weight percent bentonite. The particle density of the lower and upper foundation layers was assigned as 2.63 g/cm^3 that of control compacted backfill from WSRC-STI-2006-00198.

The particle density of the middle backfill layer was also assigned that of control compacted backfill from WSRC-STI-2006-00198 (i.e., 2.63 g/cm^3). The lateral drainage and erosion barrier layers were assigned a particle density typical of quartz (i.e., 2.65 g/cm^3).

Infiltration through the closure cap materials over time, as the closure cap degraded was evaluated using the HELP model. [WSRC-STI-2007-00184] Values for total porosity and volumetric moisture content for the closure cap materials and foundation layers were taken from this analysis. These values were used to calculate the average saturation and the air-filled porosity for the closure cap materials. The maximum air-filled porosity for each material layer over the 10,000-year simulation was utilized, since this represented the greatest air-filled porosity in which a gas could diffuse.

Table 4.5-2 provides the values of particle density (ρ_n), total porosity (η_T), average saturation (S_a), and air-filled porosity (η_a) utilized for the layers used in the baseline scenario (i.e., waste material layer to the erosion barrier) for the simulation period.

Table 4.5-2: Particle Density, Total Porosity, Average Saturation, and Air-Filled Porosity by Layer for Type I and II Tanks Baseline Scenario

Layer	ρ_n (g/cm^3)	η_T	S_a	η_a
Erosion barrier layer [a, c]	2.65	0.150	0.84	0.024
Middle backfill layer [b, c]	2.63	0.371	0.82	0.067
Lateral drainage layer [a, c]	2.65	0.417	0.61	0.162
Upper Foundation layer [b, c]	2.63	0.35	0.72	0.098
Lower Foundation Layer [b, c]	2.63	0.457	0.28	0.328
Concrete Roof [d, f]	2.51	0.168	0.50	0.084
Grout [e, g]	2.51	0.266	0.50	0.133
Stabilized Contaminant Layer [f, g]	2.51	0.266	0.50	0.133

a ρ_n assumed to be that typical of quartz (SRNL-STI-2010-00135)
b Values for ρ_n taken as that of control compacted backfill from WSRC-STI-2006-00198
c η_T, S_a, and η_a values derived from WSRC-STI-2007-00184
d The concrete roof is assumed similar to the basemat surrogate as given by WSRC-STI-2007-00369 ρ_n and porosity(η) is taken from WSRC-STI-2007-00369
e ρ_n and η of grout is taken from WSRC-STI-2007-00369
f The stabilized contaminant is assumed to have the properties of grout
g The concrete roof, grout, and stabilized contaminant layer are assumed conservatively as partially saturated; therefore, the S_a is taken as 50% and the η_a is taken as one-half η_T

4.5.3 Summary of Key Air and Radon Pathway Assumptions

The following are the key air and radon pathway analyses assumptions associated with the HTF baseline scenario:

- The stabilized contaminant layer was represented as a 1-foot layer of material located at the bottom of the waste tank
- The stabilized contaminant layer, grout, and concrete roof were assumed saturated at 50%
- The stabilized contaminant layer was assumed to have properties similar to grout
- Exclusion of the top soil, upper backfill, HDPE geomembrane, GCL, and primary steel liner of the waste tank make the model more conservative
- The final closure cap as outlined with exclusions was assumed to remain intact for the duration of the simulation

In this analysis, several conditions introduce conservatism into the calculations. These include:

- Using boundary conditions that force all gaseous radionuclides to move upward from the stabilized CZ to the land surface - some gaseous radionuclides diffuse sideways and downward in air-filled pores surrounding the stabilized CZ; therefore, ignoring this has the effect of increasing flux at the land surface
- Not taking credit for removal of radionuclides via pore water moving vertically downward through the model domain - this mechanism would likely remove some dissolved radionuclides therefore its omission had the effect of increasing the estimate of instantaneous radionuclide flux at the land surface in simulations
- Exclusion of the HDPE geomembrane, GCL, and the primary steel liner of the waste tank - inclusion of these materials in the model would significantly reduce the gaseous flux at land surface due to material properties (i.e., low air-filled porosity)
- Excluding cover materials above the erosion barrier (i.e., top soil and upper backfill layers) - this material exclusion shortens the diffusion pathway and could increase flux at the land surface
- Assuming stabilized contaminant layer, grout, and the concrete roof are only 50% saturated - these materials are likely at or near saturation making the air-filled porosity equal to one-half the total porosity and increasing diffusive transport through the materials since gaseous flux is through air-filled porosity
- Using Type I and Type II tanks with minimum closure cap thickness
- Concentrating entire estimated HTF residual inventory to a 1-foot stabilized contaminant layer to determine maximum dose and flux

4.5.4 Air Pathway Analysis

For the air pathway analysis, a list of radionuclides of interest was chosen based on a NCRP atmospheric screening methodology. [NCRP-123] The radionuclides of concern for the airborne pathway are constrained by the actual waste tank inventory and the limited number of radionuclides susceptible to volatilization. These radionuclides included C-14, Cl-36, I-129, Se-79, Sb-125, Sn-126, H-3, and Tc-99. In accordance with DOE O 435.1 Chg 1, Rn-222 is addressed separately. A summary of the radionuclides and compounds of interest is presented in Table 4.5-3.

Table 4.5-3: Radionuclides and Compounds of Interest for Air and Radon Pathway Analyses

Radionuclide	Half-life (yr)	at wt	Mol in Gas Phase	mol wt
C-14	5.70E+03	14	CO_2	45.99
Cl-36	3.01E+05	36	Cl_2	72
I-129	1.57E+07	129	I_2	258
Sb-125	2.76E+00	125	Sb	125
Se-79	2.95E+05	79	Se	79
Sn-126	2.30E+05	126	Sn	126
H-3	1.23E+01	3	H_2	6
Tc-99	2.11E+05	99	Tc	99
Rn-222	1.05E-02	222	Rn	222

[SRNL-STI-2010-00135]

4.5.4.1 Source Term Development

The assumed source term for the simulations was 1 curie of each radionuclide, which was distributed uniformly throughout the liquid filled porosity of the stabilized contaminant layer. The radionuclides were allowed to partition between the pore fluid and the air-filled porosity. Apparent inverse Henry's Law coefficients for each radionuclide for several possible pore fluids for both submerged and non-submerged waste tanks are estimated. [SRNL-TR-2010-00096] Apparent inverse Henry's Law coefficients with units of kilogram atmospheres per mole are reported so that a large value indicates the constituent partitions strongly in the liquid phase. They are also considered apparent because most of the gases dissociate in solution to species other than the aqueous species of the gas. [SRNL-TR-2010-00096] These coefficients are presented in Table 4.5-4. The minimum apparent inverse Henry's Law coefficients for all possible conditions for a particular radionuclide was used to calculate the partitioning coefficient used in the air pathway modeling.

Table 4.5-4: Apparent Inverse Henry's Law Coefficients for Various Pore Solutions for Waste Tanks

	Non-Submerged Waste Tank			Submerged Waste Tank				
	Reducing Region II	Oxidizing Region II	Oxidizing Region III	Condition A[a]	Condition B[b]	Condition C[c]	Condition D[d]	Minimum[e]
Isotope	**H**	**H**	**H**	**H**	**H**	**H**	**H**	**H**
C-14	7.966E+04	8.138E+04	2.807E+00	3.790E-02	3.586E+01	1.569E+02	1.617E+02	3.790E-02
Cl-36	2.961E+17	3.211E+17	3.580E+14	5.160E+11	4.147E+15	1.406E+16	1.439E+16	5.160E+11
I-129	3.632E+20	1.068E+33	1.346E+29	6.329E+14	5.089E+18	1.725E+19	6.959E+29	6.329E+14
Sb-125	1.785E+35	8.726E+70	4.883E+38	6.868E+32	4.294E+44	3.509E+34	9.862E+44	6.868E+32
Se-79	1.789E+06	2.505E+101	3.798E+87	2.822E+25	2.356E+44	8.525E+04	1.594E+96	8.525E+04
Sn-126	1.262E+61	1.806E+71	6.086E+61	9.597E+53	5.115E+69	4.728E+60	4.787E+98	9.597E+53
H-3	2.139E+03	2.139E+03	2.138E+03	2.138E+03	2.138E+03	2.138E+03	2.138E+03	2.138E+03
Tc-99	4.831E+67	5.741E+51	7.168E+45	1.490E+40	9.625E+47	2.108E+68	1.159E+49	1.490E+40

a Condition A = groundwater
b Condition B = groundwater equilibrated with calcite
c Condition C = mixture 0.9 groundwater + 0.1 Reduced Region II
d Condition D = mixture 0.9 groundwater + 0.1 Oxidized Region II
e The minimum apparent $k_{H,inv}$ is for all pore solutions (submerged and non-submerged)
SRNL-STI-2010-00135 (Table 4)

4.5.4.2 Implementation of Partitioning Coefficients in PORFLOW

PORFLOW has the capability of partitioning radionuclides between the solid and liquid phases through a distribution coefficient. However, PORFLOW does not have the capability of directly partitioning radionuclides between the liquid and gas phases through Henry's Law. Therefore, in order to use PORFLOW to represent transport of radionuclides through the gas phase while considering liquid-gas partitioning, Henry's Law constants must be converted to equivalent distribution coefficient.

The minimum apparent inverse Henry's Law coefficient for each radionuclide was converted into pseudo-partitioning coefficients for use in PORFLOW. The conventional application of partitioning in PORFLOW involves the transfer of contaminant from solid to liquid phase via a linear and completely reversible reaction. The reaction is represented in the form of distribution coefficient, which is used in the calculation of the retardation factor (equation in Section 4.5.2, retardation factor). The distribution coefficient is the concentration of contaminants in the solid phase relative to the concentration of contaminant in solution with typical units of milliliter per gram. The air pathway analysis partitioned contaminants from the liquid to the gas phase rather than from the solid to the liquid phase. Therefore, it was necessary to develop a relationship between the apparent inverse Henry's Law coefficients and the distribution coefficient concept used in PORFLOW. The resulting partitioning coefficients used in the PORFLOW air pathway analysis are given in Table 4.5-5.

Table 4.5-5: Apparent Inverse Henry's Law Coefficients and Distribution Coefficient by Radionuclide (Type I and II Tanks)

Radionuclide	$k_{H,inv}$ (mol/atm-kg)	K_d (mL/g)
C-14	3.790E-02	9.111E-01
Cl-36	5.160E+11	1.241E+13
I-129	6.329E+14	1.522E+16
Sb-125, 126	6.868E+32	1.651E+34
Se-79	8.525E+04	2.050E+06
Sn-121m, 126	9.597E+53	2.307E+55
Tc-99	1.490E+40	3.582E+41
Tritium	2.138E+03	5.141E+04

[SRNL-STI-2010-00135]

To implement the partitioning coefficients correctly in PORFLOW it was necessary to redefine the material properties of the stabilized CZ. The typical simulation in PORFLOW involves a solid, liquid, and a gas, with partitioning of contaminants between the solid and liquid phase (via distribution coefficient) and advective or diffusive transport occurring through the liquid phase. Inputs include the bulk density of the solid phase and the porosity of the gas-liquid phase. For gaseous diffusion problems, the particle density is that of the solid material, the porosity is the void space occupied by the gas (air-filled porosity), and the fluid density is the density of air. If the gaseous contaminants are assumed to be totally in the gas phase and the waste is assumed dry, then the air-filled porosity equals the total porosity and there is no partitioning. For this air pathway analysis, the waste was assumed to be 50% saturated with the radionuclides of interest partitioned between the gas and liquid phase based on the material properties presented in Table 4.5-2.

In order to implement the distribution coefficient approach to partitioning, the liquid takes on the role usually played by the solid in a typical groundwater transport problem. Likewise, the gas takes on the role usually played by the liquid. The solid phase can be thought of as having the role typically played by gas where it is not involved in the transport process. In this implementation, the total porosity is the content of the solid and gas phases. The air-filled porosity, which is the porosity used in the transport analysis, is determined by multiplying the total porosity by the gas saturation.

Air is the fluid through which the radioactive gasses diffuse to the ground surface. As such, the fluid density input to PORFLOW was the density of air. For each simulation, a 1-curie inventory of each radionuclide was placed in the waste layer and partitioned between the liquid and gas phases according to the partitioning coefficients presented in Table 4.5-5. Once in the gas phase, the radionuclides diffused to the land surface based on the effective diffusion coefficients presented in Table 4.5-6 and the transport equation provided in Section 4.5.2.

4.5.4.3 Effective Air Diffusion Coefficients

The effective air diffusion coefficient of each radionuclide or compound within each material zone was determined. A relationship was established between moisture saturation and the radon effective air-diffusion coefficient for various pore sizes of earthen materials. Using

this method, a radon effective air-diffusion coefficient was determined for each material type based upon the average moisture saturation for the material. [SRNL-STI-2010-00135] Subsequently, using Graham's Law, the effective air-diffusion coefficient of each radionuclide or compound evaluated was determined for each material type based on the radon effective air-diffusion coefficient using the following relationship:

$$D = D' \sqrt{\frac{MWT'}{MWT}}$$

Where:

D = the effective diffusion coefficient of the radionuclide of interest (m^2/yr) within the material zone of interest

D' = the effective diffusion coefficient of Rn-222 (m^2/yr) within the material zone of interest

MWT' = the molecular weight of the reference radionuclide (Rn-222)

MWT = the molecular weight of the element or compound of interest

A summary of the radon effective air-diffusion coefficients and the calculated effective air-diffusion coefficients for each radionuclide/compound by material zone are presented in Table 4.5-6.

Table 4.5-6: Effective Air-Diffusion Coefficients by Radionuclide/Compound and Material for Type I and II Tanks and Closure Cap

Radionuclide	Tank Stabilized Contaminants, Grout, and Concrete Roof Layer (m^2/yr)	Lower Foundation Layer (m^2/yr)	Upper Foundation Layer (m^2/yr)	Lateral Drainage Layer (m^2/yr)	Middle Backfill Layer (m^2/yr)	Erosion Barrier Layer (m^2/yr)
C-14	1.358E+01	2.658E+01	5.752E+00	9.213E+00	3.196E+00	2.858E+00
Cl-36	1.085E+01	2.124E+01	4.597E+00	7.364E+00	2.555E+00	2.284E+00
H-3	3.760E+01	7.359E+01	1.593E+01	2.551E+01	8.850E+00	7.912E+00
I-129	5.734E+00	1.122E+01	2.429E+00	3.890E+00	1.350E+00	1.207E+00
Rn-222	6.181E+00	1.210E+01	2.618E+00	4.194E+00	1.455E+00	1.301E+00
Sb-125	8.237E+00	1.612E+01	3.489E+00	5.589E+00	1.939E+00	1.734E+00
Se-79	1.036E+01	2.028E+01	4.389E+00	7.030E+00	2.439E+00	2.181E+00
Sn-126	8.205E+00	1.606E+01	3.475E+00	5.567E+00	1.931E+00	1.727E+00
Tc-99	9.256E+00	1.812E+01	3.921E+00	6.280E+00	2.179E+00	1.948E+00

Note The effective diffusion coefficient for Rn-222 was used to determine the effective air diffusion coefficient of each radionuclide/compound based on Graham's Law (Graham's Law states that the rate of diffusion of a gas in inversely proportional to the square root of its molecular weight).

[SRNL-STI-2010-00135]

4.5.5 Air Pathway Model Factors for a Unit Curie

4.5.5.1 Air Pathway Flux to Ground Surface

Model simulations were conducted to evaluate the peak flux of each radionuclide (other than radon) emanating from the top of the model domain. A unit inventory of 1 curie was assigned to the HTF Type I and Type II tanks stabilized CZ for each radionuclide considered in the analysis. Results were output in curies per year, consistent with the set of units employed in the model, and are presented for each radionuclide in Figure 4.5-3 for Type I tanks and in Figure 4.5-4 for Type II tanks. The peak fluxes emanating at the land surface are presented for Type I tanks in Table 4.5-7 and for Type II tanks in Table 4.5-8 for each period. The results are reported in this way to facilitate calculation of human exposure at the SRS boundary, at 100 meters from HTF, and at 2,360 meters from HTF (i.e., UTR representative seepline distance).

Figure 4.5-3: Flux at Land Surface per Curie of Radionuclide Remaining Type I Tanks

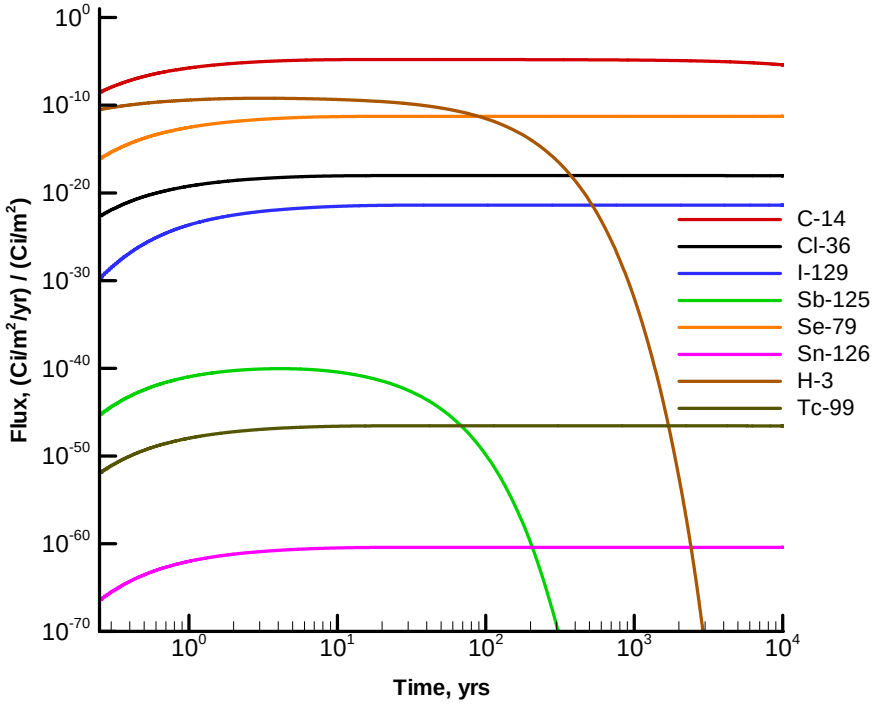

[SRNL-STI-2010-00135]

Figure 4.5-4: Flux at Land Surface per Curie of Radionuclide Remaining in Type II Tanks

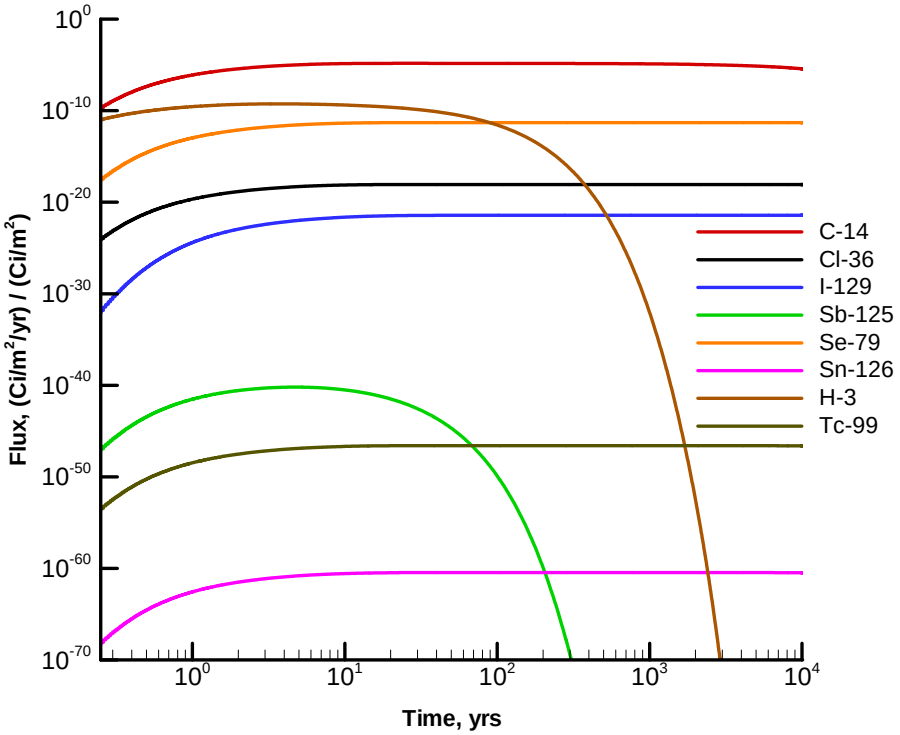

[SRNL-STI-2010-00135]

Table 4.5-7: Peak Fluxes for Each Radionuclide for Type I Tanks

Radionuclide	Activity in Residual Waste (Ci)	Peak Flux (Ci/yr/Ci)	
		0 - 100 Yrs	100 - 10,000 Yrs
C-14	1.0	1.62E-05	1.60E-05
Cl-36	1.0	9.53E-19	9.53E-19
H-3	1.0	6.33E-10	2.93E-12
I-129	1.0	4.11E-22	4.11E-22
Sb-125	1.0	9.10E-41	1.31E-50
Se-79	1.0	5.51E-12	5.51E-12
Sn-126	1.0	3.88E-61	3.88E-61
Tc-99	1.0	2.82E-47	2.82E-47

[SRNL-STI-2010-00135]

Table 4.5-8: Peak Fluxes for Each Radionuclide for Type II Tanks

Radionuclide	Activity in Residual Waste (Ci)	Peak Flux (Ci/yr/Ci)	
		0 - 100 Yrs	100 - 10,000 Yrs
C-14	1.0	1.47E-05	1.45E-05
Cl-36	1.0	8.65E-19	8.64E-19
H-3	1.0	5.53E-10	2.66E-12
I-129	1.0	3.73E-22	3.73E-22
Sb-125	1.0	6.35E-41	1.19E-50
Se-79	1.0	5.00E-12	5.00E-12
Sn-126	1.0	3.52E-61	3.52E-61
Tc-99	1.0	2.56E-47	2.55E-47

[SRNL-STI-2010-00135]

4.5.5.2 Air Pathway Dose Calculations

An evaluation was conducted to assess the potential dose to a MEI located 100 meters from HTF, the UTR seepline, and Fourmile Branch seepline. [SRNL-STI-2010-00135] The DRFs were calculated for each radionuclide potentially released from the HTF using CAP88, the EPA model for NESHAP. The dose to the receptor exposed to 1 curie of the specified radionuclide potentially released to the atmosphere is represented by DRFs. For the receptor located at the seepline locations, the distance from the HTF is sufficient for an assumption of a point source. However, the DRFs for the 100-meter receptor required evaluation of an area source because of the close proximity of HTF to the 100-meter receptor. For radionuclides not contained within the CAP88 library (Se-79, Cl-36) atmospheric transport was estimated by assigning surrogates with similar radiological properties. [SRNL-STI-2010-00018] Doses for radionuclides not contained within the CAP88 library were estimated by applying their dosimetric properties to the surrogate's relative air concentrations estimated by the model.

The SRS-specific 100-meter DRFs and the calculated Type I and Type II tank exposure levels for the 10,000-year MEI are presented in Table 4.5-9 and Table 4.5-10. Site-specific seepline DRFs and the calculated Type I and Type II tank exposure levels for the 10,000-year MEI at the seepline locations are presented in Table 4.5-11 through Table 4.5-14.

Table 4.5-9: 100m DRFs and 10,000-Year Type I Tank Exposure Levels

Radionuclide	Peak Flux (Ci/yr/Ci)	SRS 100m DRF[a] (mrem/Ci)	Dose to MEI at 100m Boundary[b] (mrem/yr/Ci)
C-14	1.60E-05	8.1E-03	1.3E-07
Cl-36	9.53E-19	1.7E-02	1.6E-20
H-3	2.93E-12	1.7E-04	5.0E-16
I-129	4.11E-22	1.2E+01	4.9E-21
Sb-125	1.31E-50	2.3E-01	3.0E-51
Se-79	5.51E-12	2.3E-02	1.3E-13
Sn-126	3.88E-61	1.1E+01	4.3E-60
Tc-99	2.82E-47	6.4E-02	1.8E-48

a SRNL-STI-2010-00018
b Dose to MEI at 100 meters = Peak Flux × DRF (SRNL-STI-2010-00135)

Table 4.5-10: 100m DRFs and 10,000-Year Type II Tank Exposure Levels

Radionuclide	Peak Flux (Ci/yr/Ci)	SRS 100m DRF[a] (mrem/Ci)	Dose to MEI at 100m Boundary[b] (mrem/yr/Ci)
C-14	1.45E-05	8.1E-03	1.2E-07
Cl-36	8.64E-19	1.7E-02	1.5E-20
H-3	2.66E-12	1.7E-04	4.5E-16
I-129	3.73E-22	1.2E+01	4.5E-21
Sb-125	1.19E-50	2.3E-01	2.7E-51
Se-79	5.00E-12	2.3E-02	1.1E-13
Sn-126	3.52E-61	1.1E+01	3.9E-60
Tc-99	2.55E-47	6.4E-02	1.6E-48

a SRNL-STI-2010-00018
b Dose to MEI at 100m = Peak Flux × DRF (SRNL-STI-2010-00135)

Table 4.5-11: UTR Seepline (2,360m) DRFs and 10,000-Year Type I Tank Exposure Levels

Radionuclide	Peak Flux (Ci/yr/Ci)	UTR 2,360m DRF[a] (mrem/Ci)	Dose to MEI at 2,360m Boundary[b] (mrem/yr/Ci)
C-14	1.60E-05	1.2E-03	1.9E-08
Cl-36	9.53E-19	3.2E-03	3.0E-21
I-129	4.11E-22	9.3E-01	3.8E-22
Sb-125	1.31E-50	5.2E-02	6.8E-52
Se-79	5.51E-12	4.8E-03	2.6E-14
Sn-126	3.88E-61	2.4E+00	9.3E-61
H-3	2.93E-12	2.5E-05	7.3E-17
Tc-99	2.82E-47	1.4E-02	3.9E-49

a SRNL-STI-2010-00018
b Dose to MEI at 100m = Peak Flux × DRF (SRNL-STI-2010-00135)

Table 4.5-12: UTR Seepline (2,360m) DRF and 10,000-Year Type II Tank Exposure Levels

Radionuclide	Peak Flux (Ci/yr/Ci)	UTR 2,360m DRF[a] (mrem/Ci)	Dose to MEI at 2,360m Boundary[b] (mrem/yr/Ci)
C-14	1.45E-05	1.2E-03	1.7E-08
Cl-36	8.64E-19	3.2E-03	2.8E-21
I-129	3.73E-22	9.3E-01	3.5E-22
Sb-125	1.19E-50	5.2E-02	6.2E-52
Se-79	5.00E-12	4.8E-03	2.4E-14
Sn-126	3.52E-61	2.4E+00	8.4E-61
H-3	2.66E-12	2.5E-05	6.7E-17
Tc-99	2.55E-47	1.4E-02	3.6E-49

a SRNL-STI-2010-00018
b Dose to MEI at 100m = Peak Flux × DRF (SRNL-STI-2010-00135)

Table 4.5-13: Fourmile Branch Seepline (1,170m) DRFs and 10,000-Year Type I Tank Exposure Levels

Radionuclide	Peak Flux (Ci/yr/Ci)	Fourmile Branch 1,170m DRF[a] (mrem/Ci)	Dose to MEI at 1,170m Boundary[b] (mrem/yr/Ci)
C-14	1.6E-05	3.9E-03	6.2E-08
Cl-36	9.53E-19	9.5E-03	9.1E-21
I-129	4.11E-22	3.6E+00	1.5E-21
Sb-125	1.31E-50	1.5E-01	2.0E-51
Se-79	5.51E-12	1.4E-02	7.7E-14
Sn-126	3.88E-61	6.6E+00	2.6E-60
H-3	2.93E-12	8.0E-05	2.3E-16
Tc-99	2.82E-47	4.0E-02	1.1E-48

a SRNL-STI-2010-00018
b Dose to MEI at 100m = Peak Flux × DRF (SRNL-STI-2010-00135)

Table 4.5-14: Fourmile Branch Seepline (1,170m) DRFs and 10,000-Year Type II Tank Exposure Levels

Radionuclide	Peak Flux (Ci/yr/Ci)	Fourmile Branch 1,170m DRF[a] (mrem/Ci)	Dose to MEI at 1,170m Boundary[b] (mrem/yr/Ci)
C-14	1.45E-05	3.9E-03	5.7E-08
Cl-36	8.64E-19	9.5E-03	8.2E-21
I-129	3.73E-22	3.6E+00	1.3E-21
Sb-125	1.19E-50	1.5E-01	1.8E-51
Se-79	5.00E-12	1.4E-02	7.0E-14
Sn-126	3.52E-61	6.6E+00	2.3E-60
H-3	2.66E-12	8.0E-05	2.1E-16
Tc-99	2.55E-47	4.0E-02	1.0E-48

a SRNL-STI-2010-00018
b Dose to MEI at 100m = Peak Flux × DRF (SRNL-STI-2010-00135)

4.5.6 Radon Analysis

The permissible radon flux for DOE facilities is addressed in DOE M 435.1-1 IV.P.(c) stating the radon flux requirement is that the release of radon shall be less than an average yearly flux of 20 pCi/m^2/sec at the surface of the facility. The performance objective refers only to radon, and the correct species must be analyzed depending on the characteristics of the residual waste stream. The instantaneous Rn-222 flux at the land surface was evaluated for the compliance period.

The potential parent radionuclides that can contribute to the creation of Rn-222 are illustrated in Figure 4.5-5. The diagram indicates the specific decay chains that lead to the formation of Rn-222, as well as the half-lives for each radionuclide. The extremely long half-life of U-238 (4.468E+9 years) causes the other radionuclides higher up on the chain of parents to be of little concern with regard to their potential to contribute significantly to the Rn-222 flux at the land surface over the period of interest. In Figure 4.5-5, the parent radionuclides that were individually evaluated are indicated with the gray shaded area (i.e., beginning with Pu-238 and U-238). Generated within the stabilized CZ, Rn-222 is in the gaseous phase and diffuses outward from this zone into the air-filled soil pores surrounding the HTF, eventually resulting in some of the radon emanating at the land surface. As such, air is the fluid through which Rn-222 diffuses, although some Rn-222 may dissolve in residual pore water.

Figure 4.5-5: Radioactive Decay Chains Leading to Rn-222

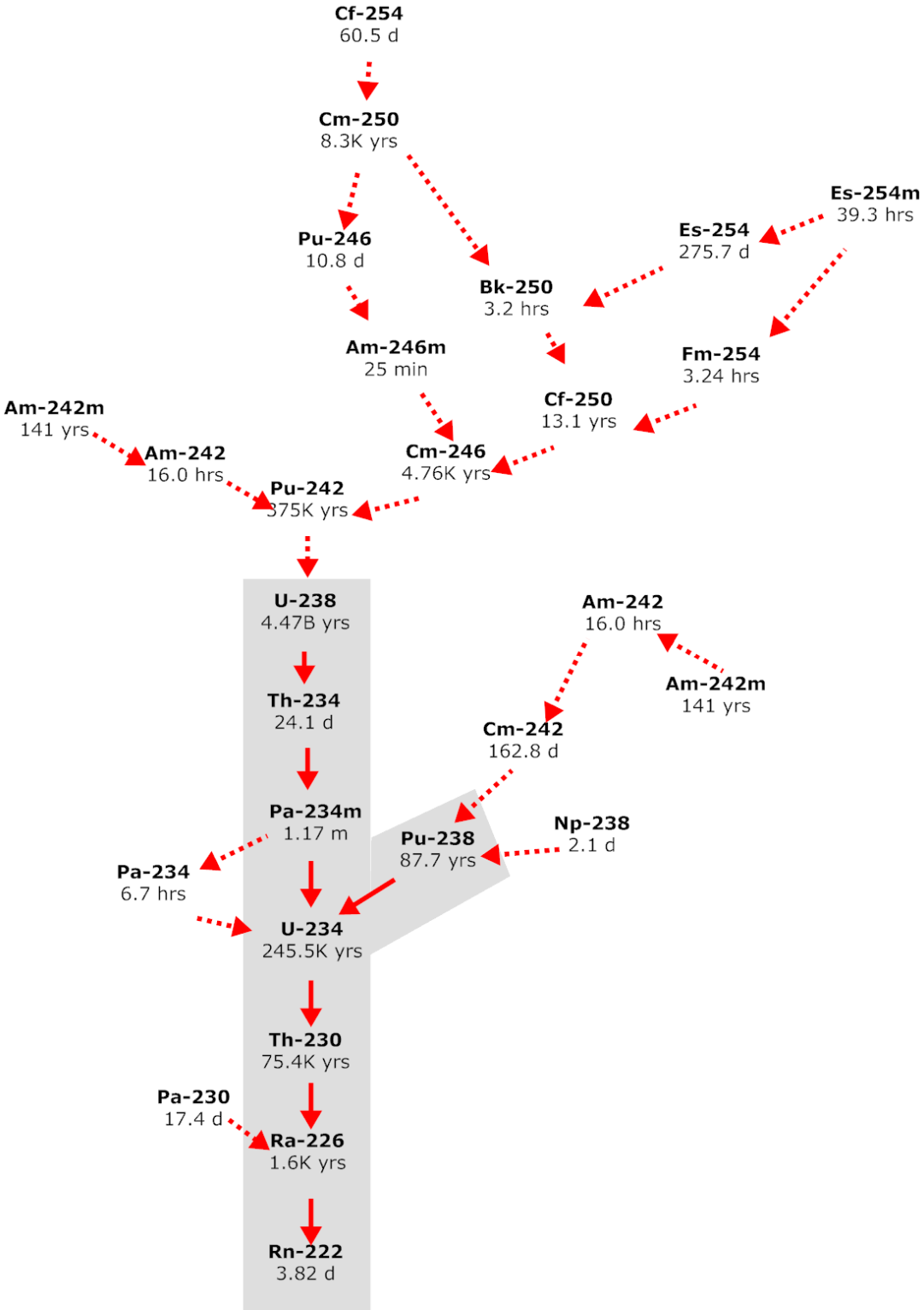

The parent radionuclides are assumed to exist in the solid phase and therefore do not migrate upward through the air-filled pore space, although they could be leached and transported downward from the stabilized CZ by pore water movement. This potential downward migration of the parent radionuclides was not considered in the radon analysis.

Decay chains evaluated were U-238→Th-234→Pa-234m→U-234→Th-230→Ra-226→Rn-222 and Pu-238→U-234→Th-230→Ra-226→Rn-222. Each parent in these chains, except Th-234 and Pa-234m, was simulated separately as the starting point of the decay chain. [SRNL-STI-2010-00135] Compared to the other parent radionuclides in these chains, Th-234 and Pa-234m have extremely short half-lives. Only a fraction of the Rn-222 generated by the decay of each parent is available for migration away from its source and into open pore space. Since the Rn-222 parent radionuclides exist as oxides or in other crystalline forms, only a fraction of Rn-222 generated by decay of Ra-226 has sufficient energy to migrate away from its original location into adjacent pore space before further decay occurs (3.82-day half-life for Rn-222).

The emanation coefficient is generally defined as the fraction of the total amount of Rn-222 produced by radium decay that escapes from soil particles and enters the pore space of the medium (the fraction of the Rn-222 that is available for transport). In the case of the HTF, the parent radionuclides are not embedded in soil but are contained within stabilized contaminants entombed in concrete/grout. Literature values for the Rn-222 emanation factor for these conditions are not available. Studies have shown the emanation factor to vary between 0.02 and 0.7 for various soil types depending primarily on moisture content. Generally, higher emanation factors are associated with higher moisture contents. [SRNL-STI-2010-00135]

RESidual RADioactivity (RESRAD) computer software is a model used to estimate radiation dose and risk from residual radioactive materials. [ANL-EAD-4] This DOE and NRC approved code assumes an emanation factor of 0.25 for Rn-222, which is representative of a silty, loam soil with low moisture content. For the HTF radon pathway analysis, the RESRAD default emanation factor of 0.25 was chosen recognizing that literature values for residual wastes similar to the HTF are not available. [SRNL-STI-2010-00135] The use of 0.25 was conservative since the assumption is that the stabilized contaminant is partially saturated and emanation factors reported in the literature for drier soils are much lower. To account for the emanation factor in the model, an effective source term of 0.25 curie of parent radionuclide was utilized for each curie disposed within the facility. [SRNL-STI-2010-00135]

Some radon dissolves in pore water but since diffusion proceeds more slowly in fluid air, diffusion was the only transport process by which Rn-222 was allowed to reach the land surface of the HTF. The molecular diffusion coefficient of Rn-222 in open air is 347 m^2/yr (1.1E+00 m^2/sec). [SRNL-STI-2010-00135] A relationship between moisture saturation and the radon effective air-diffusion coefficient for various pore sizes of earthen materials was established. This method was used to calculate a radon effective air-diffusion coefficient for each material type based upon the average moisture saturation for the material. Tortuosity was assigned a unit value for each material type. A summary of the radon air-diffusion coefficients by material type are presented in Table 4.5-6.

4.5.7 Radon Pathway Model Results

Model simulations were conducted to evaluate the peak instantaneous Rn-222 flux at the land surface for the compliance period for Type I and Type II tanks.

Model results were output in curie per meter squared per year for each curie of inventory per meter squared, consistent with the set of units employed in the model. A graph of these results is shown in Figure 4.5-6 for Type I tanks and in Figure 4.5-7 for Type II tanks. The units are converted to picocurie per meter squared per second for each curie per meter squared, which are the units used to define the regulatory flux limit in DOE M 435.1-1. The peak fluxes represent the peak flux Rn-222 Ci/m^2 at the land surface, and are given in Table 4.5-15 for Type I tanks and in Table 4.5-16 for Type II tanks.

Figure 4.5-6: Rn-222 Flux at Land Surface Resulting from Unit Source Term for Type I Tanks

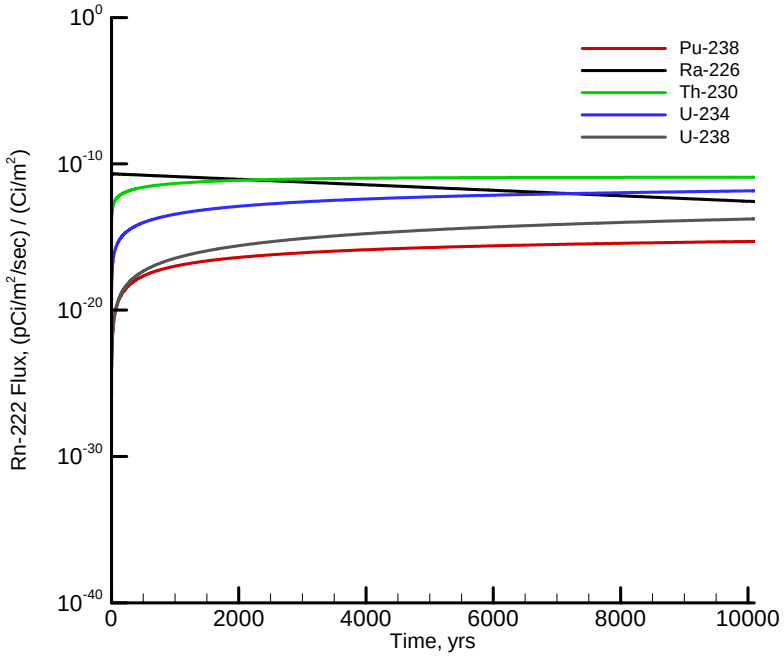

[SRNL-STI-2010-00135]

Figure 4.5-7: Rn-222 Flux at Land Surface Resulting from Unit Source Term for Type II Tanks

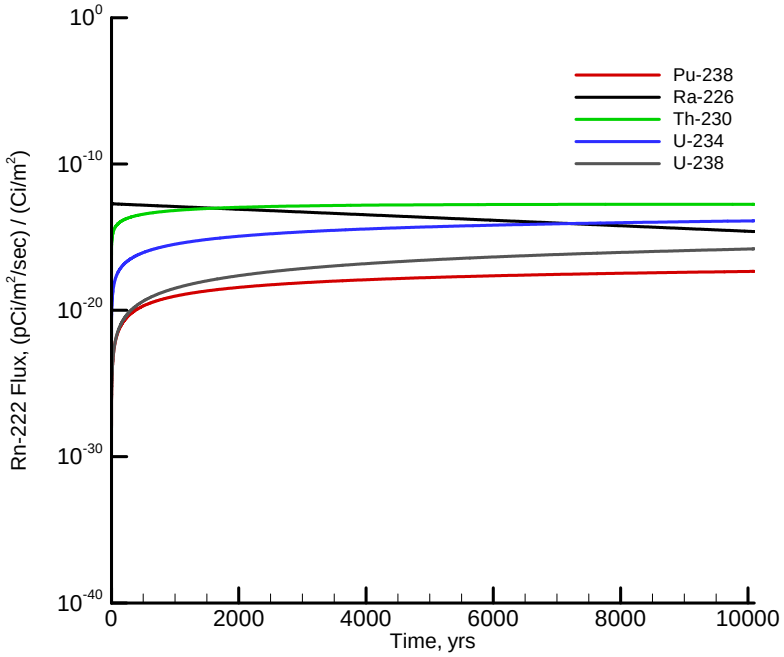

[SRNL-STI-2010-00135]

Table 4.5-15: Simulated Peak Instantaneous Rn-222 Flux over 10,000 Years at the Land Surface for Type I Tanks

Parent Rn-222 Source (1 Ci/m^2)	Flux (pCi/m^2/sec) / (Ci/m^2)
Pu-238	5.01E-16
Ra-226	2.08E-11
Th-230	1.19E-11
U-234	1.42E-12
U-238	1.72E-14

[SRNL-STI-2010-00135 Table 25]

Table 4.5-16: Simulated Peak Instantaneous Rn-222 Flux over 10,000 Years at the Land Surface for Type II Tanks

Parent Rn-222 Source (1 Ci/m^2)	Flux (pCi/m^2/sec) / (Ci/m^2)
Pu-238	4.59E-18
Ra-226	1.91E-13
Th-230	1.75E-13
U-234	1.30E-14
U-238	1.58E-16

[SRNL-STI-2010-00135 Table 26]

4.6 Biotic Pathways

The purpose of this section is to document the Bioaccumulation Factors and Human Health Exposure parameters used in the HTF PA modeling effort. Exposure pathways for the HTF PA are discussed in Section 4.2.3. Bioaccumulation Factors and Human Health Exposure parameters are used to calculate doses for each of the pathways.

4.6.1 Bioaccumulation Factors

For PA analyses at SRS, soil-to-vegetable (also known as soil-to-plant ratios or plant-to-soil ratios), feed-to-milk, feed-to-beef, water-to-fish, feed-to-poultry, and feed-to-egg transfer factors are the bioaccumulation factors considered. Soil-to-vegetable transfer factors determine the fraction of an element that is drawn from the soil into the edible plant. Feed-to-milk transfer factors represent the element-specific fraction transferred from fodder to milk. Feed-to-beef transfer factors represent the element-specific fraction transferred from fodder-to-beef. Water-to-fish transfer factors are the equilibrium ratios between concentration in finfish and concentration in water. Feed-to-poultry transfer factors represent the element-specific fraction transferred from fodder to poultry. Feed-to-egg transfer factors represent the element-specific fraction transferred from fodder to eggs.

The factors utilized were developed based on comparison to a number of other DOE facilities and generic national and international references to establish relevance of the parameters selected and as needed, verify the regional differences for the Southeastern United States.

4.6.1.1 Bioaccumulation Factor Methodology

A report entitled *Land and Water Use Characteristics and Human Health Input Parameters for use in Environmental Dosimetry and Risk Assessments at the Savannah River Site* documents the SRS evaluation and reviews of transfer factors. [SRNL-STI-2010-00447] This report presents additional details on factors utilized in the past and discussion on factors developed for SRS use. This report also established a standardized source for bioaccumulation factor parameters that represent current data.

In developing SRNL-STI-2010-00447, a comprehensive literature review was completed and references were updated to include the latest available information. These values from the more recent compilations were recommended, rather than those in older publications. The general hierarchy on document use at SRS for bioaccumulation factors is listed below:

- Site-specific
  - WSRC-TR-96-0231
  - SRT-EST-2003-00134
  - SRNL-STI-2009-00178
- IAEA-472
- PNNL-13421
- ORNL-5786
- NCRP-123, Volume 1

Issued in 2010, the *Handbook of Parameter Values for the Prediction of Radionuclide Transfer in Terrestrial and Freshwater Environments* (IAEA-472) provides parameter values for radionuclide, bioaccumulation, and transfer in terrestrial and freshwater environments.

This report supersedes IAEA-364 (*Handbook of Parameter Values for the Prediction of Radionuclide Transfer in Temperate Environments)* which was a key source of data in previous PA models.

Baseline Parameter Update for Human Health Input and Transfer Factors for Radiological Performance Assessments at the Savannah River Site (WSRC-STI-2007-00004) provides an evaluation of several sources of transfer factors and recommends values for use at SRS. WSRC-STI-2007-00004 recommends PNNL-13421 as the secondary source of values if site-specific values are not available. The hierarchy of documents in PNNL-13421 used to establish transfer factors is IAEA-364, NUREG-CR-5512, and NCRP-123 Volume 1. IAEA-364 encompasses a variety of plant types however; it has been superseded by IAEA-472. *Residual Radioactive Contamination from Decommissioning: Technical Basis for Translating Contamination Levels to Annual Total Effective Dose Equivalent*, NUREG-CR-5512, is frequently referenced because it contains a large set of data and traceable references. *Screening Models for Releases of Radionuclides to Atmosphere, Surface Water, and Ground*, NCRP-123, is chosen because it is a generally accepted reference for a generic model. WSRC-STI-2007-00004 also recommended values from ORNL-5786 as a third source. In ORNL-5786, the hierarchy of documents used to establish transfer factors is Regulatory Guide 1.109, then the TERRA code values.

A survey of land and water usage characteristics within a 50-mile region of the SRS was conducted and documented in WSRC-RP-91-17. The results indicate that chickens are raised on farms within 50 miles of SRS; however, chickens eat commercial feed. Since poultry production is an indoor operation with feed provided by the parent companies responsible for marketing the final product, SRNL-STI-2010-00447 did not include feed-to-poultry and feed-to-egg transfer factors. In order to account for local poultry and egg farmers that use free-range methods or home-grown fodder as feed, a methodology similar to that described above for SRNL-STI-2010-00447 was used to determine the feed-to-poultry and feed-to-egg transfer factors. The PNNL-13421 transfer factors were used and updated with the transfer factors from the IAEA-472. Elements in the model that feed-to-poultry or feed-to-egg transfer factors were not found were assigned a zero value.

4.6.1.1.1 Bioaccumulation Parameters

The transfer factors that SRS utilized for the PA appear in Tables 4.6-1 through 4.6-6. The data in these tables was taken from SRNL-STI-2010-00447, PNNL-13421, and IAEA-472.

Table 4.6-1: Soil-to-Vegetable Transfer Factors (Unitless)

Atomic No.	Element	Value	Atomic No.	Element	Value	Atomic No.	Element	Value
89	Ac	6.11E-05	32	Ge	1.56E-02	84	Po	4.30E-04
47	Ag	1.19E-04	1	H	4.80E+00	59	Pr	3.90E-03
13	Al	1.27E-04	108	Ha	2.00E-03	78	Pt	4.88E-03
95	Am	7.33E-05	2	He	1.00E-20	94	Pu	1.97E-05
18	Ar	1.00E-20	72	Hf	1.95E-04	88	Ra	1.19E-02
33	As	2.73E-03	80	Hg	9.03E-02	37	Rb	1.39E-01
85	At	2.93E-02	67	Ho	3.90E-03	75	Re	1.21E-01
79	Au	2.64E-03	53	I	1.32E-02	104	Rf	3.00E-03
5	B	3.90E-01	49	In	2.43E-04	45	Rh	1.76E-01
56	Ba	9.75E-04	77	Ir	4.76E-03	86	Rn	1.00E-20
4	Be	6.83E-04	19	K	2.54E-01	44	Ru	6.29E-03
83	Bi	9.75E-02	36	Kr	1.00E-20	16	S	2.93E-01
97	Bk	1.00E-03	57	La	9.09E-04	51	Sb	2.61E-04
35	Br	2.93E-01	3	Li	7.80E-04	21	Sc	4.24E-04
6	C	1.37E-01	103	Lr	2.00E-03	34	Se	1.89E-02
20	Ca	3.90E+00	71	Lu	7.80E-04	14	Si	2.65E-02
48	Cd	1.49E-01	101	Md	2.00E-03	62	Sm	3.90E-03
58	Ce	1.63E-03	12	Mg	1.28E-01	50	Sn	2.27E-03
98	Cf	6.11E-05	25	Mn	6.39E-02	38	Sr	1.23E-01
17	Cl	3.49E+00	42	Mo	8.71E-02	73	Ta	4.88E-03
96	Cm	1.27E-04	7	N	7.43E-03	65	Tb	3.90E-03
27	Co	2.48E-02	11	Na	5.85E-03	43	Tc	1.79E+01
24	Cr	1.95E-04	41	Nb	2.18E-03	52	Te	5.85E-02
55	Cs	6.85E-03	60	Nd	3.90E-03	90	Th	3.14E-04
29	Cu	1.56E-01	10	Ne	1.00E-20	22	Ti	5.85E-04
66	Dy	3.90E-03	28	Ni	2.18E-02	81	Tl	2.43E-04
68	Er	3.90E-03	102	No	2.00E-03	69	Tm	7.80E-04
99	Es	1.00E-03	93	Np	3.91E-03	92	U	6.69E-03
63	Eu	3.90E-03	8	O	6.00E-01	23	V	5.85E-04
9	F	3.65E-03	76	Os	6.45E-03	74	W	1.95E-02
26	Fe	1.10E-02	15	P	1.95E-01	54	Xe	1.00E-20
100	Fm	2.00E-03	91	Pa	6.11E-05	39	Y	3.90E-04
87	Fr	5.85E-03	82	Pb	5.18E-03	70	Yb	7.80E-04
31	Ga	2.43E-04	46	Pd	1.28E-02	30	Zn	1.71E-01
64	Gd	3.90E-03	61	Pm	2.32E-02	40	Zr	7.80E-04

Table 4.6-2: Feed-to-Milk Transfer Factors (d/L)

Atomic No.	Element	Value	Atomic No.	Element	Value	Atomic No.	Element	Value
89	Ac	2.00E-05	32	Ge	7.21E-02	59	Pr	3.00E-05
47	Ag	1.58E-03	1	H	1.50E-02	78	Pt	5.15E-03
13	Al	2.06E-04	105	Ha	5.00E-06	94	Pu	1.00E-05
95	Am	4.20E-07	2	He	1.00E-20	88	Ra	3.80E-04
33	As	6.00E-05	72	Hf	5.50E-07	37	Rb	1.20E-02
85	At	1.03E-02	80	Hg	4.70E-04	75	Re	1.50E-03
79	Au	5.50E-06	67	Ho	3.00E-05	104	Rf	2.00E-05
5	B	1.55E-03	53	I	5.40E-03	45	Rh	1.00E-02
56	Ba	1.60E-04	49	In	2.00E-04	86	Rn	1.00E-20
4	Be	8.30E-07	77	Ir	2.00E-06	44	Ru	9.40E-06
83	Bi	5.00E-04	19	K	7.20E-03	16	S	7.90E-03
97	Bk	2.00E-06	57	La	2.00E-05	51	Sb	3.80E-05
35	Br	2.00E-02	3	Li	2.06E-02	21	Sc	5.00E-06
6	C	1.20E-02	103	Lr	5.00E-06	34	Se	4.00E-03
20	Ca	1.00E-02	71	Lu	2.06E-05	14	Si	2.00E-05
48	Cd	1.90E-04	101	Md	5.00E-06	62	Sm	3.00E-05
58	Ce	2.00E-05	12	Mg	3.90E-03	50	Sn	1.00E-03
98	Cf	1.50E-06	25	Mn	4.10E-05	38	Sr	1.30E-03
17	Cl	1.70E-02	42	Mo	1.10E-03	73	Ta	4.10E-07
96	Cm	2.00E-05	7	N	2.50E-02	65	Tb	3.00E-05
27	Co	1.10E-04	11	Na	1.30E-02	43	Tc	1.87E-03
24	Cr	4.30E-04	41	Nb	4.10E-07	52	Te	3.40E-04
55	Cs	4.60E-03	60	Nd	3.00E-05	90	Th	5.00E-06
29	Cu	2.00E-03	28	Ni	9.50E-04	22	Ti	7.53E-05
66	Dy	3.00E-05	102	No	5.00E-06	81	Tl	2.00E-03
68	Er	3.00E-05	93	Np	5.00E-06	69	Tm	2.06E-05
99	Es	2.00E-06	76	Os	5.00E-03	92	U	1.80E-03
63	Eu	3.00E-05	15	P	2.00E-02	23	V	2.06E-05
9	F	1.00E-03	91	Pa	5.00E-06	74	W	1.90E-04
26	Fe	3.50E-05	82	Pb	1.90E-04	39	Y	2.00E-05
87	Fr	2.06E-02	46	Pd	1.00E-02	70	Yb	2.06E-05
31	Ga	5.00E-05	61	Pm	3.00E-05	30	Zn	2.70E-03
64	Gd	3.00E-05	84	Po	2.10E-04	40	Zr	3.60E-06

Table 4.6-3: Feed-to-Beef Transfer Factors (d/kg)

Atomic No.	Element	Value	Atomic No.	Element	Value	Atomic No.	Element	Value
89	Ac	4.00E-04	64	Gd	2.00E-05	78	Pt	4.00E-03
47	Ag	3.00E-03	32	Ge	7.00E-01	94	Pu	1.10E-06
13	Al	1.50E-03	1	H	0.00E+00	88	Ra	1.70E-03
95	Am	5.00E-04	105	Ha	5.00E-06	37	Rb	1.00E-02
33	As	2.00E-03	72	Hf	3.16E-05	75	Re	8.00E-03
85	At	1.00E-02	80	Hg	2.50E-01	45	Rh	2.00E-03
79	Au	5.00E-03	67	Ho	3.00E-04	86	Rn	1.00E-20
5	B	8.00E-04	53	I	6.70E-03	44	Ru	3.30E-03
56	Ba	1.40E-04	49	In	8.00E-03	16	S	2.00E-01
4	Be	1.00E-03	77	Ir	1.50E-03	51	Sb	1.20E-03
83	Bi	4.00E-04	19	K	2.00E-02	21	Sc	1.50E-02
97	Bk	2.50E-05	57	La	1.30E-04	34	Se	1.50E-02
35	Br	2.50E-02	3	Li	1.00E-02	14	Si	4.00E-05
6	C	3.10E-02	103	Lr	2.00E-04	62	Sm	3.16E-04
20	Ca	1.30E-02	71	Lu	4.50E-03	50	Sn	8.00E-02
48	Cd	5.80E-03	12	Mg	2.00E-02	38	Sr	1.30E-03
58	Ce	2.00E-05	25	Mn	6.00E-04	73	Ta	1.34E-05
98	Cf	4.00E-05	42	Mo	1.00E-03	65	Tb	2.00E-05
17	Cl	1.70E-02	7	N	7.50E-02	43	Tc	6.32E-03
96	Cm	4.00E-05	11	Na	1.50E-02	52	Te	7.00E-03
27	Co	4.30E-04	41	Nb	2.60E-07	90	Th	2.30E-04
24	Cr	9.00E-03	60	Nd	2.00E-05	22	Ti	1.73E-04
55	Cs	2.20E-02	28	Ni	5.00E-03	81	Tl	4.00E-02
29	Cu	9.00E-03	102	No	2.00E-04	69	Tm	4.50E-03
66	Dy	2.00E-05	93	Np	1.00E-03	92	U	3.90E-04
68	Er	2.00E-05	76	Os	4.00E-01	23	V	2.50E-03
99	Es	2.50E-05	15	P	5.50E-02	74	W	4.00E-02
63	Eu	2.00E-05	91	Pa	4.47E-04	39	Y	1.00E-03
9	F	1.50E-01	82	Pb	7.00E-04	70	Yb	4.00E-03
26	Fe	1.40E-02	46	Pd	4.00E-03	30	Zn	1.60E-01
100	Fm	2.00E-04	61	Pm	2.00E-05	40	Zr	1.20E-06
87	Fr	2.50E-03	84	Po	5.00E-03			
31	Ga	5.00E-04	59	Pr	2.00E-05			

Table 4.6-4: Water-to-Fish Bioaccumulation Factors (L/kg)

Atomic No.	Element	Value	Atomic No.	Element	Value	Atomic No.	Element	Value
89	Ac	2.50E+01	64	Gd	3.00E+01	78	Pt	3.50E+01
47	Ag	1.10E+02	32	Ge	4.00E+03	94	Pu	3.00E+01
13	Al	5.10E+01	2	He	1.00E+00	88	Ra	4.00E+00
95	Am	2.40E+02	1	H	1.00E+00	37	Rb	4.90E+03
33	As	3.30E+02	72	Hf	1.10E+03	75	Re	1.20E+02
85	At	1.50E+01	80	Hg	6.10E+03	45	Rh	1.00E+01
79	Au	2.40E+02	67	Ho	3.00E+01	45	Rn	7.55E-10
56	Ba	1.20E+00	53	I	3.00E+01	44	Ru	5.50E+01
4	Be	1.00E+02	49	In	1.00E+04	16	S	8.00E+02
83	Bi	1.50E+01	77	Ir	1.00E+01	51	Sb	3.70E+01
97	Bk	2.50E+01	19	K	3.20E+03	21	Sc	1.90E+02
35	Br	9.10E+01	57	La	3.70E+01	34	Se	6.00E+03
6	C	3.00E+00	71	Lu	2.50E+01	14	Si	2.00E+01
20	Ca	1.20E+01	12	Mg	3.70E+01	62	Sm	3.00E+01
48	Cd	2.00E+02	25	Mn	2.40E+02	50	Sn	3.00E+03
58	Ce	2.50E+01	42	Mo	1.90E+00	38	Sr	2.90E+00
98	Cf	2.50E+01	7	N	2.00E+05	73	Ta	3.00E+02
17	Cl	4.70E+01	11	Na	7.60E+01	65	Tb	4.10E+02
96	Cm	3.00E+01	41	Nb	3.00E+02	43	Tc	2.00E+01
27	Co	7.60E+01	60	Nd	3.00E+01	52	Te	1.50E+02
24	Cr	4.00E+01	28	Ni	2.10E+01	90	Th	6.00E+00
55	Cs	3.00E+03	93	Np	2.10E+01	22	Ti	1.90E+02
29	Cu	2.30E+02	8	O	1.00E+00	81	Tl	9.00E+02
66	Dy	6.50E+02	76	Os	1.00E+03	92	U	9.60E-01
68	Er	3.00E+01	15	P	1.40E+05	23	V	9.70E+01
99	Es	2.50E+01	91	Pa	1.00E+01	74	W	1.00E+01
63	Eu	1.30E+02	82	Pb	2.50E+01	39	Y	4.00E+01
9	F	1.00E+01	46	Pd	1.00E+01	30	Zn	3.40E+03
26	Fe	1.70E+02	61	Pm	3.00E+01	40	Zr	2.20E+01
87	Fr	3.00E+01	84	Po	3.60E+01			
31	Ga	4.00E+02	59	Pr	3.00E+01			

Table 4.6-5: Feed-to-Poultry Transfer Factors (d/kg)

Atomic No.	Element	Value	Atomic No.	Element	Value	Atomic No.	Element	Value
89	Ac	6.00E-03	63	Eu	2.00E-03	78	Pt	0.00E+00
47	Ag	2.00E+00	9	F	1.40E-02	94	Pu	3.00E-03
13	Al	0.00E+00	26	Fe	1.00E+00	88	Ra	3.00E-02
95	Am	6.00E-03	64	Gd	2.00E-03	51	Sb	6.00E-03
33	As	8.30E-01	1	H	0.00E+00	34	Se	9.70E+00
56	Ba	1.90E-02	80	Hg	3.00E-02	62	Sm	2.00E-03
83	Bi	9.80E-02	53	I	8.70E-03	50	Sn	8.00E-01
6	C	0.00E+00	19	K	4.00E-01	38	Sr	2.00E-02
20	Ca	4.40E-02	71	Lu	0.00E+00	43	Tc	3.00E-02
48	Cd	1.70E+00	25	Mn	1.90E-03	90	Th	6.00E-03
98	Cf	6.00E-03	42	Mo	1.80E-01	92	U	7.50E-01
17	Cl	3.00E-02	41	Nb	3.00E-04	30	Zn	4.70E-01
96	Cm	6.00E-03	28	Ni	1.00E-03	40	Zr	6.00E-05
27	Co	9.70E-01	93	Np	6.00E-03			
24	Cr	2.00E-01	91	Pa	6.00E-03			
55	Cs	2.70E+00	82	Pb	8.00E-01			
29	Cu	5.00E-01	46	Pd	3.00E-04			

Table 4.6-6: Feed-to-Egg Transfer Factors (d/kg)

Atomic No.	Element	Value	Atomic No.	Element	Value	Atomic No.	Element	Value
89	Ac	4.00E-03	63	Eu	4.00E-05	78	Pt	0.00E+00
47	Ag	5.00E-01	9	F	2.70E+00	94	Pu	1.20E-03
13	Al	0.00E+00	26	Fe	1.80E+00	88	Ra	3.10E-01
95	Am	3.00E-03	64	Gd	4.00E-05	51	Sb	7.00E-02
33	As	2.60E-01	1	H	0.00E+00	34	Se	1.60E+00
56	Ba	8.70E-01	80	Hg	5.00E-01	62	Sm	4.00E-05
83	Bi	2.60E-01	53	I	2.40E+00	50	Sn	1.00E+00
6	C	0.00E+00	19	K	1.00E+00	38	Sr	3.50E-01
20	Ca	4.40E-01	71	Lu	0.00E+00	43	Tc	3.00E+00
48	Cd	1.00E-01	25	Mn	4.20E-02	90	Th	4.00E-03
98	Cf	4.00E-03	42	Mo	6.40E-01	92	U	1.10E+00
17	Cl	2.70E+00	41	Nb	1.00E-03	30	Zn	1.40E+00
96	Cm	4.00E-03	28	Ni	1.00E-01	40	Zr	2.00E-04
27	Co	3.30E-02	93	Np	4.00E-03			
24	Cr	9.00E-01	91	Pa	4.00E-03			
55	Cs	4.00E-01	82	Pb	1.00E+00			
29	Cu	5.00E-01	46	Pd	4.00E-03			

4.6.2 Human Health Exposure Parameters (Consumption Rates)

This section documents the human health exposure parameters (i.e., consumption rates) used in the HTF PA modeling effort. The factors utilized were developed based on comparison to a number of other DOE facilities and generic national and international references to establish relevance of the parameters selected and as needed, verify the regional differences for the Southeastern United States. The parameter values recommended were based on expected values along with a range for these values versus providing parameters for estimating an annual dose to the MEI. The consumption rates that SRS utilized for the PA appear in Tables 4.6-7 through 4.6-9. Distribution ranges for Tables 4.6-7 through 4.6-9 are presented in Section 5.6.3 tables.

Table 4.6-7: Crop Exposure Times and Productivity

Parameter	GoldSim Parameter Name	Value	
Vegetable crop exposure times to irrigation (d)	VeggieExposureTime	70	
Buildup time of radionuclides in soil (d)[a]	SoilBuildupTime	9,125	
Agricultural productivity (kg/m^2)[a]	VegetationProductionYield	2.2	
Fraction of Foodstuff Produced Locally		**All-Pathway**	**Intruder**
Leafy vegetables and produce	LocalGrown and LocalGrown_Intr	0.173	0.308
Meat	FracLocalBeef_MOP and FracLocalBeef_Intr	0.306	0.319
Milk	FracLocalMilk_MOP and FracLocalMilk_Intr	0.207	0.254
Poultry and Eggs[b]	FracLocalChic_MOP and FracLocalChic_Intr	0.306	0.319

[WSRC-STI-2007-00004, Table 3-1 except as noted]
a SRNL-STI-2010-00447
b ML083190829, Table A-1

Table 4.6-8: Physical Parameters

Parameter	GoldSim Parameter Name	Value
Water Density (g/ml)	*WaterDens*	1.0
Areal surface density of soil (kg/m^2)	*SurfaceSoilDensity*	240
Density of Sandy Soil (kg/m^3)[a]	*DryBulkDensity_SandySoil*	1,650
Airborne release fraction[b]	*ARF*	1.0E-04
Soil loading in air (kg/m^3)	*AirMassLoadingSoil*	1.0E-07
Depth of garden (cm)	*TillDepth and SoilThickness*	15
Water contained in air at ambient conditions (g/m^3)[c]	*AirWaterContent*	10
Water contained in air at shower conditions (g/m^3)[c]	*ShowerAirWaterContent*	41
Soil moisture content[d]	*SoilMoistureContent*	0.2086
Precipitation rate (in/yr)[d]	*PR*	49.1
Evapotranspiration rate (in/yr)[d]	*ER*	32.6
Irrigation rate (in/yr)	*IR*	52*
Irrigation rate ($L/d/m^2$)	*IrrigationRate*	3.6*
Fraction of the time that vegetation is irrigated	*FracYearIrrigate*	0.2
Weathering decay constant (1/d)	*WeatheringDecayConst*	0.0495
Fraction of material deposited on leaves that is retained	*LeafRetention*	0.25
Fraction of material deposited on leaves that is retained after washing	*WashingFactor*	1.0
Area of garden for family of four (m^2)	*GardenSize*	100
Well diameter (ft)[e]	*WellDiameter*	0.667
Transfer line circumference (ft)[e]	*PipeAreaperLength*	0.803
Well depth (ft)[e]	*WellDepth*	100

[WSRC-STI-2007-00004, Table 3-2 except as noted]

a WSRC-STI-2006-00198, Table 5-18

b DOE-HDBK-3010-94

c HNF-SD-WM-TI-707

d WSRC-STI-2007-00184

e SRR-CWDA-2010-00054

* Based on an assumption of 1-in/wk = 0.36 cm/d. A $1m^2$ area, 0.36 cm/d x 10,000 cm^2/m^2 x 1L/1,000 cm^3=3.6 $L/d/m^2$.

Table 4.6-9: Individual Exposure Times and Consumption Rates

Parameter	GoldSim Parameter Name	Value
Breathing rate (m^3/yr)	*AirIntake*	5,548
Consumption Rate		
Soil (kg/year)	*SoilConsumptionRate*	0.0365
Leafy vegetable (kg/yr)	*Leafy*	21
Other vegetable (kg/yr)	*Veg*	163
Meat (kg/yr)	*BeefConsumptionRate*	43
Poultry (kg/yr)[a]	*ChicConsumptionRate*	25
Eggs (kg/yr)[a]	*EggConsumptionRate*	19
Finfish (kg/yr)	*FishConsumptionRate*	9
Milk (L/yr)	*MilkConsumptionRate*	120
Water (L/yr)	*WaterConsumptionRate*	337
Fodder-Beef cattle (kg/d)	*ConsumptionFodderBeef*	36
Fodder-Milk cattle (kg/d)	*ConsumptionFodderMilk*	52
Fodder-Poultry (kg/d)[a]	*ConsumptionFodderChic and ConsumptionFodderEgg*	0.1
Fraction of milk-cow feed is from pasture (fodder)	*FodderFractionMilk*	0.56
Fraction of beef-cow feed is from pasture (fodder)	*FodderFractionBeef*	0.75
Fraction of poultry feed is from pasture (fodder)	*FodderFractionChic and FodderFractionEgg*	1
Water (beef cow) (L/d)	*CattleWaterConsumptionBeef*	28
Water (milk cow) (L/d)	*CattleWaterConsumptionMilk*	50
Water (poultry) (L/d)[a]	*ChicWaterConsumption and EggWaterConsumption*	0.3
Exposure Time		
Swimming (hr/yr)[b]	*AnnualSwimming*	7
Boating (hr/yr)[b]	*AnnualBoating*	22
Showering (min/d)	*ExposureFractionShower*	10
Fraction of time spent working in garden	*ExposureFractionGarden*	0.01
Boating geometry factor[c]	*BoatingGF*	0.5
Swimming geometry factor[c]	*SwimmingGF*	1
Fraction of year acute intruder is exposed to drill cuttings[d]	*FractionExposedtoCuttings*	0.0023

[WSRC-STI-2007-00004, Table 4-1 except as noted]
a ML083190829, Table A-1
b SRNL-STI-2010-00447
c Conservative assumption
d Assumes 20 hours to complete well drilling

4.6.2.1 Human Health Exposure Parameters Methodology

Baseline Parameter Update for Human Health Input and Transfer Factors for Radiological Performance Assessments at the Savannah River Site (WSRC-STI-2007-00004) documents the results of the SRS evaluation and reviews of consumption rates. The report includes information to establish a range of values for each parameter that was used to perform the

uncertainty analyses. Refer to this report for additional discussion on parameters such as water ingestion rates, crop yields, garden fractions, and sizes along with soil exposure times. *Land and Water Use Characteristics and Human Health Input Parameters for use in Environmental Dosimetry and Risk Assessments at the Savannah River Site* (SRNL-STI-2010-00447) relies heavily on WSRC-STI-2007-00004, and reproduces nearly all of the human health exposure parameters from that report. Since WSRC-STI-2007-00004 also provides a range of values used to perform uncertainty analyses, the human health exposure parameters and ranges used in the HTF PA were taken from WSRC-STI-2007-00004 with a few parameters updated by SRNL-STI-2010-00447 as noted in the tables.

In developing WSRC-STI-2007-00004, a comprehensive literature review was completed. A hierarchy of data sources was established to select values for human health exposure parameters. The utilization of site-specific values from the most recent and comprehensive references are given priority. Values promulgated by national or international organizations were used as representative of the SRS area practices in the absence of site-specific values. The *Risk-Based Screening of Radionuclide Releases from the Savannah River Site* was used as a source to validate the receptor practices in the areas surrounding SRS. [CDC-2006] The values given for the parameters are given as expected values, together with an observed range.

Site-specific information is available for most of the human health exposure parameters required to estimate doses. Report WSRC-RP-91-17, *Land and Water-Use Characteristics in the Vicinity of the Savannah River Site and Site-Specific Parameter Values for the Nuclear Regulatory Commission's Food Pathway Dose Model*, surveyed county agents in South Carolina and Georgia and compiled county-specific statistics on land and water use within a 50 mile radius of SRS. When the report does not provide site-specific information for physical parameters and consumption rates, global data are used. The EPA report *Exposure Factors Handbook, National Center for Environmental Assessment*, summarizes and recommends human health exposure parameter data for human exposure to environmental contaminants based on studies published through August 30, 1997. [EPA-600-P-95-002] Documents ANL-EAD-4 and ANL-EAIS-8 provide data for use in RESRAD, a DOE and NRC supported dose model based on literature review of standard values and publications. NUREG-CR-5512 provides generic and site-specific human health data for estimating dose from exposure to residual radioactive contamination.

4.7 Dose Analysis

Over time, the mobile contaminants in the HTF waste tanks and ancillary equipment will gradually migrate downward through unsaturated soil to the hydrogeologic units comprising the shallow aquifer underlying the HTF. Some contaminants will be transported via groundwater through the aquifers, to the outcrops at Fourmile Branch and UTR. Upon reaching the surface water, the contaminants could be present at the seepline, in sediments at the bottom of streams, and at the shoreline. Human receptors could be exposed to contaminants through various pathways associated with the aquifers and surface water as described in Section 4.2.3.

The potential dose to MOP via the air pathway was also evaluated as described in Section 4.5.

4.7.1 Dose Conversion Factors

The purpose of this section is to present the set of DCFs used in dose calculations for the HTF PA modeling effort. A comprehensive list of DCFs was prepared and included in Table 4.7-1, even though only a subset of the values listed was actually utilized in the PA modeling.

Radiation doses to humans may result from internal inhalation or ingestion of radionuclides by or from external exposure to radionuclides present in the environment. Dose assessment at SRS is carried out by considering radionuclide concentrations in environmental media, factoring in human exposure conditions, and performing the conversion of exposure to dose. For internal exposure, radionuclide activity intake is calculated by combining the radioactivity concentration in environmental media (e.g., food, soil, air, and water) with the amount of environmental medium taken into the body. Then, using internal DCFs, radionuclide intake is converted into dose. To assess exposure from external sources, SRS uses external DCFs that convert radionuclide concentrations in environmental media to doses for the duration of exposure.

4.7.1.1 Internal DCFs

Previous SRS PA analyses utilized the DCFs from EPA Federal Guidance Report 11, published in 1988. [EPA-520-1-88-020] The International Commission on Radiological Protection (ICRP) published new DCFs based upon updated dosimetric models in ICRP Publication 72 in 1996. The DOE has begun using the ICRP models for occupational exposure internal dose assessments at different sites including SRS, and they are also used for SRS safety basis calculations. Safety Basis Documents, as defined in 10 CFR 830, Subpart B, are the DSA and hazard controls that provide reasonable assurance that a DOE nuclear facility can be operated safely in a manner that adequately protects workers, the public, and the environment. Only internal DCFs for adults, as opposed to internal DCFs for children or infants, were utilized in the HTF PA, consistent with guidance in DOE Guide 435.1-1, Section IV.P.(2).

The DCFs are converted to standard units for input into the calculations by multiplying the ICRP-72 DCFs by 3.7E+06 (Sv/Bq/rem/μCi). The internal DCFs in rem per microcurie (rem/μCi) are presented in Table 4.7-1 for the various radionuclides. For inhalation DCFs, the most likely lung absorption type from Table 2 of ICRP-72 was used if available, and if not available, the most conservative type was assumed.

For radionuclides with daughter products that are expected to be in secular equilibrium with the parent radionuclide, the DCFs of the daughter products are summed with the DCF of the parent radionuclide to match the modeling code transport output. The equilibrium is calculated using the individual ICRP-72 DCF and adjusted by the branching fraction for the daughter products to the parent. For example, the ICRP-72 ingestion DCF for Pb-210, Bi-210, and Po-210 is 2.6 rem/μCi (6.9E-07 Sv/Bq), 4.8E-03 rem/μCi (1.3E-09 Sv/Bq), and 4.4 rem/μCi (1.2E-06 Sv/Bq) respectively. Based on a branching fraction of 1.0 for Bi-210 and 1.0 for Po-210, the adjusted Pb-210 DCF is 2.6 rem/μCi + 4.8E-03 rem/μCi + 4.4 rem/μCi = 7.0 rem/μCi. Radionuclides that have short-lived daughter product DCFs included in the parent DCF are noted in Table 4.7-1.

Because the ICRP data is the most recent data available and is based on the most recent dosimetric models, the ICRP-72 DCFs were used for this HTF PA analyses and have been approved for use by DOE Office of Health Safety and Security. [ICRP-72, DOE_02-23-2011]

4.7.1.2 External DCFs

External DCFs for uniformly distributed contamination in soil at an infinite depth with no shielding and at 15 cm are taken from EPA Federal Guidance Report 12. [EPA-402-R-93-081] The external DCFs in EPA-402-R-93-081 represent the dose rate per unit of activity of soil contaminated at various depths, reported in sievert (Sv) per second per becquerel (Bq) per cubed meter. The DCFs are converted to standard units for input into PA calculations by multiplying the EPA-402-R-93-081 DCFs by 1.168E+14 ((rem/yr per μCi/m^3) / (Sv/s per Bq/m^3)). External DCFs are presented in Table 4.7-1 for various radionuclides for both contaminated soil and for immersion in contaminated water. [EPA-402-R-93-081]

For radionuclides with daughter products that are expected to be in secular equilibrium with the parent radionuclide, the DCFs of the daughter products are summed with the DCF of the parent radionuclide to match the modeling code transport output. The equilibrium is calculated using the individual EPA-402-R-93-081 DCF and adjusted by the branching fraction for the daughter products to the parent, similar to the calculation described for the internal DCFs. Radionuclides, which have short-lived daughter product DCFs included in the parent DCFs are noted in Table 4.7-1.

Table 4.7-1: Internal and External DCFs

Radionuclide	Internal DCFs (rem/μCi)		External DCFs (rem/yr per μCi/m^3)		
	Ingestion	Inhalation	Infinite Depth	15 cm	Water Immersion
Ac-227 [a]	4.47E+00	2.10E+03	1.26E-03	1.18E-03	4.74E-03
Ag-108m	8.51E-03	2.74E-02	6.02E-03	5.38E-03	1.97E-02
Al-26	1.30E-02	7.40E-02	1.09E-02	9.03E-03	3.43E-02
Am-241	7.40E-01	1.55E+02	2.73E-05	2.73E-05	2.20E-04
Am-242m [a]	7.41E-01	1.53E+02	4.25E-05	4.10E-05	2.03E-04
Am-243 [a]	7.43E-01	1.52E+02	5.59E-04	5.44E-04	2.57E-03
Bi-210m [a]	5.55E-02	1.26E+01	8.65E-04	8.14E-04	3.14E-03
C-14	2.15E-03	7.40E-03	8.41E-09	8.41E-09	5.13E-08
Ca-41	7.03E-04	3.52E-04	0.00E+00	0.00E+00	0.00E+00
Cf-249	1.30E+00	2.59E+02	1.16E-03	1.07E-03	4.03E-03
Cf-251	1.33E+00	2.63E+02	3.29E-04	3.22E-04	1.45E-03
Cl-36	3.44E-03	2.70E-02	1.49E-06	1.42E-06	5.23E-06
Cm-243	5.55E-01	1.15E+02	3.64E-04	3.53E-04	1.52E-03
Cm-244	4.44E-01	9.99E+01	7.87E-08	7.87E-08	1.34E-06
Cm-245	7.77E-01	1.55E+02	2.13E-04	2.10E-04	1.03E-03
Cm-246	7.77E-01	1.55E+02	7.26E-08	7.26E-08	1.23E-06
Cm-247 [a]	7.03E-01	1.44E+02	1.16E-03	1.08E-03	4.09E-03
Cm-248	2.85E+00	5.55E+02	5.49E-08	5.49E-08	9.30E-07
Co-60	1.26E-02	3.70E-02	1.01E-02	8.47E-03	3.20E-02
Cs-135	7.40E-03	2.55E-03	2.39E-08	2.39E-08	1.28E-07
Cs-137 [a]	4.81E-02	1.70E-02	2.13E-03	1.89E-03	6.92E-03
Eu-152	5.18E-03	1.55E-01	4.38E-03	3.76E-03	1.44E-02
Eu-154	7.40E-03	1.96E-01	4.80E-03	4.11E-03	1.55E-02
Eu-155	1.18E-03	2.55E-02	1.14E-04	1.14E-04	6.55E-04
Gd-152	1.52E-01	7.03E+01	0.00E+00	0.00E+00	0.00E+00
H-3	6.66E-05	1.67E-04	0.00E+00	0.00E+00	0.00E+00
I-129	4.07E-01	1.33E-01	8.09E-06	8.09E-06	1.04E-04
K-40	2.29E-02	7.77E-03	6.50E-04	5.34E-04	2.03E-03
Lu-174	9.99E-04	1.55E-02	3.58E-04	3.09E-04	1.40E-03
Mo-93	1.15E-02	2.18E-03	3.69E-07	3.69E-07	6.91E-06
Nb-93m	4.44E-04	1.89E-03	6.50E-08	6.50E-08	1.21E-06
Nb-94	6.29E-03	4.07E-02	6.05E-03	5.29E-03	1.95E-02
Ni-59	2.33E-04	4.81E-04	0.00E+00	0.00E+00	0.00E+00
Ni-63	5.55E-04	1.78E-03	0.00E+00	0.00E+00	0.00E+00
Np-237 [a]	4.10E-01	8.51E+01	6.86E-04	6.52E-04	2.66E-03
Pa-231	2.63E+00	5.18E+02	1.19E-04	1.12E-04	4.41E-04

Table 4.7-1: Internal and External DCFs (Continued)

Radionuclide	Internal DCFs (rem/μCi)		External DCFs (rem/yr per μCi/m^3)		
	Ingestion	Inhalation	Infinite Depth	15 cm	Water Immersion
Pb-210 [a]	7.00E+00	1.66E+01	3.81E-06	3.73E-06	2.28E-05
Pd-107	1.37E-04	2.18E-03	0.00E+00	0.00E+00	0.00E+00
Pt-193	1.15E-04	7.77E-05	3.54E-09	3.54E-09	1.08E-07
Pu-238	8.51E-01	1.70E+02	9.46E-08	9.42E-08	1.33E-06
Pu-239	9.25E-01	1.85E+02	1.84E-07	1.77E-07	1.12E-06
Pu-240	9.25E-01	1.85E+02	9.17E-08	9.15E-08	1.30E-06
Pu-241	1.78E-02	3.33E+00	3.69E-09	3.68E-09	1.89E-08
Pu-242	8.88E-01	1.78E+02	8.00E-08	8.00E-08	1.09E-06
Pu-244 [a]	8.92E-01	1.74E+02	1.26E-03	1.11E-03	4.11E-03
Ra-226 [a]	1.04E+00	1.31E+01	6.99E-03	5.89E-03	2.25E-02
Ra-228 [a]	3.08E+00	1.70E+02	1.01E-02	8.37E-03	3.25E-02
Se-79	1.07E-02	4.07E-03	1.16E-08	1.16E-08	6.92E-08
Sm-147	1.81E-01	3.55E+01	0.00E+00	0.00E+00	0.00E+00
Sm-151	3.63E-04	1.48E-02	6.15E-10	6.15E-10	9.92E-09
Sn-126 [a]	1.88E-02	1.05E-01	7.40E-03	6.61E-03	2.45E-02
Sr-90 [a]	1.14E-01	1.39E-01	1.54E-05	1.44E-05	4.41E-05
Tc-99	2.37E-03	1.48E-02	7.85E-08	7.82E-08	3.67E-07
Th-229 [a]	2.27E+00	3.17E+02	9.98E-04	9.21E-04	3.83E-03
Th-230	7.77E-01	5.18E+01	7.56E-07	7.46E-07	4.60E-06
Th-232	8.51E-01	9.25E+01	3.26E-07	3.25E-07	2.32E-06
U-232 [a]	1.75E+00	1.89E+02	6.37E-03	5.15E-03	2.04E-02
U-233	1.89E-01	1.33E+01	8.73E-07	8.45E-07	4.25E-06
U-234	1.81E-01	1.30E+01	2.51E-07	2.50E-07	2.04E-06
U-235 [a]	1.75E-01	1.15E+01	4.73E-04	4.61E-04	1.99E-03
U-236	1.74E-01	1.18E+01	1.34E-07	1.33E-07	1.35E-06
U-238 [a]	1.79E-01	1.08E+01	9.49E-05	8.48E-05	3.45E-04
Zr-93	4.07E-03	3.70E-02	0.00E+00	0.00E+00	0.00E+00

a Based on the parent radionuclide plus daughter products

4.7.2 MOP Dose Analysis

Two distinct release scenarios were analyzed to assess the potential MOP doses associated with the HTF. The difference in the scenarios was the primary water source, 1) a well drilled into the groundwater aquifers and 2) an HTF stream. The MOP dose pathways used in the PA analyses are discussed in detail in Section 4.2.3.1.

The consumption rates and bioaccumulation factors that are used in conjunction with the proposed pathways are discussed in detail in Section 4.6.

4.7.3 Intruder Dose Analysis

Two distinct release scenarios were analyzed to assess the potential intruder doses associated with the HTF. The intruder scenarios of concern are the Acute Intruder-Drilling Scenario

and the Chronic Intruder Agricultural (Post-Drilling) Scenario. The intruder dose pathways used in the PA analyses are discussed in detail in Section 4.2.3.2.

The consumption rates and bioaccumulation factors that are used in conjunction with the proposed pathways are discussed in detail in Section 4.6.

4.7.4 Analysis Approach

The MOP and intruder exposure scenarios were analyzed for HTF to provide results to demonstrate compliance with the performance criteria. The analysis provides not only the maximum projected dose and time of occurrence, but also the dominant pathway contributing to the dose and the radionuclides responsible for the maximum dose.

The groundwater and surface water concentrations and resulting human health impacts are calculated for the Base Case using the PORFLOW computer code. The analysis approaches used for HTF are based upon the radionuclide inventories (Sections 3.3.2 and 3.3.3), stabilized contaminant release mechanisms (Section 4.2.1), and radionuclide transport models (Section 4.2.2) as described previously in this document.

4.8 RCRA/CERCLA Risk Evaluation

Protocols have been developed, with approval of SCDHEC and the EPA to support the SRS ACP remediation activities. The protocols provide instructions for the development of conceptual site models used in the RCRA Facility Investigation Work Plan and CERCLA Remedial Investigation (RI) process. [ERD-AG-003_F.17, ERD-AG-003_P.1.4, ERD-AG-003_P.1.5, ERD-AG-003_P.5.2, and ERD-AG-003_P.10.1] These same protocols were used to evaluate the potential for adverse affects associated with exposure to constituents present at the HTF in the stabilized contaminants. Groundwater concentrations at the HTF were compared to the SDWA MCLs. In the absence of MCLs, groundwater radionuclide concentrations were compared to PRGs, and non-radionuclide concentrations were compared to RSLs.

The PRGs are risk-based tools used to evaluate and clean up contaminated sites. The use of PRGs to evaluate risk/hazard is a simple and accepted method; however, this method does not replace the current Constituent of Potential Concern (COPC) identification process that considers the residential soil PRGs in the initial screening step. [http://epa-prgs.ornl.gov/radionuclides/download/rad_master_prg_table_pci.pdf]

The May 2010 version of the EPA RSL tables is the source of RSLs for non-radiological constituents. It combines current EPA toxicity values with standard exposure factors to estimate contaminant concentrations in environmental media (soil, air, and water) that the agency considers protective of humans (including sensitive groups), over a lifetime. Region 3 RSL concentrations are based on direct contact pathways for which generally accepted methods, models, and assumptions have been developed (i.e., quantitative ingestion, dermal contact, and inhalation factors) for specific land use conditions. Additional information can be found at the EPA website:

http://www.epa.gov/reg3hwmd/risk/human/rb-concentration_table/Generic_Tables/index.htm

Oak Ridge National Laboratory (ORNL) has derived risk-based radiological PRG values using default parameters and the latest toxicity values. The EPA website provides specific details regarding use of the database tool to calculate the PRGs and generic tables that were used for

comparison to the modeled radionuclide concentrations evaluated in this PA. [http://epa-prgs.ornl.gov/radionuclides/download/rad_master_prg_table_pci.pdf]

4.8.1 Integrated Conceptual Model

The ICM for HTF (Figure 4.8-1) depicts the understanding of the site and focuses on identifying potential contaminant migration from the sources to potential receptors. The ICM identifies potential sources of contamination, release mechanisms, media of concern, exposure routes, and potential receptors. For the purposes of the ICM, the surface soil interval is defined as the 0 to 0.3-meter (0 to 1-foot) interval and is evaluated for human and ecological exposure. The subsurface soil interval is the 0.3 to 1.2-meter (1 to 4-foot) interval and is evaluated for ecological exposure. The deep soil interval (> 1.2 meters) is defined on a subunit specific basis and is evaluated for Principal Threat Source Material (PTSM) (future excavation scenario) and contaminant migration potential. The approved risk evaluation approach used in the RCRA Facility Investigation and CERCLA RI process differs slightly from the general analysis approach used in calculating the PA dose results in Sections 5 and 6, such that there will be some differences between the risk analyses release scenarios (shown in Figure 4.8-1), and the dose analyses pathways and scenarios (Section 4.2.3).

Figure 4.8-1: Integrated Conceptual Site Model for HTF

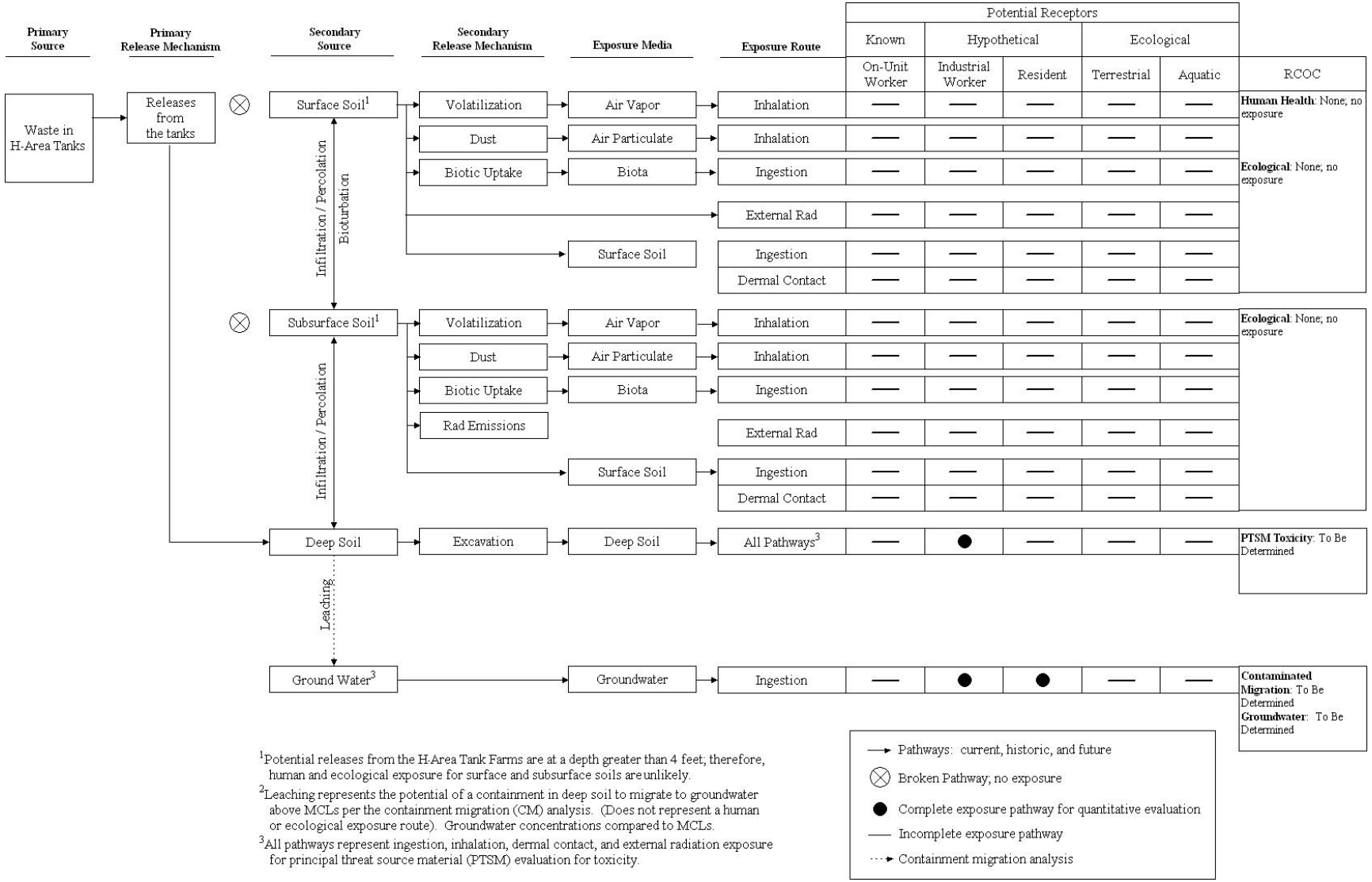

Initially, the ICM provides a representation of the contamination source. It also includes potential release mechanisms and exposure routes based on existing understanding of the nature and extent of contamination. For this evaluation, because the HTF will remain operational while the individual waste tanks are closed, only the stabilized contamination in the waste tanks is considered. Final facility closure of the HTF will include the evaluation of potential surface soil contamination.

4.8.1.1 Primary Source of Contamination

The primary source of contamination was the stabilized contaminants in the HTF waste tanks and ancillary equipment. Contaminants may be released from primary sources through release (migration) of contaminants from the waste tanks and ancillary equipment.

4.8.1.2 Secondary Sources of Contamination

Environmental media impacted by the release of primary source contamination becomes a secondary source. After grouting the waste tanks and ancillary equipment, at least 10 feet of material will be placed as backfill. Potential releases from the HTF are then at depths greater than 1.2 meters; therefore human and ecological exposure for surface or subsurface soils is unlikely (incomplete pathway). Secondary sources of contamination include deep soils beneath the waste tanks and groundwater.

Environmental media may serve as both a contaminant reservoir, via chemical bonding and biotic uptake, and/or secondary release mechanism of contaminants. Secondary release mechanisms include, leaching of constituents from deep soils to groundwater and excavation of deep soils.

4.8.1.3 Exposure Pathways (Media)

Contact with contaminated environmental media creates exposure pathways for human receptors. Potential exposure media includes excavation of deep soil and groundwater.

4.8.1.4 Exposure Routes

Potential exposure routes for human receptors may include the following:

- Ingestion of excavated soil
- Inhalation of air vapor and particulates from excavated soil
- Dermal contact with excavated soil
- External radiation exposure from radiological constituents in excavated soil
- Ingestion of groundwater

4.8.1.5 Receptors

Potential releases from the HTF are at a depth greater than 1.2 meters (4 feet); therefore, the standard human and ecological receptor scenarios do not apply. A future industrial worker scenario is considered for deep soils at the PTSM toxicity threshold to take into account potential exposure through excavation.

4.8.2 Risk Assessment

The risk assessment for the HTF closure follows the ACP protocols for human health and ecological risk assessments. [ERD-AG-003_F.17, ERD-AG-003_P.1.4, ERD-AG-003_P.1.5] Based on available characterization data and estimated volume of residual material expected to remain in each of the waste tanks and ancillary equipment, the chemical and radiological inventory used for PA modeling has been calculated for HTF as discussed in Section 3.3. Modeling was conducted to determine the peak concentrations of the non-radiological and radiological contaminants in the groundwater over the 10,000 years following closure. When each waste tank is closed, analyses will be performed to compare the actual residual inventory versus the calculated values used in the modeling.

4.8.2.1 Human Health Risk Assessment

The SRS ACP protocols call for evaluation of surface soils for exposure to a future industrial worker from 0 to 1 foot. Some of the ancillary equipment may currently be within the 0 to 1-foot depth. However, since the waste tanks and ancillary equipment will be stabilized and covered with at least 10 feet of backfill, there will be no pathway for future industrial worker exposure. Therefore, based on the evaluation using the SRS ACP protocols, no human health risk assessment is required at this time. [ERD-AG-003_F.17, ERD-AG-003_P.1.4, ERD-AG-003_P.1.5]

4.8.2.2 Ecological Risk Assessment

The ACP protocols call for evaluation of surface soils for ecological exposure from 0 to 4 feet. Some of the ancillary equipment may currently be within the 0 to 4-foot depth. However, since the waste tanks and ancillary equipment will be stabilized and covered with at least 10 feet of backfill, there will be no pathway for ecological exposure. Therefore, based on the evaluation using the ACP protocols, no ecological risk assessment is required at this time. [ERD-AG-003_F.17, ERD-AG-003_P.1.4, ERD-AG-003_P.1.5]

4.8.2.3 Principal Threat Source Materials

The PTSM are those materials that include or contain hazardous substances, pollutants, or contaminants that act as a reservoir for migration of contamination to groundwater, surface water, or air, or that act as a source for direct exposure. [OSWER 9380.3-06FS] Source characterizations are necessary to determine whether the source(s) can be designated as PTSM, Low-Level Threat Source Material, or non-hazardous materials.

The closed HTF waste tanks and ancillary equipment are, by definition, PTSM. The waste tanks and the residue remaining in the waste tanks will be stabilized and then covered with at least 10 feet of backfill. This approach is consistent with ACP remediation of reactor seepage basins, which contained contaminated soils determined to be PTSM. [ERD-AG-003_F.17, ERD-AG-003_P.1.4, ERD-AG-003_P.1.5, ERD-AG-003_P.10.1]

4.8.2.4 Contaminant Migration Constituents of Concern

Contaminant migration constituents of concern (CMCOC) were identified through a system that is consistent with both the ACP protocols and the HTF PA. The CMCOC were identified by modeling the release of contaminants and their travel through the vadose zone. The same model utilized in the HTF PA to meet 10 CFR 61 requirements is used as the basis of the CMCOC evaluation. Any radiological contaminants that are modeled to reach the water table are compared to MCL, PRG, or other appropriate standards in cases where the constituent does not have an MCL. Non-radiological contaminants are compared to MCLs or RSLs. Any constituents that are predicted to exceed these standards in the groundwater directly beneath HTF (within the 1-meter boundary) in 10,000 years are identified as CMCOC. The CMCOC are often addressed by the placement of a low permeability cap such as is planned for the HTF closure. [ERD-AG-003_F.17, ERD-AG-003_P.1.4, ERD-AG-003_P.1.5, ERD-AG-003_P.5.2] Values for CMCOC are included for 10,000 years at both the HTF 100-meter boundary and the seepline. Risk Assessment modeling results are discussed in detail in Section 5.7.